Lower Great Miami River Nutrient Management Project

MCD
MIAMI CONSERVANCY DISTRICT

LimnoTech
Water Environment | Scientists Engineers

Prepared by
LimnoTech
Under Contract to the
Miami Conservancy
District

February 28, 2017

Blank

TABLE OF CONTENTS

LIST OF FIGURES

LIST OF TABLES

ACRONYMS

A2EM	Advanced Aquatic Ecosystem Model
ADCP	Acoustic Doppler Current Profiler
CBOD5	5-Day Carbonaceous Biochemical Oxygen Demand
CFD	Cumulative Frequency Distribution
CFS	Cubic Feet per Second
CHl *a*	Chlorophyll *a*
DIP	Dissolved Inorganic Phosphorus
DO	Dissolved Oxygen
DOC	Dissolved Organic Carbon
DPO_4	Dissolved Inorganic Phosphorus
EFDC	Environmental Fluid Dynamics Code
FEMA	Federal Emergency Management Agency
GCWW	Greater Cincinnati Water Works
LGMR	Lower Great Miami River
LTOC	Labile Total Organic Carbon
MCD	Miami Conservancy District
NCDC	National Climatic Data Center
NO_2	Nitrite
NO_3	Nitrate
NH_3	Ammonia
NLCD	National Land Cover Dataset
NPDES	National Pollutant Discharge Elimination System
OEPA	Ohio Environmental Protection Agency
ORSANCO	Ohio River Valley Water Sanitation Commission
PAR	Photosynthetically Active Radiation
PBIAS	Percent Bias
PO_4	Orthophosphate
POC	Particulate Organic Carbon
PIP	Particulate Inorganic Phosphorus
RM	River Mile

SRP	Soluble Reactive Phosphorus
TKN	Total Kjeldahl Nitrogen
TN	Total Nitrogen
TOC	Total Organic Carbon
TOP	Total Organic Phosphorus
TP	Total Phosphorus
TSS	Total Suspended Solids
USEPA	United States Environmental Protection Agency
USGS	United States Geological Survey
VSS	Volatile Suspended Solids
WRRF	Water Resource Recovery Facility
WWH	Warm Water Habitat
WWTP	Waste Water Treatment Plant

Blank

Executive Summary

This report documents work related to the development, calibration and initial application of a water quality model of the lower Great Miami River (LGMR), Ohio. This work was conducted by LimnoTech under contract to the Miami Conservancy District (MCD), on behalf of a partnership of Water Resource Recovery Facilities (WRRFs). The partnership includes: the cities of Dayton, Englewood, Fairfield, Franklin, Hamilton, Miamisburg, Middletown, Springboro, Troy, Union, and West Carrollton; Tri-Cities Wastewater Authority on behalf of the cities of Huber Heights, Vandalia, and Tipp City; and Montgomery County. The purpose of this work was to conduct a scientifically sound evaluation of the potential effects of nutrient load reduction on water quality in the LGMR.

As a result of a water quality investigation of the LGMR conducted by the Ohio Environmental Protection Agency (OEPA) and policy set forth in the 2013 Ohio Nutrient Reduction Strategy, the OEPA notified NPDES permittees in the LGMR that the OEPA was planning to write numeric phosphorus limits into permits starting with the next permit renewal cycle. Although extensive data collection up to this point had defined conditions in the LGMR that were potentially attributed to excessive nutrient loading, specifically large diurnal DO variation and high sestonic chlorophyll, a model had not been developed to evaluate that relationship and estimate the effect of reducing phosphorus loading on these conditions. Several of the WRRFs that would be subject to phosphorus limits in their NPDES permits decided to fund the development of such a model.

After reviewing available model platforms and in consideration of project objectives, the Environmental Fluid Dynamics Code (EFDC) was selected to simulate LGMR hydrodynamics and the Advanced Aquatic Ecosystem Model (A2EM) was selected to simulate LGMR water quality. Available date were compiled and reviewed to determine suitability for model development and data collected between 2011 and 2013 were chosen for use in calibration of the LGMR water quality model, as these years represent a range of hydrologic conditions on the river. The LGMR water quality model domain is depicted in Figure ES-1.

The calibrated LGMR water quality model provides a reasonable, although not exact, representation of the system. The consensus opinion of the modeling team and expert reviewers is that the calibration is as good as can be accomplished given the available data. An improved understanding of the LGMR system and an improved model calibration is possible, but would require additional data collection, as described in the body of this report. In addition to data limitations, the results from a limited field investigation conducted during this project suggest that significant lateral variability of key water quality parameters, especially dissolved oxygen, can occur in the river and these lateral variations cannot be captured by the one-dimensional framework of the current model. Data collected during this project demonstrate that concurrent DO concentrations can vary by up to 6 mg/l across the channel. Although further field investigation is needed to corroborate these observations, they suggest that no single-point DO measurement in the LGMR should be construed as representative of the entire cross-section of the river.

The work conducted in this study and documented in this report supports the following key findings and results:

- The calibrated LGMR water quality model provides a very good representation of the system and is as good a water quality model as can be accomplished given the available data. The model framework and calibration are robust, scientifically sound and were developed based on good modeling practices.
- Although calibration of the LGMR water quality model can potentially be improved in the future with collection of additional data (see Section 6.2), the current calibrated model is appropriate for use in comparatively evaluating nutrient load reduction scenarios.

- While both sestonic and benthic algae contribute to the large diurnal DO variations observed in the LGMR, benthic algae production and respiration appear to be the most significant drivers of diurnal DO range based on available data and model predictions.
- The current cumulative phosphorus loading to the LGMR is so large that even after drastic reductions in phosphorus loading are simulated, including the elimination of phosphorus in effluent from major WRRFs, significant improvements in DO and algal growth are not predicted.
- Information developed as part of this project indicates that lateral variability of DO up to 6 mg/l can occur concurrently in the LGMR. This indicates that a DO measurement at a single point in the river cannot be assumed to be representative of DO across the entire river, which is significant for two reasons:
    1. It means that the LGMR water quality model, which represents laterally-averaged conditions in the river, can never be expected to reproduce data at a single point precisely.
    2. The single-point measurement may not be appropriate for determining attainment of water quality standards or other water quality endpoints.

Specific recommendations for additional data collection that could improve understanding of the river, as well as accuracy and reliability of the LGMR water quality model, are made in the final section of the report.

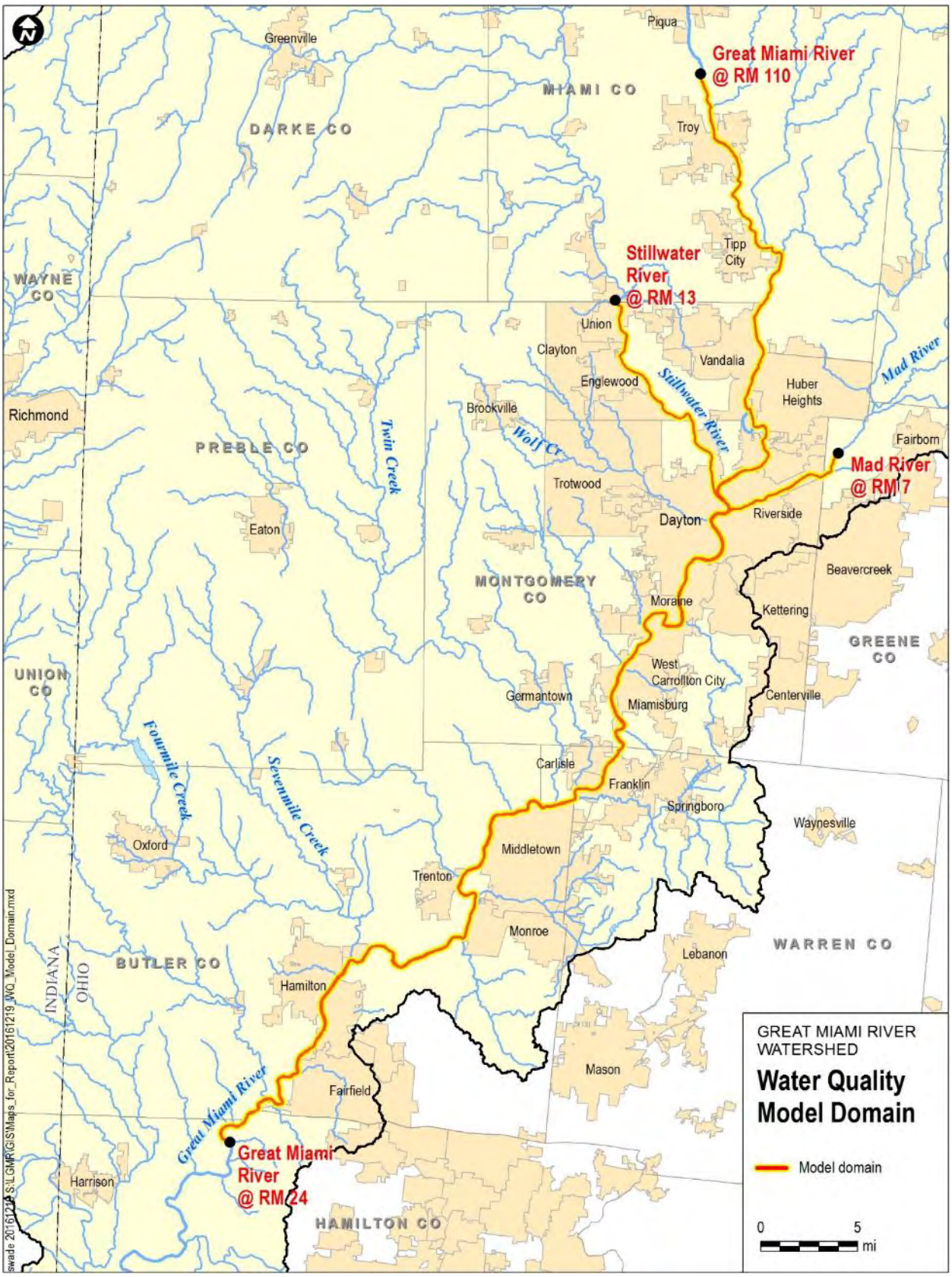

Figure ES-1. Extent of the LGMR Water Quality Model

1 Introduction

This report documents work related to the development, calibration and initial application of a water quality model of the lower Great Miami River (LGMR), Ohio. This work was conducted by LimnoTech under contract to the Miami Conservancy District (MCD), on behalf of a partnership of Water Resource Recovery Facilities (WRRFs). The purpose of this work was to conduct a scientifically sound evaluation of the potential effects of nutrient load reduction on water quality in the LGMR.

This introductory section provides the following information:

- A description of the LGMR study area;
- Background on the LGMR Nutrient Management Project;
- Project objectives; and
- Report organization.

A description of the contents and organization of this report is provided at the end of this section.

1.1 Study Area Description

The Great Miami River is located in southwestern Ohio and flows approximately 170 miles from its headwaters in southern Hardin County, southwest to the Ohio River (Figure 1-1). The entire Great Miami River watershed drains approximately 5,367 square miles of land, which includes 3,942 square miles in Ohio and 1,425 square miles in Indiana.

For purposes of this project, the LGMR is defined as the portion of the Great Miami River downstream of Troy (this is different than the LGMR defined by the OEPA). The study area for this project (Figure 1-2) includes the LGMR, as well as portions of the Stillwater River (downstream of Englewood) and the Mad River (downstream of the Huffman flood protection dam). These upper bounds were defined by the presence of water quality monitoring stations maintained by MCD and the LGMR partners. It should be noted that the spatial extent of various models developed and used in this project do not all conform to the study area extent. For that reason, the spatial extent of each model is described in the section of this report dealing with that model's development.

The City of Dayton is located at the confluence of the Stillwater River, the Great Miami River and the Mad River. Downstream of Dayton, major tributaries to the LGMR are (with their drainage areas):

- Wolf Creek (70.5 sq. mi.)
- Twin Creek (316.6 sq. mi.)
- Four Mile Creek (315.2 sq. mi.)

These tributaries flow into the LGMR from the west/northwest. Flow to the LGMR from the east/southeast is from smaller tributaries draining a much smaller portion of the watershed as shown in Figure 1-1.

Figure 1-1. Great Miami River Watershed

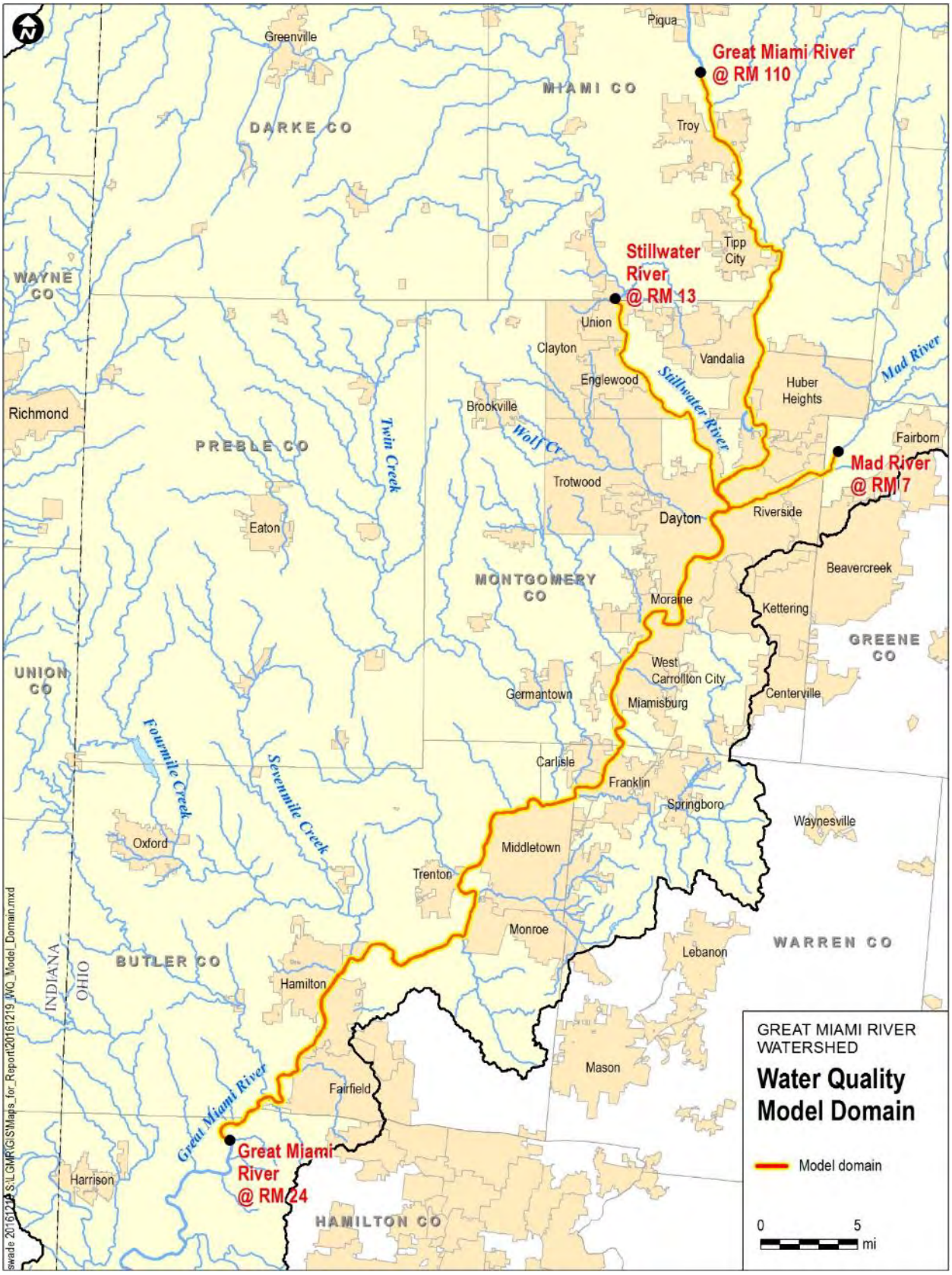

Figure 1-2. Lower Great Miami River Study Area.

1.1.1 Land Cover

Current land cover in the Great Miami Watershed was obtained from the most recent (2011) National Land Cover Dataset (NLCD) and used to assess the distribution of land cover types in both the overall watershed and the study area. The NLCD uses 15 different land cover categories, which were collapsed into three categories for presentation in this report as follows:

- NLCD categories "pasture/hay" and "cultivated crops" were combined into "agricultural".
- NLCD categories "open water, deciduous forest, evergreen forest, mixed forest, shrub/scrub, grasslands/herbaceous, woody wetlands and emergent herbaceous wetlands" were combined into "undeveloped".
- NLCD categories categorized as developed "open space", "low intensity", "medium intensity" and "high intensity" were combined into "developed".

Using these aggregations, the dominant land cover in the Great Miami watershed is agricultural (66%). The overall Great Miami River land cover distribution is depicted in Figure 1-3.

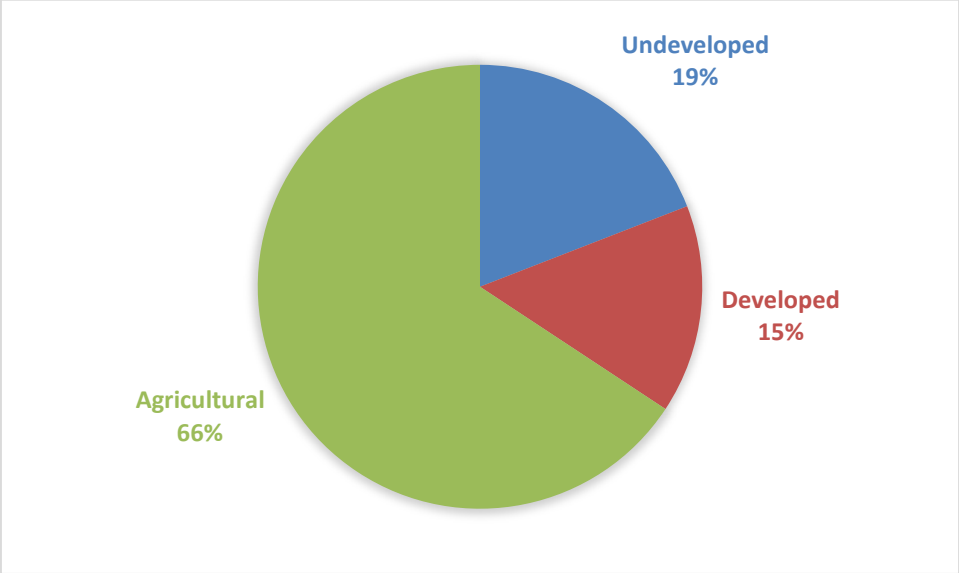

Figure 1-3. Great Miami River Watershed Land Cover Distribution (NLCD, 2011).

1.1.2 Low Head Dams

The LGMR has undergone significant physical modification through the construction of dams over the past hundred years or more. Some dams were built for recreation or water diversion/supply purposes. There are currently ten low head dams on the mainstem LGMR within the study area, as listed in Table 1-1 and shown on Figure 1-4.

Table 1-1. Low Head Dams on the Lower Great Miami River.

Dam Name	Dam Location[1] (River Mile)	Owner	Year Constructed	Height (ft)	Purpose
Needmore Road Wellfield Dam	86.74	City of Dayton	1975	n/a	Recharge for City Wellfield
Island Park Dam	82.31	City of Dayton	1915	5.9	Recreation
Monument Avenue Dam	80.88	Five Rivers Metroparks	1978	5	Recreation, undergoing partial removal
Tait Station Dam	77.64	MCD	1935	4	None (originally for cooling water diversion), scheduled for removal in 2017
South Montgomery County Dam (a.k.a. West Carrollton Dam near Moraine Airpark)	72.7	MCD	1987	11	Recreation
Hutchings Station Dam	64.52	Dayton Power & Light Company	1948	8.5	None (originally for cooling water diversion)
AK Steel Dam	51.72	AK Steel	1942	6	Water diversion
Dam South of Rentschler MetroPark	41.47	MetroParks of Butler County	1800s	5	Water diversion
Two Mile Dam (Near Combs Park, North of Black Street)	37.18	MCD	1922	11	Grade control
Hamilton Low Dam	34.57	MCD	1987	9	Recreation

[1] River mile stationing used in this report is based on stationing developed for this project by LimnoTech using available spatial data in GIS; as such, station values may differ slightly from those reported elsewhere.

Figure 1-4. Dams on the LGMR within the Study Area.

1.1.3 Water Resource Reclamation Facilities

Within the study area, there are 14 major (i.e. having an average design flow of 1.0 million gallons per day (MGD) or greater) WRRFs. In addition to these publicly-owned facilities, there are three major industrial dischargers. These WRRFs and industrial dischargers are listed in Table 1-2, along with their National Pollutant Discharge Elimination System (NPDES) permit numbers and average design flows. Their locations are shown on Figure 1-5.

Table 1-2. Major WRRFs Discharging to the Lower Great Miami River (Source: OEPA NPDES Permit Fact Sheets)

WRRF Name	Permittee	Discharge Location (River Mile)	NPDES Permit Number	Average Design Flow (MGD)
Troy Wastewater Treatment Plant	City of Troy	105.62.	1PD00019*LD	7.0
Union Wastewater Treatment Plant	City of Union	11.75 (Stillwater R.)	1PB00030*FD	1.0
Englewood Wastewater Treatment Plant	City of Englewood	8.86 (Stillwater R.)	1PD00001*OD	2.5
Tri-Cities North Regional Wastewater Treatment Plant	Tri-Cities North Regional Wastewater Authority	87.47	1PD00020*JD	11.2
Dayton Wastewater Treatment Plant	City of Dayton	76.11	1PF00000*OD	72
Western Regional Wastewater Treatment Plant	Montgomery County	71.48	1PL00002*ND	20
West Carrollton Wastewater Treatment Plant	City of West Carrollton	68.85	1PD00014*KD	1.4
City of Miamisburg Water Reclamation Facility	City of Miamisburg	65.05	1PD00017*MD	4.0
Franklin Regional Wastewater Treatment Plant	Veolia Water North America LLC, Cities of Franklin, Carlisle and Germantown	59.65	1PD00004*QD	4.5
Middletown Wastewater Treatment Plant	City of Middletown	48.29	1PE00003*OD	26
LeSourdsville Regional Water Reclamation Facility	Butler County Board of Commissioners	45.65	1PK00011*ND	15
Hamilton Water Reclamation Facility	City of Hamilton	34.0	1PE00002*ND	32
Fairfield Wastewater Treatment Plant	City of Fairfield	32.0	1PD00003*QD	10
Wausau Paper (industrial)	Wausau Paper Towel & Tissue, LLC	51.62	1IA00119*HD	4.0
AK Steel	AK Steel Corp.	51.45	1ID00001*KD	N/A
MillerCoors	MillerCoors, LLC	43.7	1IH00011*FD	1.75

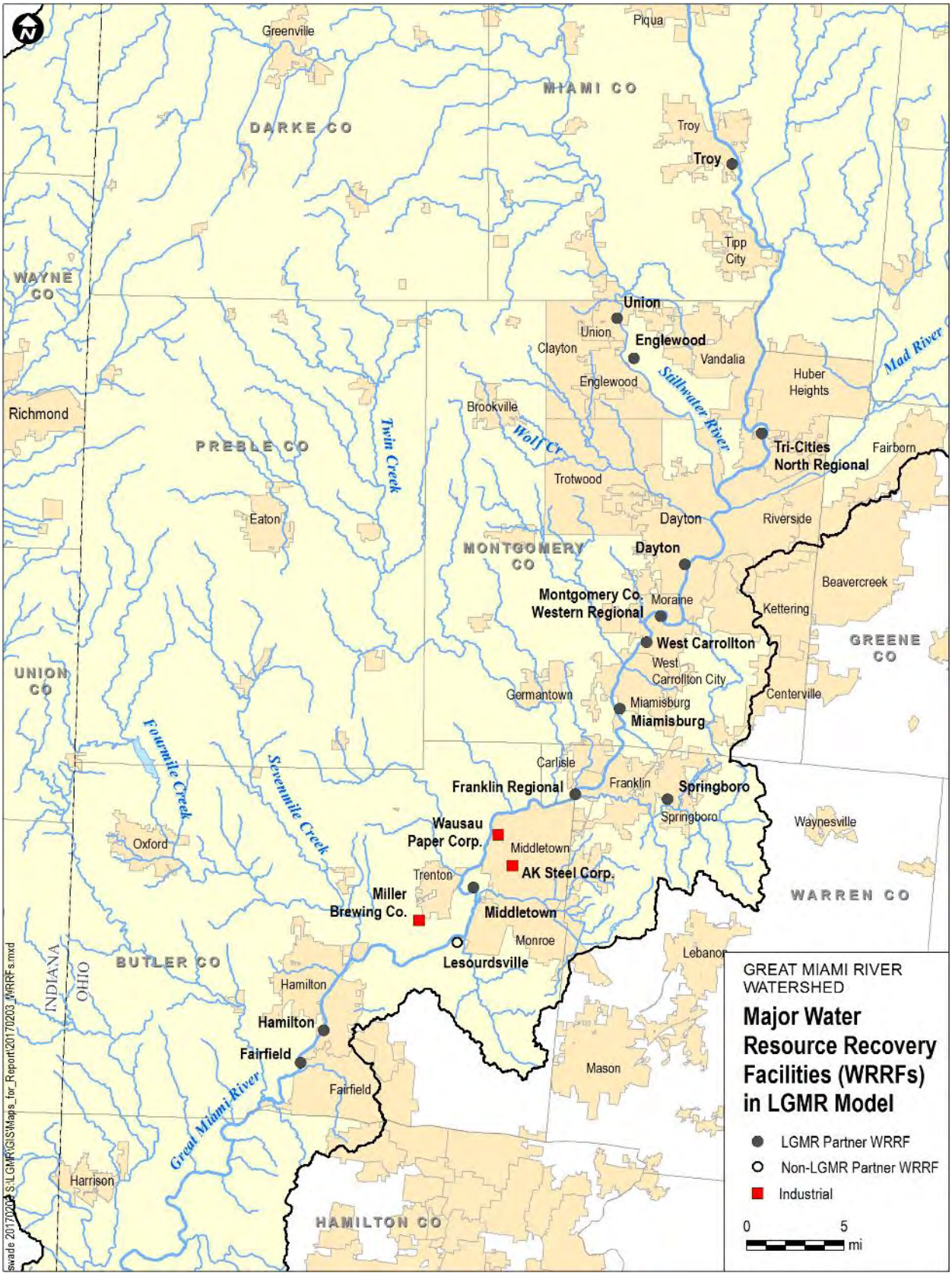

Figure 1-5. Major Wastewater Treatment Plants on the LGMR within the Study Area.

1.2 Project Background and Scope

This project is focused solely on nutrient loading to the LGMR and the water quality effects associated with nutrient loading. Specifically, data collected and observations made by the OEPA have led to concerns over the effects of nutrient loading, as indicated by large diurnal variation in dissolved oxygen, as well as the associated large amount of algae growing in the river under certain conditions. Further background on the water quality drivers for this project is discussed below.

1.2.1 Aquatic Life Use Designation of the LGMR

The aquatic life use of the Great Miami River, as designated by the State of Ohio (Ohio Administrative Code 3745-1-21), is warm water habitat (WWH). WWH is defined in the State water quality standards as follows (Ohio Administrative Code 3745-1-07(B)(1)(a)):

> "…these are waters capable of supporting and maintaining a balanced, integrated, adaptive community of warm water aquatic organisms having a species composition, diversity, and functional organization comparable to the twenty-fifth percentile of the identified reference sites within each of the following ecoregions: the interior plateau ecoregion, the Erie/Ontario lake plains ecoregion, the western Allegheny plateau ecoregion and the eastern corn belt plains ecoregion. For the Huron/Erie lake plains ecoregion, the comparable species composition, diversity and functional organization are based upon the ninetieth percentile of all sites within the ecoregion. For all ecoregions, the attributes of species composition, diversity and functional organization will be measured using the index of biotic integrity, the modified index of well-being and the invertebrate community index as defined in "Biological Criteria for the Protection of Aquatic Life: Volume II, User's Manual for Biological Field Assessment of Ohio Surface Waters," as cited in paragraph (B) of rule 3745-1-03 of the Administrative Code."

The OEPA (2012) further describes WWH by saying that "this use designation defines the "typical" warm water assemblage of aquatic organisms for Ohio rivers and streams; this use represents the principal restoration target for the majority of water resource management efforts in Ohio."

1.2.2 LGMR Water Quality Background

The biological and water quality condition of the LGMR has been the focus of evaluation for more than two decades. In 1995, the OEPA conducted an extensive biological and water quality investigation of about 90 miles of the Great Miami River, which they referred to as the "Middle and Lower Great Miami River" (OEPA, 1997), from upstream of Dayton (RM 90) to the Ohio River. This investigation included assessment of biological, chemical and physical conditions at 164 stations on the mainstem Great Miami River and its tributaries. This investigation concluded that, of the 90 miles of mainstem Great Miami River investigated, 55.3% (approximately 50 miles) was in full attainment of the designated aquatic life use, 40.3% (approximately 36 miles) was in partial attainment and 4.4% was in non-attainment (approximately 4 miles).

In 2010, the OEPA again conducted a biological and water quality assessment of 75 miles of the LGMR to determine attainment of the river's designated aquatic life use. Of these 75 miles, 60.6 miles were found to be in full attainment of the WWH aquatic life use designation, and 14.4 miles were found to be in partial attainment (OEPA, 2012). In their report, the OEPA concluded that "of the 14.4 miles in non-attainment, nutrient over-enrichment was the principal cause of impairment." The report also stated that:

> "Nutrient over-enrichment was clearly evidenced by anomalously high sestonic chlorophyll levels, and 24-hour swings in dissolved oxygen (DO) in excess of 15 mg/l – or 3 times what is typical for large rivers. Chlorophyll levels averaged 124 μg/l over the summer, with values over 200 μg/l measured in

July. These levels are five to ten times higher than what are typical for large rivers, even those considered enriched. Nutrient over-enrichment was the primary cause of non-attainment for 13.9 miles of the 14.4 impaired miles."

The OEPA report made several general recommendations for reducing nutrient loading and mitigated the effects of nutrient loading, including (OEPA, 2012):

- Changes to management of nutrients and drainage on agricultural lands;
- Rebuilding floodplain capacity to increase assimilative capacity;
- Dam removal and
- Phosphorus limits for major point sources.

In 2013, the State of Ohio published the Ohio Nutrient Reduction Strategy (OEPA, 2013) which recommended "voluntary practices and regulatory based initiatives designed to reduce nutrient losses in runoff and subsurface drainage and to remove nutrients through point source treatment technologies." The document was prepared in response to requests from U.S. EPA Region 5 to produce a State strategy as called for in the 2008 Gulf (of Mexico) Hypoxia Action Plan. The Ohio Nutrient Reduction Strategy identified the Great Miami River watershed as a priority and stated that the watershed "contributes significant nutrient loading from both agricultural land use and urban nonpoint and point sources." Based on SPARROW modeling results from the United States Geological Survey (USGS), the strategy cited the Great Miami River as being among those Ohio watersheds that have the "highest nutrient flux" in the Ohio River Basin. The strategy also published guidelines for assigning initial phosphorus NPDES limits for major publicly-owned treatment works (POTWs); for POTWs in the Ohio River Basin discharging to receiving waters identified as impaired for nutrients, the guideline stated "Set initial permit limit at the lower of 1.0 mg/l at design flow or existing permitted load (with trading option, habitat fixes)."

As a result of its 2010 investigation findings and policy set forth in the 2013 Ohio Nutrient Reduction Strategy, the OEPA notified NPDES permittees in the LGMR that the OEPA was planning to write numeric phosphorus limits into permits starting with the next permit renewal cycle. Although extensive data collection up to this point had defined conditions in the LGMR that were potentially attributable to excessive nutrient loading, specifically large diurnal DO variation and high sestonic chlorophyll, a model had not been developed to estimate the effect of reducing phosphorus loading on these conditions. Fifteen communities that own and/or manage WRRFs, in conjunction with the MCD, decided to fund the development of such a model. The partnership includes: the cities of Dayton, Englewood, Fairfield, Franklin, Hamilton, Miamisburg, Middletown, Springboro, Troy, Union, and West Carrollton; Tri-Cities Wastewater Authority on behalf of the cities of Huber Heights, Vandalia, and Tipp City; and Montgomery County. In 2015, the OEPA issued permits for the City of Dayton Wastewater Treatment Plant and Montgomery County's Western Regional Water Reclamation Facility containing phosphorus limits. The permit fact sheets provided the following rationale (OEPA, 2015a; OEPA, 2015b):

- *"For the Dayton and Montgomery County Western Regional WWTPs* – A seasonal aggregate total phosphorus loading limit that applies for the period July through October. The limit was calculated using the plant's median seasonal flow for the years 2010 through 2014 and a total phosphorus concentration of 1 mg/l. The permits allow 36 months for the plants to meet the seasonal loading limit.

  These two plants are the largest and most upstream discharges of the lower Great Miami River watershed and contribute to a significant increase in the total phosphorus concentrations, dissolved oxygen swings and chlorophyll *a* values in the river."

- *"For the other major WWTPs* – Continued monitoring of total phosphorus in their effluent as well as upstream and downstream of their discharges. These plants also must develop a study that evaluates the technical and financial capability of their existing treatment facilities to reduce total phosphorus to 1 mg/l or lower. This study is required by Ohio Senate Bill 1, which was signed by the Ohio Governor on April 2, 2015. The study must be submitted to OEPA by December 1, 2017. OEPA is implementing this Ohio Senate Bill 1 requirement outside of NPDES permits. Instead, OEPA will send a letter instructing all applicable facilities how to comply with the evaluation study required by Ohio Senate Bill 1."

In December 2015, the WRRF partners and MCD selected LimnoTech to conduct the work documented in this report.

In 2016, OEPA conducted in-stream monitoring in the LGMR study area to assess attainment of Ohio's aquatic life use standards. Within the extent of the LGMR water quality model discussed in this report, there were 64 monitoring stations, as shown in Figure 1-6. Of these, 51 stations (80%) were found to be in full attainment. Thirteen stations (20%) were found to be in partial attainment. None were found to be in non-attainment.

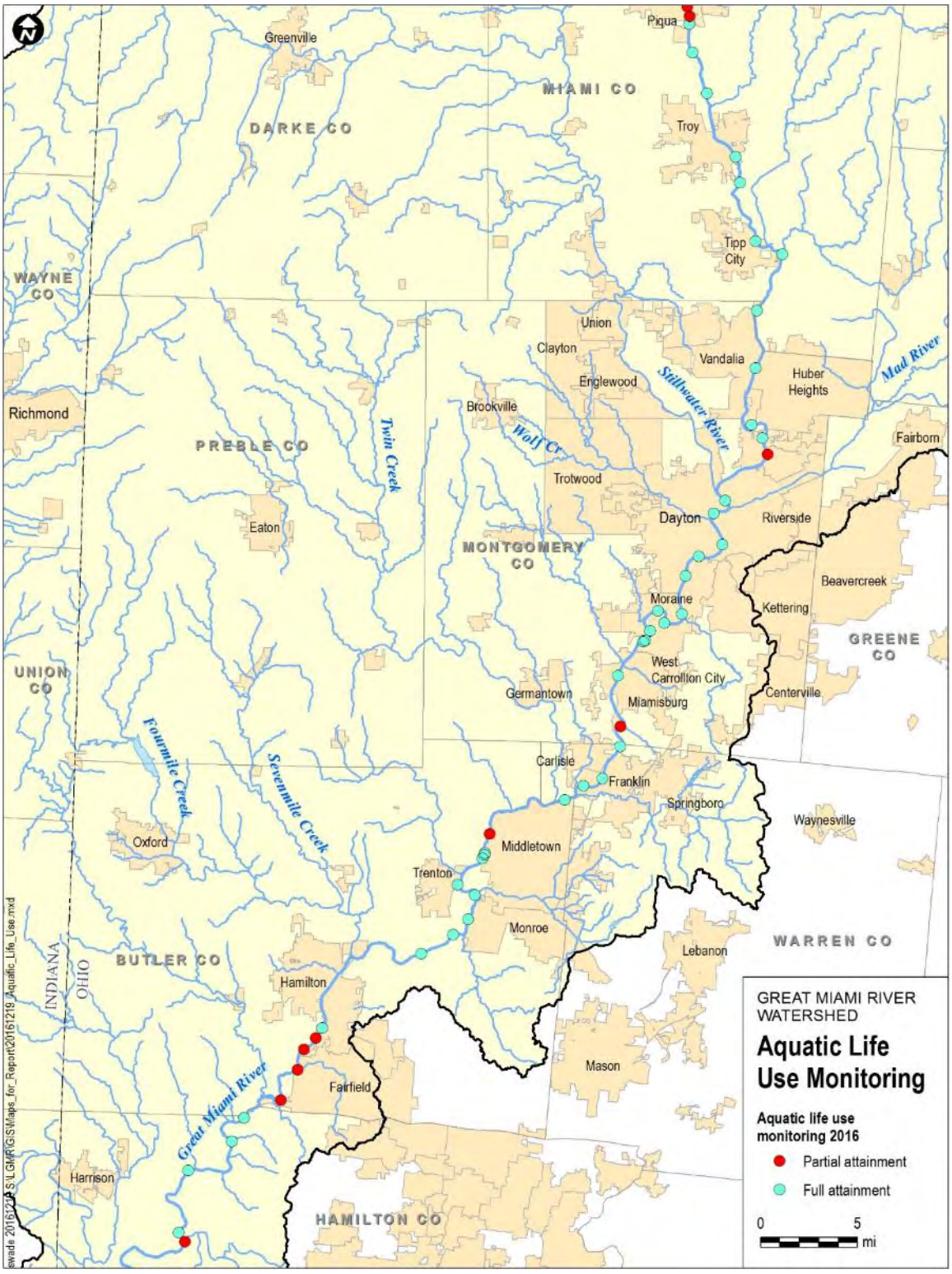

Figure 1-6. 2016 Aquatic Life Use Attainment Results[2].

[2] Based on data from the OEPA Map and Geographic Data Site (http://data.oepa.opendata.arcgis.com/datasets?sort_by=updated_at), accessed December 2016.

1.3 Objectives

The main objectives of the lower Great Miami River Nutrient Management project are:

- Develop and calibrate a water quality model of the LGMR that can be used to evaluate the effects of potential nutrient load reduction on dissolved oxygen and algae conditions in the river.
- Apply the LGMR water quality model to hypothetical load reduction scenarios and compare the results.
- Identify significant data and/or information gaps that, once filled, might improve understanding of the LGMR system and improve decision-making.
- Insure that all work is scientifically sound.

The extent to which the work completed has achieved these objectives is discussed in Section 6 of this report.

1.4 Report Organization

There are five major sections to this report, following this introduction:

- Section 2 (Summary of Supporting Data) provides a summary of background data compiled for this project. A more detailed discussion of supporting data is provided in a technical memorandum included as Appendix A.
- Section 3 (Model Development) describes the development of the LGMR hydrodynamic and water quality models, including a summary discussion of model platform selection. Appendix B contains a technical memorandum discussing the model selection process in more detail.
- Section 4 (Model Calibration) includes a discussion of calibration of the LGMR hydrodynamic and water quality models, including methods and results.
- Section 5 (Water Quality Scenarios) describes seven phosphorus load reduction scenarios that were simulated using the calibrated LGMR water quality model and the results of those simulations.
- Section 6 (Findings and Recommendations) summarizes the overall findings of this project and provides some recommendations for additional investigation to improve the reliability and utility of the models developed in this project.

Blank

2 Summary of Supporting Data

2.1 Data Summary

The Great Miami River and its tributaries have been studied with monitoring dating back several decades. This section presents an inventory and review of data relevant to the development of a water quality model of the lower Great Miami River, which was a necessary initial step in that model development process. LimnoTech has compiled and reviewed the available data provided by MCD, WRRFs, the OEPA, USGS, and local researchers, as well as from commonly used data clearinghouses such as the Water Quality Portal and the Permit Compliance System (PCS). The objective of this task was to inventory the amount and types of data and to review the datasets and their associated quality, to support the following water quality model development activities:

- Assessment of watershed characteristics to inform model forcing functions;
- Assessment of in-stream data to inform model calibration and corroboration, including identification of potential model calibration locations based on data availability;
- Assessment of in-stream data to inform model processes; and
- Identification of data gaps that may adversely affect the development and calibration of the model and thus its reliability for application to management scenarios.

LimnoTech has compiled available measured data describing in-stream surface water quality, sediment quality, hydraulics, biological community health (fish and macroinvertebrates), habitat, floating (sestonic) and fixed (benthic) algae levels, groundwater quality, point source discharge characteristics, and stream geomorphometry. Data for the entire Great Miami River (GMR) watershed were considered to inform not only the water quality model development and calibration, but also to inform the development of a watershed model that was used to specify upstream and tributary flows and nutrient loads. Data spanning roughly the last 20 years (1996 – 2015) were obtained. The focus of this data compilation effort was on data directly related to issues associated with dissolved oxygen and algal production in the LGMR, as well as hydrologic and hydraulic data. Over 1,500,000 records were reviewed and compiled in a project database (Table 2-1). Most of these observations are located within the lower portion of the LGMR that is represented in the water quality model (roughly the lower 110 miles of the LGMR, the lower 13 miles of the Stillwater River and the lower seven (7) miles of the Mad River).

Table 2-1. Summary of Available Data Reviewed and Compiled for the LGMR Project.

Sample Media	Count of Compiled Observations (Great Miami River Watershed)	Count of Compiled Observations (Water Quality Model Domain)
In-stream flow	133,596	49,850
Surface water quality[a]	1,528,180	1,308,006
Sediment quality	906	311
Biological/Habitat[b]	1,440	1,440
Point source discharge	45,549	30,243
Groundwater quality[b]	4,329	4,329

[a] Continuous monitoring data from sondes located within the lower Great Miami River watershed were compiled and reviewed.
[b] Locations within the lower Great Miami River watershed were compiled and reviewed.

LimnoTech also compiled spatial datasets using Geographic Information Systems (GIS) to complement the measured data in characterizing the watershed and informing the development of the water quality model. In addition, information on river bathymetry, dam features, and in-stream transport was also acquired and reviewed.

Overall, the available data were sufficient to develop and calibrate the water quality model. The hydrology and water quality data available throughout the entire Great Miami River watershed are sufficient to conduct a multi-year calibration of the watershed model being used to generate upstream and tributary flows and nutrient loads. Data-rich periods include 2010, when OEPA conducted extensive spatial sampling to inform their 2010 Biological and Water Quality Survey of the Lower Great Miami River and Selected Tributaries (OEPA, 2012), and the years 2011-2015, when the MCD and YSI Incorporated water quality data sondes deployed in the Great Miami River and Mad River provide the most extensive continuous monitoring dataset for dissolved oxygen.

2.2 Data Review

Data were compiled for surface water, bedded river sediment, groundwater and point sources. The data compiled for the model are described in this section based on three categories of data needs for the water quality model: 1) calibration data; 2) external forcing functions; and 3) data to inform key model processes. Other data that provided additional understanding of the watershed and waterways are also included as a separate data category. The data available for each of these data categories are described in the following subsections. Additional detail on each of the data sources and types is included in Appendix A.

2.2.1 Calibration Datasets

Calibration data include in-stream hydraulic and/or water quality observations that can be used for comparison to model simulated values. Theoretically, any location within the model domain that has data could potentially serve as a calibration location. However, the strength of the model calibration is best demonstrated against sampling locations with a high frequency of records, especially over a range of conditions. Therefore, the data were reviewed to identify sampling locations that could provide robust calibration datasets.

2.2.1.a Potential Hydraulic Calibration Datasets

The hydraulic component of the model moves flows through the model domain without regard to pollutant loads. It is important to calibrate this movement of water (e.g. hydraulics) so that characteristics that affect the water quality predictions, such as dilution and travel times, are reasonably represented prior to beginning the water quality calibration. Hydrologic and hydraulic data from the gages installed by the USGS and maintained by the MCD provide the most extensive flow and field measurement (e.g. flow, velocity, depth, cross-sectional area) surveys for use in calibrating the hydraulic portion of the water quality model (Figure 2-1).

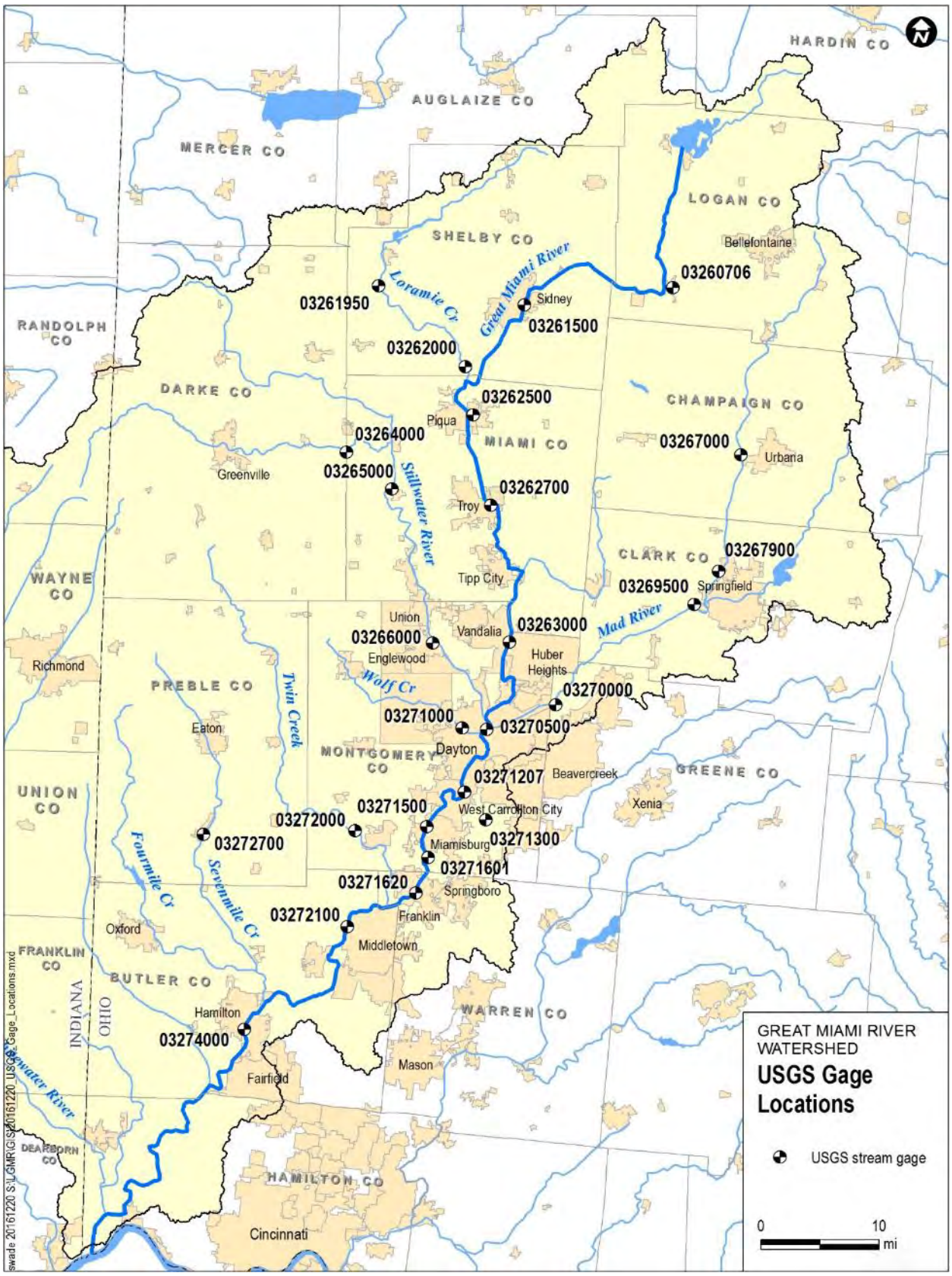

Figure 2-1. Locations of Hydrologic and Hydraulic Data in the Great Miami River Watershed.

Data from 1998-2015 for twenty-five (25) gages were compiled into the project database. Most of these gages had data spanning the entire date range. Eleven (11) of the gages are within the water quality model domain, and seven of these gages had over 100 field measurements and over 6,000 daily flow observations. The fourteen gages located outside of the water quality model domain were used to constrain the tributary and upstream flows in the watershed model.

MCD also provided a time-of-travel study in the LGMR between Dayton and Cleves conducted in 1966 by the USGS. These data, which are summarized in a report, provided a dataset to calibrate longitudinal transport in the model. Additional detail on the hydraulic datasets is provided in Appendix A, and the use of the data in the hydraulic model calibration is described in Section 4.1 of this report.

2.2.1.b Potential Water Quality Calibration Datasets

The objective of the LGMR model calibration is to simulate the eutrophic conditions (including algae) resulting in the range of dissolved oxygen (DO) levels observed in the monitoring data. With DO and algae as the focus of the calibration, the model calibration needed to also be well constrained with respect to the parameters affecting the eutrophic processes, including nutrient conditions. The primary water quality calibration variables were: 1) dissolved oxygen; 2) nutrients including total phosphorus (TP), ortho-phosphate (PO4), total nitrogen (TN) and its species (total ammonia (NH3), nitrate and nitrite (NO3+NO2)) , total Kjeldahl nitrogen (TKN); and 3) sestonic algae (expressed as chlorophyll *a* [Chl *a*]). Secondary calibration variables, which are systems the model simulates but had less rigorous calibration targets, included: 1) benthic algae (due to relative dearth of data) and 2) biochemical oxygen demand (BOD, due to potential measurement interference by algal respiration). Water quality data were compiled for all of the calibration variables.

A number of agencies have monitored in-stream water quality in the Great Miami River watershed, including: MCD, Heidelberg University, OEPA, Greater Cincinnati Water Works, USGS, ORSANCO, and the WRRFs. MCD generated the highest density of data through its continuous DO and Chl *a* monitoring collaboration with YSI Incorporated (Figure 2-2). Most of the data in this dataset were collected during 2011 to the present, and there are over 10,000 observations each for DO and Chl *a* at each location. In addition, the other primary calibration parameters are sampled approximately daily at Miamisburg (by Heidelberg University) and Fairfield (by MCD), respectively. Each of the WWRFs also sample upstream and downstream of their discharge locations and report monthly average concentrations for several of the calibration variables, most notably TP. Data from each of these sources span 5-20 years, a robust period of record for consideration as calibration datasets. These data sources offered the most potential for use as calibration datasets due to the large number of observations and long period of monitoring.

OEPA conducted sampling for an extensive number of parameters but at much lower frequency than MCD or the WWTPs. However, their sampling program includes data for the secondary calibration variables and represents the only source of benthic algae data. OEPA also conducted continuous monitoring for DO at multiple locations for several days at each location between 2010 and 2012. The continuous monitoring datasets provided additional spatial coverage for assessing the model calibration with high density DO data.

ORSANCO conducted regular monitoring in the Great Miami River for over 10 years but only at one location near the mouth of the river. Monitoring by Greater Cincinnati Water Works (GCWW) and the USGS was conducted less frequently. These data were compiled but ultimately deemed unusable for the model calibration and corroboration for the following reasons: 1) the ORSANCO sampling location is downstream of the water quality model extent (described in Section 3); 2) the GCWW data do not have the temporal frequency to be useful as calibration targets; and 3) the USGS water quality data for in-stream gages are not contemporary. Additional detail on the water quality data from each organization is

provided in Appendix A, and the use of the data in the water quality calibration is described in Section 4.2 of this report.

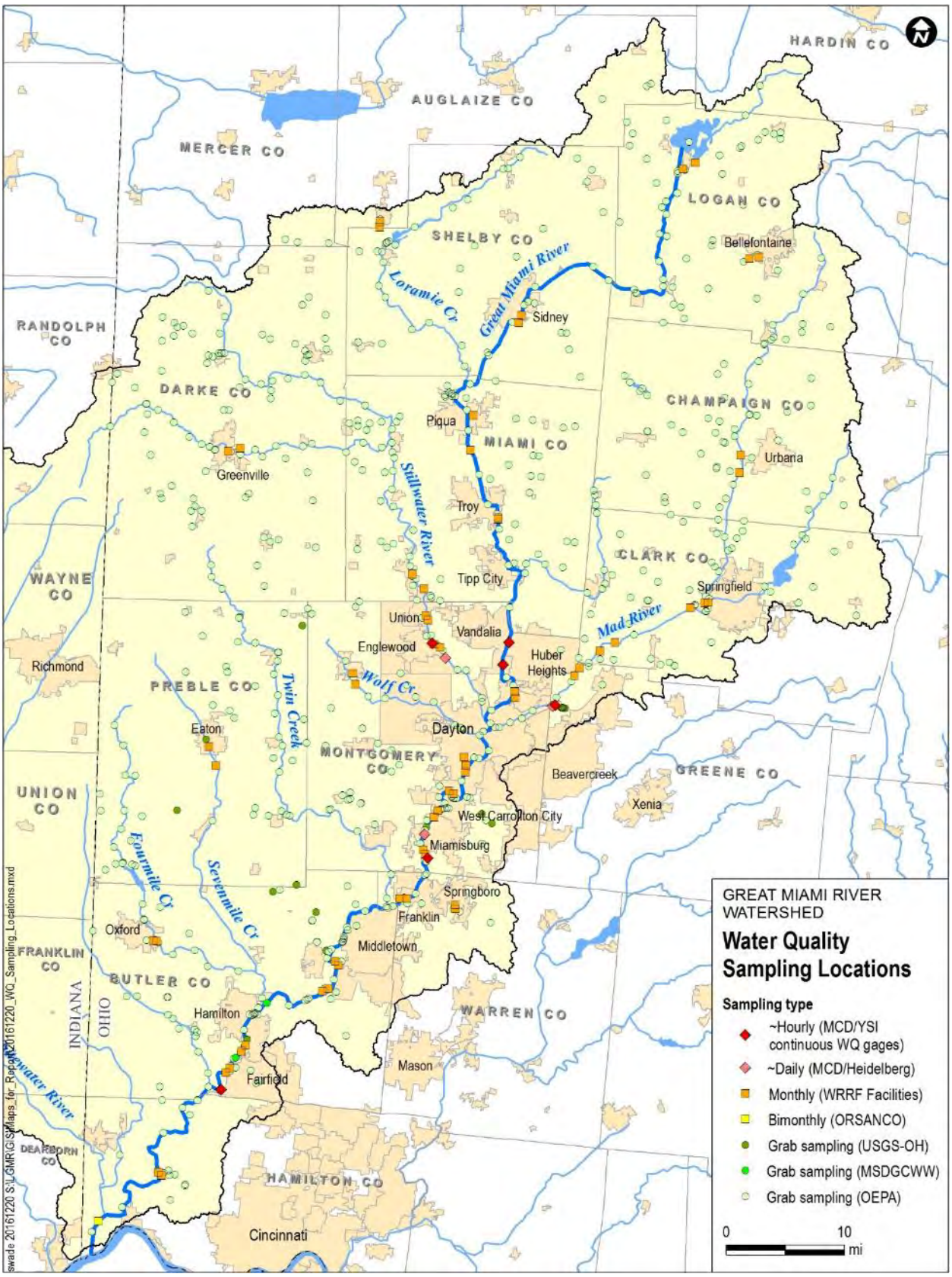

Figure 2-2. Water Quality Monitoring Locations in the Great Miami River Watershed.

2.2.2 External Forcing Functions

External forcing functions refer to model input time series that are specified to, and not simulated by, the model. The most important forcing functions these are the flows and loads from various pollutant sources in the watershed. Other forcing functions affect the kinetics of the processes represented in the model, such as solar radiation. This section describes the data used to specify the different types of external forcing functions.

2.2.2.a Point Source Flows and Loads

Major WRRF and industrial facilities are permitted to discharge nutrients and other constituents to local waterways under the NPDES. These loads may be the predominant source of both flow and nutrients to the local waterways during low flow periods.

The WRRF facilities provided data on monthly average flow, phosphorus and nitrate/nitrite results from 2008 to present for their treated effluents. Data for other parameters (other nutrients, DO, BOD) that the WRRFs monitor in their effluents and other permitted outfalls (e.g. combined sewer overflow (CSO), sanitary sewer overflow (SSO), bypass locations) were downloaded via the OEPA permit website. Older monthly flow and water quality data were downloaded from USEPA's Permit Compliance System (PCS) database. These data nominally span 1998-2011 and were used to fill gaps in the period covered by other data sources. A similar process was followed for the major industrial facility permittees in the LGMR. The monitoring requirements for parameters vary by facility. Additional detail is provided in Appendix A.

2.2.2.b Watershed Flows and Loads

Flows in the portion of the watershed upstream of and tributary to the LGMR model domain were obtained from the USGS, as described in Section 2.2.1.a. Flow and field measurement data were obtained for fourteen gages in the portion of the watershed.

Water quality data for the areas outside of the LGMR model domain were obtained from the same data sources described in Section 2.2.1.b. MCD has monitoring stations located near the upstream boundary of the LGMR model domain in the Great Miami River (Huber Heights), the Stillwater River (Englewood) and the Mad River (Dayton). Data are extensive in terms of monitoring period (>10 years) and number of parameters. Parameters of interest include the primary and secondary calibration variables and parameters affecting the kinetics of the modeled parameters, such as total organic carbon (TOC) and total suspended solids (TSS).

MCD and YSI Incorporated also conduct continuous DO and Chl *a* monitoring at stations located near the upstream boundaries of the LGMR model (Figure 2-2). Most of the data were collected from 2011 to the present, and there are over 10,000 observations each for DO and Chl *a* at each location. Data from these stations were used to specify the concentration inputs at each of the upstream boundaries of the LGMR model.

Water quality data for the tributaries to the Great Miami River were collected by OEPA, the USGS, and WRRFs in these tributary watersheds. Sampling in the tributaries tended to be less frequent than the sampling described for the calibration/corroboration and upstream boundary datasets. Additional detail is provided in Appendix A.

2.2.2.c Climatological Conditions

Climatological data are used in the model to capture daily and/or seasonal effects of the changing environment on transformation processes represented in the model. Climatological conditions include cloud cover, wind speed, and daylight period. Daily data were obtained from the National Climatic Data Center (NCDC) for six stations:

1) Dayton International Airport (GHCND ID USW00093815);
2) Fairfield, Ohio (GHCND ID USC00332651);
3) Butler County (GHCND ID USW00053855; BASINS ID 725217);
4) Winchester, Indiana airport (GHCND ID US1NRN0006; BASINS ID IN129678);
5) Greenville water plant (GHCND ID USC00333375); and
6) Sidney Highway Department (GHCND ID US10chey028, BASINS ID OH337698).

These data were obtained for use in the model but were not included in the water quality project database.

Hourly water temperature data were compiled for the six continuous monitoring stations maintained by MCD/YSI (Figure 2-2). As with the DO and Chl *a* calibration data, water temperature data were collected from 2011 to the present, and over 10,000 observations are available at each location. Additional detail is provided in Appendix A.

2.2.3 Key Model Processes

This section describes data used to inform the site-specific characteristics of the model's fate processes for the water quality parameters. Examples of fate processes include reaeration, algal (benthic and sestonic) growth and respiration, and the nutrient cycle. Typically, data to inform these processes are unavailable or highly limited. Site-specific data for the key model processes are presented in the following subsections.

2.2.3.a Sediment Phosphorus Flux

Phosphorus release from the sediments under anoxic conditions is another potential source of phosphorus that can affect algal production and contribute to large diurnal swings in dissolved oxygen. MCD and Wright State University collaborated on a sediment phosphorus flux study in summer 2015. Phosphorus flux rates were estimated above and below three dams in the river at a total of eight stations. These data, provided in May 2016, were compiled for use in calibrating sediment flux rates in the soft sediment areas represented in the model.

2.2.3.b Light Extinction

Light extinction inputs dictate the extent to which solar radiation at the water's surface is attenuated with depth in the water column, and affect the rate of benthic and sestonic algal growth. Light extinction can be characterized with collection of chlorophyll *a*, TSS (or turbidity), TOC and/or volatile suspended solids (VSS), Secchi depth and/or photosynthetically active radiation (PAR). If PAR data are available, correlations between PAR and TOC (and/or VSS), chlorophyll *a* and TSS (or turbidity) can be developed to better inform modeling of light extinction. No PAR data were identified for the LGMR.

Hourly turbidity and chlorophyll *a* data were compiled at the six continuous monitoring stations maintained by MCD/YSI (Figure 2-2). As with the DO and Chl *a* calibration data, turbidity data were collected from 2011 to the present, and over 10,000 observations are available at each location. Over 20,000 TSS measurements were compiled, with the bulk (over 76%) of the measurements collected by MCD and Heidelberg University (Figure 2-2). TOC data were more limited than the TSS data, with approximately 500 data points obtained from the monitoring agencies listed in Section 2.1. MCD does not routinely monitor TOC. OEPA collected approximately two-thirds of the TOC data that were compiled for use in the model. Additional detail is provided in Appendix A.

2.2.3.c Reaeration

Reaeration coefficients are used in water quality models to represent the transfer of oxygen between the water column and the atmosphere. Site-specific measurements of the reaeration coefficients can be made using several methods, most commonly, with a tracer gas. No reaeration studies have been conducted in the Great Miami River as of the writing of this report.

2.2.3.d Nutrient Factor Limitation

The growth of benthic and sestonic algae can be limited by the amount of nutrients available as a food source (as well as by water temperature conditions and light availability). Water quality models use a growth rate tempered by coefficients that attenuate the algal growth and uptake of nutrients during periods with low nutrient concentrations. These coefficients can be estimated for site-specific conditions with bench scale studies. However, as of the writing of this report, no studies have been conducted to develop site-specific nutrient factors for the LGMR.

2.2.4 Supporting Data

Other data types provide useful information about the watershed conditions even though they may not be used directly in the water quality model. These data types include bed sediment quality, groundwater quality, biological community and habitat assessments and stream bathymetry. Each of these data types is briefly discussed in the sub-sections below. More detail is available in Appendix A.

2.2.4.a Bed Sediment

In-stream sediment quality provides information to characterize the role of sediment in nutrient fate and transport and eutrophication. Data from OEPA and the USGS included measurements of benthic algal density, total phosphorus, ammonia and total organic carbon. Approximately 750 observations were obtained, reviewed and compiled in the database prepared as part of the LGMR Nutrient Management Project.

2.2.4.b Groundwater

Groundwater is a potential source of nutrients to the LGMR waterway since it is a primary source of base flow to the surface waters. Groundwater quality sampling has been conducted at many locations in the GMR watershed, but each location has a limited number of sampling surveys. Data from MCD, the USGS, the Ohio Division of Drinking and Ground Water, and Greater Cincinnati Water Works (GCWW) were obtained, reviewed, and compiled in the project database.

2.2.4.c Biological and Habitat

The OEPA conducted biological community and habitat assessments in the lower Great Miami River in 2010. Other portions of the Great Miami River watershed were assessed in other years. Although the water quality model does not extend to simulating biological community health, the community and habitat data were compiled to provide additional context for relating the water quality model results to aquatic life conditions. The habitat data were also used to inform the representation of sediment bed characteristics in the model. Results associated with 68 locations were reviewed for the project.

2.2.4.d Bathymetry

River bathymetry data are used to construct the physical representation of the river in the model. The presence of detailed bathymetry data generally increases reliability in the model's simulation of transport characteristics (e.g. stream velocity, depth, loss rates via settling mechanisms). Sources of bathymetry

data included Acoustic Doppler Current Profiler (ADCP) transect surveys collected by MCD and the USGS, and hydraulic models developed by MCD and/or the U.S. Army Corps of Engineers for flooding analyses. Additional detail on the use of bathymetry data is provided in Section 3.2.

2.3 Data Gaps

The data described in this section and Appendix A were reviewed by the project team to determine whether there are significant data gaps with respect to constructing and calibrating the water quality model and the model/methods used to specify upstream/tributary conditions. The gap analysis considered factors such as:

- Spatial extent of available data;
- Temporal extent of key parameters;
- Quality of available data; and
- Availability of related parameters at a given location.

Overall, the available data were deemed sufficient to support development of the water quality and watershed models. However, three potential data gaps were identified:

1. Bathymetry;
2. Light extinction information; and
3. Process data for calibration.

Through process of model calibration and application, additional data gaps were identified. Several recommendations for additional data collection to better constrain processes in the model were developed and are discussed in Section 6.2.

Blank

3 Model Development

This section documents the LGMR model development process, including selection of the model platform, development of the hydrodynamic model, and development of the water quality model, and water quality model expert review.

3.1 Model Platform Selection

The overall modeling platform used to simulate water quality in the LGMR consists of two linked models: 1) a hydrodynamic model that simulates river flows, velocities, and depths, and 2) a water quality model that simulations concentrations of the water quality endpoints of concern. The model selection process is documented in a June 20, 2016, technical memo, included here as Appendix B.

The model framework used to compute flows, velocities, and depths (i.e. hydrodynamics) in the LGMR was EFDC (Environmental Fluid Dynamics Code). EFDC is a state-of-the-art finite difference model that can be used to simulate hydrodynamic and water quality behavior in one, two, or three dimensions in riverine, lacustrine, and estuarine environments (TetraTech 2007a, 2007b). The model was developed by John Hamrick at the Virginia Institute of Marine Science in the 1980s and 1990s, and is currently maintained under support from the U.S. EPA. The model has been applied to hundreds of water bodies, including Chesapeake Bay and the Housatonic River. Recently, LimnoTech successfully applied EFDC to a number of riverine sites including the Ohio River and the Maumee River and Western Basin of Lake Erie. The EFDC model is both public domain and open source, meaning that the model can be used free of charge, and the original source code can be tailored to the specific needs of a particular application. As a result, EFDC provides a powerful and highly flexible framework for simulating hydrodynamic behavior in the LGMR.

The model platform used in this project for water quality simulation was the Advanced Aquatic Ecosystem Model (A2EM). A2EM was developed by LimnoTech to simulate water quality dynamics on a fine-scale, three-dimensional computational grid, based on a linkage to an external hydrodynamic model application (in this case, EFDC). A2EM is capable of simulating all necessary processes related to dissolved oxygen and algal growth in the LGMR. Furthermore, it is capable of transient (non-steady state) simulation, which is important in this project. A2EM was selected over other modeling platforms for several reasons. First, LimnoTech has developed an extensive set of processing and visualization tools to support the EFDC and A2EM models, which improves the efficiency of applying the linked EFDC-A2EM modeling framework for the LGMR. Also, LimnoTech has a wealth of experience applying the linked EFDC-A2EM model code, and is fully confident in the accuracy of the water quality model calculations. Lastly, A2EM includes processes that are likely to be significant in the LGMR, such as benthic algae, which are not included in some other model platforms.

3.2 Hydrodynamic Model Development

The LGMR hydrodynamic model domain extends along the Great Miami River from Troy, Ohio, located roughly twenty miles upstream of Dayton, and downstream to the Ohio River. Also included in the model are lower portions of the Mad River (seven miles) and Stillwater River (thirteen miles). These reaches were included so that the model represents the major flood protection structures on these rivers, and so that the model extends to the USGS gages on these tributaries.

In the hydrodynamic model, each stream is segmented into grid cells. Hydrodynamic calculations of velocities and depths are made by the model at the edges and centers of the grid cells. The cells are typically 265 feet long (approximately 20 cells per mile). The Great Miami River grid cells vary in width from approximately 90 feet to 750 feet, with a mean width of 290 feet.

Key features influencing hydrodynamics that are represented in the hydrodynamic model include stream bathymetry (i.e. sediment bed elevations), low head dams, flood protection dams, and tributary and point source inflows. Model inputs defining these features were based on site specific data as summarized in Table 3-1.

Table 3-1. Data Sources Supporting the Hydrodynamic Model

Stream Feature	Data Sources	Details
Stream Bathymetry	USGS ADCP Data HEC-2 Model Bathymetry	Obtained from USGS Ohio Water Science Center and USACE Louisville District, respectively
Flood Protection Dams	HSPF model rating curves (see Section 3.3.3.b and Appendix C)	Original HSPF model with rating curves provided by MCD
Low Head Dams	Mike Ekberg, MCD (personal communication)	MCD provided table of dam heights and elevations
Tributary Inflows	HSPF model output	Re-calibrated HSPF model described in Appendix C
Upstream Inflows	USGS Discharge Data	15-minute discharge data: • Stillwater River Gage #03265000 • Great Miami River Gage #03267000 • Mad River Gage #03270000

Stream bed elevation and dams, which strongly influence computed water depths and velocities, are illustrated in Figure 3-1. The LGMR is characterized by a relatively uniform slope (0.07%) over the entire 110-mile modeled reach, punctuated by some short locally shallower and steeper reaches. Eleven low head dams, which are also shown in Figure 3-1, are distributed through most of the modeled reach. These low head dams range in height from 5 to 11 feet tall, and they form small upstream pools that are appreciably deeper than the free flowing reaches.

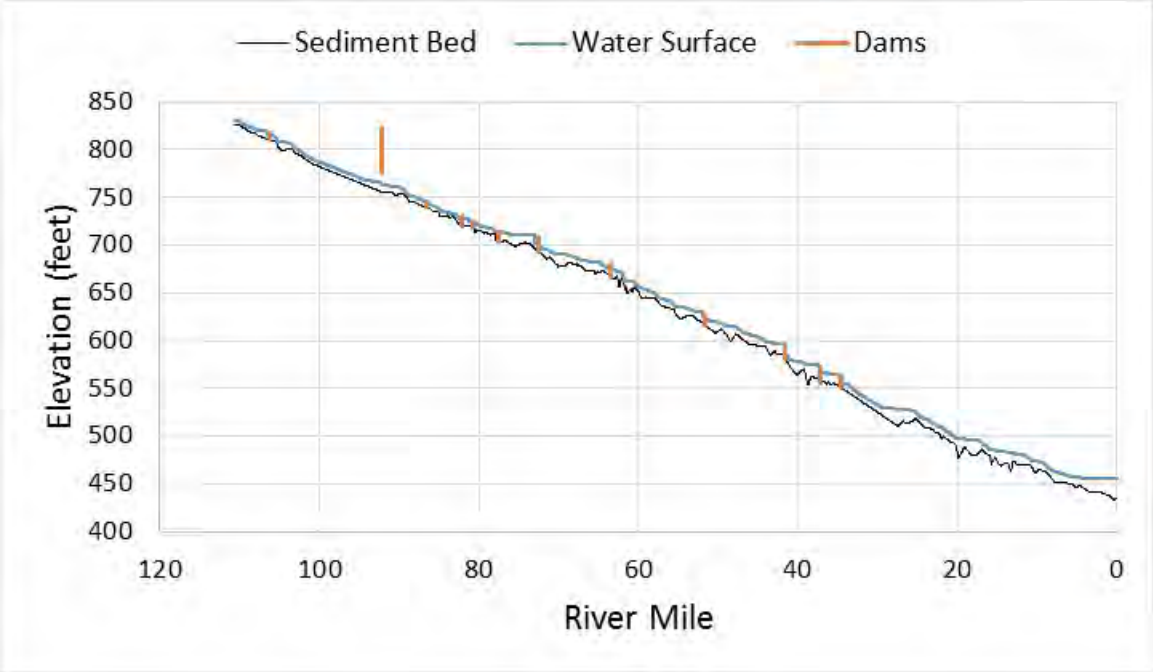

Figure 3-1. Great Miami River Stream Bed Profile and Dam Locations and Heights

Three flood protection dams are represented in the model: 1) the Taylorsville Dam on the Great Miami River above Dayton, 2) the Englewood Dam on the Stillwater River, and 3) the Huffman Dam on the Mad River. Each dam is formed by an earthen embankment and includes conduits that freely convey lower to moderate flows beneath the embankment (Miami Conservancy District, 2016).

Rating curves (i.e., relationships between hydraulic potential energy and discharge over the dam) for the low head dams were developed using the broad crested weir equation and dam elevation information provided by MCD. Dam widths were estimated from aerial photography.

Flows to the upstream most reaches of the model are based on USGS discharge data as defined in Table 3-1. Tributary inflows accounting for all watershed areas draining to the modeled reaches were compiled from the HSPF model. Point source inflows from WRRFs and permitted industrial discharges were represented in the HSPF watershed model or directly in the EFDC model, depending on proximity to the river. Point sources discharging at locations farther from the river were represented in the watershed model while more proximate sources were represented directly in the EFDC model.

Figure 3-2 maps the key features described above related to the hydrodynamic model, including the model extent, dam locations, and USGS gage locations.

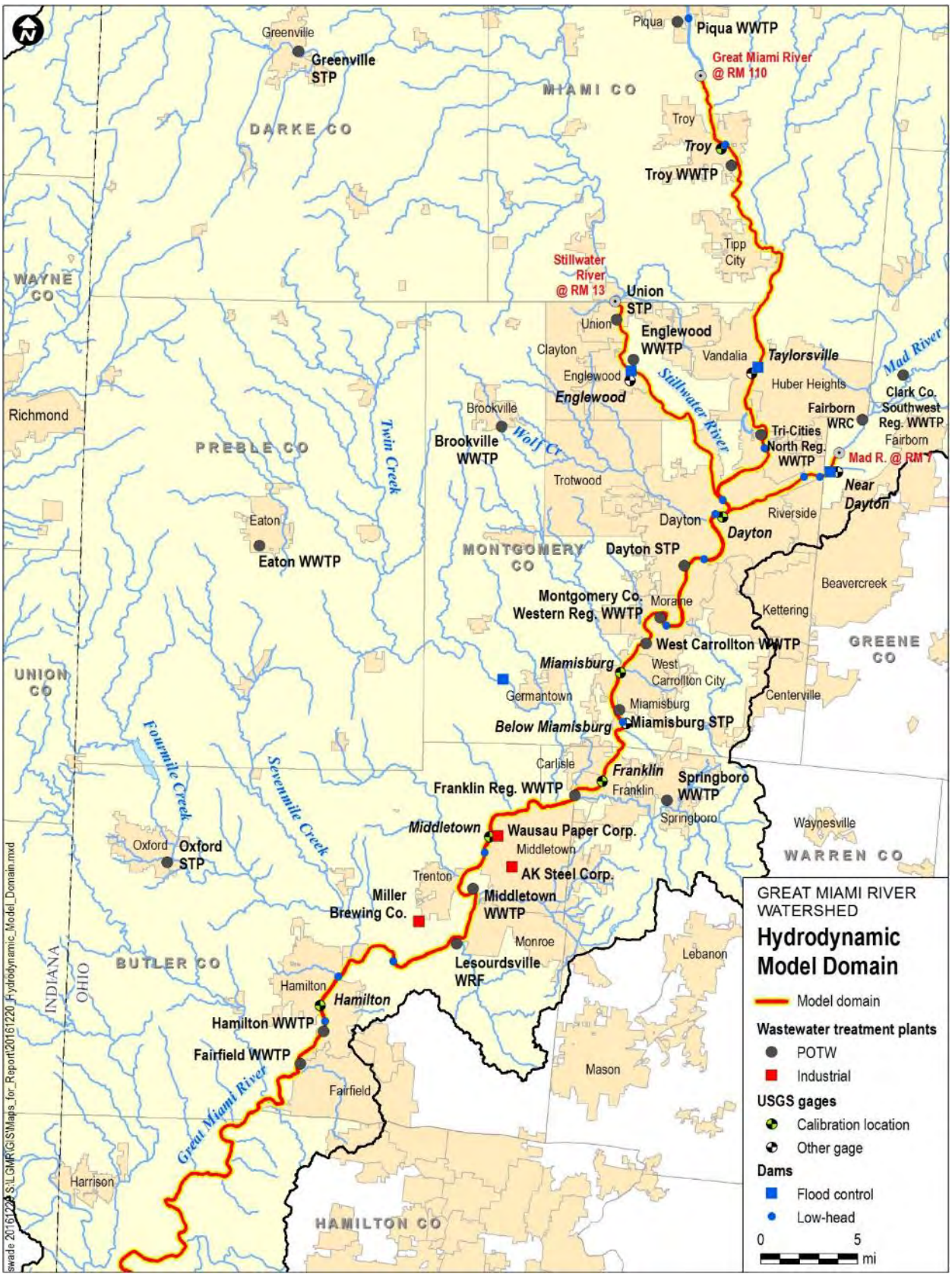

Figure 3-2. Key Features Related to the Hydrodynamic Model

3.3 Water Quality Model Development

This section provides a discussion of the water quality modeling framework used for the LGMR, model segmentation, boundary conditions and kinetic function inputs, eutrophication processes represented, and representation of the sediment bed.

3.3.1 Model Framework Description

As discussed in Section 3.1, the Advanced Aquatic Ecosystem Model (A2EM) was selected as the modeling framework to simulate water quality conditions in the LGMR system. A2EM is a publically available advanced eutrophication model that was developed by LimnoTech based on the open source Row-Column AESOP (RCA) model, which was developed by HydroQual and made publically available in 2004 (HydroQual, 2004). A2EM includes a number of enhancements relative to the original RCA framework, including a linkage to the EFDC hydrodynamic model (Verhamme et al., 2016). A2EM is capable of simulating:

- Suspended solids;
- Transport and fate of organic and inorganic nutrients;
- Dissolved oxygen kinetics;
- Multiple sestonic algal functional groups (maximum of five);
- A benthic algae functional group;
- Zooplankton (up to three classes);
- Benthic filter filters (e.g., to represent *Dreissenid* mussels); and
- Diagenesis processes and nutrient release within the sediment bed.

A2EM has been successfully applied at a number of freshwater sites across the U.S. to answer management questions concerning eutrophication and ecosystem function (Verhamme et al., 2016; LimnoTech, 2009; Bierman et al., 2005; DePinto et al., 2009a; DePinto et al., 2009b). The model is capable of simulating eutrophication processes in one, two, or three dimensions at whatever spatial resolution is appropriate to answer management questions and justifiable based on available monitoring data.

The remainder of this section describes the linkage of A2EM to the EFDC model and the water quality / eutrophication state variables simulated by the A2EM framework for the LGMR.

3.3.1.a Linkage to EFDC

A key feature of the A2EM framework is the linkage that it provides to the EFDC hydrodynamic model. This linkage allows for A2EM to simulate water quality and eutrophication processes in one, two, or three dimensions based on either the same grid used in the hydrodynamic model or a "collapsed" version of the hydrodynamic grid. The linkage capability built into the EFDC and A2EM framework not only allows the hydrodynamic and water quality models to "talk" to each other, but also importantly avoids the need to re-run the entire hydrodynamic simulation each time a water quality simulation is run. Running the water quality simulation independent of the hydrodynamic simulation results in reduced model runtimes and improves the efficiency with which calibration and scenario simulations can be completed with the A2EM model.

As an EFDC simulation progresses, physical and time-variable hydraulic information is written to a suite of linkage files in a binary format (*.bin), at a time interval defined by the modeler (e.g., every hour).

Static grid information passed between the models includes model grid dimensions (i.e., cell width, length, and bottom elevation) and vertical layer configuration and locations where external flow sources enter the model domain. Dynamic results from the EFDC simulation that are included as time series in the A2EM linkage files include:

- Flow rates at horizontal and vertical interfaces between adjacent model grid cells;
- Dispersion rates at horizontal and vertical interfaces between cells;
- Water surface elevation (relative to initial cell depth);
- Inflow rates associated with individual external flow sources (e.g., discrete point and non-point sources);
- Flow rates across dams represented within the model; and
- Water temperature (an optional linkage variable).

While segment depths and velocities are not explicitly included in the linkage file, A2EM internally calculates these variables based on the linkage input time series as the simulation proceeds. For the LGMR application, water temperature was neither simulated by EFDC nor included in the linkage to A2EM. Excellent water temperature data are available from continuous water quality data sonde measurements made at various locations in the Great Miami River, Stillwater River, and Mad River, and these data were used to specify temperature time series directly for A2EM (see Section 3.3.4 for more details). The linkage between EFDC and A2EM is depicted in Figure 3-3.

As discussed in the previous section, the grid developed to represent the LGMR system in the EFDC hydrodynamic model contained very detailed spatial resolution, with grid cell lengths of ~0.05 mile. This resolution was necessary to capture transitions in bathymetry and other conditions in the hydrodynamic simulation. However, this level of resolution is unnecessary for the water quality sub-model and would result in prohibitive model simulation runtimes (i.e., a single water quality simulation would take many days to complete). To address the need for a less-resolved water quality grid, LimnoTech developed a linkage processing algorithm that "collapses" the parent hydrodynamic model grid into a coarser version of the grid, while preserving the water balance and hydraulic information at the coarser scale and maintaining the same time interval for the linkage. An additional useful feature of the collapsing algorithm is that it computes the optimal time step across the entire collapsed version of the grid for each linkage time interval. This in turn allows the modelers to optimize the time steps input to A2EM to ensure that water quality model simulations are completed as efficiently as possible. Two collapsed water quality grids were developed to represent the LGMR system, and these grids are further discussed in Section 3.3.2 (Model Segmentation).

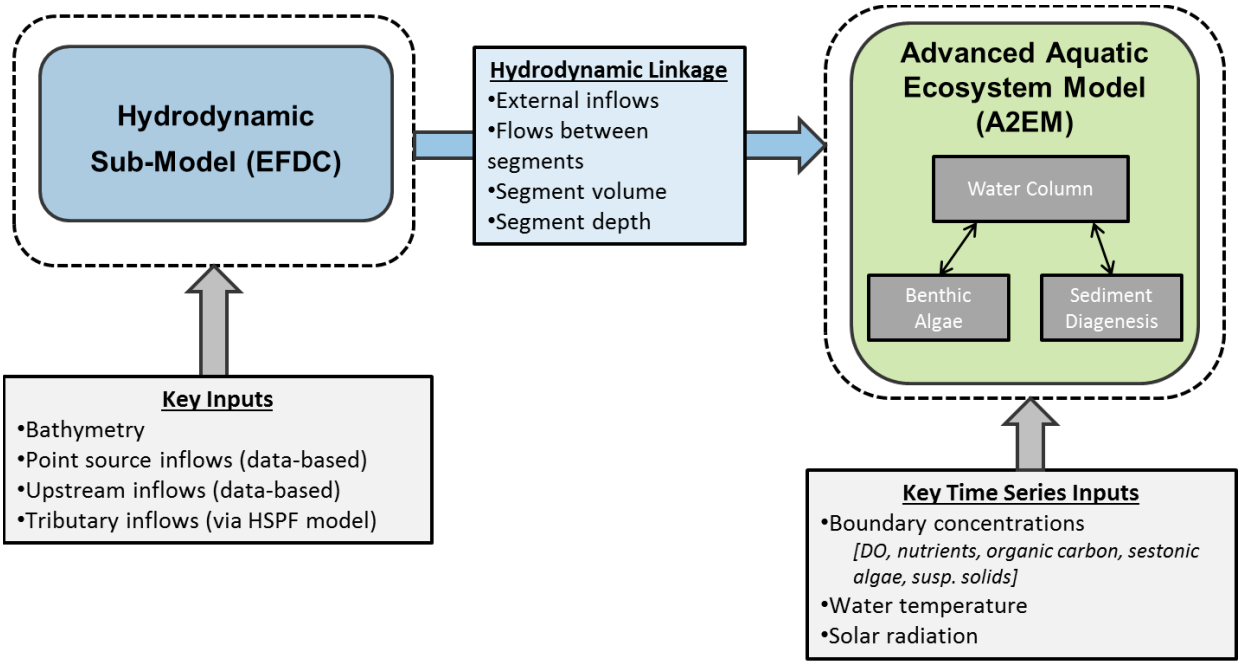

Figure 3-3. EFDC-A2EM Framework and Linkage Flow Chart

3.3.1.b Eutrophication State Variables

The A2EM framework includes a total of forty (40) state variables that can be used to describe nutrient transport and fate and eutrophication processes in the water column; however, only 28 of these variables are employed in the LGMR model (Table 3-2). The other (12) A2EM state variables were excluded from the model because: 1) they represent constituents or processes that are not relevant to the current LGMR modeling evaluation, and/or 2) they are not sufficiently supported by existing data and so would add unwarranted complexity. Examples of excluded systems include additional sestonic algae groups, zooplankton groups, and additional classes of particulate and dissolved organic carbon.

Table 3-2. Eutrophication State Variables in LGMR Model (water column only)

System No	System ID	System Description	Units[1]
2	PHYT1	Blue-green algal group	mg-C/L
3	PHYT2	Diatom algal group	mg-C/L
4	PHYT3	Summer assemblage/other algal group	mg-C/L
7	RPOP	Particulate Organic Phosphorus - refractory	mg-P/L
8	LPOP	Particulate Organic Phosphorus - labile	mg-P/L
9	RDOP	Dissolved Organic Phosphorus - refractory	mg-P/L
10	LDOP	Dissolved Organic Phosphorus - labile	mg-P/L
11	PO4T	Total Inorganic + Algal Phosphorus	mg-P/L
12	RPON	Particulate Organic Nitrogen - refractory	mg-N/L
13	LPON	Particulate Organic Nitrogen - labile	mg-N/L
14	RDON	Dissolved Organic Nitrogen - refractory	mg-N/L
15	LDON	Dissolved Organic Nitrogen - labile	mg-N/L
16	NH4T	Total Ammonia + Algal Nitrogen	mg-N/L
17	NO23	Nitrite + Nitrate	mg-N/L
18	BSI	Biogenic Silica	mg-Si/L
19	SIT	Total Available Silica	mg-Si/L
20	RPOC	Particulate Organic Carbon - refractory	mg-C/L
21	LPOC	Particulate Organic Carbon - labile	mg-C/L
22	RDOC	Dissolved Organic Carbon - refractory	mg-C/L
23	LDOC	Dissolved Organic Carbon - labile	mg-C/L
24	EXDOC	Dissolved Organic Carbon - algal exudate	mg-C/L
27	O2EQ	Aqueous SOD	mg-O_2/L
28	DO	Dissolved Oxygen	mg-O_2/L
29	SS1	Suspended Solids, fine	mg/L d.w.
30	SS2	Suspended Solids, coarse	mg/L d.w.
35	DYE	Conservative Tracer (for testing purposes)	mg/L
36	LPIP	Exchangeable Particulate Inorganic Phosphorus	mg-P/L
37	RPIP	Non-Exchangeable Particulate Inorganic Phosphorus	mg-P/L

[1] "C", "N", "P", and "Si" refer to carbon, nitrogen, phosphorus, and silicon, respectively; "d.w." refers to dry weight.

As indicated by the PHYT1, PHYT2, and PHYT3 System IDs listed in Table 3-2, the LGMR model simulates three sestonic algae functional groups that are intended to be representative of blue-green algae, winter diatoms, and summer assemblage/other algae. The key relationships between water column state variables and other quantities of interest are described in the sub-sections following for sestonic algae, carbon, nitrogen, and phosphorus components. Further discussion of the eutrophication processes represented in A2EM that influence these components, including both sestonic and benthic algae processes, is provided in Section 3.3.5. It should be noted that benthic algae is simulated by A2EM in association with the sediment bed and not the water column, which is why benthic algae is not included with the water column state variables listed in Table 3-2.

Biological Components

The A2EM framework simulates phytoplankton biomass on a carbon basis (e.g. g-C/m^3). Algal-bound carbon is provided directly by the combination of the [PHYT1], [PHYT2], and [PHYT3] systems. For simplicity, [AlgC], [AlgP], and [AlgN] can be used to represent phytoplankton biomass expressed in carbon, phosphorus, and nitrogen equivalents, respectively:

$$[A\lg C] = [PHYT1] + [PHYT2] + [PHYT3] \quad (3\text{-}1)$$

$$[A\lg P] = \frac{[PHYT1]}{\left(R_{C:P,PHYT1}\right)} + \frac{[PHYT2]}{\left(R_{C:P,PHYT2}\right)} + \frac{[PHYT3]}{\left(R_{C:P,PHYT3}\right)} \quad (3\text{-}2)$$

$$[A\lg N] = \frac{[PHYT1]}{\left(R_{C:N,PHYT1}\right)} + \frac{[PHYT2]}{\left(R_{C:N,PHYT2}\right)} + \frac{[PHYT3]}{\left(R_{C:N,PHYT3}\right)} \quad (3\text{-}3)$$

In Equations 3-2 and 3-3, $R_{C:P,\ PHYTi}$ and $R_{C:N,\ PHYTi}$ represent the carbon-to-phosphorus (C:P) and carbon-to-nitrogen (C:N) ratios, respectively, for phytoplankton class *i*. A2EM varies these ratios per user-defined limits based on the nutrient conditions simulated by the model (e.g., ranging from "luxury" to "starvation" conditions). The ratios employed for the three sestonic algal groups represented in the LGMR model are consistent with those used for prior A2EM applications for riverine and lake systems: 5.68 – 8.5 g-C/g-N for nitrogen, and 40-90 g-C/g-P for phosphorus.

Organic Carbon Components

The carbon (C) components represented in the A2EM framework can be summarized by Equations 3-4 through 3-6 (all quantities have units of g-C/m^3). It should be noted that inorganic carbon is not represented in the A2EM framework, as it does not significantly influence the processing and recycling of nutrients that principally drive the LGMR system response.

- *Total Organic Carbon (TOC):*

$$[TOC] = ([RPOC] + [LPOC]) + ([RDOC] + [LDOC]) + [EXDOC] + [A\lg C] \quad (3\text{-}4)$$

- *Particulate Organic Carbon (POC):*

$$[POC] = [RPOC] + [LPOC] + [A\lg C] \quad (3\text{-}5)$$

- *Dissolved Organic Carbon (DOC):*

$$[DOC] = [RDOC] + [LDOC] + [EXDOC] \quad (3\text{-}6)$$

Nitrogen Components

The nitrogen (N) components represented in the A2EM framework can be summarized by Equations 3-7 through 3-12 (all quantities have units of g-N/m^3). It should be noted that particulate inorganic nitrogen (PIN) is not represented in the framework, as this component has been widely accepted as being inconsequential.

- *Total Nitrogen (TN):*

$$[TN] = ([RPON] + [LPON]) + ([RDON] + [LDON]) + ([NH4] + [NO23]) + [A\lg N] \quad (3\text{-}7)$$

- *Total Organic Nitrogen, non-algal (TON):*

$$[TON] = ([RPON] + [LPON]) + ([RDON] + [LDON]) \quad (3\text{-}8)$$

- *Particulate Organic Nitrogen (PON):*

$$[PON] = [RPON] + [LPON] + [A\lg N] \quad (3\text{-}9)$$

- *Dissolved Organic Nitrogen (DON):*

$$[DON] = [RDON] + [LDON] \tag{3-10}$$

- *Dissolved Inorganic Nitrogen (DIN):*

$$[DIN] = [NH4] + [NO23] \tag{3-11}$$

- *Total Inorganic Nitrogen (TIN):*

$$[TIN] = [DIN] = [NH4] + [NO23] \tag{3-12}$$

Phosphorus Components

The phosphorus (P) components represented in the A2EM framework can be summarized by Equations 3-13 through 3-19 (all quantities have units of g-P/m^3). It should be noted that in A2EM, [DPO4] represents actual dissolved P, [LPIP] represents inorganic P (g-P/m^3) adsorbed to solids that can be exchanged with [DPO4], and [RPIP] represents inorganic P (g-P/m^3) that is permanently adsorbed to solids.

- *Total Phosphorus (TP):*

$$\begin{aligned}[TP] = ([RPOP] + [LPOP]) + ([RDOP] + [LDOP]) \\ + [DPO4] + ([LPIP] + [RPIP]) + [A\lg P]\end{aligned} \tag{3-13}$$

- *Total Organic Phosphorus (TOP):*

$$\begin{aligned}[TOP] = ([RPOP] + [LPOP]) + ([RDOP] + [LDOP]) \\ + [A\lg P]\end{aligned} \tag{3-14}$$

- *Particulate Organic Phosphorus (POP):*

$$[POP] = [RPOP] + [LPOP] + [A\lg P] \tag{3-15}$$

- *Dissolved Organic Phosphorus (DOP):*

$$[DOP] = [RDOP] + [LDOP] \tag{3-16}$$

- *Total Inorganic Phosphorus (TIP):*

$$[TIP] = [DPO4] + ([LPIP] + [RPIP]) \tag{3-17}$$

- *Particulate Inorganic Phosphorus (PIP):*

$$[PIP] = [LPIP] + [RPIP] \tag{3-18}$$

- *Dissolved Inorganic Phosphorus (DIP):*

$$[DIP] = [DPO4] \tag{3-19}$$

3.3.2 Model Segmentation

As described in Section 3.1, the EFDC hydrodynamic sub-model represents the LGMR between approximately River Mile (RM) 110 of the Great Miami River to its confluence with the Ohio River (RM 0). The hydrodynamic model domain also includes the Stillwater River below RM 13.3 and the Mad River below RM 7.0. As discussed in Section 3.2, the hydrodynamic grid has detailed spatial resolution,

with cells lengths of approximately 0.05 mile. As noted in the linkage discussion above, using the same grid resolution for the water quality sub-model was neither necessary nor practical, given that A2EM simulation runtimes would have been on the order of days to weeks when using the full hydrodynamic grid. Therefore, a linkage collapsing algorithm was developed and applied to generate two collapsed versions of the grid for use in A2EM, a "fine" version and a "coarse" version. The key characteristics of the three grids used for the LGMR model are summarized in Table 3-3 below.

Table 3-3. Summary of LGMR Model Grids

Grid Type	Purpose	Segment Count	Typical Segment Length (mile)	Runtime per Calendar Year (hours)[1]
Detailed Hydrodynamic	For running hydrodynamic simulations of LGMR and generating initial linkage output for A2EM	2,611	0.05	4
"Fine" Water Quality	For conducting final calibration/baseline simulations and final versions of the water quality simulations	700	0.25	8
"Coarse" Water Quality	For conducting rapid calibration iterations and running initial tests of water quality scenarios (taking advantage of runtimes of less than 10 minutes)	106	1.0	0.1

[1] The runtime noted for the "detailed hydrodynamic" grid is for the hydrodynamic model only; A2EM simulations were not run for this grid, but would have been on the order of days to more than a week for each calendar year simulated.

The spatial domains of the "fine" and "coarse" water quality grids are identical and include the following extents:

- Great Miami River, from RM 110.3 to 24.0;
- Stillwater River (lower 13.3 miles); and
- Mad River (lower 7.0 miles).

The upstream extents of the water quality model are identical to those for the hydrodynamic sub-model; however, the water quality grids extend downstream only to RM 24.0 in the Great Miami River, while the hydrodynamic model extends to the confluence with the Ohio River. There are currently insufficient data and/or results from watershed models to inform nutrient and other constituent loadings in the lower 24 miles of the Great Miami River; therefore, this reach was not represented in the water quality model in the interest of reducing model runtimes and avoiding the potential for producing misleading results (i.e., due to lack of loading information preventing model calibration). The extent of the water quality grid is depicted in Figure 3-4.

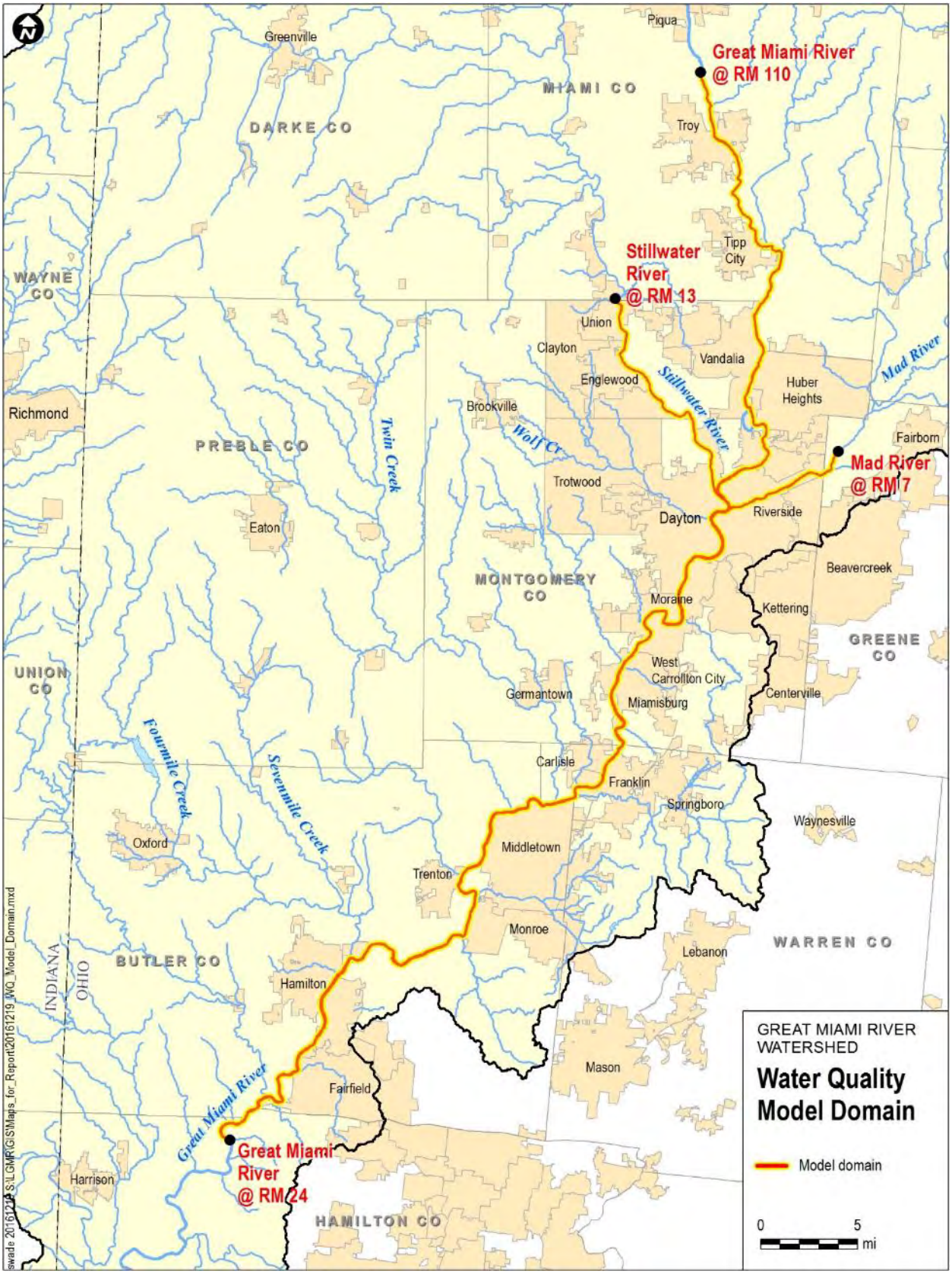

Figure 3-4. Extent of A2EM "Fine" and "Coarse" Model Grids

As indicated in Table 3-3, there is a significant difference between the number of grid cells and the computational runtime required for the "fine" and "coarse" versions of the water quality grid. After their initial development, comparative A2EM test simulations were run using each of these grids, and the results were evaluated to assess how closely the results generated for the "coarse" grid reproduced results based on the "fine" grid. In general, the "coarse" grid reproduces the "fine" grid results quite well, and therefore was relied on to facilitate more rapid iterations on the calibration, as well as to initially test load reduction and other scenario simulations. The "fine" grid preserves a greater degree of detail with respect to riffle and impoundment reaches and the transition between those reaches; therefore, it was used as the basis for the final versions of the calibration, baseline, and scenario water quality simulations.

3.3.3 Boundary Conditions

Three distinct types of flow boundaries were used for the A2EM model and concentration time series for phytoplankton, phosphorus, nitrogen, carbon, silica, dissolved oxygen, and suspended solids were specified for each, including:

- Upstream Boundaries;
- HSPF Boundaries; and
- Point Sources Boundaries.

The following sub-sections provide discussion on how boundary conditions were developed for each of these types.

3.3.3.a Upstream Boundaries

Three MCD-operated nutrient monitoring stations in the Great Miami River watershed were used to define upstream boundary concentrations for the water quality model: Great Miami River at Huber Heights, Stillwater River at Englewood, and Mad River near Dayton. These stations provided TP, soluble reactive phosphorus (SRP), ammonia (NH3), nitrate (NO3), nitrite (NO2), total Kjeldahl nitrogen (TKN), TSS, DO, and chlorophyll *a* measurements. The approach to define phosphorus, nitrogen, and suspended solids inputs was to: 1) compute a daily average concentration for days when measurements were taken, or 2) use daily average USGS flow data to estimate the concentration for days when no water quality measurements were taken by using station-specific flow-concentration relationships (Appendix D, Table D-1). The nearest USGS gages used to determine daily average flow were Great Miami River at Taylorsville (#03263000), Stillwater River at Englewood (#03266000), and Mad River near Dayton (#03270000). Organic P and N were subdivided into particulate/dissolved and refractory/labile according to the assumptions depicted in Table 3-4.

Continuous sonde measurements of DO and chlorophyll *a* were used to define upstream boundary concentrations for DO and three phytoplankton functional groups. Hourly DO time series for the Upper Great Miami River and Mad River boundaries were specified using sonde measurements from the Great Miami River Dayton Canoe Club and Mad River at Huffman Dam monitoring stations, respectively. An hourly DO time series for the Stillwater River boundary was derived from sonde measurements at Great Miami River Dayton Canoe Club and Mad River at Huffman Dam. The Stillwater River time series was constructed using a sinusoidal function and a 30-day rolling average of the daily minimum and maximum DO measurements at the two indicated locations (Appendix D, Figure D-1). Gaps in the chlorophyll *a* dataset were filled using a daily variable time series for the Upper Great Miami River and Stillwater River boundaries (Appendix D, Figure D-2) or a constant 6 μg/l assumed concentration for the Mad River boundary. Sestonic algae composition was specified for the three functional groups based on the distribution of maximum growth rates as a function of water temperature and average monthly water temperatures (Appendix D, Figure D-3).

Unlike for nutrients, data for DO, and chlorophyll *a*, organic carbon were not available at the upstream boundaries. Instead, results from sampling efforts in the GMR watershed were used to define organic carbon inputs. TOC was defined using a relationship between flow percentile and measured concentrations (Appendix D, Figure D-4), and TOC was partitioned into DOC and POC using a DOC:TOC relationship (Appendix D, Figure D-5).

3.3.3.b HSPF Boundaries

An overview of the development and calibration of the Great Miami River Watershed *Hydrologic Simulation Program - FORTRAN* (GMRWHSPF) model, which was used to define flow and nutrient boundaries for EFDC and A2EM, is provided in Appendix C. Daily variable boundary concentration time series were defined for twenty-seven locations where GMRWHSPF model output was linked to A2EM. Three forms of phosphorus (DIP, PIP, and TOP) and three forms of nitrogen (NH4, NO23, and TON) were simulated in HSPF. Organic P and N were subdivided into particulate/dissolved and refractory/labile components according to the assumptions depicted in Table 3-4.

Boundary concentrations for state variables not simulated in the HSPF model were defined using various Great Miami River watershed datasets. Sestonic algae boundary time series were defined using the daily variable chlorophyll *a* time series that was used to fill in gaps for the Upper Great Miami River and Stillwater River boundaries (Appendix D, Figure D-2). Sestonic algae composition was defined for the three functional groups using the same distribution developed for the Upper Great Miami River and Stillwater River boundaries (Appendix D, Figure D-3). The same hourly DO time series developed for the Stillwater River boundary, as described in the "Upstream Boundaries" section above, was used for the HSPF boundaries. TOC concentration and the split between DOC and POC were defined using the same method as described in the "Upstream Boundaries" section above.

3.3.3.c Point Source Boundaries

Boundary concentration time series for the 14 major municipal WWRFs and three major industrial dischargers in the water quality model domain were defined using the data described in Section 2.2.2 and Appendix A. Monthly variable phosphorus and nitrogen concentration time series were used for all point sources except the three industrial dischargers, which used constant concentrations. Facility averages were used to specify constant concentrations for suspended solids and CBOD5 (used to specify organic C state variables). A monthly variable DO time series was also specified for each facility. Total phosphorus was partitioned into 70% DIP and 30% organic P. Organic P and N were subdivided into particulate/dissolved and refractory/labile components according to the assumptions depicted in Table 3-4. The following steps were followed using CBOD5 measurements to calculate components of TOC: 1) CBOD5 concentrations were multiplied by a factor of two to obtain an estimate of the ultimate CBOD which was assumed to be oxygen demand from only labile total organic carbon (LTOC), 2) ultimate CBOD was converted from oxygen units to carbon units based on stoichiometric ratios (12 mg C/ 32 mg O^2), 3) LTOC was multiplied by four to obtain an estimate of TOC (assuming LTOC is 25% of TOC), and (4) TOC was split into particulate/dissolved and refractory/labile components according to the assumptions depicted in Table 3-4.

Table 3-4. Assumed breakdown of organic carbon, phosphorus, and nitrogen for upstream, HSPF, and point source boundaries to the water quality model

Upstream and HSPF Boundaries				Point Source Boundaries			
CARBON							
Particulate		Dissolved		Particulate		Dissolved	
see Figure D-5		*see Figure D-5*		10%		90%	
Refractory	Labile	Refractory	Labile	Refractory	Labile	Refractory	Labile
85%	15%	85%	15%	75%	25%	75%	25%
PHOSPHORUS							
Particulate		Dissolved		Particulate		Dissolved	
50%		50%		40%		60%	
Refractory	Labile	Refractory	Labile	Refractory	Labile	Refractory	Labile
85%	15%	85%	15%	75%	25%	75%	25%
NITROGEN							
Particulate		Dissolved		Particulate		Dissolved	
25%		75%		40%		60%	
Refractory	Labile	Refractory	Labile	Refractory	Labile	Refractory	Labile
85%	15%	85%	15%	75%	25%	75%	25%

3.3.4 Kinetic Functions

Time series for total daily solar radiation, duration of daylight, wind speed, ice cover, and water temperature were defined as follows. Inputs for solar radiation and wind speed were derived from data downloaded from the NCDC station for the Dayton Airport (NOAA, 2016). Solar radiation was computed by converting qualitative, hourly cloud cover observations to a quantitative measure (tenths) and using the WDMUtil program to generate a solar radiation time series from the cloud cover time series and latitude of the Dayton Airport. The duration of daylight, expressed as a fraction of daylight hours to total hours, was derived from data obtained by querying the U.S. Naval Observatory "Duration of Daylight" database for Dayton, OH (USNO, 2016). For simplicity, the entire model domain was assumed to be free of ice for the duration of the simulation period (i.e., a constant ice coverage of 0% was used). A total of six water temperature time series were used to define unique temperature regimes for the LGMR (split into 3 segments; Mad River confluence to above Hutchings Dam, below Hutchings Dam to above Two Mile Dam, and below Two Mile Dam), Upper Great Miami River, Stillwater River, and Mad River.

3.3.5 Eutrophication Processes

The A2EM represents a fully integrated eutrophication and sediment diagenesis and nutrient flux modeling framework, and the LGMR model includes a customized application of this framework to best address site-specific management questions and eutrophication processes. The A2EM framework is based on the principle of mass conservation, which states that all mass leaving a given model compartment (i.e., segment) must be accounted for by incoming/outgoing transport (with adjacent cells or the boundary) and/or gains or losses via transformation processes simulated within the segment itself. The following sub-sections provide an overview of key processes related to sestonic algae production, benthic algae production, light extinction, sediment diagenesis, dissolved oxygen kinetics, and the cycling of carbon, nitrogen, and phosphorus components simulated within the A2EM framework. When represented in

equations in this section, the A2EM state variables are denoted by the same "System ID" included in Table 3-2.

The interactions between dissolved oxygen (DO) and algal (sestonic and benthic) production, respiration, and death are particularly important for the LGMR, as algal processes and the breakdown of organic matter (i.e., BOD) in the water column are principal drivers for DO daily average concentrations and diurnal variability. Figure 3-5 provides a schematic that depicts the general relationship between algal growth (production) and loss processes and key processes affecting dissolved oxygen concentrations in the LGMR model. Further discussion of these relationships is provided below.

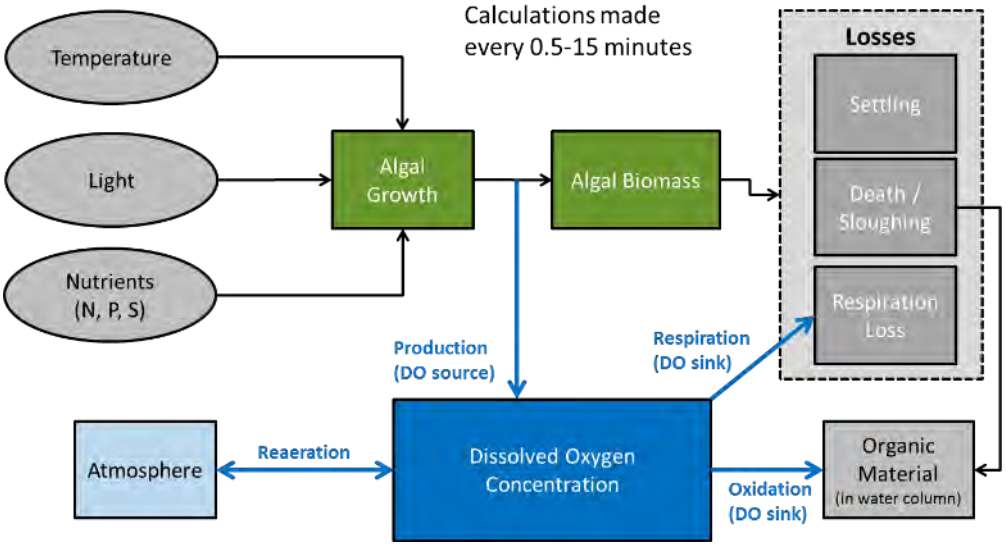

Figure 3-5. General Depiction of Algal and Dissolved Oxygen Processes

3.3.5.a Sestonic Algae

As discussed previously, the LGMR application of the A2EM framework includes three sestonic algal functional groups that represent the biomass of blue-green algae (PHYT1), winter diatoms (PHYT2), and summer assemblage / other algae (PHYT3). A2EM internally represents algal biomass on a carbon weight basis; however, the concentration of viable (pheophytin-corrected) chlorophyll *a* is typically used to quantify algal biomass based on monitoring. Chlorophyll *a* concentration is related to carbon-based biomass in A2EM by the following relationship:

$$C_{chl,tot} = \frac{1000ug/mg}{\left(R_{C:Chla,PHYT1}\right)} * [PHYT1] + \frac{1000ug/mg}{\left(R_{C:Chla,PHYT2}\right)} * [PHYT2] + \frac{1000ug/mg}{\left(R_{C:Chla,PHYT3}\right)} * [PHYT3] \quad (3\text{-}20)$$

where $C_{chl,tot}$ represents the total viable chlorophyll *a* concentration (µg/L), and $R_{C:Chla,\ PHYT*}$ represents the carbon:chlorophyll *a* ratio for each phytoplankton class (specified as 33 g-C/g-Chl *a* for blue-greens and summer assemblage, and 50 g-C/g-Chl *a* for winter diatoms). It should be noted that the term "chlorophyll *a*" used throughout this report always refers to the viable (i.e., pheophytin-corrected) chlorophyll *a* concentration.

Net production ($S_{sa,i}$, g-C/m^3/day) of each sestonic algae functional group *i* is computed as the difference between gross growth ($G_{sa,i}$, day^{-1}) and death ($D_{sa,i}$, day^{-1}) via endogenous respiration and other losses (e.g., due to zooplankton grazing), as shown below:

$$S_{sa,i} = (G_{sa,i} - D_{sa,i}) * C_{sa,i} \quad (3\text{-}21)$$

where $C_{sa,i}$ is the initial biomass concentration (g-C/m^3) of sestonic algae functional group *i*. Gross production of sestonic algae is computed as the product of a maximum (i.e., saturated) growth rate (day^{-1}) and a correction factor that reflects water temperature conditions and Michaelis-Menton assumptions regarding potential light, phosphorus, and nitrogen limitations.

The growth rate ($G_{sa,i}$, day^{-1}) in Equation 3-21 is computed assuming a multiplicative relationship with ambient water temperature, light, and nutrient availability:

$$G_{sa,i} = G_{sa,i,\max} * \left[G_{T,i}(T) * G_{I,i}(I) * G_{N,i}(N)\right] \quad (3\text{-}22)$$

where: $G_{sa,i,max}$ is the maximum growth rate – i.e., at the optimum temperature (day^{-1});

$G_{T,i}(T)$ is the effect of temperature on growth rate;

$G_{I,i}(I)$ is the effect of light intensity on growth rate; and

$G_{N,i}(N)$ is the effect of nutrient limitation on growth rate.

The temperature correction for maximum growth rate ($G_{sa,i,max}$) is calculated by A2EM based on the water temperature via the following equations:

$$\begin{aligned} G_{T,i}(T) &= e^{-\beta_1 (T_{opt,i} - T)^2} \qquad for\ T \le T_{opt,i} \\ G_{T,i}(T) &= e^{-\beta_2 (T_{opt,i} - T)^2} \qquad for\ T > T_{opt,i} \end{aligned} \quad (3\text{-}23)$$

where $T_{opt,i}$ (°C) is the optimal temperature and β_1 and β_2 are shaping coefficients for sestonic algae group *i*. Figure 3-6 shows the temperature-corrected maximum growth rate as a function of water temperature for the three sestonic algae groups simulated in the current model: blue-greens, winter diatoms, and summer assemblage. As indicated in this figure, the optimal temperature for winter diatoms (12°C) is considerably lower than that for blue-greens and summer assemblage. Therefore, cooler temperatures in winter, spring, and fall tend to favor diatom growth, while higher temperatures in the summer favor the growth of summer assemblage and blue-green algae.

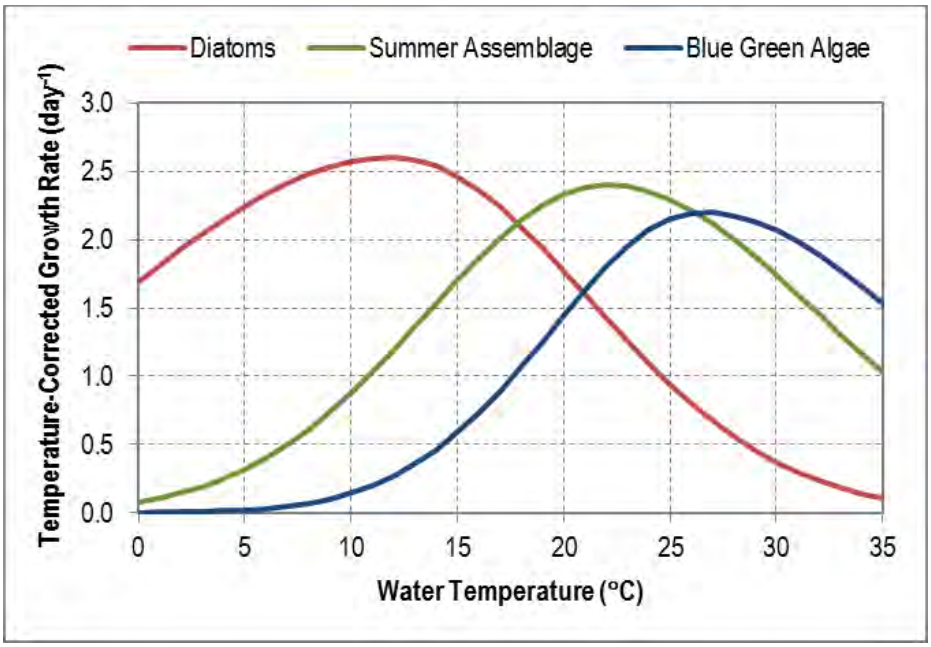

Figure 3-6. Sestonic Algae Maximum Growth Rates as a Function of Water Temperature

Light availability is an important factor governing the growth of algae in many systems, and this is also true in the LGMR system where water depth and turbidity vary spatially and through time. Light intensity is at a maximum at the water body's surface, with attenuation due to absorbance and reflection occurring with increasing depth through the water column. Photo-inhibition may occur right at the surface due to light intensities exceeding the saturating intensity, while minimal light will be available lower in the water column due to attenuation by non-living suspended solids, dissolved solids, and algae. The A2EM application for the LGMR computes the depth-averaged light reduction factor for growth based on the half-saturation approach employed in the QUAL2K model (see equation 86 in Chapra et al., 2012):

$$G_{I,i}(I) = \frac{1}{k_e * d} * \ln\left[\frac{K_{Lp} + I_0(t)}{K_{Lp} + I_0(t) * e^{-k_e d}}\right] \quad (3\text{-}24)$$

where: d = depth of water column segment (m);

k_e = light extinction coefficient (m^{-1});

$I_o(t)$ = incident light intensity at the water surface at time t (ly/day); and

K_{Lp} = half-saturation light intensity parameter (ly/day).

The incident light intensity at the water surface (I_o, ly/day) is calculated based on the current time of day (t_d), the time of sunrise ($t_{sunrise}$), and the fraction of day experiencing daylight (f):

$$I_0 = \frac{I_{tot}}{0.635 * f} \sin\left[\frac{\pi(t_d - t_{sunrise})}{f}\right] \quad (3\text{-}25)$$

where I_{tot} is the total daily incident solar radiation (ly/day). The light intensity at any point within the water column ($I(d)$) is calculated as a function of the incident surface intensity (I_o), the light extinction coefficient (k_e), and water depth (d):

$$I(d) = I_0 * \exp(-k_e d) \tag{3-26}$$

The effect of nutrient concentrations on sestonic algal growth is represented in A2EM using functions based on the Michaelis-Menten equation. The Michaelis-Menten expression is calculated for each nutrient (phosphorus, nitrogen, and silica), and the minimum value is then used to calculate the nutrient correction factor for sestonic algal growth ($G_{N,i}(N)$):

$$G_{N,i}(N) = MIN\left(\frac{C_{DIN}}{K_{mN} + C_{DIN}}, \frac{C_{DIP}}{K_{mP} + C_{DIP}}, \frac{C_{DIS}}{K_{mS} + C_{DIS}}\right) \tag{3-27}$$

where K_{mN}, K_{mP}, and K_{mS} are the half-saturation constants (g/m^3) and C_{DIN}, C_{DIP}, and C_{DIS} are the inorganic concentrations (g/m^3) for nitrogen, phosphorus, and silica, respectively.

The sestonic algae total death or loss rate ($D_{sa,i}$) in Equation 3-21 is calculated as the sum of the total respiration rate and the zooplankton grazing rate per Equation 3-28:

$$D_{sa,i} = k_{resp,sa,i}(T) + k_{grz,i} \tag{3-28}$$

where $k_{resp,sa,i}(T)$ is the temperature-dependent respiration rate (day^{-1}), including basal/resting respiration and growth-dependent respiration; and $k_{grz,i}$ is first-order rate of zooplankton grazing on sestonic algae functional group i (day^{-1}), as specified by the modeler.

In addition to the growth and death processes described in Equations 3-22 and 3-28, sestonic algae biomass is transported between model segments via advection and dispersion, as well as potentially settled to the sediment bed within model segments. Once sestonic algae biomass has deposited on the sediment bed, immediate death and recycling of the biomass to organic pools of carbon, nitrogen, and phosphorus is assumed.

A complete discussion of the sestonic algae algorithms implemented in the A2EM model is provided in the RCA Version 3.0 user's manual (HydroQual, 2004).

3.3.5.b Benthic Algae

Previous versions of the A2EM framework included a sub-model for *Cladophora*, a benthic alga that is commonly found in the nearshore areas of the Great Lakes, for example. Based on the data acquisition and evaluation process for the LGMR, it was determined that it would be important to represent benthic algae and its impact on nutrients and dissolved oxygen in the system. While it may have been possible to use the existing *Cladophora* sub-model for this purpose, it is not known which benthic algae species are present in the LGMR. Therefore, it was determined that the most technically defensible approach was to incorporate the key features of the QUAL2K model's (Chapra et al. 2012) general benthic algae sub-model, which is suitable for riverine systems (Flynn et al., 2013), to the A2EM framework, while retaining the "subzone" approach used in A2EM for calculating varying benthic algae density over a range of water depths within a given segment.

Consistent with the approach used for sestonic algae, A2EM internally represents benthic algal biomass on a carbon weight basis; however, the density, rather than in-water concentration, of viable (i.e., pheophytin-corrected) chlorophyll *a* is typically used to quantify benthic algal biomass based on field sample collection and analysis. Chlorophyll *a* concentration is related to the carbon-based biomass in A2EM by the following relationship:

$$C_{chla,ba} = \frac{1000\,mg/g}{\left(R_{C:Chla,ba}\right)} * BALG \tag{3-29}$$

where *BALG* is the carbon-based biomass density (g-C/m²), $C_{chla,ba}$ represents the equivalent total viable chlorophyll *a* density (g-Chl *a*/m²), and $R_{C:Chla,\,ba}$ represents the carbon-to-chlorophyll *a* ratio for benthic algae (specified as 40 g-C/g-Chl *a* for the LGMR model).

Net production (S_{ba}, g-C/m²/day) of benthic algae is computed as the difference between gross production resulting from growth (G_{ba}, g-C/m²/day) and losses due to endogenous respiration (R_{ba}, day^{-1}) and death (D_{ba}, day^{-1}), as shown below:

$$S_{ba} = G_{ba} - (R_{ba} + D_{ba}) * BALG_0 \tag{3-30}$$

where $BALG_0$ is the initial benthic algae biomass density (g-C/m²).

Gross production of benthic algae is computed as the product of a maximum (i.e., saturated) zero-order growth rate (g-C/m²/day) and attenuation factors that reflect Michaelis-Menton assumptions regarding potential light, phosphorus, and nitrogen limitations. Analogous to sestonic algae growth, the actual zero-order growth rate (G_{ba}, g-C/m²/day) in Equation 3-30 is computed assuming a multiplicative relationship with ambient water temperature, light, and nutrient availability:

$$G_{ba} = G_{ba,20} * \left[G_{T,ba}(T) * G_{I,ba}(I) * G_{N,ba}(N)\right] \tag{3-31}$$

where: $G_{ba,20}$ is the zero-order growth rate at a water temperature of 20°C (g-C/m²/day);

$G_{T,ba}(T)$ is the factor representing the effect of temperature on growth rate;

$G_{I,ba}(I)$ is the factor representing the effect of light intensity on growth rate; and

$G_{N,ba}(N)$ is the factor representing the effect of nutrient limitation on growth rate.

The temperature correction for the base growth rate ($G_{ba,20}$) is calculated by A2EM based on an Arrhenius model using the time- and space-variable water temperature inputs to the model developed from available monitoring data:

$$G_{T,ba}(T) = \left(G_{ba.20}\right) * \theta_{g,ba}^{(T-20)} \tag{3-32}$$

where T (°C) is the actual water temperature, and $\theta_{g,ba}$ is the Arrhenius temperature correction coefficient.

Light availability is an important factor governing the growth of benthic algae in many systems, and this is also true in the LGMR system where water depth and turbidity vary spatially and through time. Light intensity is at a maximum at the water surface and at a minimum at the surface of the sediment bed, based on attenuation of light through the vertical water column. The A2EM framework computes the depth-averaged light reduction factor for benthic algae growth based on the half-saturation light model:

$$G_{I,ba} = \frac{I_{bot}}{K_{Lb} + I_{bot}} \tag{3-33}$$

Where K_{Lb} (ly/day) is a half-saturation light constant for benthic algae, and I_{bot} (ly/day) is the light intensity at the bottom of the water column (i.e., at the surface of the sediment bed). The light intensity at the surface of the sediment bed is calculated as a function of the incident surface intensity (I_o), the light extinction coefficient (k_e), and the water depth (d):

$$I_{bot} = I_0 * \exp(-k_e * d) \tag{3-34}$$

The effect of nutrient concentrations on benthic algae growth is represented in a more complex manner than for sestonic algae. The benthic algae algorithm tracks internal (i.e., within-cell) nutrient concentrations and accounts for potential "luxury uptake" of phosphorus and nitrogen by algal cells. The intracellular ratios of N and P are calculated on a space- and time- variable basis as:

$$q_{Nb} = \frac{C_{N,ba}}{BALG} \tag{3-35}$$

$$q_{Pb} = \frac{C_{P,ba}}{BALG} \tag{3-36}$$

where $C_{N,ba}$ and $C_{P,ba}$ are the intracellular concentrations of N (g-N/m²) and P (g-P/m²), respectively, and q_{Nb} and q_{Pb} are the intracellular ratios of N (g-N/g-C) and P (g-P/g-C), respectively.

As described in Chapra et al. (2012), the Droop formulation is used to relate the nutrient limitation factor to the intracellular nutrient concentrations as:

$$G_{N,ba}(N) = MIN\left(1 - \frac{q_{0,Nb}}{q_{Nb}}, 1 - \frac{q_{0,Pb}}{q_{Pb}}\right): \quad if\ q_{Nb} \geq q_{0,Nb}\ and\ q_{Pb} \geq q_{0,Pb} \tag{3-37}$$

where $q_{o,Nb}$ and $q_{o,Pb}$ are the minimum ratios of N:C (g-N/g-C) and P:C (g-P/g-C), respectively, required for growth to occur. If the actual intracellular ratio (e.g., q_{Pb}) is less than the minimum ratio for growth ($q_{o,Pb}$), then the growth rate is zero and no growth of benthic algae can occur at that time.

The change in the internal concentrations of nutrients (N and P) in benthic algal cells is calculated based on the uptake rate of N and P with compensation for the loss of nutrient mass from the cells via death and excretion processes:

$$\underline{\text{For N}}: \quad S_{ba,N} = U_{ba,N} + q_{Nb} * BALG * (D_{ba} + k_{ex,ba}) \tag{3-38}$$

$$\underline{\text{For P}}: \quad S_{ba,P} = U_{ba,P} + q_{Pb} * BALG * (D_{ba} + k_{ex,ba}) \tag{3-39}$$

where $S_{ba,N}$ (g-N/m²/day) and $S_{ba,P}$ (g-P/m²/day) are the change in internal N and P concentrations, respectively; $U_{ba,N}$ (g-N/m²/day) and $U_{ba,P}$ (g-P/m²/day) are the cell uptake rates for N and P; and $k_{ex,ba}$ (day^{-1}) is the first-order excretion rate for benthic algae.

The algal uptake rates depend on both the external (i.e., in the water column) and internal cell concentrations of N and P. For example, the uptake rate for phosphorus is calculated as:

$$U_{ba,P} = \rho_{\max,Pb} * \left(\frac{C_{DIP}}{k_{s,Pb} + C_{DIP}}\right) * \left(\frac{K_{q,Pb}}{K_{q,Pb} + (q_{Pb} - q_{0,Pb})}\right) * BALG \tag{3-40}$$

where:

$\rho_{max,Pb}$ = maximum uptake rate for phosphorus (g-P/g-C/day);

C_{DIP} = dissolved inorganic phosphorus (DIP) concentration in the water column (g-P/m^3);

$k_{s,Pb}$ = half-saturation constant for external P concentration (g-P/m^3); and

$K_{q,Pb}$ = half-saturation constant for intracellular phosphorus (g-P/g-C).

The calculation of uptake rate for nitrogen is completely analogous to Equation 3-40, only with N-specific parameters and the dissolved inorganic nitrogen concentration (C_{DIN}) represented by the sum of nitrate and ammonia substituted for the DIP concentration.

The first-order benthic algae respiration rate (R_{ba}, from Equation 3-30) is calculated from a base respiration rate at 20°C ($k_{r,ba}$, day^{-1}) and an Arrhenius temperature correction constant ($\theta_{r,ba}$):

$$R_{ba} = k_{r,ba} * \left(\theta_{r,ba}^{T-20}\right) \tag{3-41}$$

and the first-order death rate (D_{ba}, day^{-1}) is analogously calculated as:

$$D_{ba} = k_{d,ba} * \left(\theta_{d,ba}^{T-20}\right) \tag{3-42}$$

where $k_{d,ba}$ (day^{-1}) is the base death rate at a water temperature of 20°C, and $\theta_{d,ba}$ is the appropriate Arrhenius correction term.

Nutrient mass removed from benthic algae cells via death or excretion processes is recycled to the appropriate nutrient pools in the water column. Mass loss via excretion is handled as follows:

- Nitrogen: 100% of excreted N is added to the ammonia (NH4) pool in the water column; and
- Phosphorus: 100% of excreted P is added to the dissolved inorganic P (DIP) pool in the water column.

The destination of mass removed from benthic algae cells due to death depends on the amount of luxury N or P storage in the cells. The routing of N mass lost from cells via the death process is handled as follows:

$$\Delta_{NH4} = \left(0.30 * q_{0,Nb} + RLUX_N * \left(q_{Nb} - q_{0,Nb}\right)\right) * D_{ba} * BALG \tag{3-43}$$

$$\Delta_{LPON} = \Delta_{RPON} = \left(0.35 * q_{0,Nb} + 0.5 * \left(1 - RLUX_N\right) * \left(q_{Nb} - q_{0,Nb}\right)\right) * D_{ba} * BALG \tag{3-44}$$

where Δ_x represents the N mass derivative (g-N/m^2/day) for ammonia (NH4) or labile/refractory particulate organic N (LPON/RPON), and $RLUX_N$ is the fraction of luxury-stored N mass to be routed to the NH4 pool.

The routing of P mass lost from cells via the death process is handled similarly as follows:

$$\Delta_{DIP} = RLUX_P * \left(q_{Pb} - q_{0,Pb}\right) * D_{ba} * BALG \tag{3-45}$$

$$\Delta_{LPOP} = \Delta_{RPOP} = \left(0.5 * q_{0,Pb} + 0.5 * \left(1 - RLUX_P\right) * \left(q_{Pb} - q_{0,Pb}\right)\right) * D_{ba} * BALG \tag{3-46}$$

where Δ_y represents the P mass derivative (g-P/m^2/day) for DIP or labile/refractory particulate organic P (LPOP/RPOP), and $RLUX_P$ is the fraction of luxury-stored P mass to be routed to the DIP pool. The area-normalized changes in concentration are converted to water column concentration derivatives (e.g., CD_{DIP}, g-P/m^3) by multiplying by the area of the sediment bed (*SArea*, m^2) and dividing by the water column volume (*Vol*, m^3) associated with the segment. The values of the $RLUX_N$ and $RLUX_P$ parameters were set via model calibration (see Section 4 for more information).

Further descriptions of the benthic (or "bottom") algae algorithms implemented in the A2EM model are provided in the QUAL2K manual (Chapra et al., 2012). A number of the parameters described in the process equations presented above were modified and evaluated as part of the calibration effort. The final parameterization used for the calibration is presented and discussed in Section 4.

3.3.5.c Subzone Calculations for Light & Benthic Algae

Calculating the impact of light availability on growth rates within the benthic algae sub-model requires that the water depth in a given segment be appropriately represented. This can be challenging with a one-dimensional model, such as the LGMR model, because the simulated water depth effectively represents the average depth over two dimensions: 1) longitudinally over the extent of the segment, and 2) laterally (i.e., bank to bank) across the segment. In reality, the water depth within a reach represented by a model segment can vary considerably, especially when moving laterally across the river from one bank to the opposite bank. At a given transect location, the position of the maximum water depth (i.e., thalweg) of the river will typically occur a distance away from the banks, and areas near the banks will tend to be relatively shallow and slower moving. Changes in depth correspond to changes in light intensity, with a greater amount of light reaching the sediment bed and promoting more benthic algae growth in shallower areas, all else being assumed equal. This distinction is particularly important to make in deeper/backwater reaches in a system like the LGMR because there may be sufficient light penetration for benthic algae to grow in the near-bank areas, but not in the deeper portions of the channel.

In order to account for the variability in water depth across a model segment (both laterally and longitudinally), A2EM provides the option to partition the area of a segment into up to 10 "subzones" representing a range of water depths (Figure 3-7). Each depth subzone is associated with a specific fraction of the total segment surface area and a depth "offset" relative to the mean depth that is calculated based on the collapsed linkage information from the hydrodynamic model. The sum of all area fractions across the bins will typically sum to 1.0, such that the entire surface area of the segment is collectively represented by the bins. This approach is conceptually very similar to that used by Flynn et al. (2013) in extending the core QUAL2K benthic algae model to application to the Yellowstone River.

A total of eight (8) subzones were specified for the LGMR model application to capture the range of light intensity conditions experienced at varying depths in each segment. Each bin is associated with 12.5% of the total area in each segment, and the depth offset for each bin was set based on an analysis of the distribution of sediment bed elevations represented in all (HEC-based) transects associated with a particular model segment. A conceptual schematic of a transect representing an A2EM segment and the associated subzones is shown in Figure 3-7.

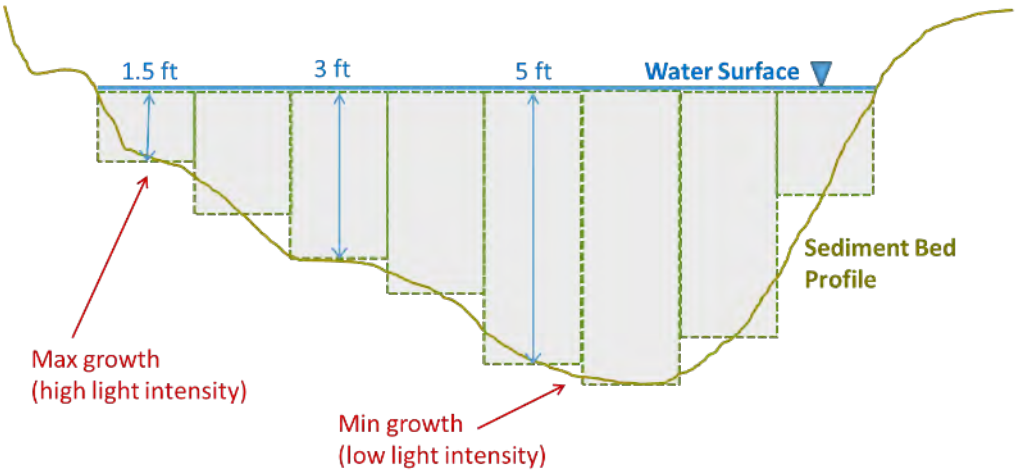

Figure 3-7. Schematic of Depth "Subzones" for Benthic Algae Light Calculations

3.3.5.d Light Extinction

As noted above, light availability is one of the three major factors influencing algal growth, along with water temperature and nutrient availability. Within the A2EM framework, the light intensity at a given water depth in the river is determined by two factors: 1) the intensity of light reaching the water surface (typically expressed in units of Langleys (ly) per day), and 2) the extinction (loss) of light due to absorption or reflection by particles and dissolved substances presence in the water column. A *light extinction coefficient* is used as the basis for calculating residual light intensity at any vertical position (depth) within the water column. Ideally, a site-specific function should be developed relating the light extinction coefficient to concentrations of different substances in the water column, including sestonic algae, organic and inorganic solids, and dissolved organic carbon. Development of such a relationship typically requires multiple monitoring events that include concurrent measurements of constituent concentrations and photosynthetically active radiation (PAR).

Because suitable datasets to develop a site-specific light extinction function are not currently available for the LGMR, a literature-based approach was followed. The light extinction formulation used in A2EM follows the default approach used in the QUAL2K model (see equation 84 and Table 6 in Chapra et al., 2012) where the total light extinction coefficient (k_e, m^{-1}) is expressed as the sum of individual extinction factors representing different types of substances:

$$k_e = k_{eb} + \alpha_i * C_i + \alpha_o * C_o + \alpha_p * C_p + \alpha_{pn} * C_p^{2/3} \quad (3\text{-}47)$$

where k_{eb} is background extinction coefficient due to water and color (m^{-1}); C_i is the inorganic suspended solids concentration (mg-d.w./L); C_o is the particulate organic matter concentration (mg-d.w./L); C_p is the chlorophyll *a* concentration (ug/L); and α_i, α_o, α_p, α_{pn} are coefficients. The coefficient for each term is defined by the modeler as an input to the A2EM simulation. The coefficients were set initially based on the default values used in the QUAL2K model (see Table 6 in Chapra et al., 2012), and then adjusted as part of the model calibration (see Section 4). Further details regarding the calculation of residual light intensity in the water column are provided in the RCA user's manual (HydroQual, 2004).

3.3.5.e Sediment Diagenesis

Sediment diagenesis involves the bacterial mineralization of organic matter to soluble end-products, including soluble forms of carbon (C), nitrogen (N), and phosphorus (P). A2EM includes a sediment

diagenesis sub-model, which is based on the framework developed by Di Toro et al. (1990). The sub-model tracks deposition of organic C, N, and P via settling of detrital organic matter and algal biomass from the water column and then simulates the breakdown of organic materials in a surficial aerobic layer and a deeper anaerobic layer (Figure 3-8). The mineralization processes simulated by the model consume oxygen, which is represented by the model as the production of sediment oxygen demand (SOD) and acts as a sink for dissolved oxygen in the water column. Mineralization processes also produce inorganic phosphorus and nitrogen (nitrate and ammonium) as end products. Fluxes of inorganic P and N species are calculated between the sediment bed and the water column based on the gradient in dissolved concentrations of the individual species. Therefore, if/when the concentration of a dissolved inorganic species (PO4, NO3, or NH4) in the bed exceeds the concentration in the water column, there will be a net flux of that dissolved species from the bed to the water column. Conversely, if the concentration of a particular dissolved inorganic species is greater in the water column than in the bed, the net flux will be from the water column into the bed. These processes are depicted in general fashion in Figure 3-8 below.

An important feature of the sediment diagenesis model is that dissolved inorganic P (DIP or DPO4) concentrations and fluxes from the sediment bed to the water column will tend to increase, often substantially, in response to very low (i.e., < 2 mg/l) DO concentrations in the water column. Very low DO concentrations in the water column result in the thinning of the surficial aerobic layer in the sediment bed and subsequent exposure of the anaerobic layer to the water column. Dissolved phosphorus concentrations in the anaerobic layer are generally much higher than for the aerobic layer due to the absence of oxidized iron species that have a high binding capacity for dissolved phosphate. A more detailed description of the sediment diagenesis sub-model can be found in Di Toro et al. (1990), Chapra (1997), and Appendix A of the RCA user's manual (HydroQual, 2004).

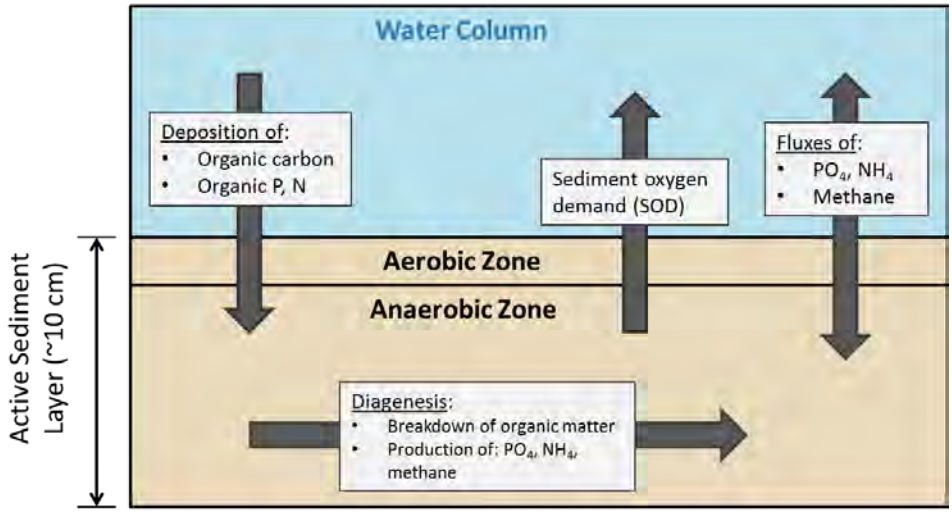

Redrawn from Di Toro et al. 1990, Chapra 1997

Figure 3-8. A2EM Sediment Diagenesis Sub-model

For the LGMR model, the A2EM framework was enhanced to allow for selective application of the sediment diagenesis sub-model to model segments in the LGMR where consistent soft sediment accumulation has been observed or is generally expected to occur based on guidance provide by OEPA. The approach used to apply and initialize concentrations for the sediment diagenesis sub-model is described in the "Sediment Bed Initialization" section below.

3.3.5.f Dissolved Oxygen Kinetics

The behavior of dissolved oxygen (DO) in a natural system is driven by a number of processes, typically including oxidation of organic matter in the water column, sediment oxygen demand (based on oxidation processes occurring in the sediment), reaeration, production via algal growth, and sinks due to algal respiration (Figure 3-5). Not only are these individual processes complex in their own right, but one process may affect another process either directly or indirectly. For example, the death of algal biomass will contribute to the pool of oxygen-demanding organic substances (i.e., BOD) in the water column. While some processes occur at a relatively steady rate (e.g., oxidation of BOD), others, such as algal production, have rates that will fluctuate considerably over the span of a day and are capable of driving significant diurnal variations in DO concentration.

Because variations in DO concentration are of principal importance in the LGMR system, all key source and sink (i.e., loss) processes were represented in the simulation of DO within the A2EM framework, including:

- Oxidation of organic carbon species in the water column (sink);
- Production via sestonic algae and benthic algae growth (source);
- Consumption via sestonic algae and benthic algae respiration (sink);
- Consumption via nitrification processes (sink);
- Oxidation of oxygen-demanding equivalents (e.g., methane) potentially released from the sediment bed (sink); and
- Reaeration (source or sink, depending on conditions).

The key algorithms used to represent several of these processes are presented below. Nitrification and oxidation of oxygen-demanding equivalents are of lesser importance in the LGMR based on model sensitivity and calibration work, and therefore these processes are not discussed in detail here. Detailed equations and discussion for each process affecting DO can be found in Appendix A of the RCA version 3 user's manual (HydroQual, 2004).

Oxidation of Organic Matter

Oxidizable dissolved or particulate forms of organic matter (carbon) can enter a water body from a variety of sources, including external point and non-point sources, and via internal processes, such as resuspension and other release of carbon from the sediment bed. A2EM represents organic matter via a set of specific organic carbon species (systems 20-24 in Table 3-2), including:

- Labile and refractory particulate organic carbon (LPOC and RPOC);
- Labile and refractory dissolved organic carbon (LDOC and RDOC); and
- Algal exudate (EXDOC).

The A2EM framework uses an Arrhenius equation to calculate the oxidation of each of these five organic carbon types, following the general form of:

$$\Delta DO_{oxid} = k_{oxid} * \theta_{oxid}^{(T-20)} * C_{DO} \quad (3\text{-}48)$$

where ΔDO_{oxid} is the rate of DO consumption (g-O^2/m^3/day); k_{oxid} is the first-order oxidation rate (day^{-1}); θ_{oxid} is the temperature correction constant; and C_{DO} is the DO concentration (g/m^3). The oxidation rates and the temperature correction constants are specified as unique input constants to A2EM for each of the five organic carbon species listed above.

Sestonic and Benthic Algae Production

The gross production (i.e., growth) of either sestonic and/or benthic algae results in a production of dissolved oxygen, with the rate of DO production dependent on the rate of algal growth. The relative impact of algal production on DO concentration depends on which form of nitrogen is being used to support growth. Generally, algae preferentially use ammonia (NH4) for growth, with nitrate (NO3) also being suitable but less preferred. A2EM computes an ammonia "preference factor" that quantifies the relative fractions of algal growth involving NH4 and NO3, depending on a preference coefficient and the relative concentrations of NH4 and NO3 present in the water column (i.e., higher NH4 concentrations will result in a higher preference factor, all else being equal). The production of DO based on sestonic algal production via NH4 ($\Delta DO_{sa,NH4}$, g/m^3/day) is calculated by the model as:

$$\Delta DO_{sa,NH4} = O_{CRB} * \sum_{i=1}^{3} \left(P_{NH4,sa,i} * G_{sa,i} * C_{sa,i} \right) \quad (3\text{-}49)$$

where $P_{NH4,sa,i}$ is the model-calculated NH4 preference factor, $G_{sa,i}$ is the growth rate (day^{-1}) and $C_{sa,i}$ is the biomass concentration for sestonic algae group *i*; and O_{CRB} is the factor for converting organic carbon mass to oxygen mass (~2.67 g-O^2/g-C). As discussed earlier in this section, the LGMR application of the A2EM framework includes a total of three sestonic algae functional groups, hence the summation expression in Equation 3-49.

The production of DO based on benthic algal production via NH4 ($\Delta DO_{ba,NH4}$, g/m^3/day) is calculated by the model as:

$$\Delta DO_{ba,NH4} = O_{CRB} * \left(P_{NH4,ba} * G_{ba} * \frac{Area}{Vol} \right) \quad (3\text{-}50)$$

where $P_{NH4,ba}$ is the model-calculated NH4 preference factor, G_{ba} is the zero growth rate (g-C/m^2/day), *Area* (m^2) is the surface area of the sediment bed, and *Vol* (m^3) is the water volume in the segment.

The calculation of DO production resulting from growth based on NO3 uptake is analogous to that shown in Equations 3-49 and 3-50, but with different coefficients used for converting carbon-based growth to oxygen mass equivalents. Further discussion regarding the impact of sestonic and benthic algal growth on DO can be found in Chapra (1997), the QUAL2K user's manual (Chapra et al., 2012), and Appendix A of the RCA version 3 user's manual (HydroQual, 2004).

Sestonic and Benthic Algae Respiration

The respiration of sestonic and/or benthic algae results in a gross consumption of dissolved oxygen, with the rate of DO consumption dependent on the rate of respiration. The consumption of DO based on sestonic algal respiration ($\Delta DO_{resp,sa}$, g/m^3/day) is calculated as:

$$\Delta DO_{resp,sa} = - O_{CRB} * \left(R_{sa,i} * C_{sa,i} \right) \quad (3\text{-}51)$$

where $R_{sa,i}$ is the first-order respiration rate (day^{-1}) for sestonic algae group *i*. The consumption of DO based on benthic algal respiration ($\Delta DO_{resp,ba}$, g/m^3/day) is calculated by the model as:

$$\Delta DO_{resp,ba} = - O_{CRB} * \left(R_{ba} * BALG * \frac{Area}{Vol} \right) \quad (3\text{-}52)$$

where R_{ba} is the benthic algae first-order respiration rate (day^{-1}).

Reaeration

Reaeration is a gradient-driven process that depends on DO concentrations in the water and overlying atmosphere as well as the water temperature. Unlike other processes affecting dissolved oxygen (e.g., oxidation, which always acts as a sink), reaeration can act to either increase or decrease DO concentration in the water depending on ambient conditions. In the case of a system with large diurnal fluctuations due to algal production and respiration like the LGMR, the reaeration process will act to compress the diurnal range as it seeks to drive the DO concentration towards the in-water saturation concentration and in equilibrium with the atmosphere. The degree to which the reaeration process will influence the diurnal range depends on the magnitude of the rate of reaeration relative to the rates of ongoing algal production and respiration processes.

The oxygen transfer coefficient (K_L, m/day) dictates the rate of oxygen exchange between the atmosphere and the water column. The first-order base reaeration rate ($k_{a,20}$) at the standard temperature of 20°C is calculated by dividing the transfer coefficient K_L by the water depth (d, m^{-1}), i.e., $k_{a,20} = (K_L / d)$. The production or consumption of DO via reaeration (ΔDO_{reaer}, $g\text{-}O^2/m^3$/day) is then calculated by:

$$\Delta DO_{reaer} = k_{a,20} * \left(\theta_{reaer}^{T-20}\right) * \left(C_{DO,sat} - C_{DO}\right) \quad (3\text{-}53)$$

where θ_{reaer} is the Arrhenius temperature constant, T is the water temperature (°C), and $C_{DO,sat}$ is the DO concentration at saturation ($g\text{-}O^2/m^3$). The DO saturation concentration varies and generally depends on the water temperature, salinity levels, and elevation. However, for a freshwater system like the LGMR, the relationship between saturation concentration and water temperature represented in A2EM can be simplified to:

$$C_{DO,sat} = 14.6244 - 0.36713 * T + 0.0044972 * T^2 \quad (3\text{-}54)$$

The DO saturation concentration is plotted as a function of water temperature in Figure 3-9 below.

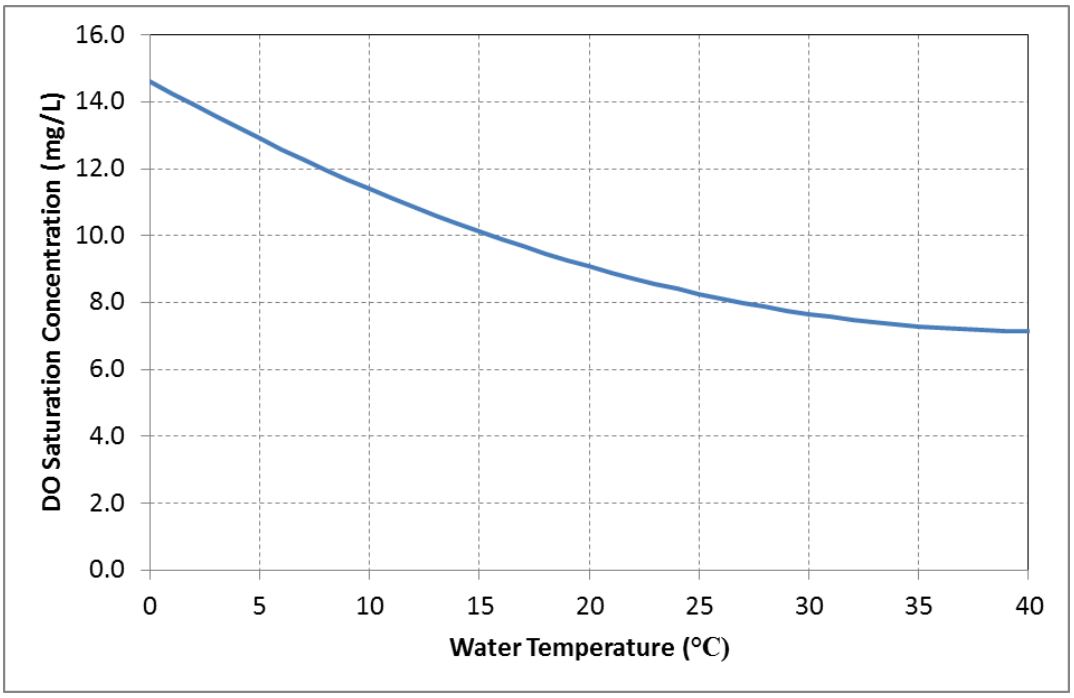

Figure 3-9. Dissolved Oxygen Saturation Concentration as a Function of Water Temperature

The value of K_L in a given system may depend on the hydraulic characteristics of a stream (i.e., depth and velocity), wind speed near the water surface, and/or the presence of waterfalls and dams. While a number of empirical approaches are available to estimate K_L (and also the first-order rate, $k_{a,20}$) under varying stream conditions, none of them provide exact predictions. For that reason, obtaining site-specific data on reaeration rates is a strongly preferred approach (Dr. Steven Chapra, personal communication). Because site-specific reaeration process data are not currently available for the LGMR, the Covar (1976) method was used to internally, dynamically calculate reaeration rates within the A2EM application. This method selects what it considers to be the most appropriate empirical method (selecting from the O'Connor-Dobbins, Churchill, and Owens-Gibbs methods) based on the water depth and velocity simulated by the model for a particular segment at a given time in the simulation. Additional A2EM spatial inputs are used to apply ceiling and/or floor values for the reaeration rates calculated via the Covar approach for segments where unrealistically low or high values of K_L or k_a are generated. Further discussion of the O'Connor-Dobbins, Churchill, and Owens-Gibbs empirical formulations and Covar approach for calculating reaeration rate is available in Chapra (1997) and in the QUAL2K user's manual (Chapra et al., 2012).

3.3.5.g Carbon, Nitrogen, and Phosphorus Cycling

A set of simplified schematics illustrating carbon, nitrogen, and phosphorus kinetics and cycling in the water column and sediment bed are provided in Figures 3-10 through 3-12. Dissolved inorganic silica and biogenic silica, which are not depicted here, are also simulated within A2EM, but they are only relevant for the growth of the winter diatom functional group. A more extensive discussion of carbon and nutrient dynamics is provided in the RCA Version 3.0 user's manual (HydroQual, 2004) and Verhamme et al. (2016).

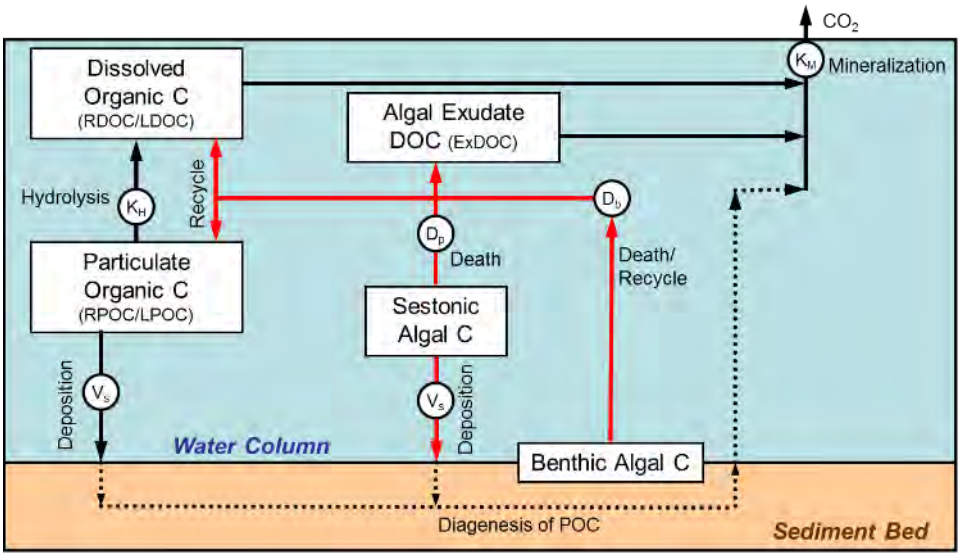

Figure 3-10. A2EM Carbon Kinetics & Cycling[3]

[3] In Figures 3-10 through 3-12, green lines represent uptake of nutrients (N, in this case) by algae; red lines represents loss of algal biomass (via death, settling/deposition). Solid green or red lines are used for sestonic algae, and dashed green or red lines are used for benthic algae. Solid black lines represent other kinetic processes that transfer N mass from one (abiotic) N species to another. Dashed black lines represent sediment bed processes involving (abiotic) N species, including transfer from the sediment bed to the water column via diffusion.

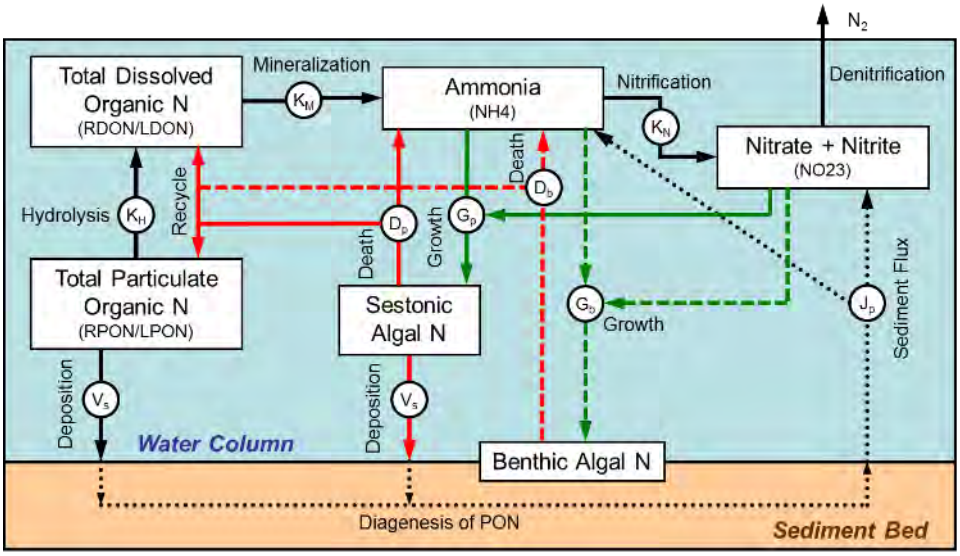

Figure 3-11. A2EM Nitrogen Kinetics & Cycling

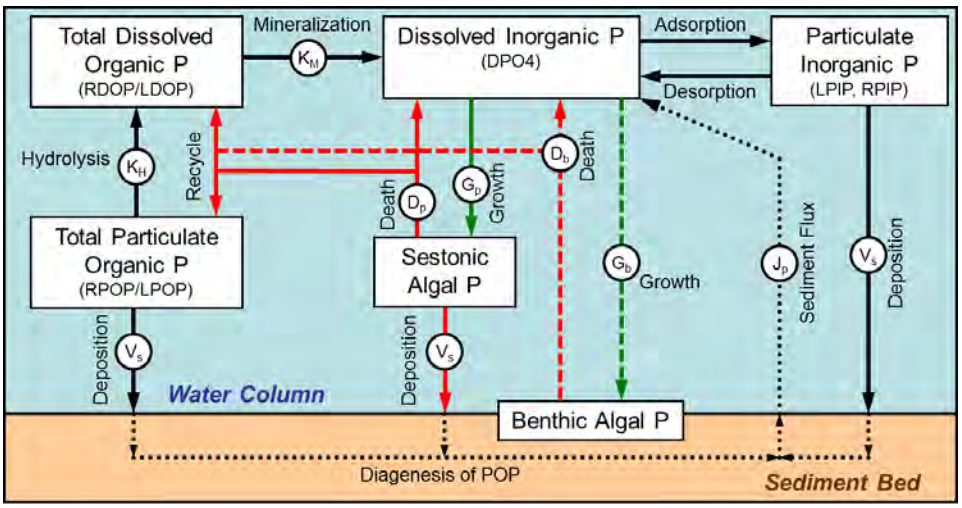

Figure 3-12. A2EM Phosphorus Kinetics & Cycling

3.3.6 Sediment Bed Initialization

As discussed above, the A2EM framework allows for selective application of the sediment diagenesis sub-model to model segments in the LGMR where consistent soft sediment accumulation is expected to occur. Delineation of a given area as possessing soft vs. hard sediment was based upon predicted shear stress at the sediment water interface. A median bottom shear stress threshold of 1.1 dynes/cm^2 as simulated by the EFDC model was used to define areas as having soft sediment. Five areas of the model domain were identified as having a median bottom shear stress of less than 1.1 dynes/cm^2, but an OEPA letter (OEPA 10/21/2016) indicated stream bed material sampling in two of those areas, the West Carrollton and Hutchings Station dam pools, revealed “a clear majority of gravel/cobble sized material.” Therefore, soft sediment was defined in just three areas of the model domain: the Great Miami River above the Island Metro Park dam, the Upper Great Miami River above the Troy low head dam, and the Mad River above Huffman Dam.

A "30-year simulation" was executed with the "coarse" version of the water quality model grid, with present-day loading conditions represented, to allow sediment concentrations (e.g. organic C, N, and P) to approach an equilibrium that could be used for sediment bed initial conditions. This was accomplished by repeating calendar year 2013 flow and loading conditions to the model domain but using the ending conditions from one year as the starting conditions for the next. Sediment concentrations for the first year were set using values from the Lake Pepin (MN) model (LimnoTech, 2009).

3.4 Water Quality Model Expert Review

As discussed in Section 1, an important objective of the project was to ensure that the model developed to represent water quality in the LGMR system was scientifically sound. Consistent with this objective, a key component of the overall water quality model development and calibration process for the LGMR system was thorough internal and external peer review of key decisions and outcomes with the A2EM model.

Internal peer review within LimnoTech was conducted by Dr. David Dilks, who has more than 30 years of experience working leading water quality and eutrophication model development across a large number of riverine, estuarine, and lake systems within the U. S. External peer review of the modeling process was conducted by Dr. Steven Chapra and Dr. Joseph DePinto. Drs. Chapra and DePinto each has more than 35 years of experience in the field of water quality modeling, as well as national and international recognition for their expertise. Brief biosketches for these experts are provided in Appendix H.

External peer review of the LGMR water quality model was facilitated by frequent email exchanges and conference calls, as well as in-person meetings with Dr. Chapra and Dr. DePinto. In early June, Dr. Chapra accompanied LimnoTech staff and representatives from MCD and the WRRFs on a full-day field visit to key LGMR locations. This field visit served to provide a good foundational understanding of the physical layout of the system for Dr. Chapra and other participants prior to water quality model development.

During the early stages of water quality model development (July-August 2016), LimnoTech kept the external experts informed and received feedback via email-based summaries of key decisions related to model inputs and process representation. Conference calls and web-based meetings were held periodically to present key input information and outcomes from model simulations. In addition to the field visit, Dr. Chapra visited LimnoTech headquarters in Ann Arbor, MI three separate times to participate in model development and calibration review sessions and provide feedback to the process. Dr. Chapra and Dr. DePinto also participated in multiple conference calls involving representatives from LimnoTech, MCD, and the WRRFs (and, on two occassions, from OEPA) to discuss the approach taken with the LGMR water quality model and to assist in answering client and agency questions.

The internal and external peer review components of the project provided considerable value to the model development/calibration process and resulted in a LGMR water quality modeling tool that is endorsed by Drs. Chapra, DePinto, and Dilks as being scientifically sound and state-of-the-science with respect to its representation of eutrophication processes, including sestonic and benthic algae dynamics and their impact on dissolved oxygen.

Blank

4 Model Calibration

This section provides an overview of the calibration approaches along with presentation and discussion of calibration results for the LGMR hydrodynamic and water quality models.

4.1 Hydrodynamic Model Calibration

4.1.1 Calibration Approach

Model calibration is described in USEPA guidance (USEPA, 1994) as the "process of adjusting model parameters within physically defensible ranges until the resulting predictions give the best possible fit to the observed data." Within the context of this model application, calibrating the model to accurately represent stream depths is important in connection with light attenuation and algal growth. Accurately representing stream velocities is important in connection with water travel times, locations of soft sediment accumulation, reaeration, and sloughing of benthic algae.

Two data sources were relied on for the hydrodynamic model calibration: 1) discharge measurement data, and 2) a dye study of the lower Great Miami River (USGS, 1966). Stream discharge data collected at seven locations along the Great Miami River were used for model calibration. For each measurement of discharge, water surface elevation and mean channel velocity have also been measured and reported. The relationships between stream discharge and water surface elevation, and between stream discharge and velocity characterize the hydraulics of a location along the stream over a wide range of flow conditions.

The dye study is a useful complement to the discharge measurement data for model calibration. While the discharge data quantify stream hydraulics at individual locations along the stream over a wide range of flow conditions, the dye study data quantify stream hydraulics over long reaches of the river for specific flow conditions of interest. Dye was injected to the river and tracked downstream on two occasions: once during a low flow condition of 380 cfs (5^{th} percentile, USGS Station #03271500 Great Miami River at Miamisburg), and for a second time during a moderately low flow conditions of 550 cfs (18^{th} percentile). The dye plume was monitored as it was transported downstream, and cumulative times of travel to successive downstream stations were reported.

4.1.2 Calibration Results

Model simulations were conducted to compare and calibrate model results to both the USGS data and the dye study data. To compare model results with the USGS data, a six-year simulation of calendar years 2010 through 2015 was run. Then the model-simulated relationship between discharge and water surface elevation and between discharge and stream velocity were compared with data at the seven calibration locations. These comparisons are shown in Figures 4-1 through 4-3. To calibrate the model, sediment bed roughness was varied within a range consistent with the substrate and form of the river channel.

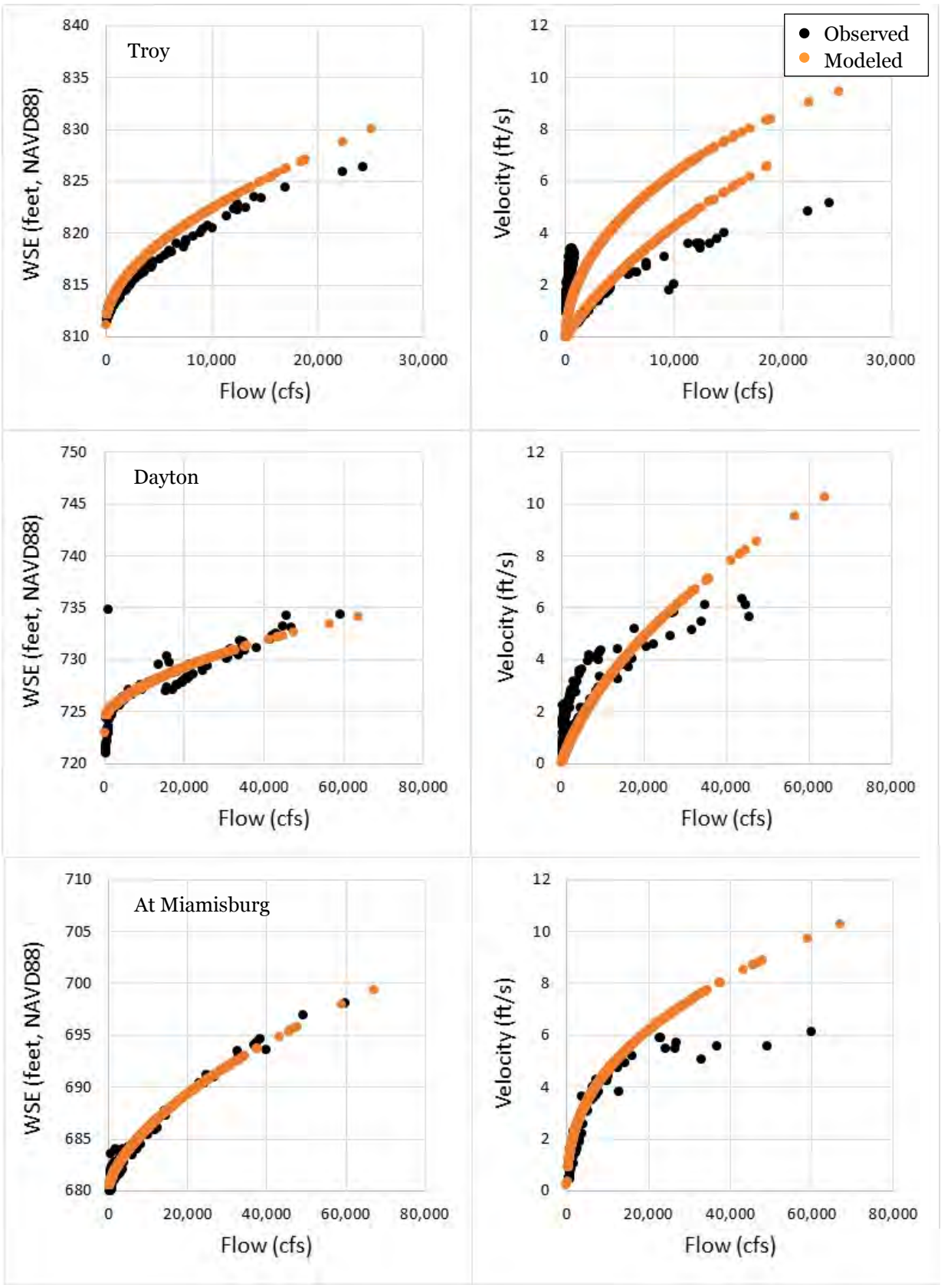

Figure 4-1. Model-Data Comparisons of Flow, Water Surface Elevation (WSE), and Velocity (1 of 3)

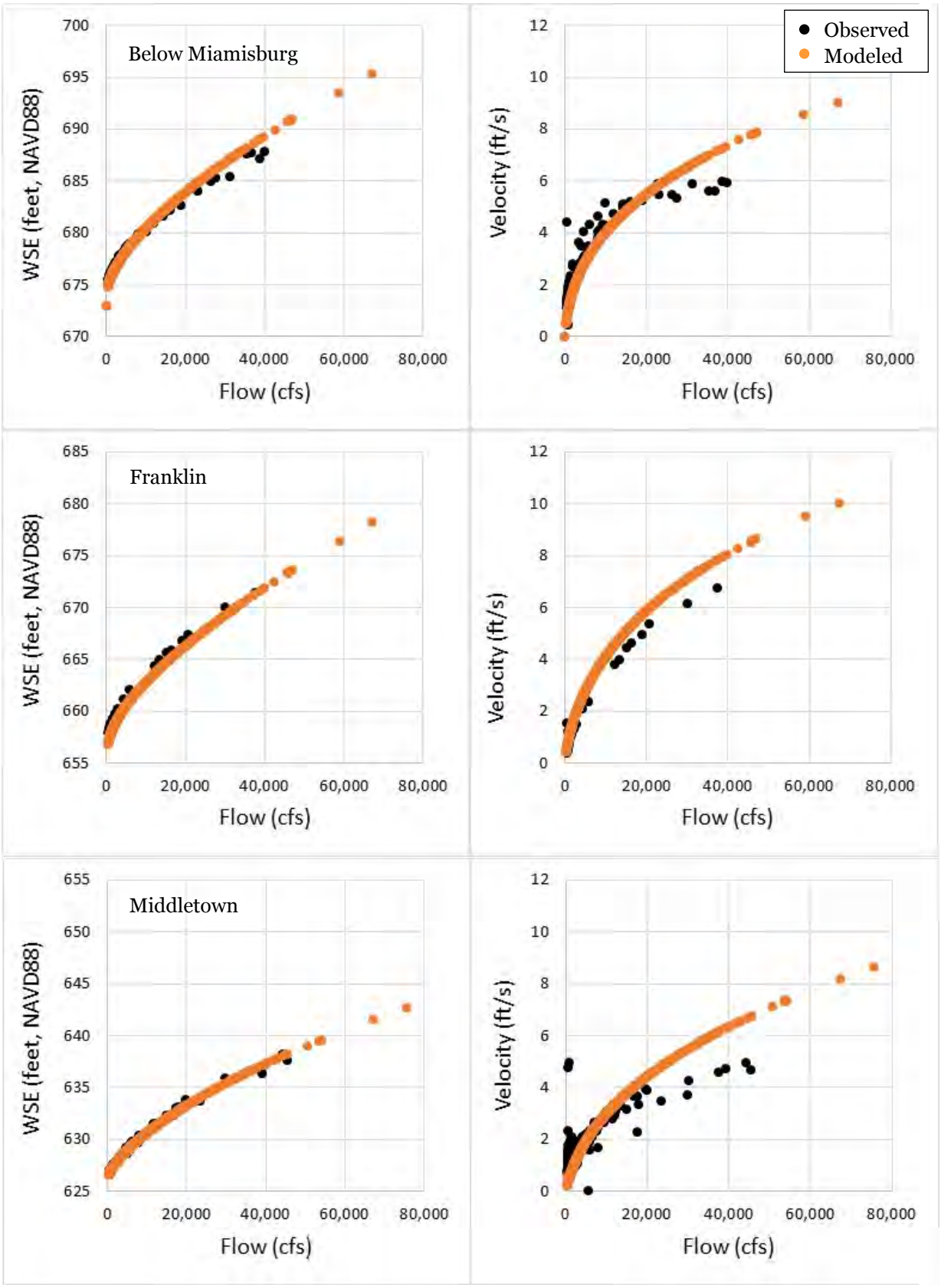

Figure 4-2. Model-Data Comparisons of Flow, Water Surface Elevation (WSE), and Velocity (2 of 3)

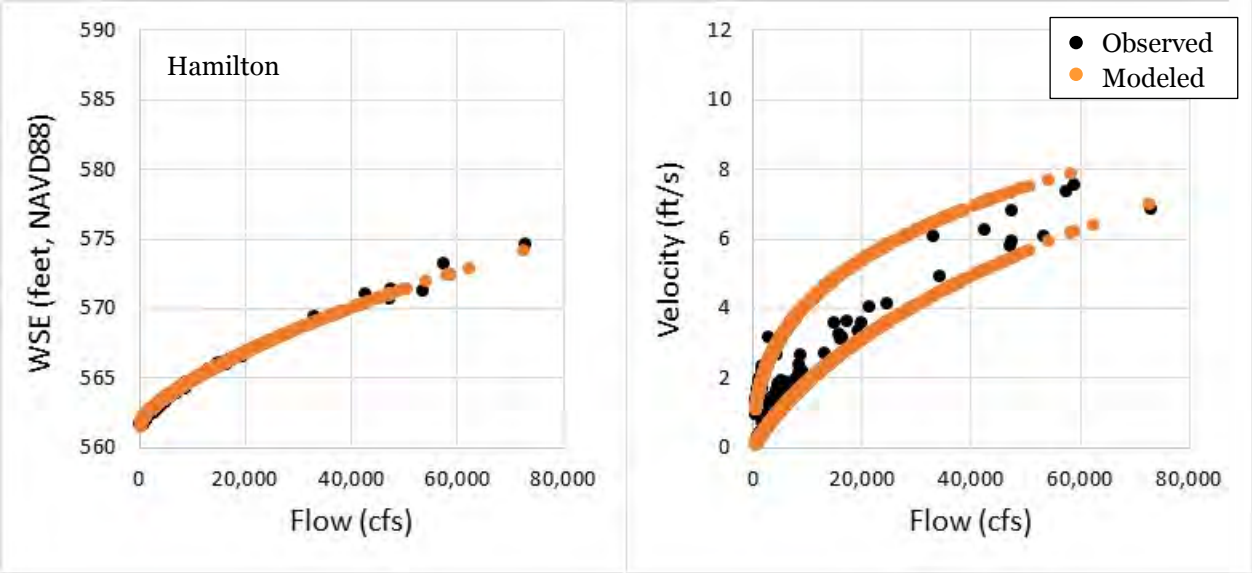

Figure 4-3. Model-Data Comparisons of Flow, Water Surface Elevation (WSE), and Velocity (3 of 3)

A calibrated bed roughness height of 10 mm was applied to all model cells, which is roughly equivalent to a Manning's "N" value of 0.034. This roughness height is consistent with roughness parameters used in flood modeling (0.021 to 0.06) conducted for the FEMA (Federal Emergency Management Agency) Flood Insurance Study for the Great Miami River (FEMA, 2005).

The hydrodynamic model results are highly consistent with the flow, water surface elevation, and velocity data over a wide range of flow conditions. Generally, modeled water surface elevations are within one half foot of the observed data, and modeled velocities are within one quarter foot per second of the observed data. Two types of deviations between model and data occur. First, at gage locations with significant floodplain areas, modeled velocities tend to be biased somewhat high under the highest observed flow conditions. This is likely because the model represents only stream channel areas and not floodplain areas, so the smaller modeled cross-section leads to higher velocities. Second, at some gage locations near low head dams, flow measurements are conducted at multiple locations depending on the intensity of flow. An example of this is the Hamilton gage where flows are measured either upstream or downstream of the nearby dam, resulting in a greater variance in the observed data. In these cases, modeled velocities both upstream and downstream of the dam are plotted to illustrate that simulated velocities span the range of the observations. Locations upstream of dams tend to experience lower velocities, while locations downstream experience higher velocities.

To compare model results with the dye study data, idealized simulations were conducted to approximate the flow conditions that occurred during the dye studies. However, the model was not adjusted to represent dam conditions and bathymetric conditions that existed at the time of the dye study. The model dam conditions and bathymetric conditions are representative of the last few decades, while the dye study was conducted six decades ago when stream bathymetry, low head dams, and conveyance through canals likely differed. Still, the dye study was considered to be a useful dataset for assessing consistency between modeled travel times and observed travel times. Known differences between stream conditions in the 1960s and present day conditions represented in the model were considered when interpreting model results. Figure 4-4 compares modeled and observed travel times for the two dye injections.

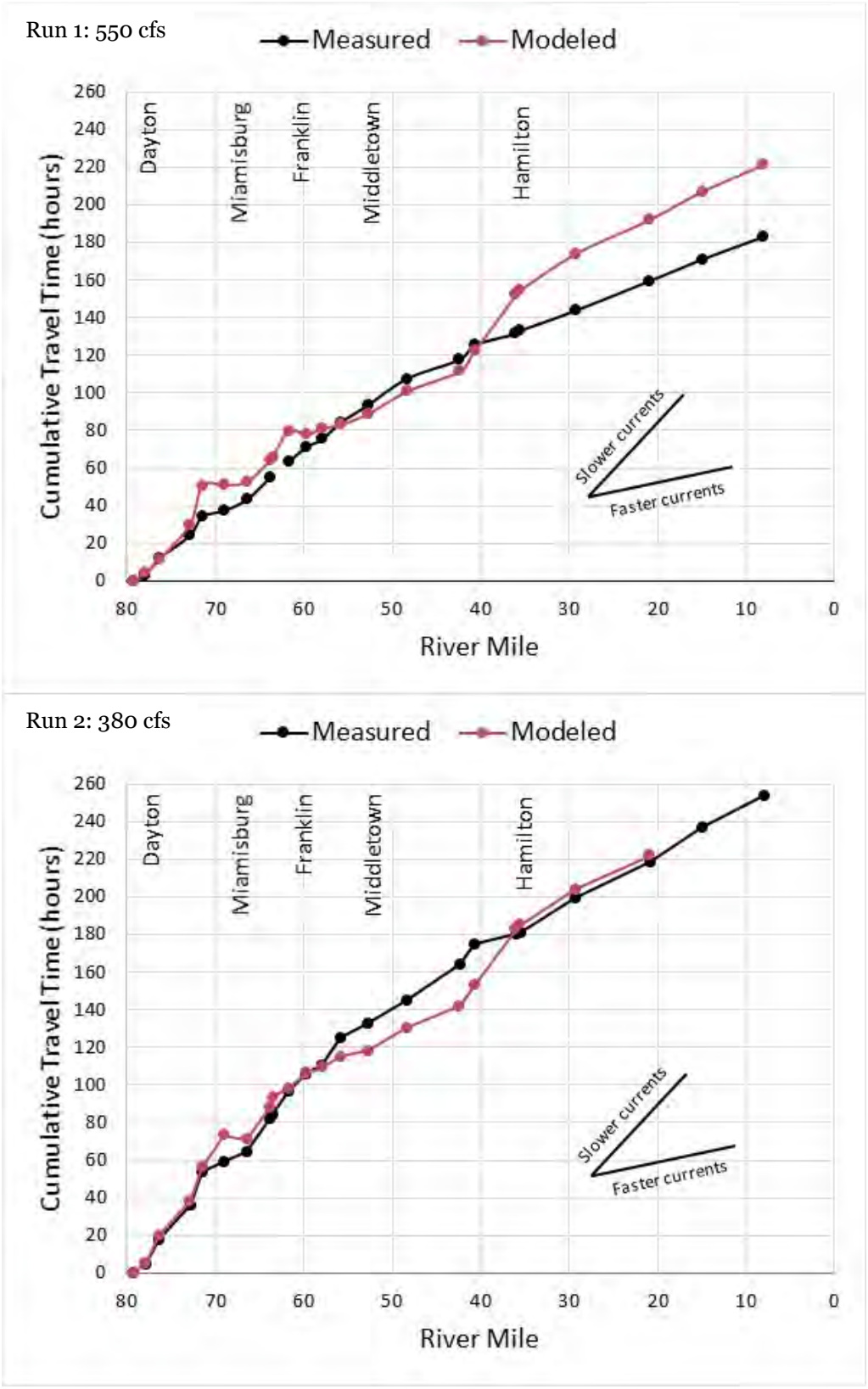

Figure 4-4. Model-Data Comparisons of Dye Travel Time

For much of the seventy-mile dye study reach, modeled and observed travel times are highly consistent with each other. For instance, the observed and modeled travel times agree within 10% of each other from river miles 80 to 40. Where deviations between modeled and observed travel times occur, there are known differences between contemporary conditions (which are represented in the model) and historical conditions when the dye surveys were conducted. For instance, the Hamilton Recreation Dam, which was constructed in 1989, is represented in the model but did not exist during the dye study. Consequently, modeled travel times are slower than observed travel times through this reach (near river mile 40).

Through reviewing and calibrating model performance against both the USGS flow measurement data and the dye study data, the model was found to produce flows, water levels, velocities, and times of travel consistent with observed data over a wide range of flow conditions.

4.1.3 Hydrodynamic Model Limitations

For the intended application of the hydrodynamic model, i.e. to support a water quality model evaluation of the impacts of nutrient sources on dissolved oxygen levels along the stream, there are no significant hydrodynamic model limitations. However, the one-dimensional nature of the model does limit it from representing bank to bank variability in stream velocities, which can influence near-bank benthic algal densities and near-bank dissolved oxygen levels. As described in Section 3.3.5.c related to "subzone" light calculations for the benthic algae sub-model, this bank to bank variability was approximated in the water quality model. A method of more explicitly representing this variability would be to model the stream in two dimensions with several grid cells spanning each cross-section. This approach would lead to higher mid-channel velocities and depths and lower near-bank velocities and depths due to greater impacts of bottom roughness on hydraulic behavior.

Another model limitation is the limited availability of recent bathymetric data. Of the 130 miles of modeled stream length, recent bathymetric data were only available for 29 miles. Survey data from the 1970s cover much of the remaining stream length and were used in addition to the more recent bathymetric data. These 1970s-era data were considered to be sufficiently representative of current stream conditions because the 1970s-era and more recent bathymetric data are similar in elevation at locations where the two datasets adjoin each other. However, use of the 1970s-era bathymetry introduces some uncertainty into the model and so is considered a model limitation.

4.2 Water Quality Model Calibration

This section provides a description of the calibration approach followed for the LGMR water quality model and presents and discusses the results of the calibration effort.

4.2.1 Calibration Approach

The general strategy for the LGMR water quality model calibration employed a weight-of-evidence approach that consisted of multiple model comparisons, both graphical and statistical, to assess model performance. Graphical comparisons includes time series (i.e., for individual model segment paired with monitoring location(s)), downriver profiles (i.e., for a specific point in time), and cumulative frequency distribution (CFD) plots. Statistical comparisons include percent bias (PBIAS) and absolute error metrics, which are both commonly used for evaluating the goodness of fit for water quality models to observed data (Donigian, 2002). While statistical performance targets for model acceptance have been established for prediction of hydrology, sediment, and nutrient variables by watershed and riverine water quality models (Donigian, 2002; Moriasi et al., 2007), the same is not true for models predicting biological (e.g. chlorophyll *a*) or biological-related (e.g. dissolved oxygen) variables. Moriasi et al., (2007) recommended the following performance ratings for simulated nitrogen and phosphorus: PBIAS $<\pm25$ as very good, $\pm25\leq$ PBIAS $<\pm40$ as good, $\pm40\leq$ PBIAS $<\pm70$ as satisfactory, and PBIAS $\geq\pm70$ as unsatisfactory.

The water quality model calibration period was selected to include calendar years 2011-12, based on the availability of key datasets for the LGMR system and varying environmental conditions observed during this period. The model calibration was corroborated by running the model without changing any model coefficients for calendar year 2013 and comparing against key datasets available for this year. The entire 2011-13 period represented a wide range of environmental forcing conditions including high and low flows and nutrient loads. In general, annual flow and nutrient loads were relatively high in 2011, low in 2012, and moderate in 2013. As discussed in Section 3, relevant water quality monitoring data to support model calibration are available at a variety of locations throughout the LGMR. As part of the calibration design, it was necessary to identify both *primary* and *secondary* monitoring stations where comparative model-data evaluations would be made. The Miamisburg and Fairfield stations were selected as the primary calibration locations because continuous, hourly measurements of dissolved oxygen, chlorophyll *a*, and nutrient concentrations were available at these locations for most of the 2011-13 period. Secondary stations included other locations within the LGMR where data on one or more of the calibration endpoints are at least sporadically available during the calibration and corroboration periods (2011-13). These secondary locations include:

- WRRF monitoring locations located upstream and downstream of facility discharge locations; and
- OEPA stations where short-term monitoring of nutrients, dissolved oxygen and sestonic chlorophyll *a* were conducted.

Both graphical and statistical evaluations were developed for the primary calibration stations; however, due to limited data coverage, only graphical model-data comparisons were evaluated for the secondary stations.

In addition to primary and secondary calibration locations/datasets, the calibration effort considered findings from a field investigation that LimnoTech conducted in the vicinity of the Miamisburg continuous monitoring station on September 16, 2016. As presented and discussed in Appendix F, discrete measurements of water depth, temperature and dissolved oxygen concentrations across two transects were made, and the observations suggested that lateral variability of dissolved oxygen and other constituents may be significant, especially under low-flow conditions in the river. Although this field investigation was limited to observations for two transects during a single day, it highlights that there is the potential for significant lateral variability in dissolved oxygen, which must be taken into consideration when evaluating model-data comparisons. This is of particular importance for measurements based on samples collected relatively close to the edges of the river, which appears to be the case for both the Miamisburg and Fairfield continuous monitoring locations.

As the calibration effort proceeded, the most sensitive coefficients, as determined by many sensitivity analysis model runs for a single year, were adjusted within an acceptable range until the endpoints (state variables) best compared with the magnitude and temporal (e.g., seasonal) and spatial trends exhibited by the observed data. Model-data comparative evaluations were made for the two primary calibration stations for each iteration, and comparisons for secondary stations were also made periodically to ensure that calibration adjustments did not result in model-data inconsistencies at those locations. Each model calibration endpoint was treated sequentially in the same manner, always checking back to previously calibrated endpoints in case there was a need for iterative re-adjustment of the coefficients for those systems.

The initial model parameterization was based on existing models of Lake Pepin (LimnoTech, 2009), Western Lake Erie (Verhamme et al., 2016), and Yellowstone River (Flynn et al., 2013). Specific parameter adjustments made to improve the water quality calibration included sestonic and benthic algal maximum growth rates and saturating algal light intensities; benthic algal respiration, death, and

excretion rates; light extinction coefficients; and nitrification and denitrification rates. Changes were made to various other parameters throughout the calibration process (e.g., optimal growth temperature of blue-greens and other algae, carbon oxidation and hydrolysis rates, sestonic algal recycle fractions, dissolved oxygen diffusivity and half-saturation constants, and temperature correction coefficients), but if model output was deemed relatively insensitive to modifications, or if the change adversely affected the calibration, then the initial value was retained. A subset of final calibrated model coefficients is listed in Table 4-1, and a complete list of all model coefficients is presented in Appendix E, Table E-1.

Table 4-1. Key calibration coefficients used for the LGMR water quality model.

Symbol	Description	Initial value(s)	Calibrated value(s)	Recommended Range (or Value)	Units	Reference(s)
General Water Quality Parameters						
K_{89C}	Mineralization rate of LDOP	0.10	0.10	0.1	/day	QEA, 2009
K_{1415C}	Nitrification rate at 20°C	0.075	0.30	0.1 – 1.0	/day	Brown and Barnwell, 1987
K_{150C}	Denitrification rate at 20°C	0.10	0.05	0.03	/day	QEA, 2009
K_{1921C}	Hydrolysis rate of LPOC	0.10	0.10	0.08	/day	QEA, 2009
K_{210C}	Oxidation rate of LDOC	0.10	0.10	0.10	/day	QEA, 2009
Sestonic Algae						
K_C	Saturated growth rate	2.0-2.3	2.2-2.6	1.5-2.5	/day	Thomann & Mueller 1987
I_S	Saturating algal light intensity	150-200	50	100-400	ly/day	Chapra 1997
K_{mN}	Half saturation constant for N	0.005-0.020	0.010-0.020	0.010-0.020	mg-N/L	Chapra 1997
K_{mP}	Half saturation constant for P	0.005	0.005	0.001-0.005	mg-P/L	Chapra 1997
Benthic Algae						
GRMAXBA	Zero-order maximum growth rate	250	400-1000	15-500	mg-Chla/m^2/day	Flynn et al. 2013
KMPBA	External P half-saturation constant	0.125	0.125	0.005-0.175	mgP/L	Flynn et al. 2013
KQPBA	Intercellular P half-saturation constant	0.00325	0.00325	0.000625-0.0125	mgP/mgC	Flynn et al. 2013
RMAXBA	Maximum respiration rate	0.2	0.4	0.02-0.8	/day	Flynn et al. 2013
EXCBA	Excretion rate	0	0.2	0-0.8	/day	Flynn et al. 2013
DTHBA	Death rate	0.3	0.2	0-0.5	/day	Flynn et al. 2013
KMLBA	Light half-saturation constant	100	50	30-90	ly/day	Flynn et al. 2013

In addition to the various model parameter changes completed during the calibration process, several enhancements were made to the A2EM code to allow greater input flexibility and/or to overcome model stability issues associated with rapid growth of benthic algae and production of dissolved oxygen. In addition to the enhancement of the benthic algal sub-model described in Section 3.3.5, A2EM code enhancements included:

- Allowing segment-specific application ceiling and/or floor constraints on the reaeration rate internally calculated by the Covar method;
- Modifying the deposition processes for inorganic and organic suspended solids to include dependence on simulated segment-specific bottom shear stress; and
- Allowing for parameterization of phosphorus and nitrogen recycling from benthic algae death.

4.2.2 Calibration Results

This sub-section provides presentation and discussion of calibration results from the LGMR water quality model for key calibration endpoints, including:

- Phosphorus (TP and DPO4);
- Nitrogen (TN and NO2+NO3, TKN, and NH3 species);
- Sestonic and benthic algae biomass (as chlorophyll *a* concentration); and
- Dissolved oxygen (daily average concentration and diurnal range).

For brevity, model-data comparison time series plots, CFD plots, and statistics are presented for the combined 2011-13 calibration/corroboration period.

4.2.2.a Phosphorus

Calibration results for total phosphorus and dissolved inorganic phosphorus (DPO4) are presented graphically in Figures 4-5 through 4-12 and statistically in Table 4-2 for the primary calibration stations at Miamisburg and Fairfield. Overall, the model predicts TP and DPO4 concentrations consistent with observations at Miamisburg and Fairfield, although concentrations are slightly over-predicted at Fairfield. In general, the model tends to somewhat over-predict TP and under-predict DPO4 concentrations at Miamisburg during the lowest flow months. At Fairfield, the model somewhat over-predicts both TP and DPO4 concentrations during the lowest flow periods. The cumulative frequency distribution (CFD) plots for these locations suggest strong agreement between simulated and observed TP concentrations across the range of observed concentrations. The agreement between simulated and observed DPO4 concentrations is also good, although some under-prediction of high observed DPO4 concentrations and over-prediction of low observed DPO4 concentrations is evident.

The statistical measures chosen to evaluate model performance, PBIAS and average absolute error, indicate acceptable model performance in predicting both TP and DPO4 concentrations at Miamisburg and Fairfield for the combined 2011-13 calibration/corroboration period. The relatively low bias and average absolute error in model predictions at both monthly and daily time scales suggest the model simulates TP and DPO4 with a reasonably level of accuracy. As expected, the average absolute error computed on a sub-daily time interval is greater than the error for the monthly time interval, reflecting greater difficulty with predicting the day-to-day variations in observed riverine concentrations, especially given that point source load inputs were specified on a monthly basis.

Additional time series comparisons of simulated and observed TP and DPO4 concentrations for three secondary calibration locations, the Great Miami River at Middletown, downstream of the LeSourdsville WRF and upstream of the Hamilton WWTP, are shown in Appendix E (Figures E-1 through E-5). Though sampling data were collected relatively infrequently, visual comparisons suggest the model predicts TP and DPO4 concentrations consistent with observations at these locations. Although the above-mentioned observation of the model over-predicting TP concentrations at Miamisburg during the lowest flow months is also evident at the Middletown station, particularly during late July 2011 OEPA sampling, model predictions during August 2011, also a low flow month, are very consistent with OEPA sampling data. Statistical performance measures were not computed for these secondary calibration stations due to an insufficient number of observations and/or lack of information on the exact date monthly grab samples were taken (i.e., for the WRRF upstream/downstream monitoring stations).

Overall, the TP and DPO4 concentrations simulated by the calibrated water quality model reproduce the annual and seasonal trends and other features of the phosphorus monitoring data available for Miamisburg and Fairfield (primary calibration stations), as well as for secondary calibration stations (e.g.,

WWRF upstream/downstream monitoring datasets). Although there are potential areas for improvement (e.g., improved model fit to observed DPO4 concentrations at lower flows), constraints associated with current input and calibration datasets limit the value of further calibrating the model at this time. Factors that contribute uncertainty to the simulation of phosphorus include the relatively coarse specification of point source loads to the LGMR (i.e., at a monthly scale) and uncertainties regarding the representativeness of samples associated with the Miamisburg and Fairfield automated monitoring stations (see discussion in Section 4.2.1 and Appendix F).

Table 4-2. Summary statistics for phosphorus for the combined calibration and corroboration periods (2011-2013)

Time Interval	Statistic	TP		DPO4	
		GMR at Miamisburg	GMR at Fairfield	GMR at Miamisburg	GMR at Fairfield
Monthly	Count	36	36	36	36
	PBIAS (%)	-1.10	-7.98	4.14	-1.42
	Absolute Error	0.05	0.06	0.04	0.03
Sub-Daily	Count	1497	531	1513	521
	PBIAS (%)	-0.97	-5.99	1.08	-1.70
	Absolute Error	0.08	0.11	0.06	0.06

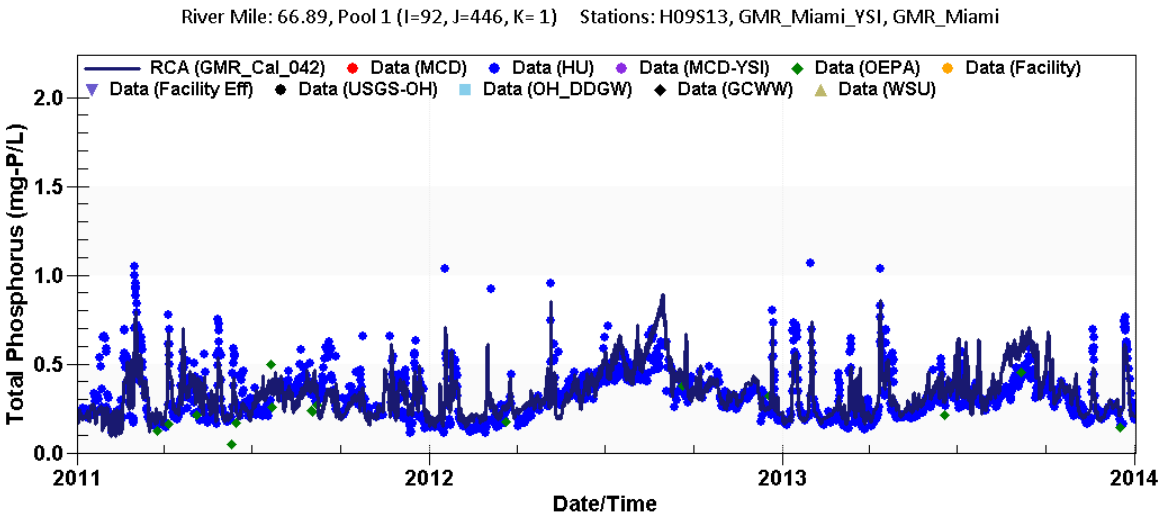

Figure 4-5. Time series comparison of simulated and observed TP concentrations for the Great Miami River at Miamisburg, 2011-2013.

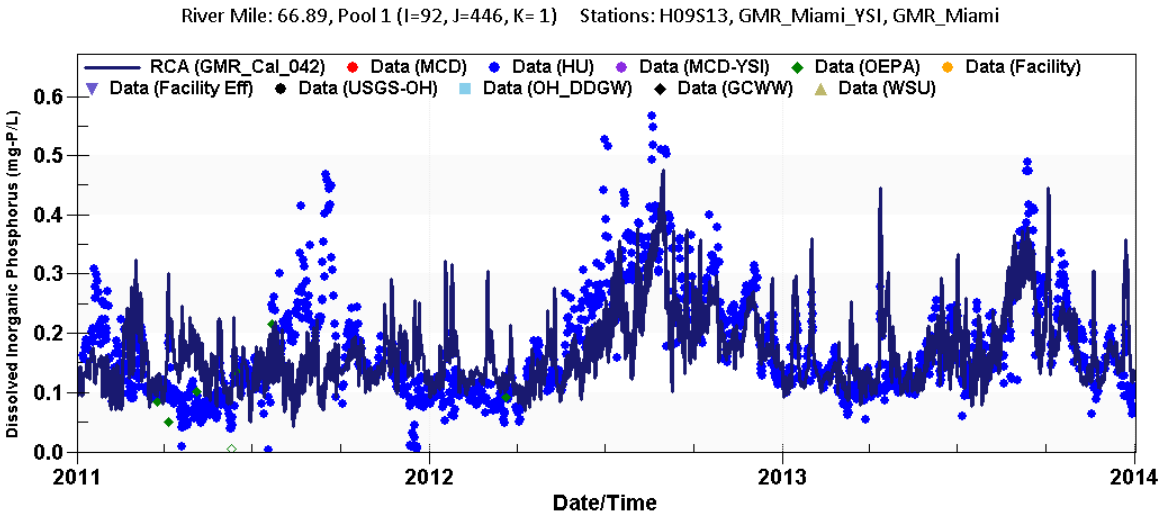

Figure 4-6. Time series comparison of simulated and observed DPO4 concentrations for the Great Miami River at Miamisburg, 2011-2013.

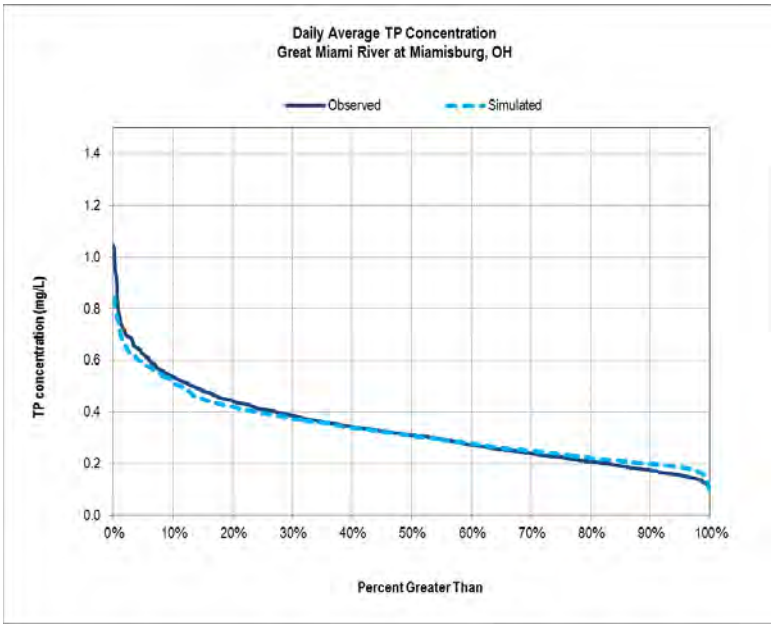

Figure 4-7. Observed and simulated TP concentration cumulative frequency distributions for the Great Miami River at Miamisburg, 2011-2013.

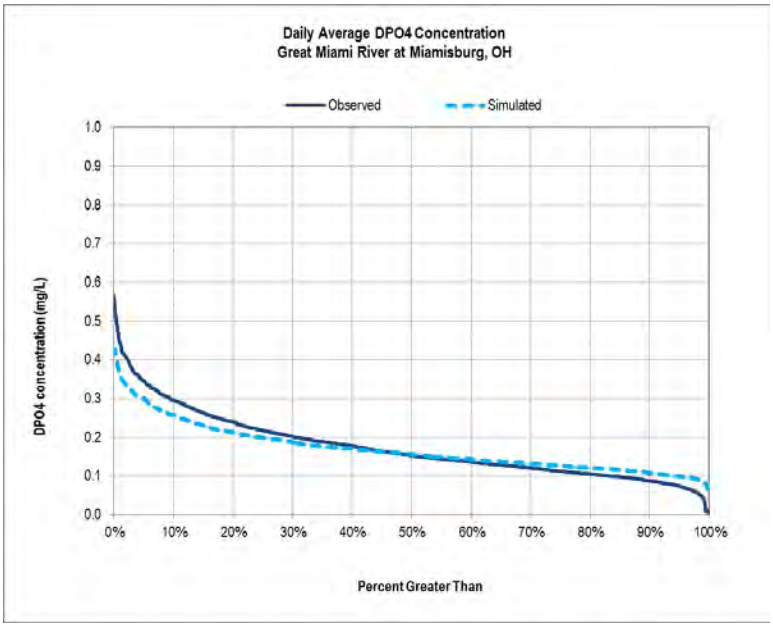

Figure 4-8. Observed and simulated DPO4 concentration cumulative frequency distributions for the Great Miami River at Miamisburg, 2011-2013.

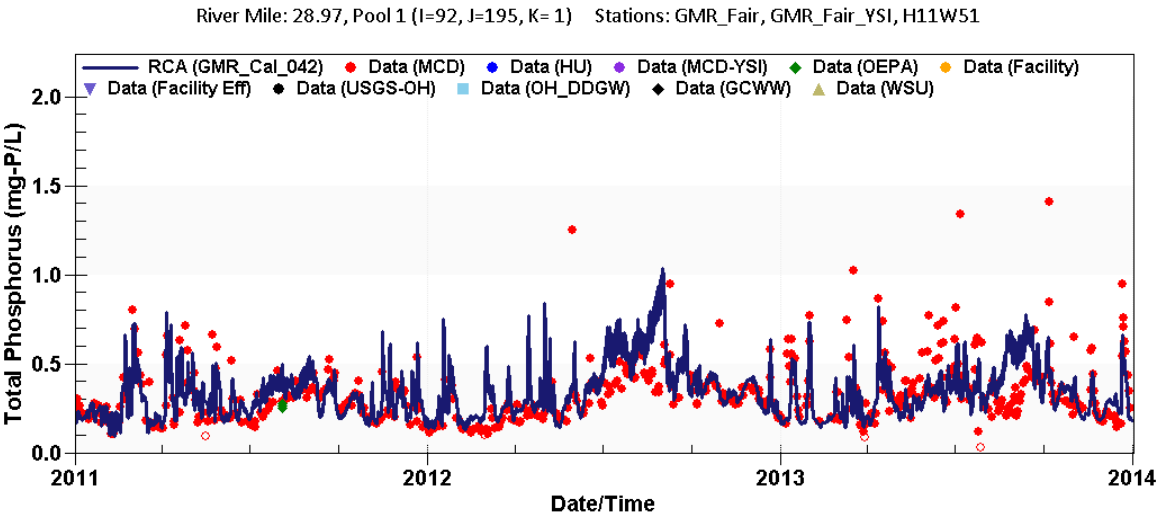

Figure 4-9. Time series comparison of simulated and observed TP concentrations for the Great Miami River at Fairfield, 2011-2013.

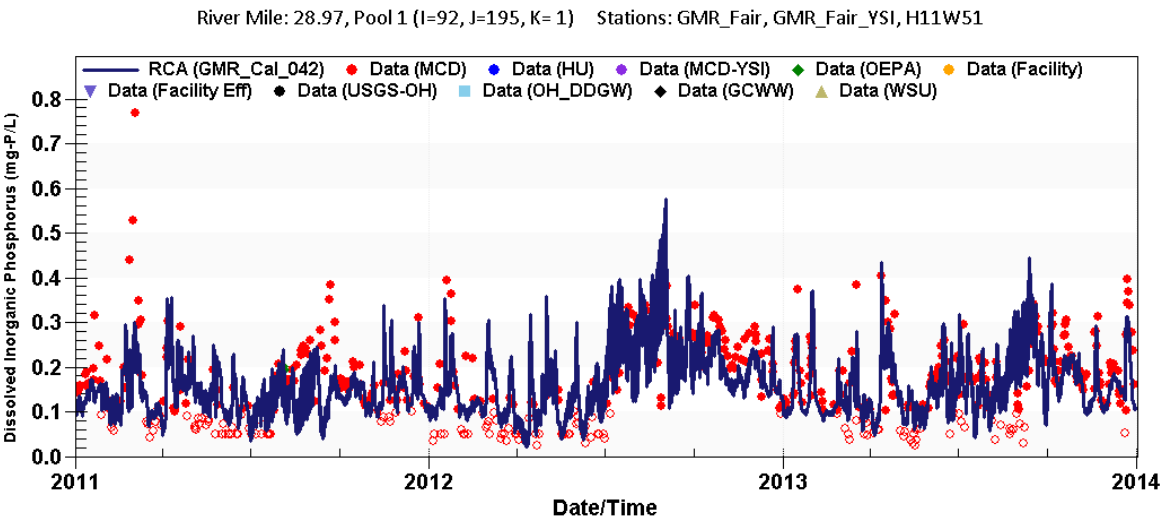

Figure 4-10. Time series comparison of simulated and observed DPO4 concentrations for the Great Miami River at Fairfield, 2011-2013.

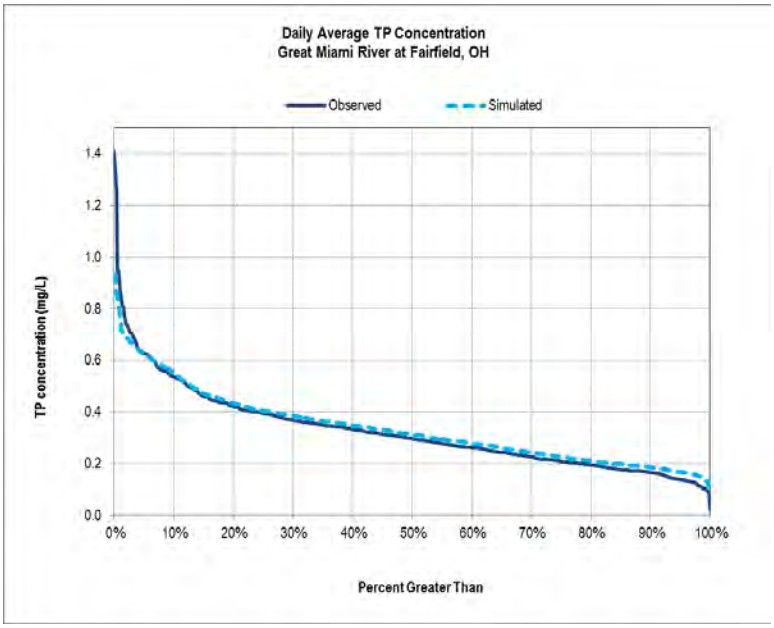

Figure 4-11. Observed and simulated TP concentration cumulative frequency distributions for the Great Miami River at Fairfield, 2011-2013.

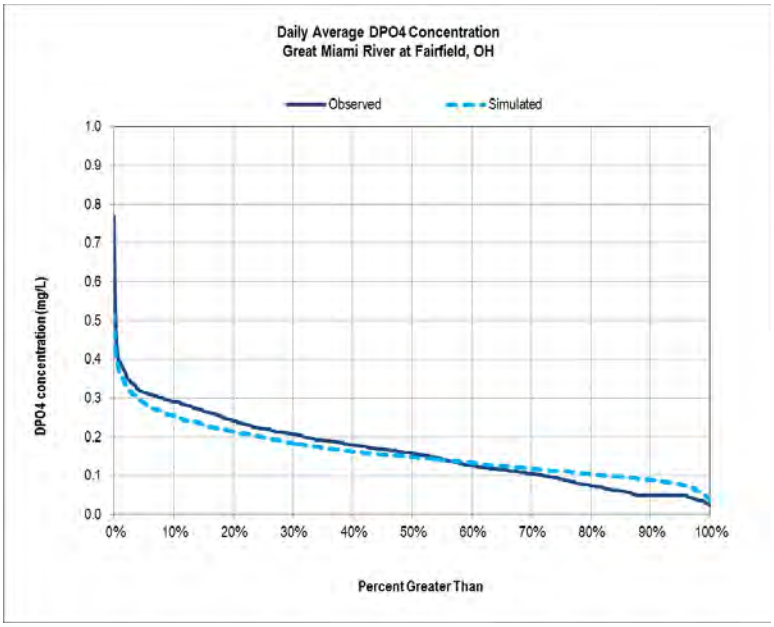

Figure 4-12. Observed and simulated DPO4 concentration cumulative frequency distributions for the Great Miami River at Fairfield, 2011-2013.

4.2.2.b Nitrogen

Model-data comparison time series plots for TN and NO2+NO3 at Miamisburg and Fairfield are presented in Figures 4-13 through 4-20, and statistical results for TN, NO2+NO3, TKN, and NH3 are provided in Table 4-3. In addition, model-data time series comparison plots for TKN and NH3 are provided in Figures E-6 through E-8 in Appendix E. Overall, the model simulates the concentrations and temporal trends of TN and the individual N species consistent with the observations at the primary calibration stations, Miamisburg and Fairfield. The model-simulated TN and NO2+NO3 concentrations tend to be slightly higher than the observed data at both locations based on the PBIAS results (Table 4-3). Model predictions of TKN concentrations tend to be higher than observations at Miamisburg and lower than observations at Fairfield based on the PBIAS results, especially during periods of relatively higher TKN concentrations (Figures E-6 and E-7). Because Heidelberg University does not report NH3 measurements for the Miamisburg location, comparisons of NH3 were only made for the Fairfield location (Table 4-3, Figure E-8). The model-predicted NH3 concentrations are similar to observed NH3 concentrations, but a large number of NH3 observations (>50%) were reported below the detection limit.

The statistical measures chosen to evaluate model performance, PBIAS and average absolute error, indicate acceptable model performance in predicting TN, NO2+NO3, TKN, and NH3 concentrations at Miamisburg and Fairfield for the combined 2011-13 calibration/corroboration period. Negative PBIAS values indicate an over-prediction of the simulated concentrations, and positive PBIAS values indicate an under-prediction of simulated concentrations relative to observed concentrations. These statistics confirm the observations described above based on the time series plots; specifically, that the model-predicted TN and NO2+NO3 concentrations tend to be higher than the observed data at both Miamisburg and Fairfield, and model predictions of TKN concentrations are high at Miamisburg and low at Fairfield relative to observations. As expected, the average absolute error computed on a sub-daily time interval is greater than the error for the monthly time interval, reflecting greater difficulty with predicting the day-to-day variations in observed riverine concentrations, especially given that point source load inputs were specified on a monthly basis.

Additional time series comparisons of simulated and observed TKN and NO2+NO3 concentrations for three secondary calibration locations, the Great Miami River at Middletown, downstream of the LeSourdsville WRF and upstream of the Hamilton WWTP, are included in Appendix E (Figures E-9 through E-14). Although sampling data were collected relatively infrequently, visual comparisons suggest that the model predicts TKN and NO2+NO3 concentrations consistent with observations at these locations. Although the above-mentioned observation of model predicted NO2+NO3 concentrations being slightly higher than observed data is also evident when comparing simulated values against OEPA sampling data for these three secondary calibration locations, the over-prediction trend is not as evident when comparing against the WWRF upstream/downstream monitoring data. Statistical performance measures were not computed for these secondary calibration stations due to an insufficient number of observations and/or lack of information on the exact date that monthly grab samples were taken (i.e., for the WRRF upstream/downstream monitoring stations).

Overall, the TN and N species concentrations simulated by the LGMR water quality model reproduce the annual and seasonal trends and other key features of the nitrogen monitoring data available for Miamisburg and Fairfield, as well as for the secondary calibration stations. As for the phosphorus calibration, there are potential areas for improvement; for example, adjustments could potentially be made to model coefficients to decrease the TN and NO2+NO3 concentrations and reduce or eliminate the over-prediction bias at Miamisburg and Fairfield. However, constraints associated with the current input and calibration datasets limit the value of further calibrating the model at this time. Factors that contribute uncertainty to the simulation of nitrogen are the same as those for phosphorus and include: 1) specification of point source loadings at a coarse (i.e., monthly) scale, and 2) uncertainties regarding the representativeness of samples associated with the Miamisburg and Fairfield automated monitoring stations (see discussion in Section 4.2.1 and Appendix F).

Table 4-3. Summary statistics for nitrogen for the combined calibration and corroboration periods (2011-2013).

Time Interval	Statistic	TN		TKN		NO2+NO3		NH3
		GMR at Miamisburg	GMR at Fairfield	GMR at Miamisburg	GMR at Fairfield	GMR at Miamisburg	GMR at Fairfield	GMR at Fairfield
Monthly	Count	36	36	36	36	36	36	36
	PBIAS (%)	-10.91	-7.82	-14.32	14.40	-5.39	-11.14	-8.01
	Absolute Error	0.71	0.72	0.20	0.26	0.55	0.69	0.04
Sub-Daily	Count	1515	527	1514	527	1507	526	504
	PBIAS (%)	-10.45	-7.36	-13.38	15.91	-5.33	-11.40	-7.67
	Absolute Error	0.95	1.06	0.32	0.51	0.76	0.93	0.09

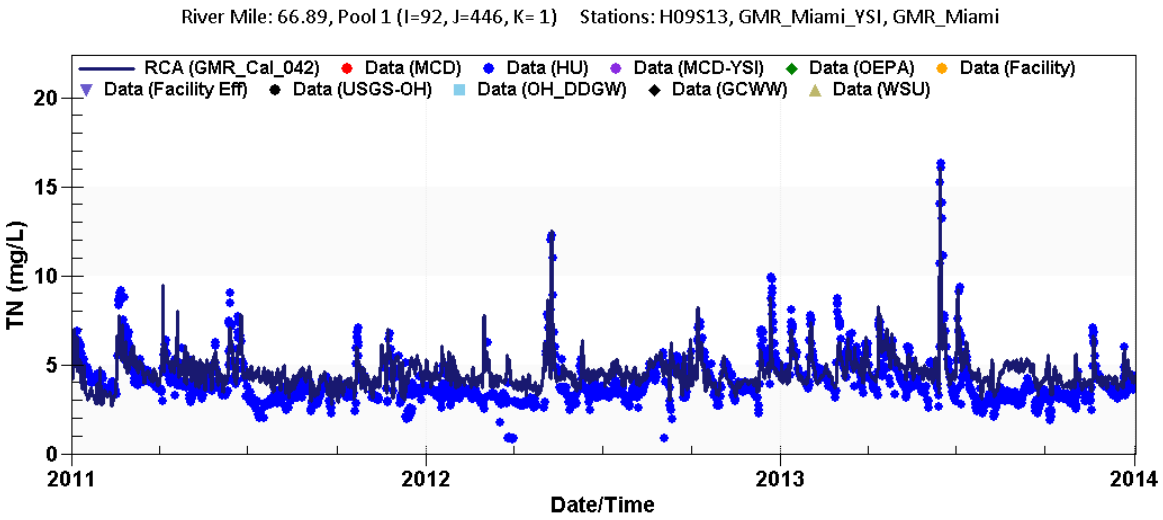

Figure 4-13. Time series comparison of simulated and observed TN concentrations for the Great Miami River at Miamisburg, 2011-2013.

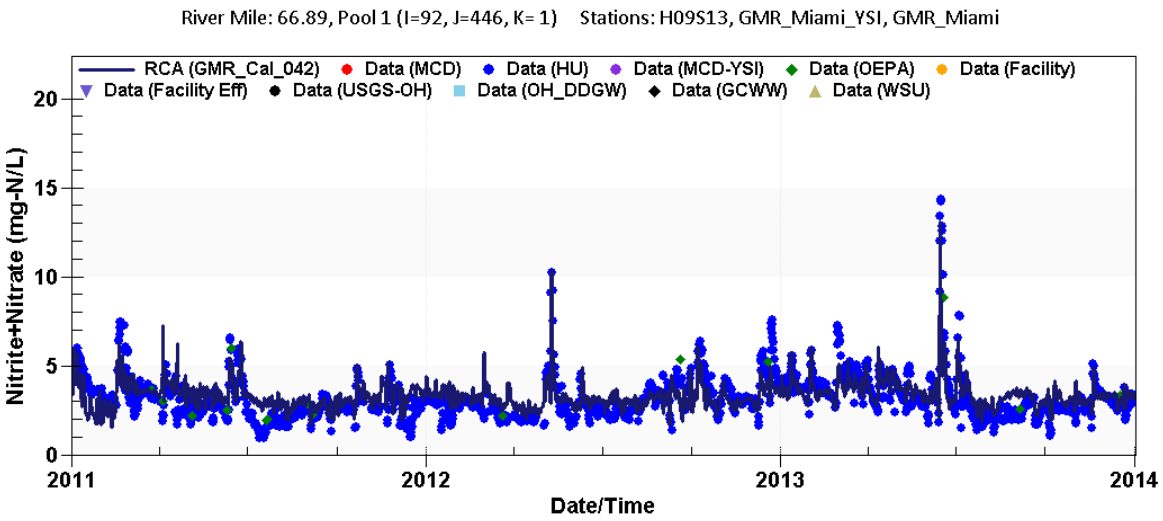

Figure 4-14. Time series comparison of simulated and observed NO2+NO3 concentrations for the Great Miami River at Miamisburg, 2011-2013.

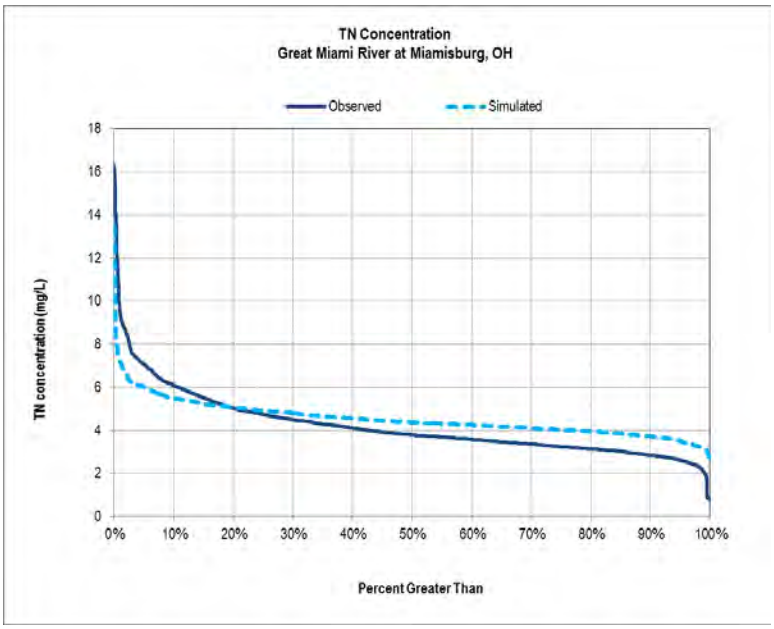

Figure 4-15. Observed and simulated TN concentration cumulative frequency distributions for the Great Miami River at Miamisburg, 2011-2013.

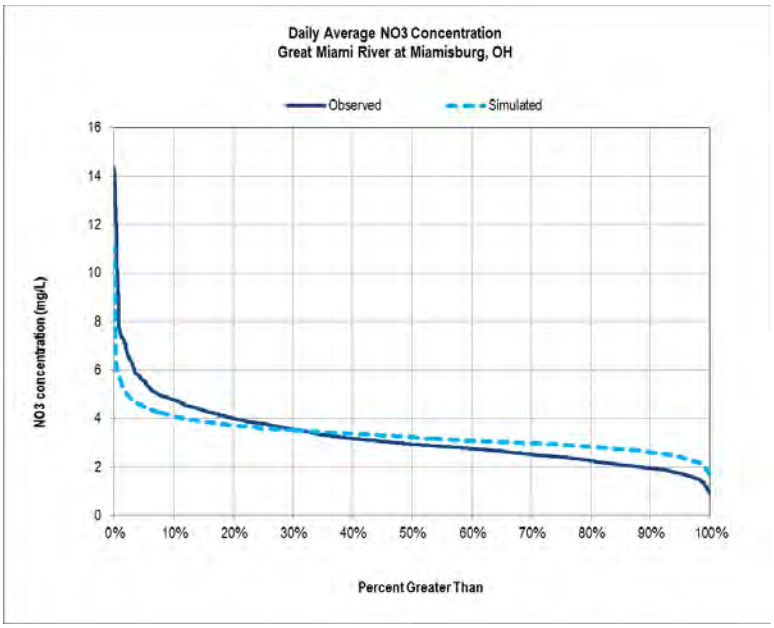

Figure 4-16. Observed and simulated NO2+NO3 concentration cumulative frequency distributions for the Great Miami River at Miamisburg, 2011-2013.

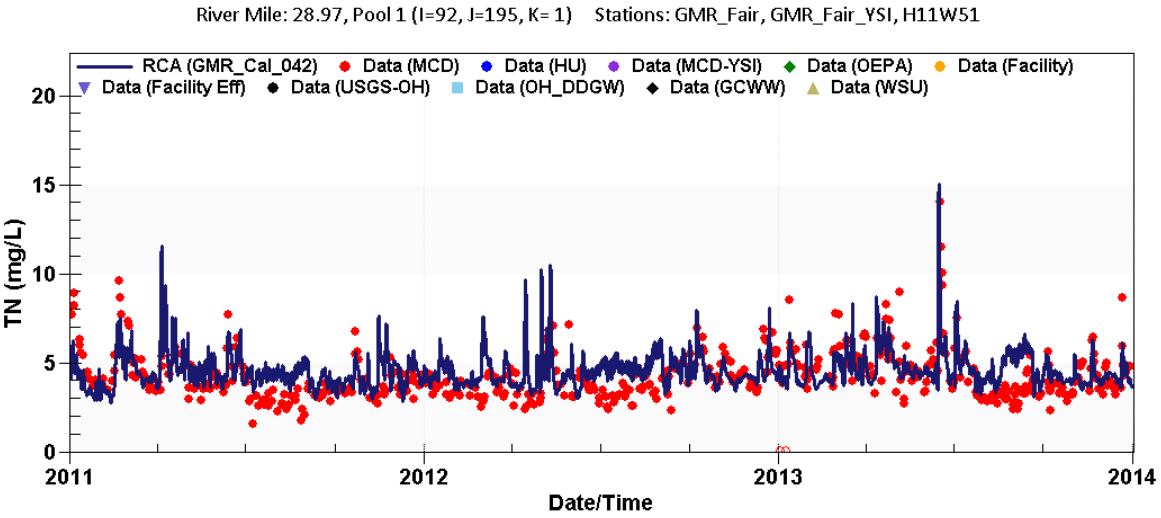

Figure 4-17. Time series comparison of simulated and observed TN concentrations for the Great Miami River at Fairfield, 2011-2013.

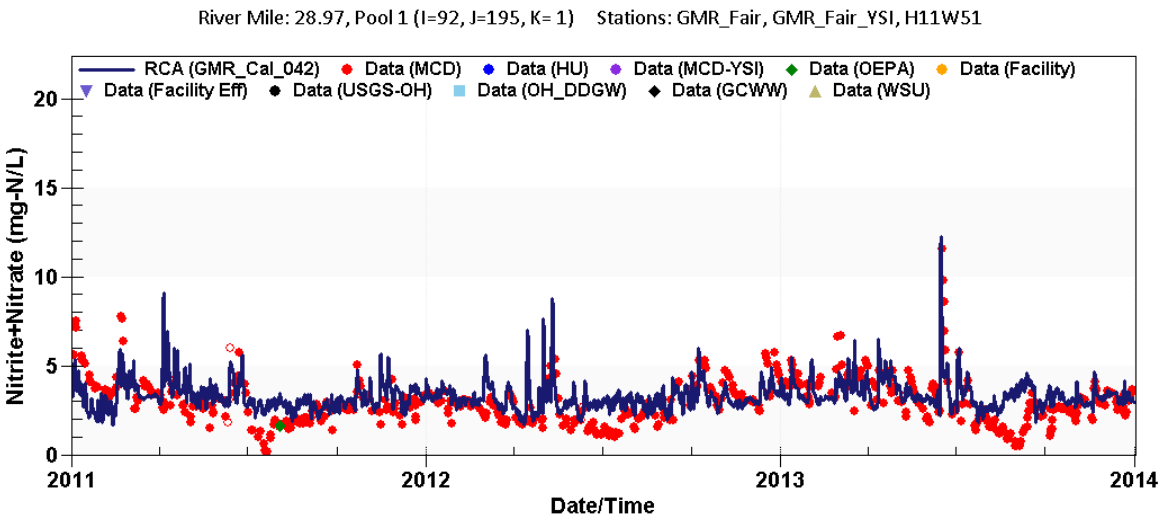

Figure 4-18. Time series comparison of simulated and observed NO2+NO3 concentrations for the Great Miami River at Fairfield, 2011-2013.

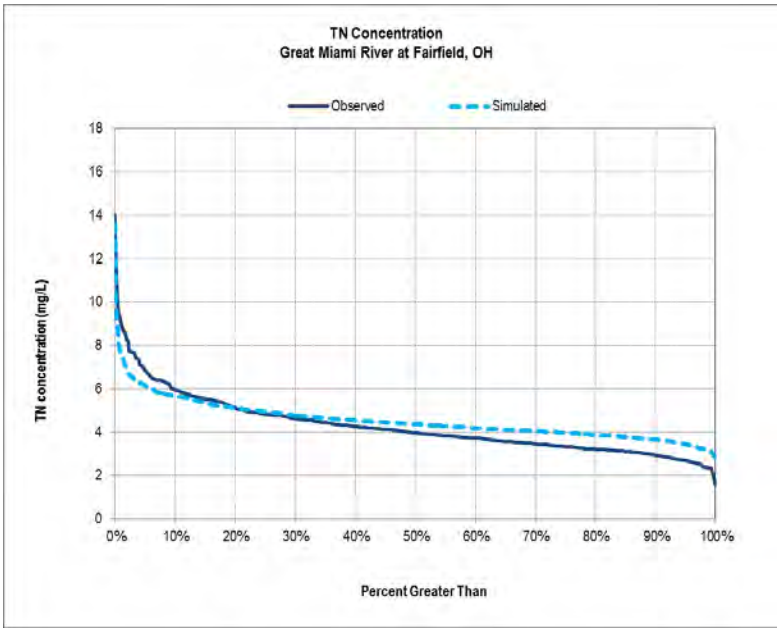

Figure 4-19. Observed and simulated TN concentration cumulative frequency distributions for the Great Miami River at Fairfield, 2011-2013.

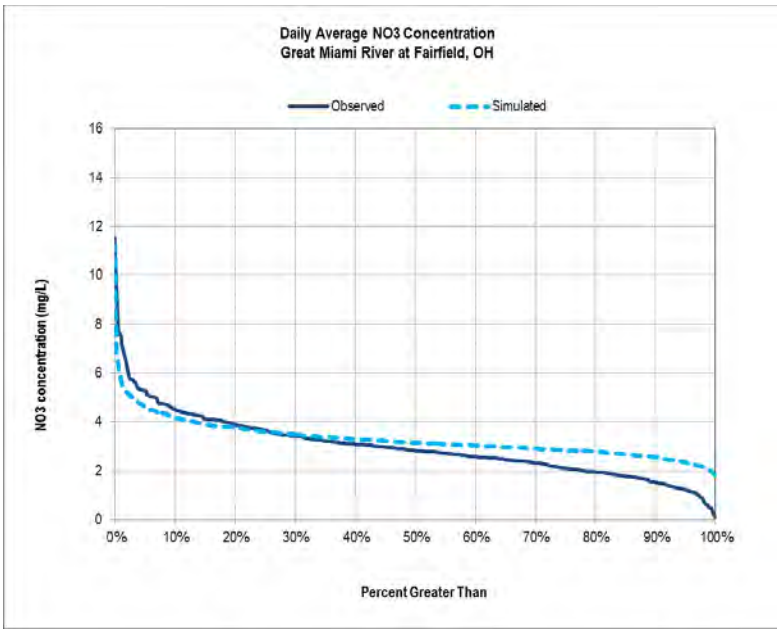

Figure 4-20. Observed and simulated NO2+NO3 concentration cumulative frequency distributions for the Great Miami River at Fairfield, 2011-2013.

4.2.2.c Algal Biomass

Calibration results for sestonic chlorophyll *a* concentration and benthic algae biomass (as chlorophyll *a*) density are presented in Figures 4-21 through 4-25 and Table 4-4. Simulated sestonic chlorophyll *a* concentrations are consistent with chlorophyll *a* observations from sonde measurements at Miamisburg for Sept 2011-Dec 2013, with a tendency to over-predict chlorophyll *a* in summer 2012 and a tendency to under-predict concentrations in August 2013 (Figure 4-21). The CFD plot for Miamisburg suggests strong agreement between simulated and observed chlorophyll *a* concentrations across the range of observed concentrations with an overall tendency of the model to somewhat over-predict observations (Figure 4-22). The model-predicted chlorophyll *a* also agrees reasonably well with sonde measurements at Fairfield in summer 2012. While some minor over-prediction is evident for summer 2012, it is relatively minor compared to the more significant under-prediction of chlorophyll *a* concentrations evident during summer 2013 (Figure 4-23). The CFD plot for Fairfield also highlights this observation; i.e., the simulated CFD deviates from the observed CFD most noticeably at the highest chlorophyll *a* concentrations, the majority of which were observed in 2013 at this location (Figure 4-24).

The reason(s) for the significant differences in chlorophyll *a* concentrations between summer 2012 and summer 2013 are not known at this time. This phenomenon does not appear to be solely related to differences in summer flow conditions between the two years, as the LGMR generally experienced lower flow conditions over longer timeframes relative to summer 2013. It should be noted that sample collection at either primary continuous monitoring station could potentially be affected by "clumps" of detached filamentous algae, which were observed in significant quantities during LimnoTech's field visit to Miamisburg in September, 2016 (see Appendix F), as well as in other photographs taken of the river.

Irrespective of the cause of the differences in sestonic algae biomass concentrations between 2012 and 2013, it was not possible to configure the LGMR water quality model to closely reproduce chlorophyll *a* observations for both years without violating established ranges for model coefficients or modifying algal growth parameters spatially or temporally. Specifically, sensitivity analyses conducted as part of the

calibration efforts suggested that it was not possible to reproduce the 2013 sestonic chlorophyll *a* observations without using maximum algal growth rates that are beyond the accepted maximum rate (2.5-3.0 day^{-1}). Furthermore, use of higher sestonic algal growth rates in the model that would more closely approximate conditions at Fairfield in 2013 would result in very significant over-predictions of chlorophyll *a* at both Miamisburg and Fairfield for 2012 and for Miamisburg in 2013. Data collection for additional summer periods at both Miamisburg and Fairfield (and perhaps intermediate locations) would be useful in determining whether the very high values measured in 2013 are commonplace, an aberration related to conditions in that particular year, or suggestive of issues with sample collection or sonde measurements at Fairfield in 2013.

The statistical measures chosen to evaluate model performance, PBIAS and average absolute error, indicate acceptable model performance in predicting chlorophyll *a* concentrations at both Miamisburg and Fairfield for the combined 2011-13 calibration/corroboration period. As noted previously, negative PBIAS values indicate an over-prediction of the simulated concentrations, and positive PBIAS values indicate an under-prediction of simulated concentrations relative to observed concentrations. These statistics confirm the observations described above regarding the time series and CFD plots; specifically that the model-predicted chlorophyll *a* concentrations are generally high compared to the observed data at Miamisburg (reflected in the negative PBIAS values). Despite the slight over-prediction of chlorophyll *a* concentrations at Fairfield in summer 2012, the significant under-prediction of chlorophyll *a* concentrations during summer 2013 result in an overall positive PBIAS value. Although the relatively smaller average absolute error at Miamisburg compared to Fairfield may suggest the model performs better at that location, the lack of chlorophyll *a* concentration data at Fairfield in 2011 and overall lower number of observations should also be considered.

Additional time series comparisons of simulated and observed chlorophyll *a* concentrations for three secondary calibration locations, the Great Miami River North of Franklin, at Middletown and upstream of the Hamilton WWTP, are shown in Appendix E (Figures E-15 through E-17). Longitudinal profile plots of simulated and observed chlorophyll *a* concentrations are shown in Appendix E for four OEPA sampling events overlapping with the 2011-2013 simulation period (Figure E-18). Both the time series for the secondary calibration locations and longitudinal plots for the OEPA survey events suggest model predictions fall within the range of observed chlorophyll *a* concentrations with the exception of the July 2011 event and the early August 2011 OPEA monitoring surveys (upstream of river mile 40 only). Statistical performance measures were not computed for these secondary calibration stations due to an insufficient number of observations.

Overall, the sestonic chlorophyll *a* concentrations simulated by the LGMR water quality model reproduce the general annual and seasonal trends and other key features of the chlorophyll *a* monitoring data available for Miamisburg and Fairfield, as well as for the secondary calibration stations. As discussed above, chlorophyll *a* observations at Fairfield for suggest significantly different behavior in the reach between Miamisburg and Fairfield in summer 2013 relative to summer 2012. The current calibration seeks a compromise between the 2012 and 2013 observations, although the model behaves much more similarly to the observations from 2012. Again, further data collection at Fairfield and/or in the reach between Miamisburg and Fairfield would be needed to develop a better understanding of temporal and spatial algal dynamics in this area of the LGMR and to support further calibration of the model. As for phosphorus and nitrogen, the uncertainty regarding the representativeness of samples associated with the Miamisburg and Fairfield automated monitoring stations should also be kept in mind when evaluating results (see discussion in Section 4.2.1 and Appendix F).

Table 4-4. Summary statistics for sestonic chlorophyll *a* for the combined calibration and corroboration periods (2011-2013).

Time Interval	Statistic	Chlorophyll *a*	
		GMR at Miamisburg	GMR at Fairfield
Monthly	Count	29	20
	PBIAS	-29.75	2.56
	Absolute Error	5.6	15.4
Daily	Count	802	476
	PBIAS	-26.14	9.56
	Absolute Error	6.8	21.0

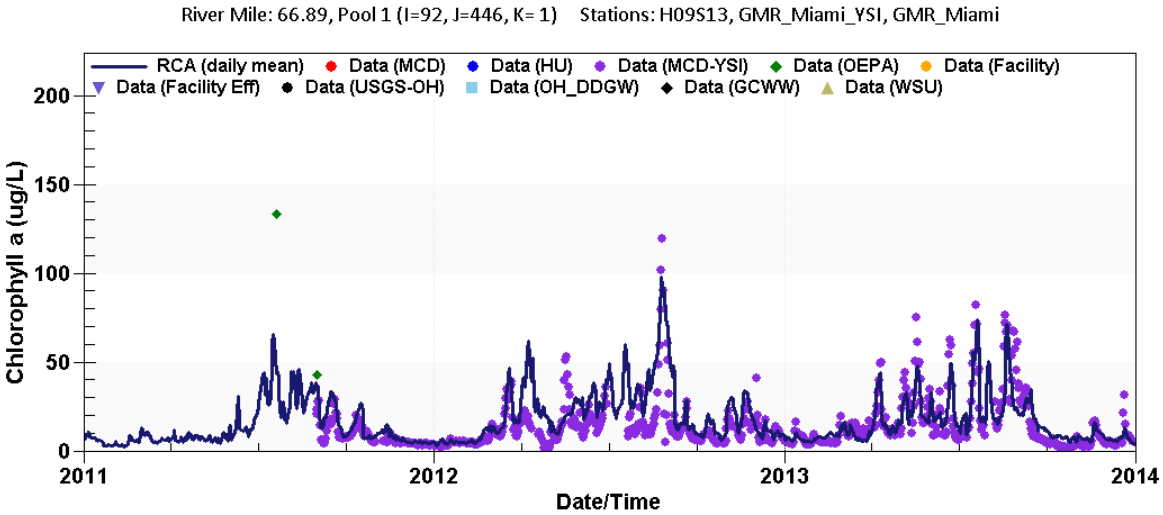

Figure 4-21. Time series comparison of simulated and observed sestonic chlorophyll *a* concentrations for the Great Miami River at Miamisburg, 2011-2013.

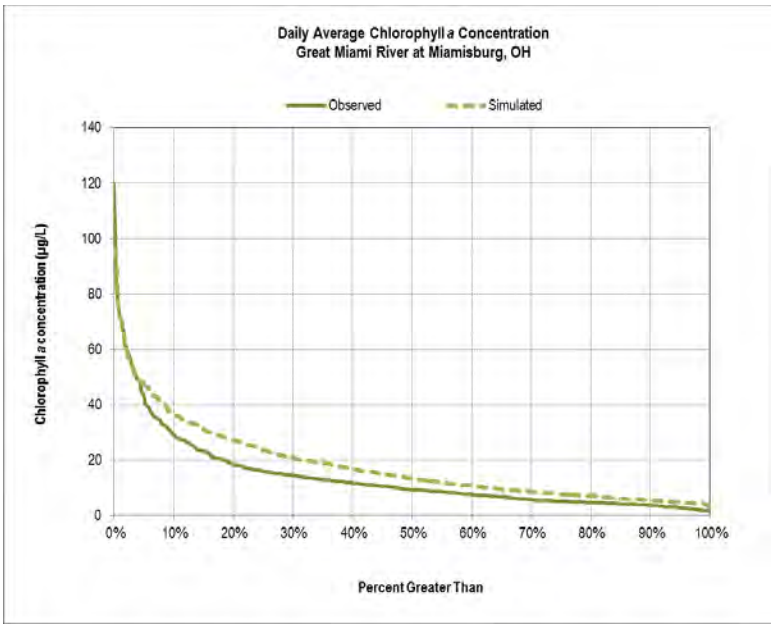

Figure 4-22. Observed and simulated sestonic chlorophyll *a* concentrations cumulative frequency distributions for the Great Miami River at Miamisburg, 2011-2013.

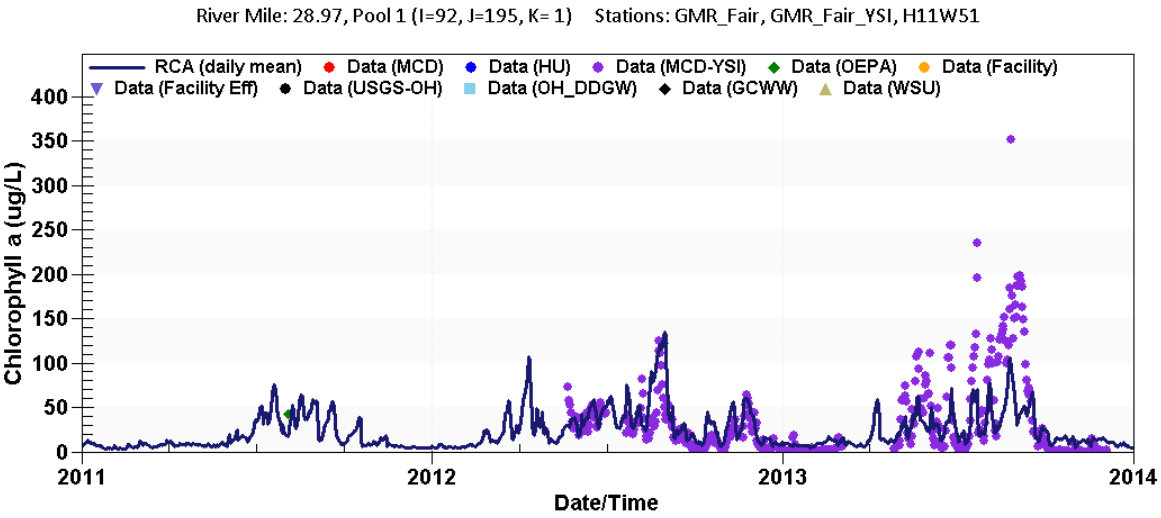

Figure 4-23. Time series comparison of simulated and observed sestonic chlorophyll *a* concentrations for the Great Miami River at Fairfield, 2011-2013.

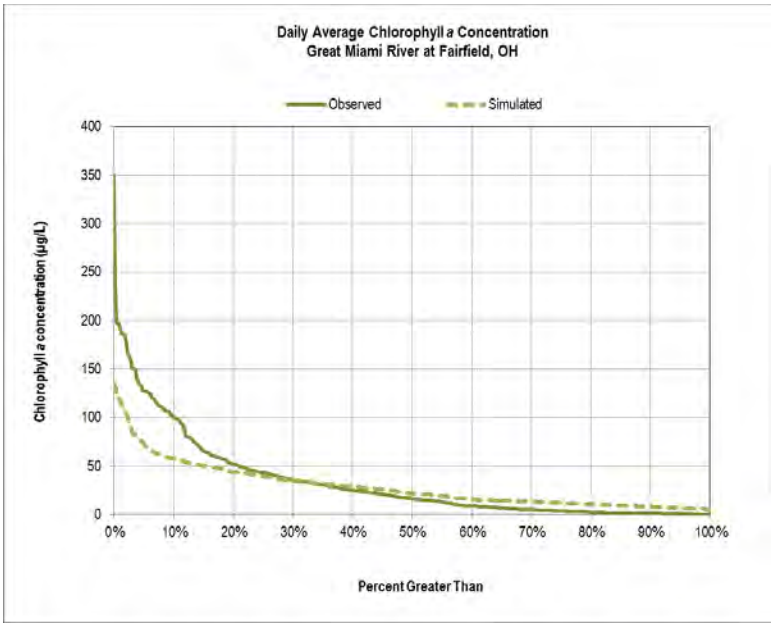

Figure 4-24. Observed and simulated sestonic chlorophyll *a* concentrations cumulative frequency distributions for the Great Miami River at Fairfield, 2012-2013.

A limited number of benthic algal density measurements were available from OEPA surveys conducted in August 2008, July-August 2011, and July 2012. These measurements were aggregated in a longitudinal plot and compared against model-predicted average benthic algal density for July-August 2011 and July-August 2012 (Figure 4-25) for the purpose of demonstrating that model-simulated benthic algal densities are consistent with field measurements. With the exception of the outlier density observation of > 900 mg-Chl *a*/m² near River Mile 35, the LGMR water quality model simulates mean benthic algae densities that are very consistent with the observations. Despite the limited number of observations available, this provides confidence that the model reasonably represents benthic algae production and loss processes and their impact on DO conditions in the LGMR.

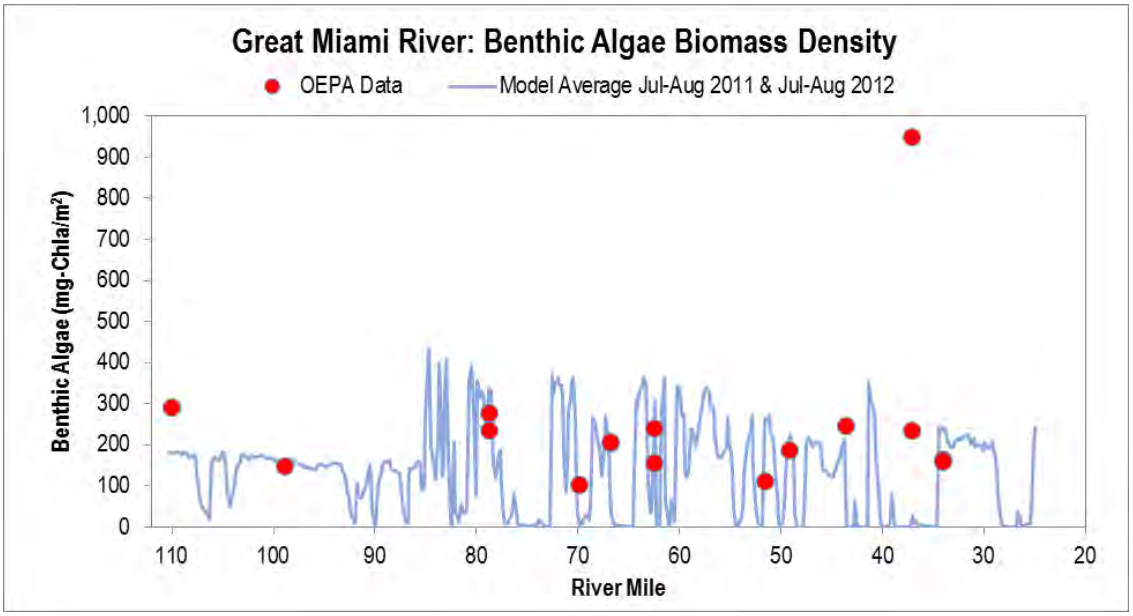

Figure 4-25. Longitudinal plot of observed and simulated benthic algae biomass density for the Great Miami River

4.2.2.d Dissolved Oxygen

Calibration results for DO are presented in Figures 4-26 through 4-34 and Table 4-5. Model-predicted daily average DO concentrations match observations from sonde measurements reasonably well at both Miamisburg and Fairfield (Figures 4-26 and 4-28). The model captures the seasonality reflected in the observed data of high average DO concentrations in the winter months and the lowest average DO concentrations in the summer months. The model tends to predict slightly higher average DO concentrations as evident in the CFD plots (Figures 4-27 and 4-29), and it does not match observed data during the relatively few days when average DO concentrations decreases below approximately 5 mg/l. It is important to note that the potential for lateral variations in DO in the LGMR system is high, based on the field investigation conducted by LimnoTech near the Miamisburg station in September, 2016 (see Appendix F). Therefore, it is not known at this time whether measurements made at Miamisburg and Fairfield based on samples drawn relatively close to the edge of the river are sufficiently representative of average DO concentrations across the full width of the river.

Diurnal DO range has been determined to be an important in the LGMR and was considered as a high priority variable during calibration. Hourly DO observations at Miamisburg and Fairfield (as well as for some secondary stations) suggest that there is considerable spatial and temporal variability in the diurnal DO range. Overall, the model reasonably reproduces diurnal DO patterns and captures the extreme diurnal ranges (i.e., instances of diurnal DO in the 15-20 mg/l range) at both Miamisburg and Fairfield (Figure 4-30 and 4-32), although the model tends to over-state diurnal DO range at both Miamisburg and Fairfield as evident by the CFD plots (Figures 4-31 and 4-33). While the model captures the seasonality of diurnal DO range well with the highest DO ranges in the summer months and lowest in the winter months, it tends to over-predict DO swings in Sep-Oct more frequently than for other months (Figures 4-30 and 4-32).

Figure 4-34 demonstrates that the model predicts suppression of diurnal DO swings in river segments behind several impoundments along the LGMR, particularly at the Island Park (RM 82), West Carrollton (RM 72), Hutchings Station (RM 63), Black Street (RM 37), and Hamilton Recreation (RM 35) dams. This trend can also be seen by careful observation of the OEPA sampling data. With the exception of the Hutchings Station dam, the lowest diurnal DO swings measured during OEPA sampling events tended to be near the same impoundments where the model predicted suppression of diurnal DO. Therefore in addition to reproducing seasonal patterns and extreme diurnal DO ranges at the Miamisburg and Fairfield continuous monitoring stations, these longitudinal profile comparisons show that the model also replicates the spatial variability in diurnal DO range (i.e., river segments with relatively high vs. relatively low diurnal DO range) demonstrated by the OEPA sampling events.

The statistical measures chosen to evaluate model performance, PBIAS and average absolute error, indicate acceptable model performance in predicting both daily average DO concentrations and diurnal DO range at Miamisburg and Fairfield for the combined 2011-13 calibration/corroboration period. These statistics confirm the observations described above regarding the time series and CFD plots; specifically, that model predictions of daily average DO concentrations tend to be slightly higher than the observed data for both Miamisburg and Fairfield on average (as reflected in the negative PBIAS values). Likewise, the negative PBIAS values for statistical evaluations of the diurnal DO range indicate the model's general tendency to over-predict the measured values despite capturing the seasonality and extremes (i.e., highest and lowest values) of diurnal DO range relatively well.

Hourly time series comparisons of simulated and observed DO concentrations for the two primary calibration locations and six secondary calibration locations are shown in Appendix E (Figures E-19 through E-27). Overall, these comparisons show that the model predicts the diurnal DO ranges, timing of minimum/maximum DO, daily minimum DO, and daily average DO reasonably well at a variety of locations throughout the LGMR. The model does not simulate maximum DO concentrations above

roughly 15 mg/l for the late July 2011 OEPA sampling event for the locations shown and therefore under-predicts both daily maximum and diurnal DO for this event; however, the model does represent the minimum daily DO and timing of min/max DO very well for this event. The model also performs better overall for the early August 2011, late August 2011, and late August 2012 OEPA sampling events. Statistical performance measures were not computed for daily average DO and diurnal DO range for the OEPA sampling stations due to an insufficient number of observations.

Overall, the average daily DO concentrations and diurnal DO range simulated by the LGMR water quality model reproduce the general annual and seasonal trends and other key features of the dissolved oxygen monitoring datasets available for Miamisburg and Fairfield, as well as for the secondary calibration stations. As discussed above, the continuous DO datasets and other supporting data suggest that there is considerable temporal and spatial variability in both of these endpoints. The water quality model performs well overall with respect to reproducing average daily DO conditions and also the extreme diurnal DO ranges observed in the system. Questions regarding the representativeness of DO measurements associated with the Miamisburg and Fairfield automated monitoring stations are of particular relevance for DO, as the results of the LimnoTech field investigation measured variations of up to 6 mg/l for DO across transects near Miamisburg (see Appendix F for more details). Therefore, further data collection at Miamisburg, Fairfield, and/or other locations to better understand and quantify lateral variability is recommended prior to conducting any additional calibration work with the water quality model.

Table 4-5. Summary statistics for DO endpoints for the combined calibration and corroboration periods (2011-2013).

Time Interval	Statistic	DO (discrete data)		Diurnal DO Range	
		GMR at Miamisburg	GMR at Fairfield	GMR at Miamisburg	GMR at Fairfield
Monthly	Count	29	19	29	19
	PBIAS	-7.47	-8.45	-58.12	-47.39
	Absolute Error	0.9	1.0	1.7	1.6
Daily	Count	816	460	816	460
	PBIAS	-8.26	-9.78	-49.25	-42.80
	Absolute Error	1.08	1.15	1.75	2.08

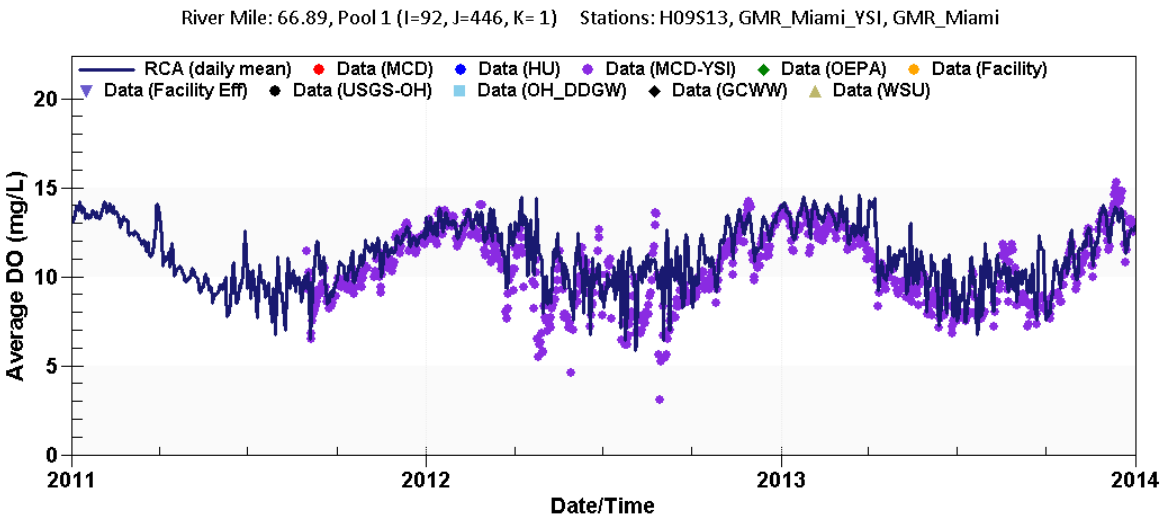

Figure 4-26. Time series comparison of simulated and observed DO concentrations for the Great Miami River at Miamisburg, 2011-2013.

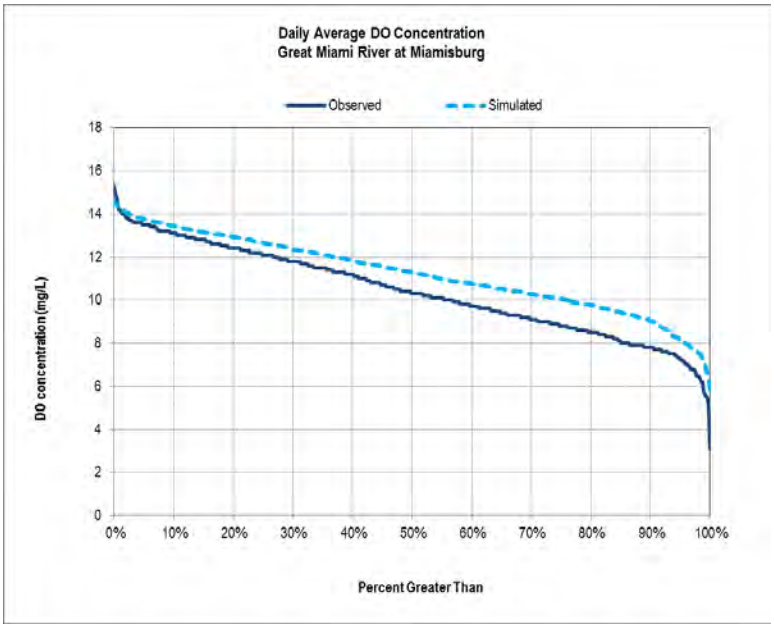

Figure 4-27. Observed and simulated DO concentration cumulative frequency distributions for the Great Miami River at Miamisburg, 2011-2013.

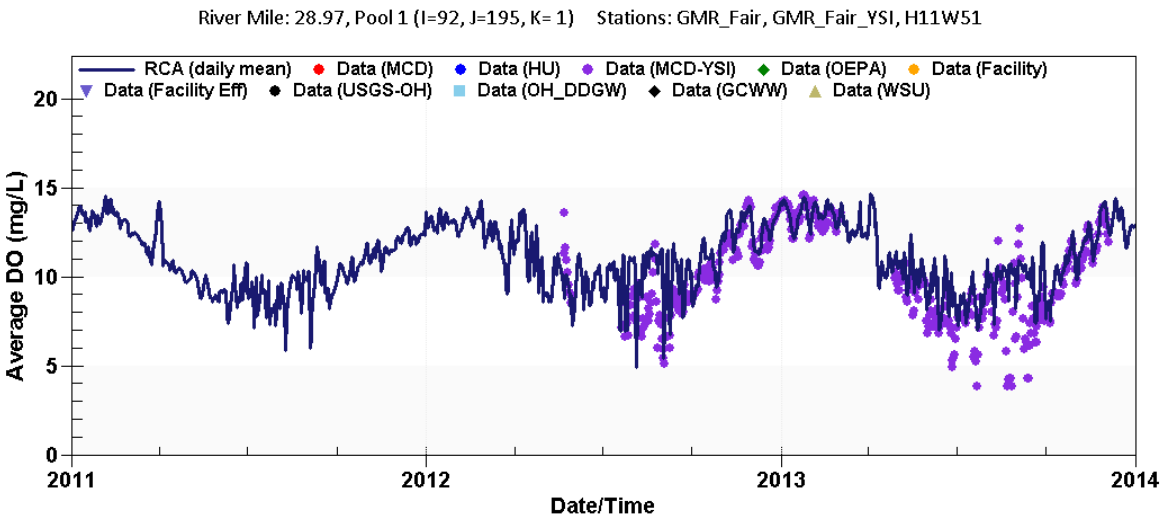

Figure 4-28. Time series comparison of simulated and observed DO concentrations for the Great Miami River at Fairfield, 2011-2013.

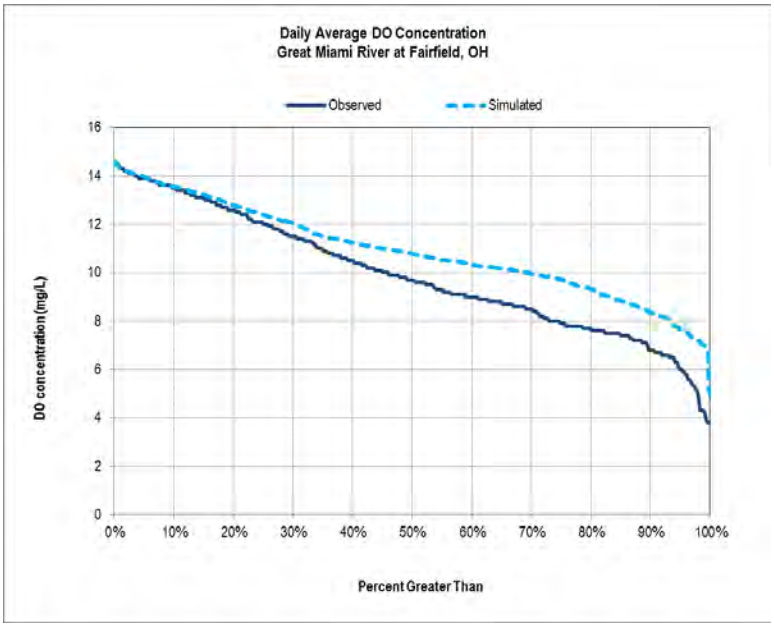

Figure 4-29. Observed and simulated DO concentration cumulative frequency distributions for the Great Miami River at Fairfield, 2012-2013.

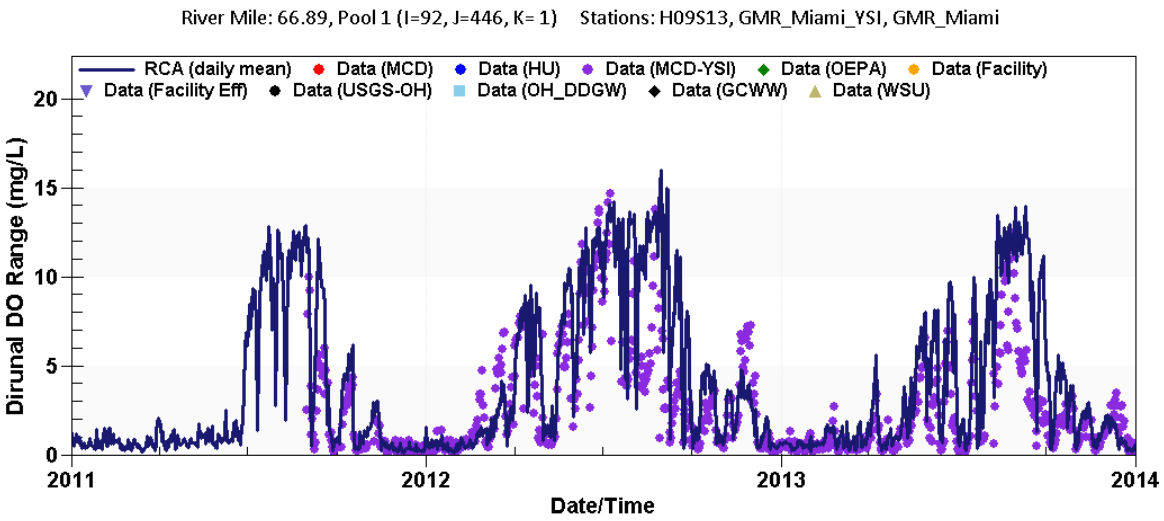

Figure 4-30. Time series comparison of simulated and observed diurnal DO range for the Great Miami River at Miamisburg, 2011-2013.

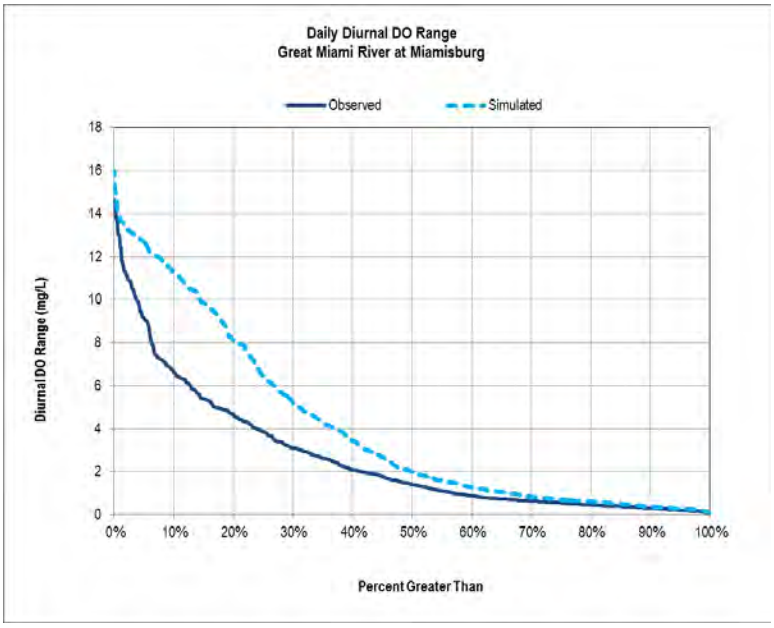

Figure 4-31. Observed and simulated diurnal DO range cumulative frequency distributions for the Great Miami River at Miamisburg, 2011-2013.

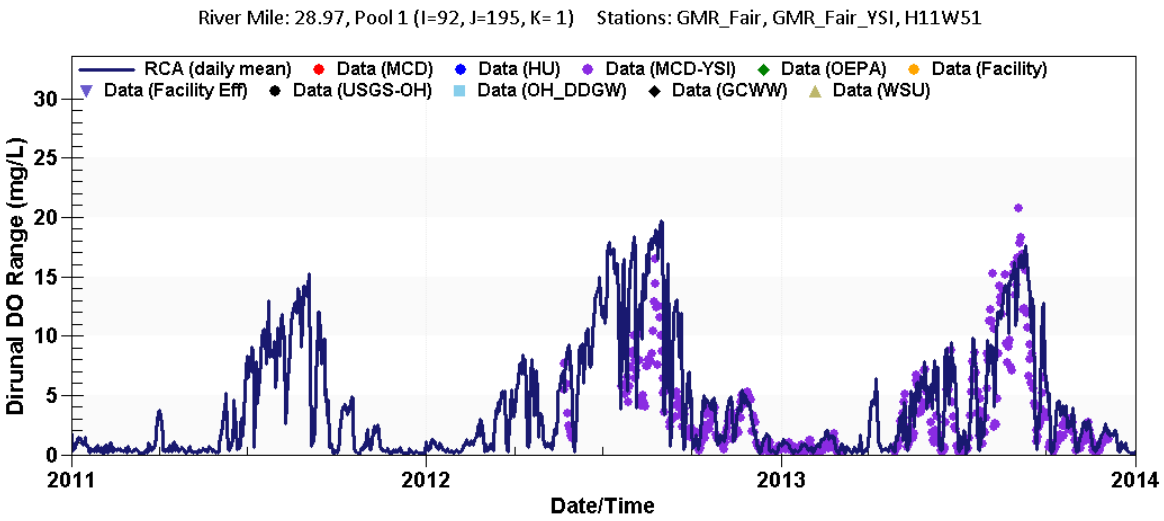

Figure 4-32. Time series comparison of simulated and observed diurnal DO range for the Great Miami River at Fairfield, 2011-2013.

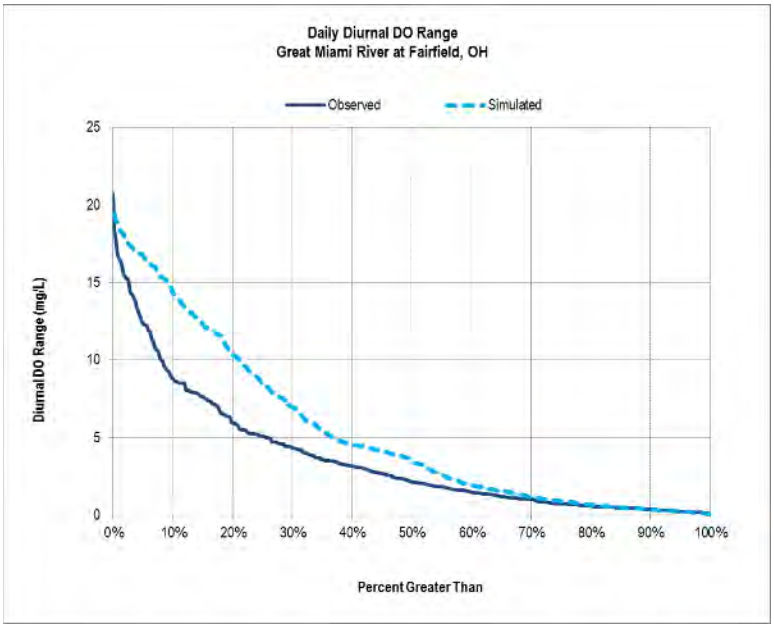

Figure 4-33. Observed and simulated diurnal DO range cumulative frequency distributions for the Great Miami River at Fairfield, 2012-2013.

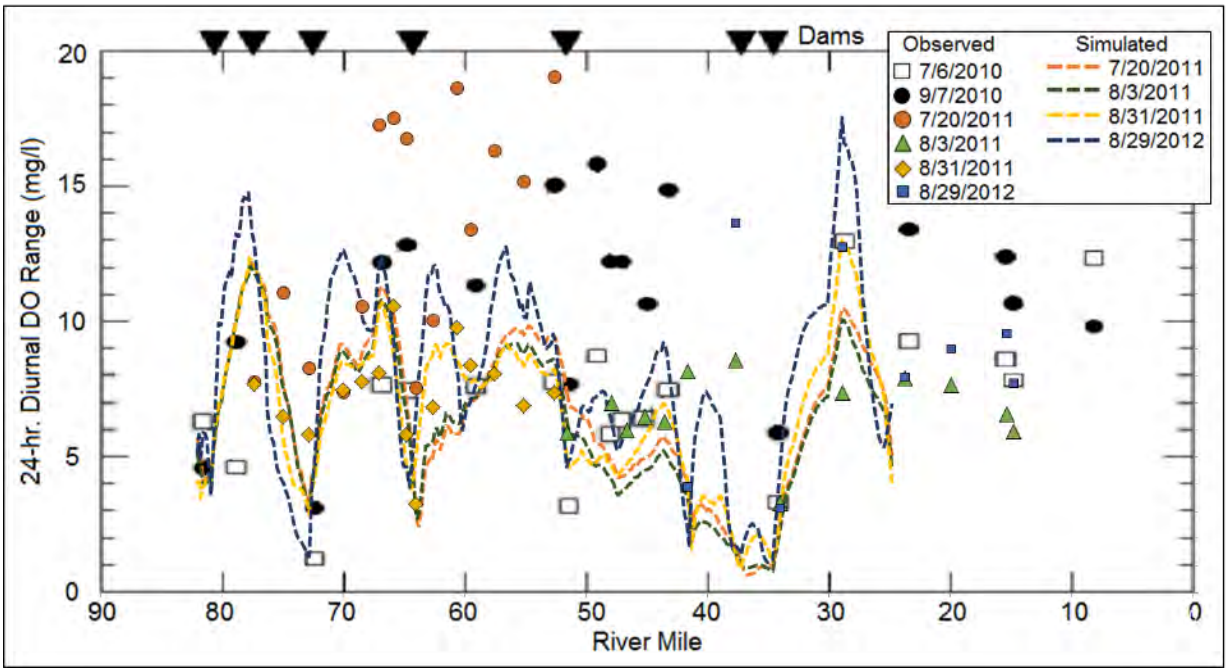

Figure 4-34. Longitudinal profile plot of diurnal DO range comparing observed data from six OEPA sampling events and simulated diurnal DO range for four of those events (Modified from Figure 29 of OEPA, 2012)

Figure 4.35 shows diagnostic results for the impact of sestonic and benthic algal growth and respiration processes on simulated DO concentrations at Miamisburg. This plot was created using custom A2EM diagnostic output variables that were added as part of this project to better assess the relative impacts of the various processes influencing simulated DO concentration and diurnal DO range. Descriptions of the processes and the algorithms used to represent them are described in Section 3.3.5.f. Although there are certain periods where the impact of sestonic algae on diurnal DO range may be of equal or greater magnitude as the impact of benthic algae, this figure demonstrates that during the majority of time and the most extreme daily diurnal DO ranges are largely impacted by benthic and not sestonic algae.

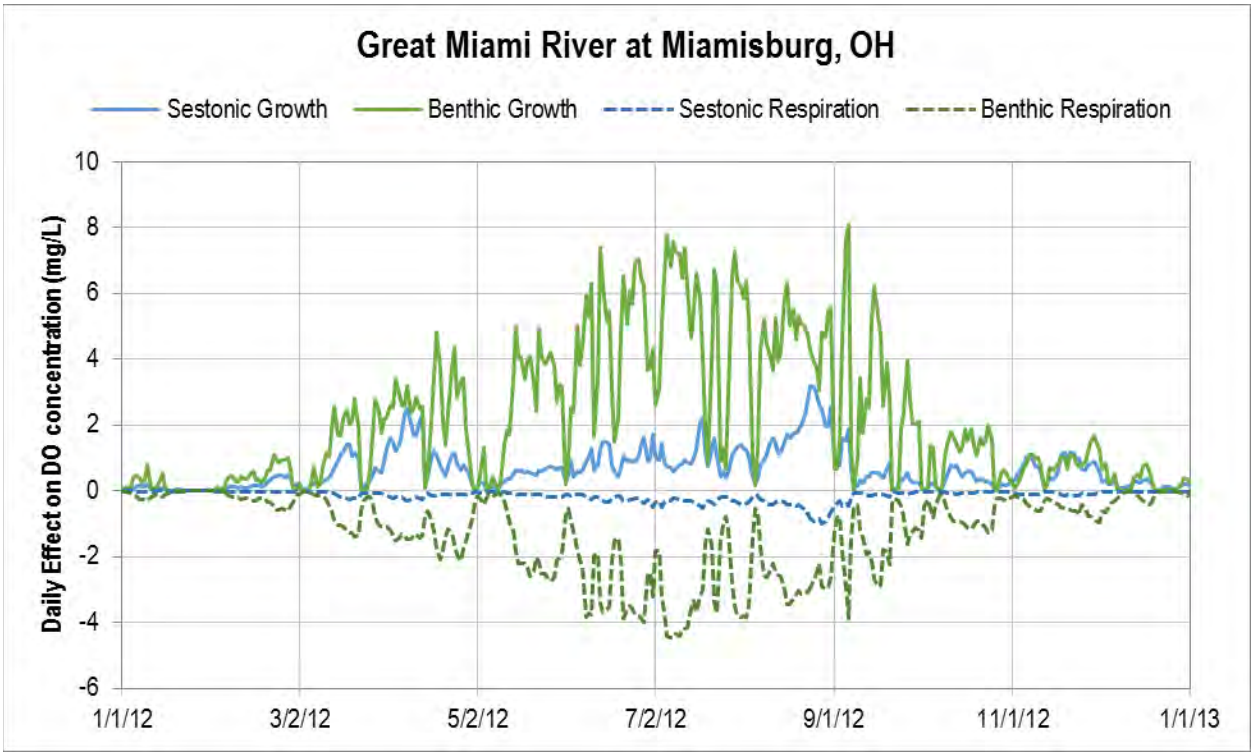

Figure 4-35. Diagnostic plot based on model output depicting the relative contribution of sestonic and benthic algal growth and respiration processes on simulated DO concentrations at Miamisburg for calendar year 2012.

4.2.3 Discussion

The calibrated LGMR water quality model provides a reasonable, although not exact, representation of the system. For the reasons discussed below, the consensus opinion of the modeling team and expert reviewers is that the calibration is as good as can be accomplished given the available data. The available data at Miamisburg and Fairfield, as well as at other locations, for nutrients, chlorophyll *a*, and dissolved oxygen suggest that the system demonstrates very different behavior in 2013 relative to 2011-12, particularly in the reach between Miamisburg and Fairfield. In addition, data suggest that significant day-to-day variability in sestonic chlorophyll *a* and other parameters can occur, and the model cannot always capture these dynamics given the current calibration constraints. An improved understanding of the LGMR system and an improved model calibration is possible, but would require additional data collection to:

- Better characterize spatial and temporal patterns for key parameters within the LGMR itself (especially sestonic and benthic algae, and dissolved oxygen);
- Characterize in greater detail point source loading of nutrients (i.e., at a daily scale) and tributary loading of nutrients and especially chlorophyll *a* to the mainstem; and
- Characterize site-specific reaeration rates and other key process parameters (e.g., related to sestonic and benthic algal growth).

The above items are further discussed in Section 6 (Findings and Recommendations).

In addition to data limitations, the results from a limited field investigation conducted during this project suggests that significant lateral variability of key water quality parameters, especially DO, can occur in the river (Appendix F), and these lateral variations cannot be captured by the one-dimensional framework of the current model. The DO data used for calibration were collected using automated data collection sondes, and these observations represent conditions at a single point location in the river, while the model represents a lateral average of the range of conditions that occur. Data collected by LimnoTech demonstrate that concurrent DO concentrations can vary by up to 6 mg/l across the channel.

Although further field investigation is needed to corroborate these observations, they suggest that no single-point DO measurement in the LGMR should be construed as representative of the entire cross-section of the river. Therefore, if a DO concentration calculated by the current LGMR water quality model, which represents laterally and longitudinally-averaged conditions for a given reach, varies from a data observation at a given point in the river at a given time, it does not directly infer that the calibration is deficient relative to the data. The effect of the above uncertainties on model scenario results are addressed via model sensitivity analysis, where certain scenarios are re-run with alternative model inputs reflecting key uncertain parameters (Section 5.7).

Blank

5 Water Quality Scenarios

The primary purpose of the LGMR water quality model is to comparatively evaluate the water quality benefits of different potential levels of nutrient load reduction, reduction of nutrients from different sources and/or other potential actions, such as dam removal. As part of this project, seven scenarios were run, each of which involved some aspect of potential nutrient load reduction. Those scenarios and their results are described in this section.

5.1 Baseline Scenario

A baseline conditions scenario was created from the calibrated A2EM model to serve as a "foundation simulation" from which management scenarios were constructed as a variation of and to assess the relative impact of various management actions. The simulation period chosen for all scenarios was the same as the calibration period; calendar years 2011-2013. The baseline scenario differed from the calibrated A2EM model in that the Butler County LeSourdsville WRF effluent TP concentrations were reduced relative to historical concentrations to reflect current conditions. Based on reported effluent TP concentrations for 2016, the baseline scenario assumed discharges of 0.11 mg-P/l for Oct-May and 0.67 mg-P/l for Jun-Sep for the LeSourdsville WRF. All other model inputs for the baseline scenario were the same as for the calibrated model; i.e. historical 2011-2013 conditions.

5.2 Key Water Quality Variables

For each scenario, tabular and graphical results were used to depict change for key water quality variables relative to the baseline conditions scenario, including the following:

- Total phosphorus and ortho-phosphorus;
- Average dissolved oxygen and diurnal dissolved oxygen swing;
- Sestonic algae; and
- Benthic algae.

Tabular results included quantification of the average July-October and average annual TP load reduction relative to the baseline conditions scenario for the 2011-2013 simulation period. Graphical results included longitudinal profile plots of various model output variables for August 31, 2012, which was the lowest flow date during the 2011-2013 simulation period (460 cfs for the Great Miami River at Hamilton). Monthly time series plots for the Great Miami River at the Fairfield water quality monitoring station were also used to depict the relative impact of the management scenarios.

5.3 Point Source Load Reduction Scenarios

The following four point source load reduction scenarios were simulated for the 2011-2013 period:

- Scenario 1 – Dayton WWTP and Montgomery County Western Regional WRF effluent TP concentrations of 0.75 mg-P/l (53% orthophosphorus) for Jul-Oct, historical conditions for Nov-Jun;
- Scenario 2 – Dayton WWTP and Montgomery County Western Regional WRF effluent TP concentrations of 0.0 mg-P/l for Jul-Oct, historical conditions for Nov-Jun;
- Scenario 3 – All major public WRRF within the A2EM domain effluent TP concentrations of 0.75 mg-P/l (53% orthophosphorus) for Jul-Oct, historical conditions for Nov-Jun; and
- Scenario 4 – All major public WRRF within the A2EM domain effluent TP concentrations of 0.0 mg-P/l for Jul-Oct, historical conditions for Nov-Jun.

5.4 Non-Point Source Load Reduction Scenario

A nonpoint source load reduction scenario was simulated for the 2011-2013 period as follows:

- Scenario 5 – Reduce agricultural (pasture and row crop) nonpoint source phosphorus loading by 15% relative to the baseline scenario

Scenario 5 was implemented by using the HSPF watershed model to inform tributary and direct drainage phosphorus loading reductions (direct inputs to the A2EM domain) and upstream boundaries.

5.5 Combination Scenario

Two combination scenarios were simulated for the 2011-2013 period:

- Scenario 6 – All major public WRRF within the A2EM domain assigned effluent TP concentrations of 0.75 mg-P/l (53% orthophosphorus) for Jul-Oct, historical conditions for Nov-Jun ***and*** reduce agricultural (pasture and row crop) nonpoint source phosphorus loading by 15% relative to the baseline scenario; and
- Scenario 7 – All major public WRRF within the A2EM domain assigned effluent TP concentrations of 0.75 mg-P/l (53% orthophosphorus) for Jul-Oct, historical conditions for Nov-Jun ***and*** reduce agricultural (pasture and row crop) nonpoint source phosphorus loading by 15% relative to the baseline scenario ***and*** remove Tait Station and Hutchings Station dams.

Scenario 6 represents a combination of scenarios 3 and 5. Scenario 7 has the same phosphorus load reductions as scenario 6 but also simulated the removal of the two impoundments listed above. The dam removal portion of scenario 7 was implemented in the LGMR modeling framework by re-running the hydrodynamic model (EFDC) with modified slopes in affected areas and re-linking hydrodynamic model output to the water quality model.

5.6 Summary of Scenario Results

Comparisons of the baseline conditions scenario and seven management scenarios are provided in Table 5-1 and Figures 5-1 through 5-13 below. Although scenarios 6 and 7 had the largest average annual TP load reduction relative to the baseline, scenario 4 had the largest average July-October TP load reduction. This resulted in scenario 4 showing the largest responses in sestonic algae, benthic algae, and dissolved oxygen model output variables relative to the baseline among the scenarios considered. Note that the time-series plots in this section show monthly average results for key water quality parameters. The daily average results for the scenarios are included as Appendix G.

Table 5-1. List of management scenarios simulated with A2EM and TP loading reductions relative to the baseline conditions scenario

Scenario No.	Description	Avg. Jul-Oct TP Load Reduction	Avg. Annual TP Load Reduction
1	Dayton & Montgomery Co. effluent 0.75 mg-P/l (53% ortho-P), Jul-Oct only	11%	1.5%
2	Dayton & Montgomery Co. effluent 0 mg-P/l, Jul-Oct only	17%	2.5%
3	All major public WRRF effluent 0.75 mg-P/l (53% ortho-P), Jul-Oct only	20%	2.8%
4	All major public WRRF effluent 0 mg-P/l, Jul-Oct only	33%	4.8%
5	15% agricultural NPS load reduction	3.6%	8.7%
6	All major public WRRF effluent 0.75 mg-P/l (53% ortho-P), Jul-Oct only and 15% agricultural NPS load reduction	23%	12%
7	Scenario 6 with Tait Station and Hutching Station dams removed	23%	12%

5.6.1 Total Phosphorus and Dissolved Phosphorus

Figure 5-1 shows monthly average total phosphorus results for the LGMR at Fairfield for the 2011 -2013 simulation period, for all seven scenarios, and Figure 5-3 shows dissolved inorganic phosphorus results in the same format. Figures 5-2 and 5-4 show a one-day snapshot of the entire modeled length of the river for total phosphorus and dissolved inorganic phosphorus, respectively. These plots are for August 31, 2012, which was the date with the lowest average daily flow during the simulation period. The average flow on that date was approximately 460 cfs for the LGMR at Hamilton, which is only slightly higher than the 7Q10 flow of 300 cfs for the river.

The following observations can be made from these results:

- Even Scenario 4, which is the most extreme (and infeasible) scenario in terms of phosphorus reduction at WRRFs, results in only a 33% TP load reduction for summer months and less than 5% reduction in annual TP load.
- The largest differences in total and dissolved inorganic phosphorus between scenarios occur between July and October, which is to be expected because effluent phosphorus reductions were specified for this period in each simulation year.
- Total and dissolved inorganic phosphorus for Scenario 5 (NPS load reduction only) are barely distinguishable from the baseline during summer months.

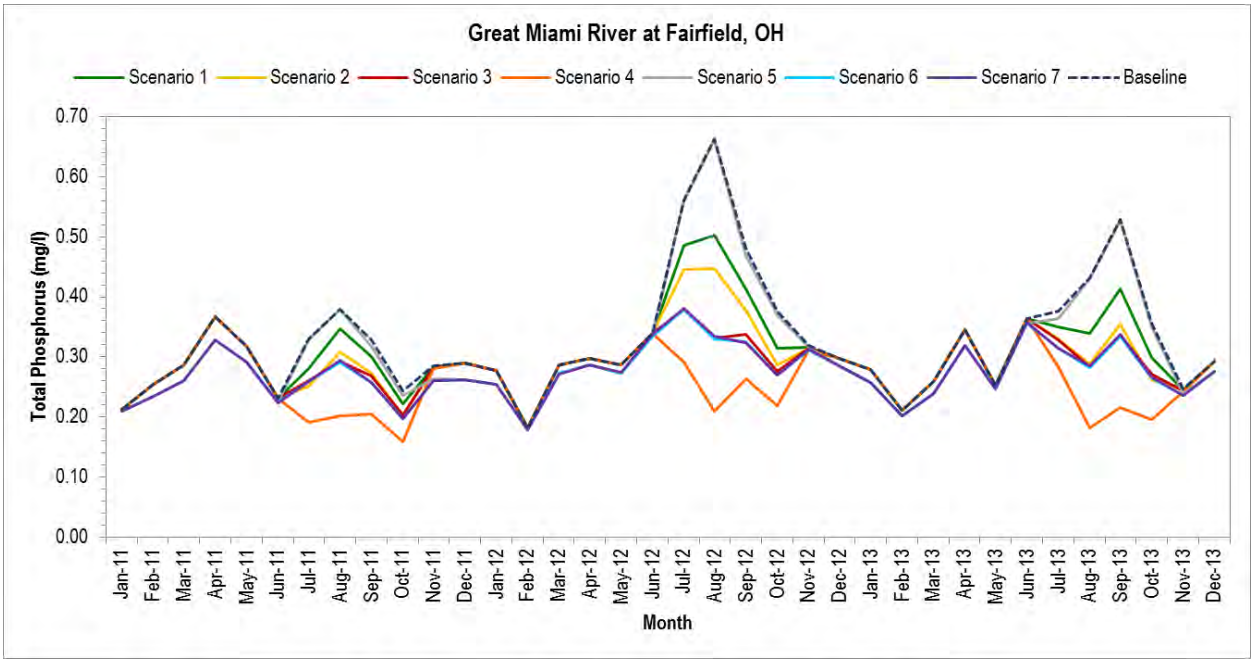

Figure 5-1. Monthly average TP time series comparison of the baseline conditions scenario and seven management scenarios for the Great Miami River at Fairfield, 2011-2013

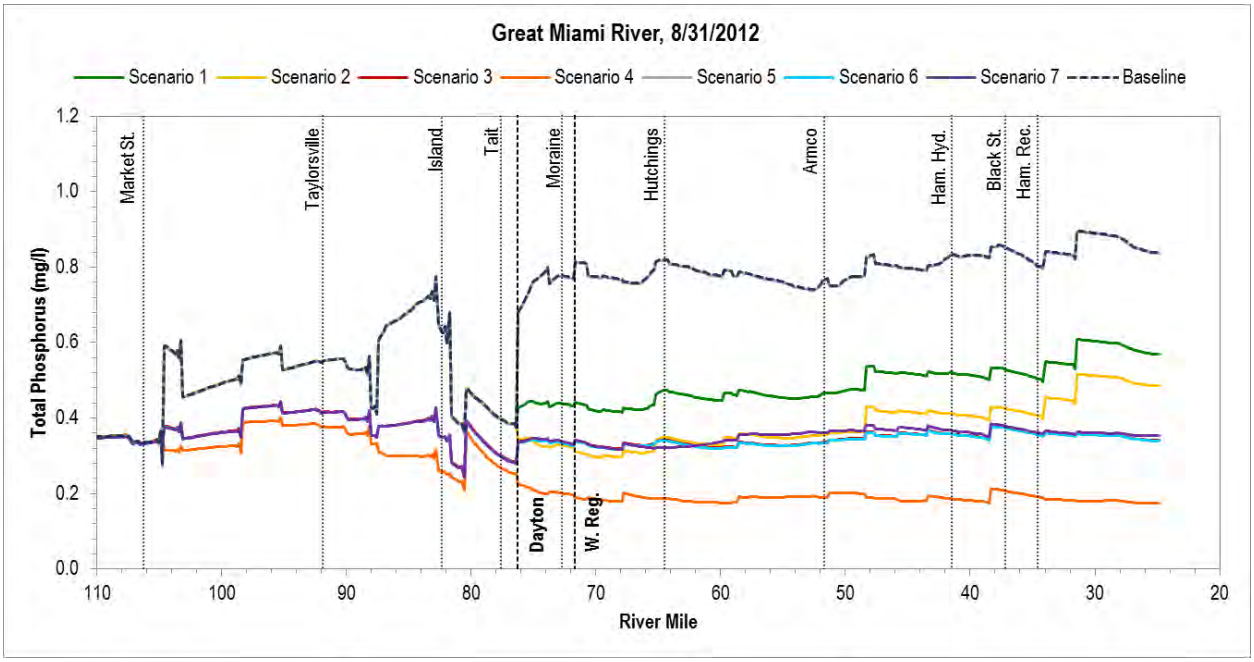

Figure 5-2. Longitudinal profile plot of TP for the baseline conditions scenario and seven management scenarios for the Great Miami River, 8/31/2012

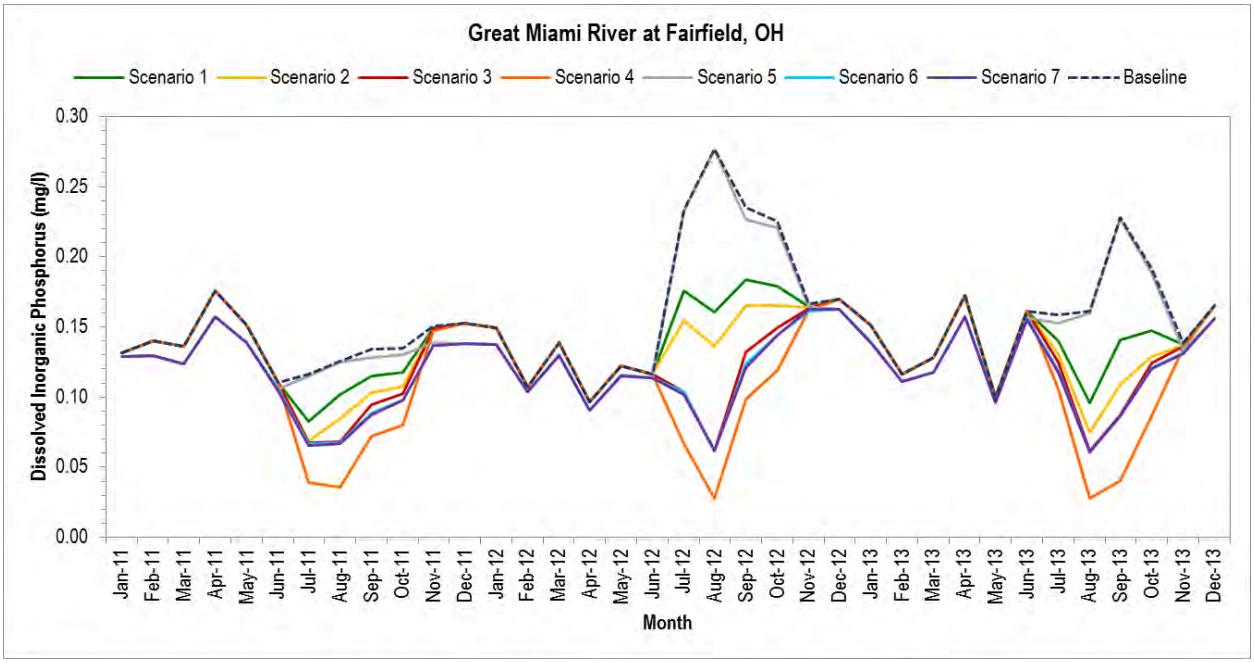

Figure 5-3. Monthly average DPO4 time series comparison of the baseline conditions scenario and seven management scenarios for the Great Miami River at Fairfield, 2011-2013

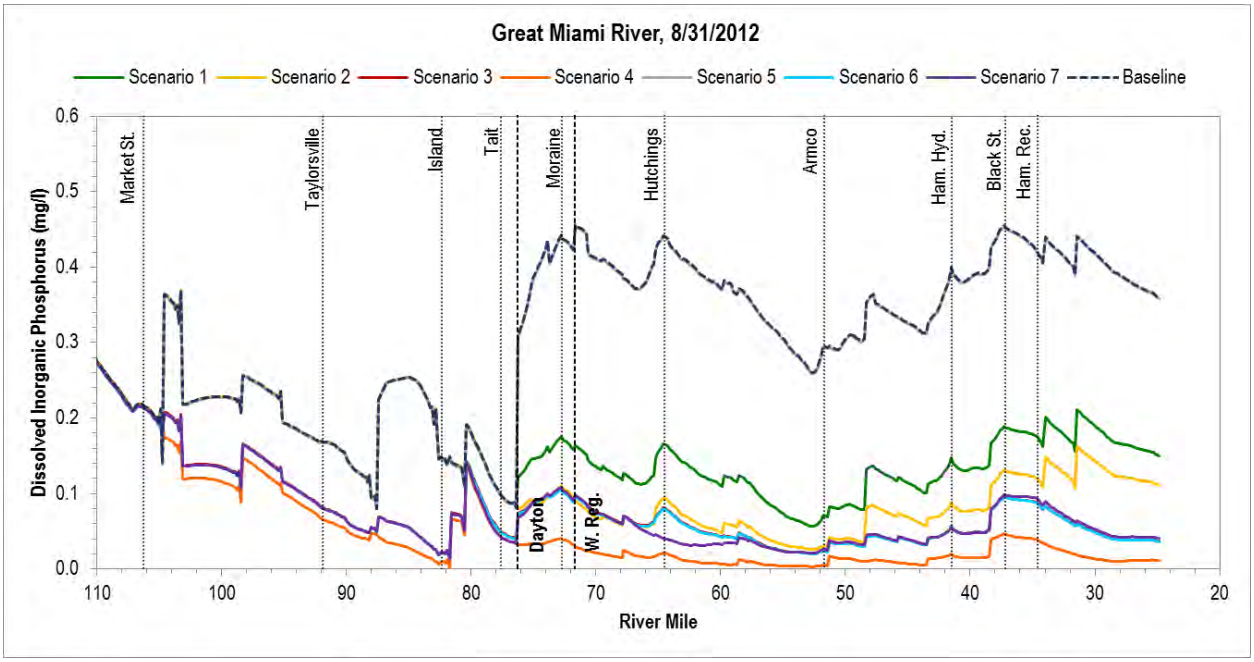

Figure 5-4. Longitudinal profile plot of DPO4 for the baseline conditions scenario and seven management scenarios for the Great Miami River, 8/31/2012

5.6.2 Dissolved Oxygen

Dissolved oxygen results for the seven scenarios are depicted in Figures 5-5 through 5-9. Monthly average DO results are depicted for the LGMR at Fairfield for the 2011 -2013 simulation period in Figure 5-5 and the monthly average daily DO diurnal range are plotted in Figure 5-7. Figures 5-6 and 5-9 show daily average DO and diurnal DO range over the entire modeled length of the river, respectively, for August 31, 2012. Daily (as opposed to monthly average) diurnal DO range is plotted for Fairfield from July 1, 2012 to November 2, 2012 in Figure 5-8. This period was chosen as the diurnal DO results showed the greatest variability between scenarios during this period.

The following observations can be made from these results:

- The phosphorus load reductions simulated in these scenarios results in almost no change in average DO between the scenarios for the LGMR at Fairfield.
- Scenario 4, which is the most extreme (and infeasible) scenario in terms of phosphorus reduction at WRRFs, resulted in the largest reduction of diurnal DO range, but this reduction was limited to a few mg/l change in the diurnal range and limited to brief periods of time.
- Scenario 7, the dam removal scenario, resulted in some local improvements in average DO and diurnal DO range, but also adversely effected DO in several locations. The adverse effect on daily average DO (i.e., lower average DO) was due primarily to (1) less settling of particulate organic material behind the dams, allowing them to stay in the downstream water column and consume DO, and (2) less settling of particulate material behind the dams, causing increased light extinction (and less production of DO) downstream of the dams.
- Summer diurnal DO ranges well above 10 mg/l are still predicted to occur for all scenarios for the LGMR at Fairfield.

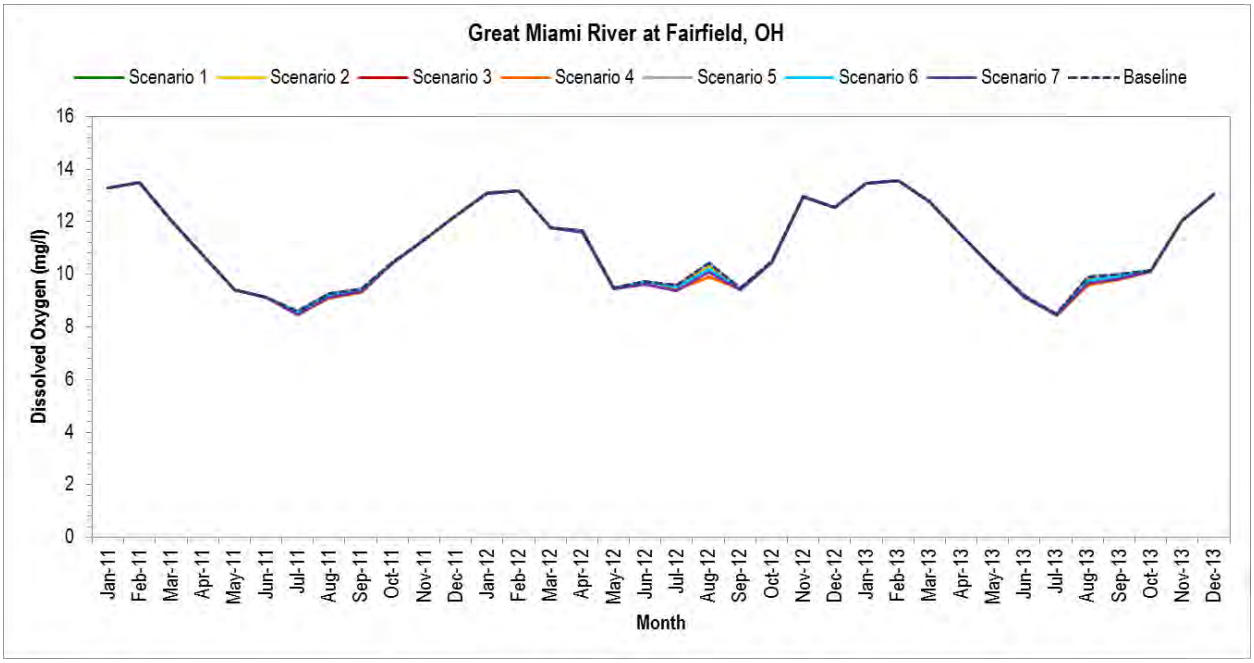

Figure 5-5. Monthly average DO time series comparison of the baseline conditions scenario and seven management scenarios for the Great Miami River at Fairfield, 2011-2013

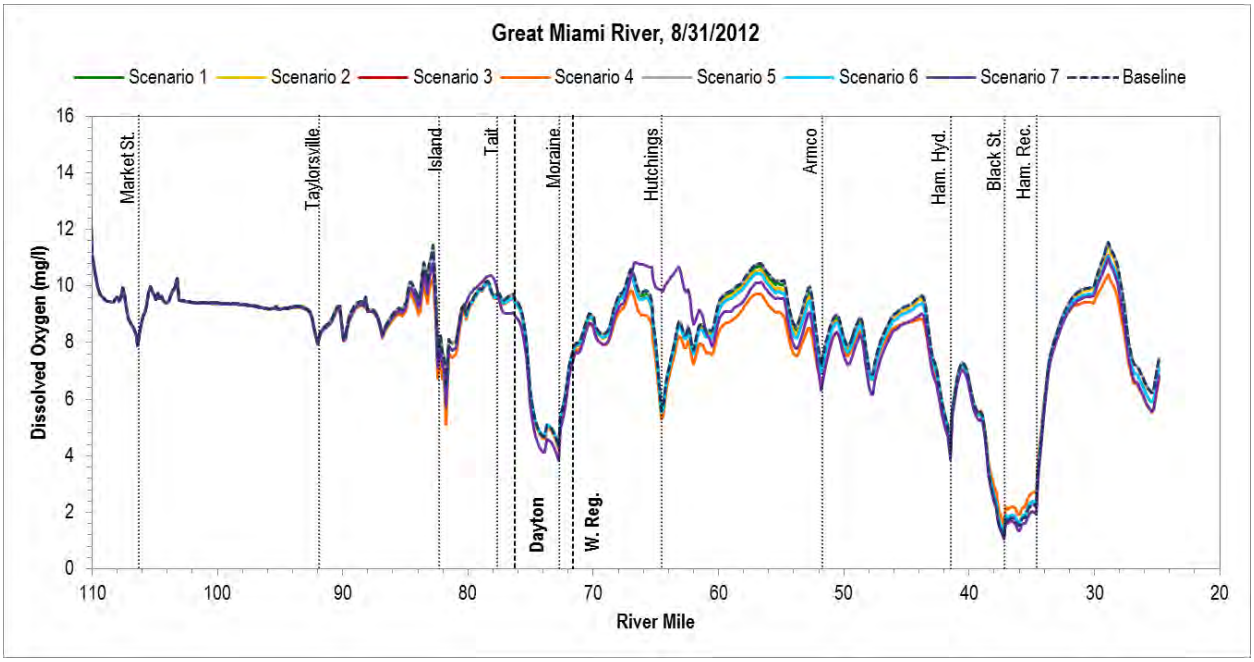

Figure 5-6. Longitudinal profile plot of DO for the baseline conditions scenario and seven management scenarios for the Great Miami River, 8/31/2012

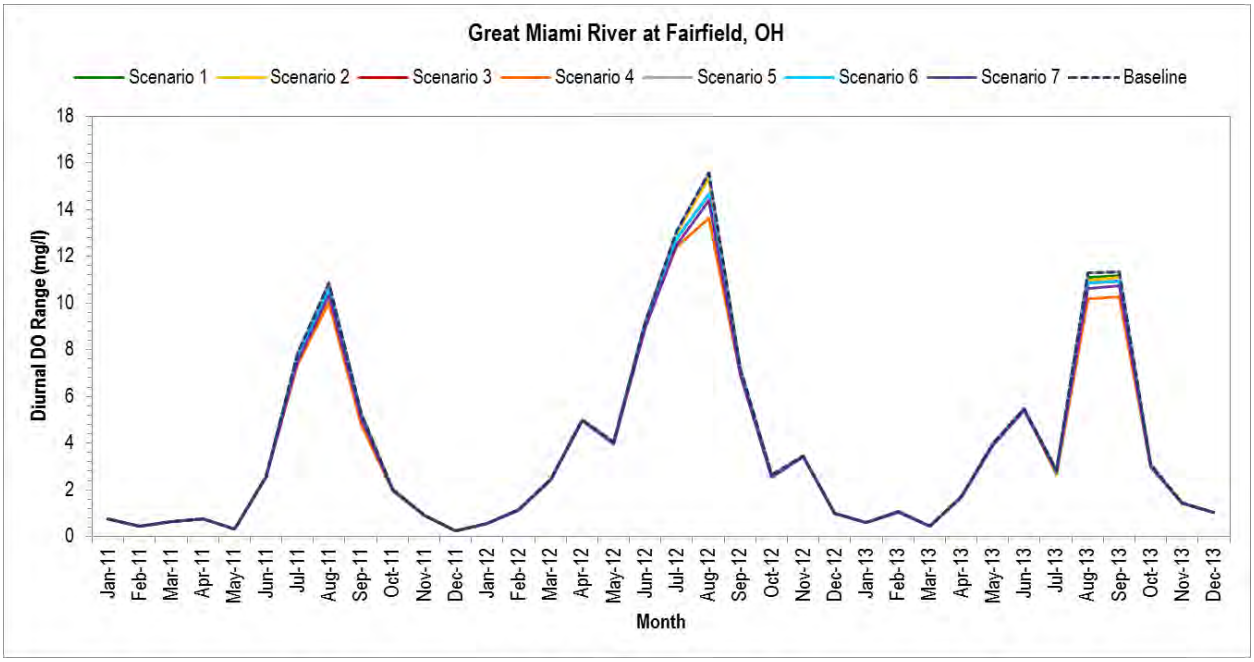

Figure 5-7. Monthly average daily diurnal DO range time series comparison of the baseline conditions scenario and seven management scenarios for the Great Miami River at Fairfield, 2011-2013

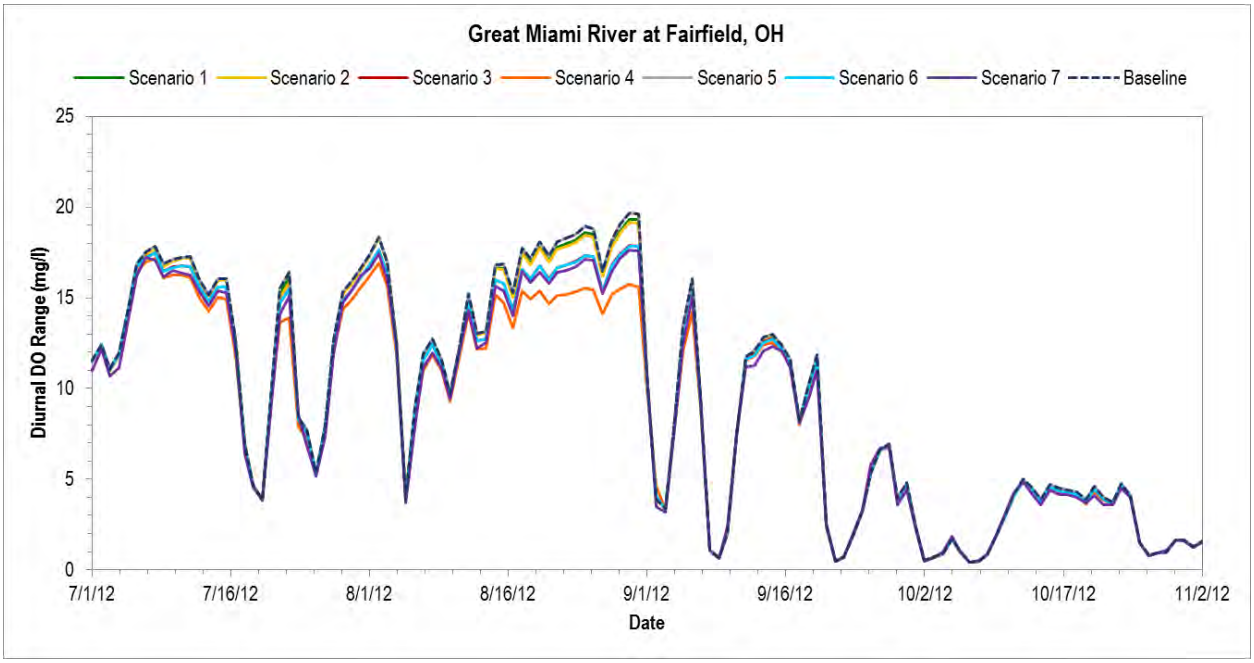

Figure 5-8. Daily diurnal DO range time series comparison of the baseline conditions scenario and seven management scenarios for the Great Miami River at Fairfield, summer 2012

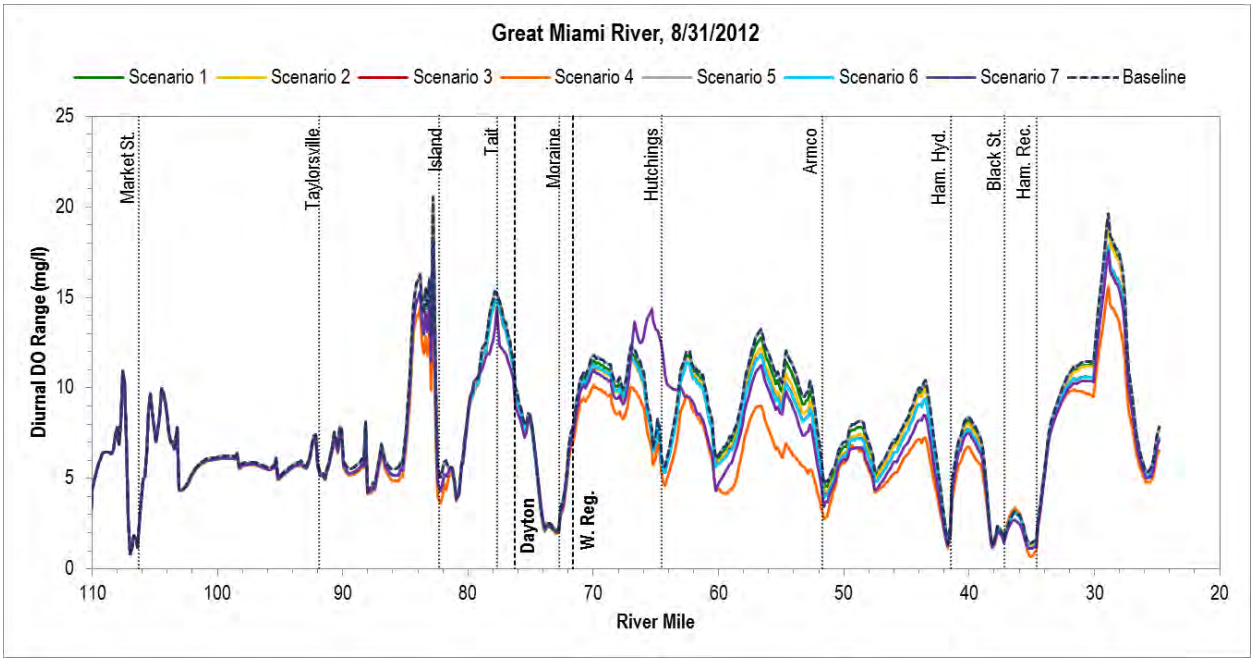

Figure 5-9. Longitudinal profile plot of diurnal DO range for the baseline conditions scenario and seven management scenarios for the Great Miami River, 8/31/2012

5.6.3 Sestonic Algae

Figures 5-10 and 5-11 depict the sestonic algae results for the seven scenarios. Figure 5-10 shows monthly average sestonic algae at Fairfield for the 2011 -2013 simulation period and Figure 5-11 shows daily average sestonic algae over the entire modeled length of the river on August 31, 2012.

The following observations can be made from these results:

- Scenario 4, which is the most extreme (and infeasible) scenario in terms of phosphorus reduction at WRRFs, resulted in the largest reduction in sestonic algae, but this reduction was limited to brief periods of time during late summer.
- Only Scenario 4 resulted in reducing sestonic algae (as chlorophyll) below 50 µg/l downstream of Dayton during summer.

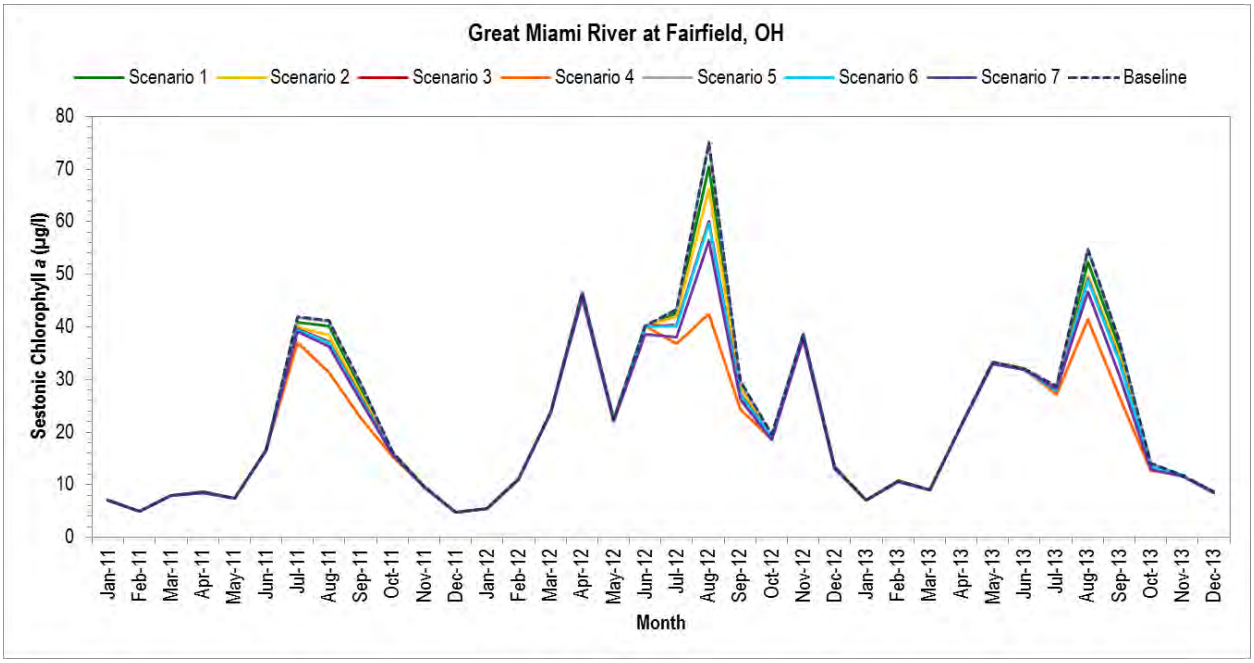

Figure 5-10. Monthly average sestonic algae chlorophyll *a* time series comparison of the baseline conditions scenario and seven management scenarios for the Great Miami River at Fairfield, 2011-2013

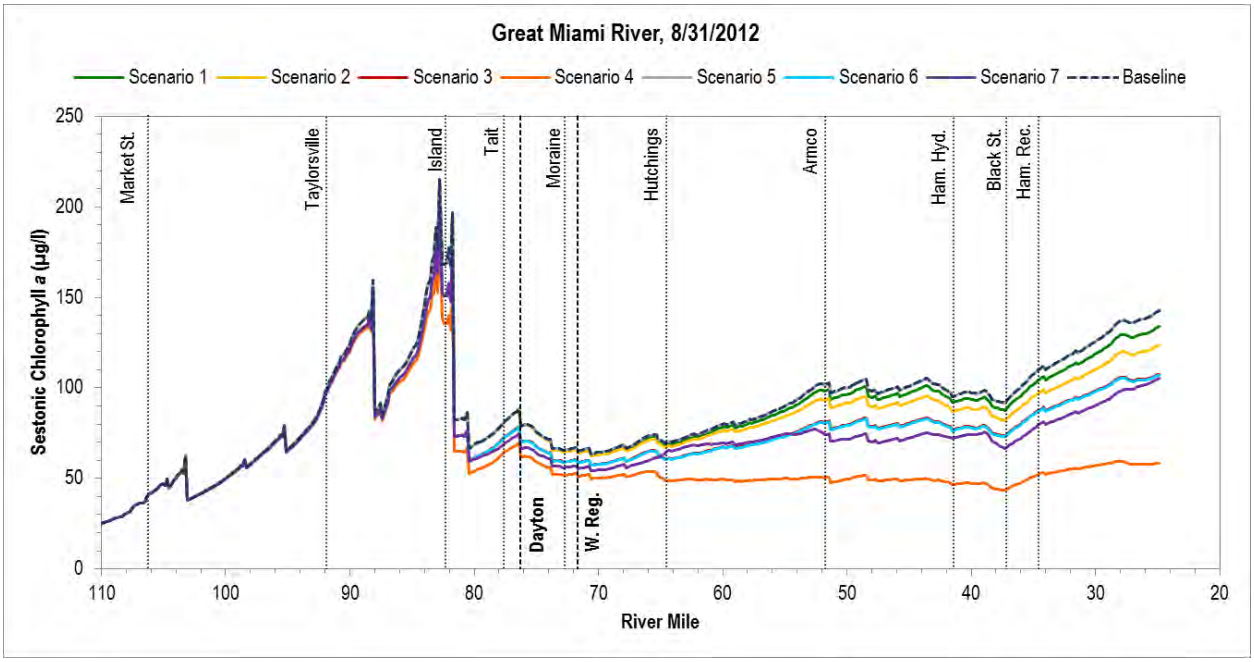

Figure 5-11. Longitudinal profile plot of sestonic algae chlorophyll *a* for the baseline conditions scenario and seven management scenarios for the Great Miami River, 8/31/2012

5.6.4 Benthic Algae

Figures 5-12 and 5-13 depict the benthic algae results for the seven scenarios. Figure 5-12 shows monthly average benthic algae at Fairfield for the 2011 -2013 simulation period and Figure 5-13 shows daily average benthic algae over the entire modeled length of the river on August 31, 2012.

The following observations can be made from these results:

- Differences in simulated monthly average benthic algae for the LGMR at Fairfield between all seven scenarios and the baseline are almost negligible, as shown in Figure 5-12.
- Scenario 4, which is the most extreme (and infeasible) scenario in terms of phosphorus reduction at WRRFs, resulted in the largest reduction in benthic algae at some locations as shown in Figure 5-13.
- Although slight reductions in benthic algae are predicted at some locations, increases are predicted at others (note results between RM 35-37 and, to lesser degree, RM 25-27 in Figure 5-13). This model-predicted increase in benthic algae is likely due to the greater light penetration occurring as a result of reduced sestonic algae.
- Scenario 7, the dam removal scenario, resulted in adverse effects (i.e., increase in benthic algae) behind the Tait Station and Hutching Station dams due to lower water depths and greater light penetration, but decreased benthic algae downstream of the dams due to less settling of particulate material behind the dams, causing increased light extinction.

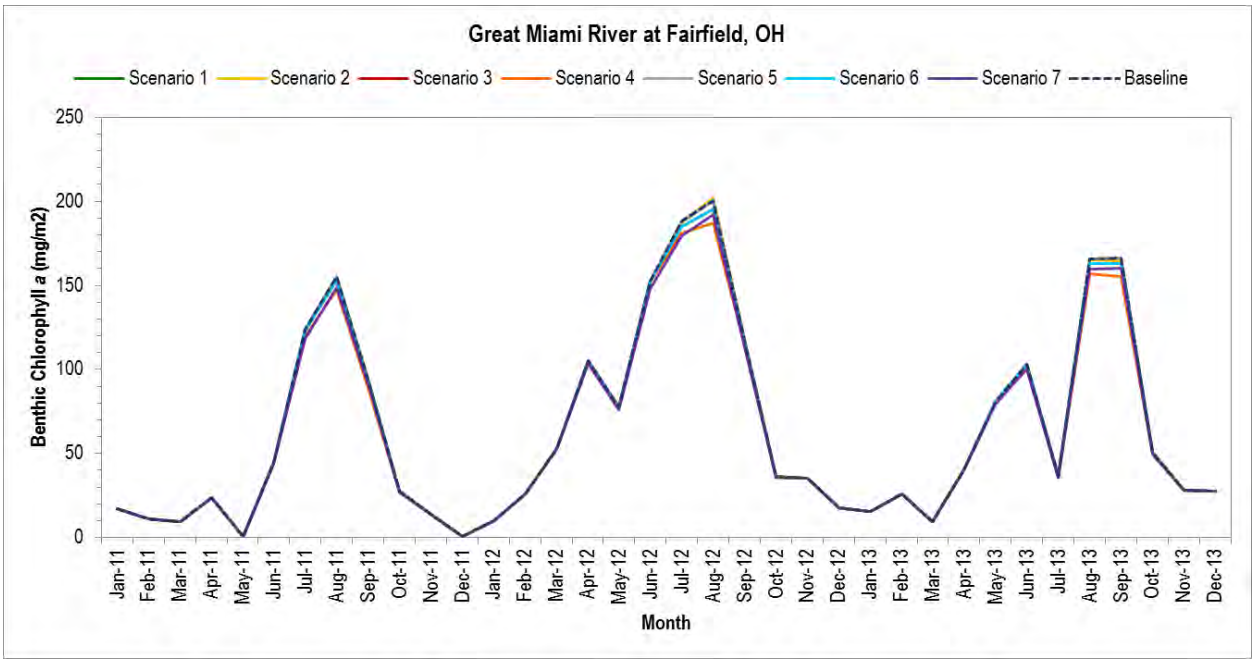

Figure 5-12. Monthly average benthic algae chlorophyll *a* time series comparison of the baseline conditions scenario and seven management scenarios for the Great Miami River at Fairfield, 2011-2013

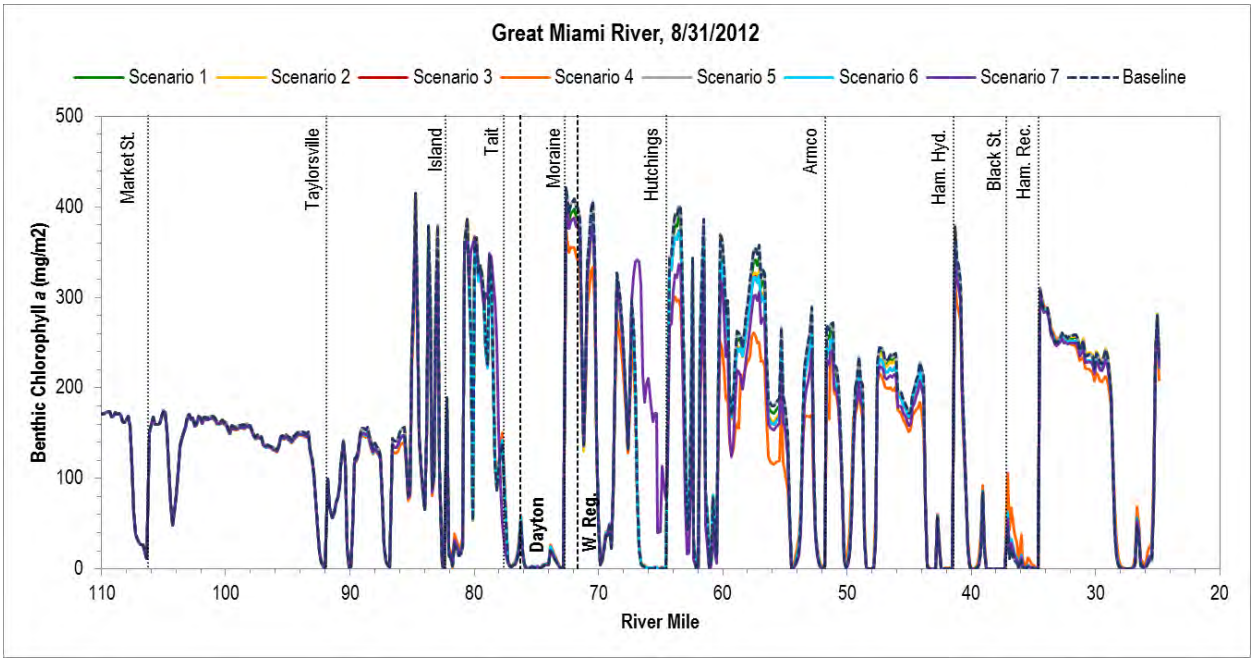

Figure 5-13. Longitudinal profile plot of benthic algae chlorophyll *a* for the baseline conditions scenario and seven management scenarios for the Great Miami River, 8/31/2012

5.7 Model Sensitivity for Key Algal Parameters

Sensitivity simulations were conducted with the calibrated water quality model to investigate the relative importance of key model input parameters on model behavior and predictions. Model inputs tested included the sestonic algal maximum theoretical growth rates and benthic algal P half-saturation constants (internal and external) and are described in Table 5-2. Sensitivity of the model to benthic algal P half-saturation constant values was only evaluated for Scenario 6 (and not the baseline) because the system rarely experiences P-limitation during baseline conditions.

Sensitivity of the model to sestonic algal P half-saturation constant was not evaluated because the baseline model input value, 5 µg-P/l, represented the maximum of recommended literature ranges (Chapra, 1997; Thomann and Mueller, 1987). This indicates that the current model calibration represent the expected upper bound in terms sensitivity to nutrient load reductions. Lowering the sestonic algal P half-saturation constant would have resulted in less system response to the external P load reduction scenarios, which was not of interest for this particular exercise.

The sensitivity values for the maximum theoretical growth rate was set at 3.0/day for all algal groups, as prior sensitivity runs had demonstrated that growth rates on this order were necessary to accurately simulate the high sestonic chlorophyll *a* levels observed in 2013 (albeit at the expense of over-predicting 2011 and 2012 sestonic chlorophyll *a* levels.) It can be deemed representative of a "worst case" condition in terms of algal growth potential. The sensitivity values for the benthic algae half-saturation constants were set at the maximum values of their expected ranges reported by Flynn et al. (2013), which represents their expected upper bound in terms sensitivity to nutrient load reductions.

Table 5-2. Details on model input parameter sensitivity tests conducted

Model Input Sensitivity Tested	Simulations Tested	Calibrated Values	Sensitivity Values
Maximum theoretical growth rates of blue-green algae, diatoms, and summer assemblage (greens)	Baseline Scenario 6	K_c, blue-greens= 2.2 day^{-1} K_c, diatoms= 2.6 day^{-1} K_c, greens= 2.4 day^{-1}	K_c, blue-greens= 3.0 day^{-1} K_c, diatoms= 3.0 day^{-1} K_c, greens= 3.0 day^{-1}
Benthic algae half-saturation constants for external P (K_{mPb}) and intracellular P (K_{qPb})	Scenario 6	K_{mPb} = 125 µg-P/l K_{qPb} = 0.00325 mg-P/mg-C	K_{mPb} = 175 µg-P/l K_{qPb} = 0.000625 mg-P/mg-C

Results of the sensitivity simulations demonstrated that both the baseline scenario and scenario 6 were very sensitive to increasing the sestonic algal maximum theoretical growth rates to 3.0 day^{-1} relative to the calibrated model input simulations (Figure 5-14). The simulated July-September sestonic chlorophyll *a* concentrations for the sensitivity run were on average over two times higher than the baseline run throughout the LGMR domain. The relative difference in simulated chlorophyll *a* between the baseline and scenario 6 was compared for both the sensitivity runs and the simulations using the calibrated values to understand the implications on model use for informing management decisions. While the simulated chlorophyll *a* concentrations under the scenario 6 loading reductions showed a larger relative change to the baseline concentrations under the sensitivity run (Table 5-3), the overall conclusions from the P loading reduction scenario remain unchanged. Namely, even under the management scenario that simulated the second largest July-October external P load reduction of the scenarios considered, enrichment indicators showed relatively marginal improvement.

Results of the sensitivity simulation for benthic algal P half-saturation constants showed more substantial differences in simulated benthic algae densities and diurnal DO ranges. For example, Figures 5-15 and 5-16 show the monthly average benthic chlorophyll *a* density (for 2011-13) and the daily diurnal DO range (for July-October, 2012), respectively, at Fairfield. While the benthic biomass simulated at Fairfield under scenario 6 was similar to the baseline scenario, the sensitivity simulation for scenario 6 produced a roughly 20% reduction in biomass during the peak growth months in the summer. Similarly, the reductions for diurnal DO range were more significant and occurred over longer time intervals than for scenario 6 simulation based on the original half-saturation parameters. For example, the only notable reductions (10-15%) in diurnal DO range for scenario 6 are observed during the latter half of August, 2012. In contrast, the scenario 6 sensitivity indicates reductions of roughly 20-25% during most of the July through mid-September period for 2012.

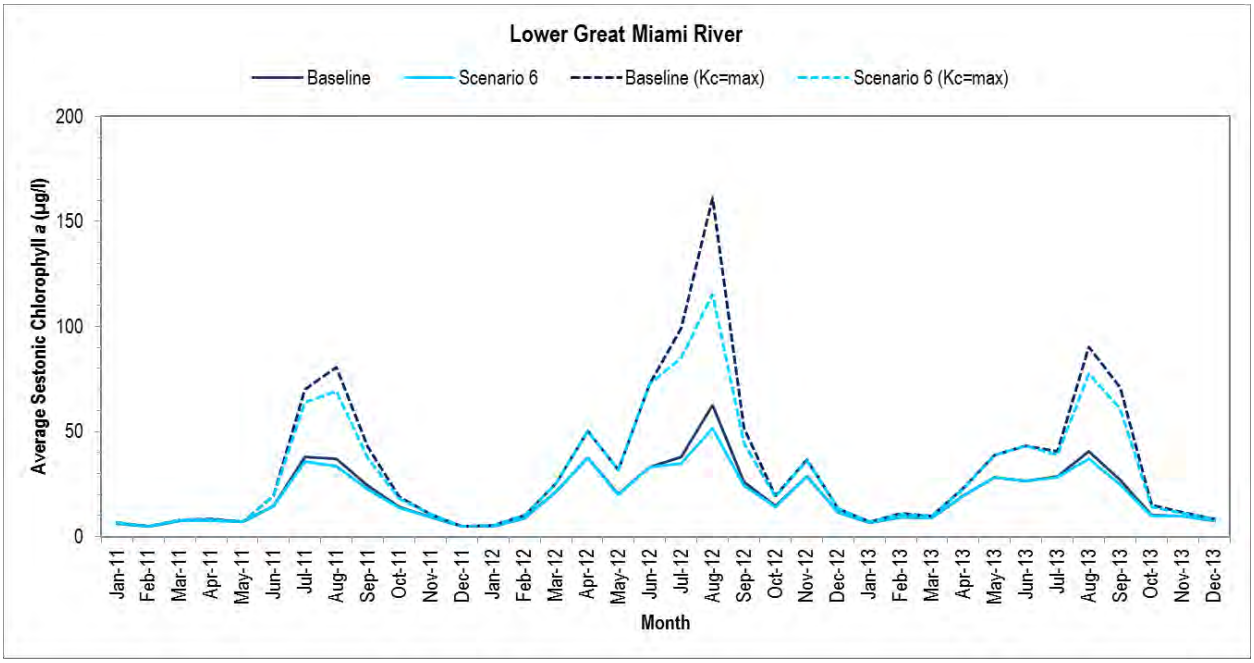

Figure 5-14. Monthly time series comparison of simulated sestonic algal chlorophyll *a* concentrations averaged over the entire LGMR for the baseline conditions scenario and scenario 6 using calibrated maximum theoretical algal growth values (solid lines) and two sensitivity runs (dashed lines)

Table 5-3. Monthly average simulated sestonic algal chlorophyll *a* concentrations (µg/l) averaged over the entire LGMR for the baseline conditions scenario and scenario 6 using calibrated maximum theoretical algal growth values and two sensitivity runs

Month	Calibrated Model			Sensitivity Runs		
	Baseline	Scenario 6	Relative Change	Baseline (Kc=max)	Scenario 6 (Kc=max)	Relative Change
Jul 2011	37.7	35.8	-5%	70.2	63.9	-9%
Aug 2011	36.8	33.7	-8%	80.5	69.3	-14%
Sep 2011	24.1	22.3	-7%	42.8	37.6	-12%
Oct 2011	14.1	13.8	-2%	18.9	18.3	-3%
Jul 2012	37.7	34.8	-8%	99.1	85.0	-14%
Aug 2012	62.5	51.6	-17%	161.2	115.3	-29%
Sep 2012	26.2	24.5	-7%	51.5	44.4	-14%
Oct 2012	14.4	14.1	-2%	19.3	18.9	-2%
Jul 2013	28.9	28.1	-3%	40.4	38.7	-4%
Aug 2013	40.6	37.2	-8%	90.4	77.6	-14%
Sep 2013	27.1	24.7	-9%	71.1	60.7	-15%
Oct 2013	10.0	9.7	-3%	14.9	14.1	-5%

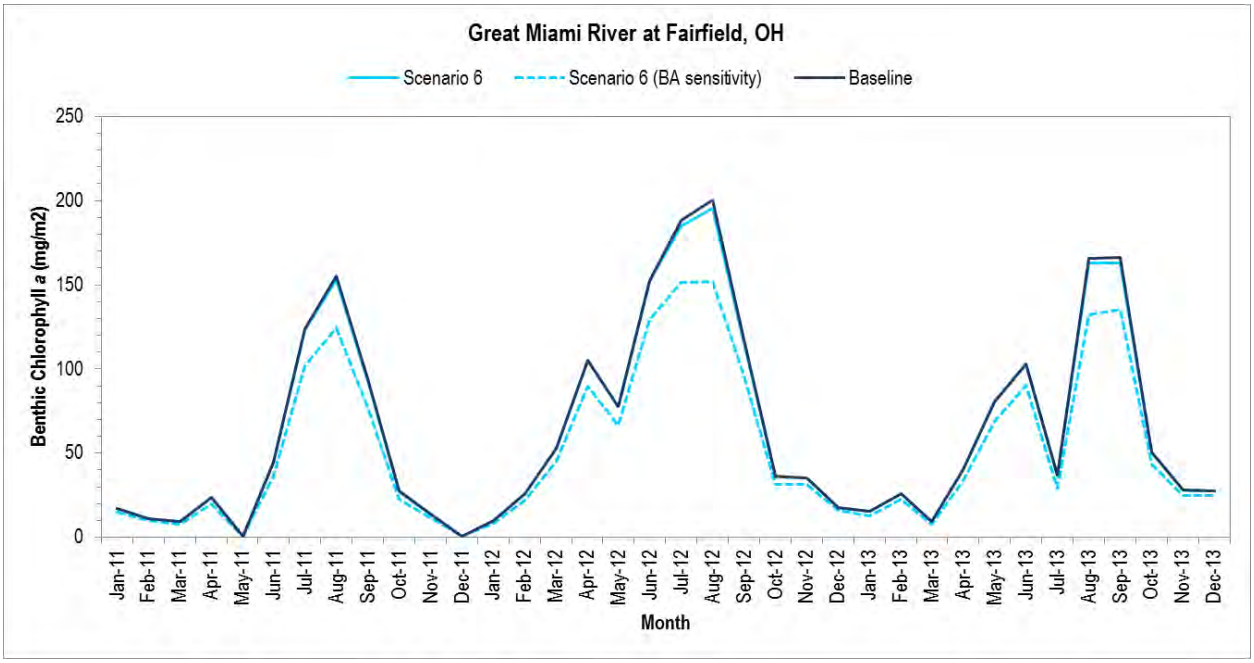

Figure 5-15. Monthly time series comparison of simulated benthic algal chlorophyll *a* densities for the Great Miami River at Fairfield for the baseline conditions scenario and scenario 6 using calibrated maximum theoretical algal growth values (solid lines) and sensitivity run (dashed line)

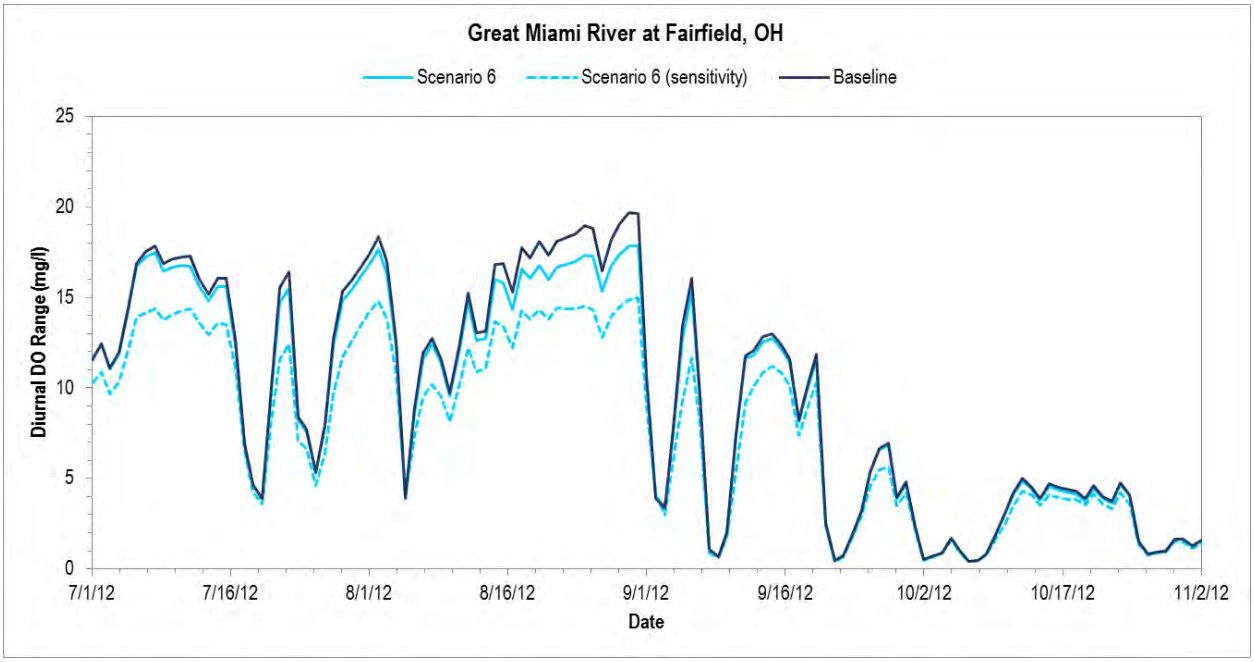

Figure 5-16. Daily time series comparison of simulated diurnal DO range for the Great Miami River at Fairfield for the baseline conditions scenario and scenario 6 using calibrated benthic algae P half-saturation values (solid lines) and sensitivity run (dashed line)

Overall, the sensitivity results demonstrate that the LGMR water quality model is highly sensitive to both algal maximum growth rates and the half-saturation parameters for benthic algae. However, only the half-saturation parameters for benthic algae significantly affect the relative reductions in biomass and diurnal DO range simulated by the model for load reduction scenarios. The sensitivity of the model to the half-saturation parameters is limited to conditions where nutrient reduction strategies result in significantly lower dissolved inorganic P (DPO4) concentrations in the river(i.e., to < 50 µg/l); however, these are the conditions of greatest interest with respect to management objectives. Given the importance of the half-saturation parameters and lack of opportunity to calibrate these parameters under present-day nutrient loading conditions, a laboratory study utilizing mesocosms experiments would be most appropriate for addressing the uncertainty with these parameters.

Blank

6 Findings and Recommendations

The main findings and recommendations of this study are presented in this section.

6.1 Findings and Results

The work conducted in this study and documented in this report supports the following key findings and results:

- The calibrated LGMR water quality model provides a reasonably accurate representation of the system and is as good a water quality model as can be accomplished given the available data. The model framework and calibration are robust, scientifically sound and were developed based on good modeling practices.
- Although calibration of the LGMR water quality model can potentially be improved in the future with collection of additional data (see Section 6.2), the current calibrated model is appropriate for use in comparatively evaluating nutrient load reduction scenarios.
- While both sestonic and benthic algae contribute to the large diurnal DO variations observed in the LGMR, benthic algae production and respiration appear to be the most significant drivers of diurnal DO range based on available data and model predictions.
- The current cumulative phosphorus loading to the LGMR is so large that even after drastic reductions in phosphorus loading are simulated, including the elimination of phosphorus in effluent from major WRRFs, significant improvements in DO and algal growth are not predicted.
- Information developed as part of this project indicates that lateral variability of DO up to 6 mg/l can occur concurrently in the LGMR. This indicates that a DO measurement at a single point in the river cannot be assumed to be representative of DO across the entire river, which is significant for two reasons:
    1. It means that the LGMR water quality model, which represents laterally-averaged conditions in the river, can never be expected to reproduce data at a single point precisely.
    2. The single-point measurement are not appropriate for determining attainment of water quality standards or other water quality endpoints, where this lateral variability in DO occurs.

The recommendations in the following section stem mainly from the above findings.

6.2 Recommendations for Future Work

Although a great deal of data have been collected from the LGMR, our understanding of the river and our ability to model dissolved oxygen and algal growth in it would be improved with some additional data collection, as identified below:

- Reaeration rate – Reaeration rate is the rate of oxygen exchange between the river and the atmosphere, and it is a both significant and uncertain variable in the model with respect to dissolved oxygen endpoints. The reaeration rate is highly variable in nature and although

equations have been developed to estimate it, they provide a range of values and there is not always agreement between estimation methods. While challenging to measure in a large river, the information provided from a carefully designed reaeration study would be very valuable and would improve our ability to accurately model DO spatial and temporal dynamics in the LGMR.

- Light extinction coefficient – As discussed in Section 3.3.5 of this report, the light extinction coefficient in the model has a strong influence on the growth rates of sestonic and benthic algae. No field data were identified to quantify light extinction in the LGMR during this project. Direct measurement of photosynthetically active radiation (PAR) with, at a minimum, concurrent TSS and chlorophyll *a* measurements would be very useful in refining this component of the model.
- Lateral variability – As discussed in Section 4.2.3 and Appendix E, significant lateral (i.e., cross-channel) variability in concurrent DO was observed at Miamisburg in 2016. However these observations were made at a single location on one day. Investigation of multiple locations under a range of flow conditions would show whether this is a localized phenomenon or a common condition.
- Chlorophyll sonde accuracy – A better understanding of the accuracy of chlorophyll *a* measurements taken using YSI sondes versus laboratory analysis of sestonic chlorophyll *a* samples would be useful in terms of guiding the use of these data to support model calibration.

The data recommendations identified above are the most significant at this point, with respect to reducing model uncertainty and improving confidence in the model. Several other data recommendations can be considered secondary to those above and include:

- Monitor chlorophyll *a* at tributary mouths downstream of Dayton (e.g., Wolf Creek, Twin Creek, Four Mile Creek) to support specification of sestonic algal biomass concentrations associated with inflows from these water bodies;
- Conduct a mesocosm study to determine optimal algal growth rates and establish nutrient limitation parameters (e.g., the half-saturation parameters discussed in Section 5.7);
- Characterize riparian shading to identify reaches where this could be a significant factor influencing light availability;
- Collect additional benthic algae data; and
- Develop improved characterization of location and extent of soft sediment.

7 References

Anchor QEA, 2009. Colorado River Environmental Models. Phase 2: Lake Travis. Prepared for: Lower Colorado River Authority, Austin, TX. March 18, 2009.

Bierman, V.J., J. Kaur, J.V. DePinto, T.J. Feist, and D.W. Dilks. 2005. "Modeling the Role of Zebra Mussels in the Proliferation of Blue-green Algae in Saginaw Bay, Lake Huron." J. Great Lakes Res. 31:32-55.

Brown, L. C. and T. O. Barnwell, Jr., 1987. The enhanced stream water quality models QUAL2E and QUAL2E-UNCAS: Documentation and User Manual. Tufts University and US EPA, Athens, Georgia.

Chapra, S.C. 1997. *Surface Water-Quality Modeling*. McGraw-Hill Companies, Inc.

Chapra, S.C., Pelletier, G.J. and Tao, H. 2012. QUAL2K: A Modeling Framework for Simulating River and Stream Water Quality, Version 2.12: Documentation and Users Manual. Civil and Environmental Engineering Dept., Tufts University, Medford, MA.

Covar, A.P. 1976. "Selecting the Proper Reaeration Coefficient for Use in Water Quality Models." Presented at the U.S. EPA Conference on Environmental Simulation and Modeling. April 19-22, 1976, Cincinnati, OH.

DePinto, J.V., V.J. Bierman Jr., D.W. Dilks, P.E. Moskus, T.A.D. Slawecki, C.F. Bell, W.C. Chapra, K.F. Flynn. 2013. Modeling Guidance for Developing Site-Specific Nutrient Goals. Final Technical Report for Water Environment Research Foundation (WERF).

DePinto, J.V., H. Holmberg, T. Redder, E. Verhamme, W. Larson, N.J. Senjem, H. Munir. 2009a. Linked hydrodynamic –sediment transport – water quality model for support of the Upper Mississippi River – Lake Pepin TMDL. Proceedings of the WEF Specialty Conference: TMDL 2009. Minneapolis, MN. August 9-12, 2009.

DePinto, J.V., M.T. Auer, T.M. Redder, E. Verhamme. 2009b. "Coupling the Great Lakes Cladophora Model (GLCM) with a whole lake Advanced Eutrophication Model (A2EM-3D)." Presented at 52nd Annual Conference on Great Lakes Research, University of Toledo, Toledo, OH (May 18- 22, 2009).

Di Toro, D. M., P. R. Paquin, K. Subburamu, and D. A. Gruber. "Sediment Oxygen Demand Model: Methane and Ammonia Oxidation." *J. Environ. Engr. Div. ASCE* 116(5):945-986.

Donigian, A. S., Jr. 2002. Watershed model calibration and validation: The HSPF experience. In Proc. WEF Natl. TMDL Science and Policy, 44-73. Alexandria, Va.: Water Environment Federation.

EPA (U.S. Environmental Protection Agency). 1994b. Report of the Agency Task Force on Environmental Regulatory Modeling: Guidance, Support Needs, Draft Criteria and Charter. EPA-500-R-94-001. Washington, D.C.: U.S. Environmental Protection Agency.

FEMA, 2005. Flood Insurance Study: Montgomery County, Ohio and Incorporated Areas. Effective January 6, 2005. #39113CV000A.

Flynn, K.F., S.C. Chapra, and M.W. Suplee. 2013. "Modeling the lateral variation of bottom-attached algae in rivers." *Ecological Modeling*: 267 (2013), p. 11-25.

HydroQual. 2004. "User's Guide for RCA (Release 3.0)." June.

LimnoTech. 2009. Upper Mississippi River –Lake Pepin Water Quality Model: Development, Calibration, and Application. Prepared for the Minnesota Pollution Control Agency. July 2009.

Miami Conservancy District, 2016. Flood Protection: MSD System. Website accessed 6/17/2016 at http://www.miamiconservancy.org/flood/dams.asp

Moriasi, D.N., Arnold, J.G., Van Liew, M.W., Bingner, R.L., Harmel, R.D. and T.L. Veith. 2007. Model evaluation guidelines for systematic quantification of accuracy in watershed simulations. Transactions of the American Society of Agricultural and Biological Engineers (ASABE), 50(3):885-900

National Oceanic and Atmospheric Administration (NOAA). 2016. National Climatic Data Center (NCDC). URL: http://www.ncdc.noaa.gov/. Accessed [May 2016].

Ohio Environmental Protection Agency (OEPA, 2013). Ohio Nutrient Reduction Strategy. OEPA Division of Surface Water. June 28, 2013.

Ohio Environmental Protection Agency (OEPAa). National Pollutant Discharge Elimination System (NPDES) Permit Program Fact Sheet Regarding an NPDES Permit To Discharge to Waters of the State of Ohio for Dayton Wastewater Treatment Plant (Revised 11/24/15).

Ohio Environmental Protection Agency (OEPAb). National Pollutant Discharge Elimination System (NPDES) Permit Program Fact Sheet Regarding an NPDES Permit To Discharge to Waters of the State of Ohio for the Western Regional Water Reclamation Facility (Revised 11/24/15).

TetraTech, Inc. 2007a. "The Environmental Fluid Dynamics Code User Manual: USEPA Version 1.01." June. URL: http://www.epa.gov/ceampubl/swater/efdc/EFDC-dl.html.

TetraTech, Inc. 2007b. "The Environmental Fluid Dynamics Code Theory and Computation – Volume 1: Hydrodynamics and Mass Transport." June. Fairfax, VA.

USGS, 1966. Time of Travel of Water in the Great Miami River. Dayton to Cleves, Ohio. June 1966.

U.S. Naval Observatory (USNO). 2016. Astronomical Applications Department, Duration of Daylight/Darkness Tables. URL: http://aa.usno.navy.mil/data/docs/Dur_OneYearphp. Accessed [July 2016].

Verhamme, E.M., J.V. DePinto, T.M. Redder, D. Rucinski. 2009. "Development of a linked fine-scale hydrodynamic and ecosystem model for assessing the impact of multiple stressors in Saginaw Bay, Lake Huron. Presented at 52nd Annual Conference on Great Lakes Research, University of Toledo, Toledo, OH (May 18- 22, 2009).

Verhamme, E.M., T.M. Redder, D.A. Schlea, J. Grush, J.F. Bratton, and J.V. DePinto. 2016. "Development of the Western Lake Erie Ecosystem Model (WLEEM): Application to connect phosphorus loads to cyanobacteria biomass." *Journal of Great Lakes Research*. In press, available online October 4. URL: http://www.sciencedirect.com/science/article/pii/S0380133016301770.

Appendix A:
Data Summary and Gap Analysis Memo

Blank

LimnoTech
Water Environment | Scientists Engineers

501 Avis Drive
Ann Arbor, MI 48108
734.332.1200
www.limno.com

Memorandum

From:	Carrie Turner	**Date:**	June 27, 2016
		Project:	Lower Great Miami River Nutrient Management Project
To:	Sarah Hippensteel (MCD)	**CC:**	Mike Ekberg (MCD)

SUBJECT: Lower Great Miami River Dataset Inventory and Quality Review – FINAL

Summary

This memo presents an inventory and review of data relevant to the development of a water quality model of the Lower Great Miami River (Figure 1) and is a necessary initial step in that model development process. LimnoTech has compiled and reviewed the readily available data provided by Miami Conservancy District (MCD), the Water Resource Recovery Facilities (WRRFs), and the Ohio Environmental Protection Agency (OEPA) as well as from commonly used data clearinghouses such as the Water Quality Portal and the Permit Compliance System (PCS). The objective of this task is to inventory the amount and types of data and review the datasets and their associated quality, to support the following project activities:

- Assessment of watershed characteristics;
- Selection of an appropriate water quality model platform;
- Identification of potential model calibration locations based on data availability; and
- Identification of data gaps that may adversely affect the development and calibration of the model and thus its reliability for application to management scenarios.

The Great Miami River and its tributaries are a well-studied system with sampling dating back several decades. LimnoTech has compiled measured data describing in-stream surface water quality, sediment quality, hydraulics, biological community health (fish and macroinvertebrates), habitat, floating (sestonic) and fixed (benthic) algae levels, groundwater quality, point source discharge characteristics, and stream geomorphometry. Data for the entire Great Miami River (GMR) watershed were considered to inform not only the water quality model development and calibration, but also to inform the development of a watershed model that will be used to specify upstream and tributary flows and nutrients loads as well as to simulate scenarios that consider controls for a mixture of sources. Data spanning roughly the last 15-20 years (1996 – 2015) were obtained. The focus of this data effort was on data directly related to issues associated with dissolved oxygen and algal development in the LGMR, as well as hydrologic and hydraulic data. Over 1,300,000 records have been reviewed and compiled in a project database (Table 1). Most of these observations are within the lower portion of the LGMR that will be represented in the water quality model (roughly the lower 110 miles of the LGMR, the lower 13 miles of the Stillwater River and the lower 6 miles of the Mad River).

Table 1. Summary of Available Data Reviewed and Compiled for the LGMR Project.

Sample Media	Count of Compiled Observations (Great Miami River Watershed)	Count of Compiled Observations (Lower Great Miami River Potential Water Quality Model Domain)
In-stream flow	133,596	49,850
Surface water quality[a]	1,331,540	1,111,366
Sediment quality	906	311
Biological/Habitat[b]	1,440	1,440
Point source discharge	45,549	30,243
Groundwater quality[b]	4,329	4,329

[a] Continuous monitoring data from sondes located within the Lower Great Miami River watershed were compiled and reviewed.
[b] Locations within the Lower Great Miami River watershed were compiled and reviewed.

LimnoTech has also compiled spatial datasets using Geographic Information Systems (GIS) to complement the measured data in characterizing the watershed and informing the development of the water quality model. In addition, information on river bathymetry, dam features, and in-stream transport has also been acquired and reviewed.

The data were taken through a simple quality assurance/quality control (QA/QC) review that was focused on identifying unreasonable values (e.g. negative pH, etc.) and unreasonable relationships (e.g. ortho-phosphate concentration higher than total phosphorus concentration). Erroneous data were rejected. The results of this task indicate that the data are generally of high quality (less than 1% of overall data were rejected) and there are extensive data for calibrating the water quality model and informing the development of watershed loads.

The data described in this memo been reviewed by the project team to determine whether there are significant data gaps with respect to constructing and calibrating the water quality model and the model/methods used to specify upstream/tributary conditions. As a result, three potential data gaps were identified:

1. Bathymetry
2. Light extinction information
3. Process data for calibration

These gaps will not affect the model development or reliability. Each of these potential gaps are discussed in more detail in this memo. Because benthic algal processes will be represented in the model, an assessment of available benthic algae data was conducted subsequent to the initial data review described in this memorandum. Through discussions with MCD and OEPA, it was determined that the available data, which consists of 19 measurements at 13 locations in the LGMR collected in 2008 – 2012, were sufficient for model development and calibration.

Overall, the available data are sufficient to develop, calibrate and corroborate the water quality model. The hydrology and water quality data available throughout the entire Great Miami River watershed are sufficient to conduct a multi-year calibration and a separate multi-year corroboration of the watershed model being used to generate upstream and tributary flows and nutrient loads. Data-rich periods that could serve as calibration and/or corroboration periods for the water quality model include 2010, when OEPA did extensive spatial sampling to inform their Lower Miami River Water Quality and Biological Study, and the years 2013-2015, when the three

MCD/YSI sondes deployed in the Great Miami River and Mad River have the most extensive continuous monitoring data. The continuous monitoring data provide the most detail on the range of dissolved oxygen levels, as well as on corresponding water temperature and algal levels. These will be important water quality model calibration datasets.

Introduction

A partnership of Water Resource Recovery Facilities (WRRFs) with permitted discharges to the Lower Great Miami River (LGMR), in conjunction with the MCD, has been investigating the causes of nutrient enrichment of the lower section of the Great Miami River (Figure 1), and are actively monitoring this issue as it relates to the renewal of individual National Pollutant Discharge Elimination System (NPDES) permits for their respective facilities. Note that Figure 1 includes a delineation of the spatial domain of the water quality model.

The Great Miami River and its tributaries are a well-studied system with sampling dating back several decades. LimnoTech has compiled and reviewed the readily available data provided by MCD, the WRRFs, and OEPA as well as from commonly used data clearinghouses such as the Water Quality Portal and the Permit Compliance System (PCS). The objective of this task is to inventory the amount and types of data and review the datasets and their associated quality, to support the following project activities:

- Assessment of watershed characteristics;
- Selection of an appropriate water quality model platform;
- Identification of potential model calibration locations based on data availability; and
- Identification of data gaps that may adversely affect the development and calibration of the model and thus its reliability for application to management scenarios.

This technical memorandum presents an inventory of the data that have been obtained for this project, an assessment of the quality of the data, and a description of how the data will be used to support the model development and calibration. To maintain continuity in the text, tables and figures have been assembled at the end of the memorandum.

Data Inventory

LimnoTech has compiled measured data describing in-stream surface water quality, sediment quality, hydraulics, biological community health (fish and macroinvertebrates), habitat, floating and fixed algae levels, groundwater quality, point source discharge characteristics, and stream geomorphometry. The focus of this data effort was on data directly related to issues associated with dissolved oxygen and algal development in the LGMR, as well as hydrologic and hydraulic data. LimnoTech has also compiled spatial datasets using Geographic Information Systems (GIS) to complement the measured data in characterizing the watershed and informing the development of the water quality model.

Data for the entire Great Miami River (GMR) watershed were considered to inform not only the water quality model development and calibration, but also to inform the development of a watershed model that will be used to specify upstream and tributary flows and nutrients loads as well as to simulate scenarios that consider controls for a mixture of sources. Data spanning roughly the last 15-20 years (1996 – 2015) were obtained. This period spans the simulation period used for MCD's HSPF flood flow models (1999 – 2009), the extensive water quality and biological

studies conducted by OEPA throughout the GMR watershed, and the more recent data-rich period (2012-2015). To date, over 1,300,000 results have been reviewed, and relevant results have been compiled in a project database using Microsoft (MS) Access (Table 1). This section presents an overview of the datasets for each data type that have been compiled and reviewed for the project.

Hydrology and Hydraulic Data

Hydrologic and hydraulic data will be used to calibrate the flow portion of the water quality model. The data will also be used to inform the hydrology inputs for the upstream and tributary areas to the water quality model. The USGS Ohio Water Science Center maintains an extensive network of gages in the Great Miami River watershed to monitor flow, velocity, depth, and precipitation (Figure 2). Daily flow and field measurement (e.g., flow, velocity, depth, cross-sectional area surveys) data for the gages shown in Figure 2 were downloaded from the USGS National Water Information System[1].

A summary of the data availability is provided in Table 2. It should be noted that there are other gages in the Great Miami River watershed; however, these gages either have limited data for use in model calibration or have been discontinued. Of the 25 gages evaluated, nearly half (eleven) are within the domain of the water quality model and may be used to calibrate the hydraulic portion of the water quality model. The entire gage network may be used to inform and update the hydrologic calibration of the watershed model.

In-stream Surface Water Quality

In-stream surface water quality datasets provide the information necessary to parameterize the water quality model's fate processes, to specify water quality conditions at the model upstream and tributary boundaries, and to calibrate the model to the measured values. In-stream surface water quality data outside the water quality model domain serve the same function for the watershed model that will be used to estimate the upstream and tributary watershed conditions.

The data review and compilation to support this project focused on the key parameters to inform nutrient and eutrophication modeling, including phosphorus and nitrogen nutrients, physico-chemical parameters (dissolved oxygen, temperature, pH, conductivity, and turbidity), suspended solids, oxygen-demanding constituents, carbon, and sestonic algae. Over 1,300,000 water quality observations have been obtained, reviewed, and compiled into the project database.

In-stream surface water quality datasets include observations from routine monitoring programs (Figure 3) as well as from periodic monitoring to support regulatory requirements and/or special studies (Figure 4). The frequency of data collected in the routine monitoring programs range from continuous monitoring (approximately hourly) to regular bi-monthly sampling, as shown in Figure 3. The periodic monitoring typically consisted of one or more measurements at a given location over a relatively short survey period spanning weeks or months. Each dataset is briefly summarized below:

- MCD/YSI Continuous Monitoring: MCD has teamed with YSI to deploy sondes at three locations in the LGMR (Figure 3). These sondes are currently measuring water temperature, pH, dissolved oxygen, turbidity, conductivity, chlorophyll *a*, blue-green algae, and fraction of dissolved organic matter. Data are recorded at a 15-minute to

[1] USGS National Water Information System: http://waterdata.usgs.gov/nwis

hourly frequency, though there are periods of time when data are not available (e.g. winter, during maintenance, records removed due to evidence of instrument drift and/or malfunction). The date that each parameter came on line varied from 2010 to 2013. From 2013 forward, the sondes have fairly comprehensive datasets for all of the parameters.

- MCD/Heidelberg University Routine Monitoring: MCD has been conducting regular water quality monitoring at four locations in the LGMR since 2002 (Figure 3). Samples are analyzed for phosphorus and nitrogen nutrients, oxygen-demanding constituents, sestonic chlorophyll *a*, suspended solids and physical characteristics. Data are reported on an approximately one to three day frequency. Heidelberg University has conducted daily sampling at one location in the LGMR since 1996 (Figure 3) for a similar set of parameters. MCD uses these data with the continuous monitoring and hydrologic data to report on annual water quality in the GMR.

- Permitted Facility Routine Monitoring: The WRRF partners have been conducting in-stream water quality sampling upstream and downstream of their facilities as part of their NPDES permit requirements (Figure 3). The facilities provided monthly measurements of phosphorus and nitrate/nitrite results from 2008 to present. Data for other parameters (other nutrients, physical parameters) that the WRRFs monitor were downloaded via the OEPA permit website[2]. The monitoring requirements for these parameters vary by facility. Similarly, in-stream monitoring data from the major industrial facility permittees in the LGMR were acquired from the OEPA permit website and span 2012-2015.

  Monthly in-stream monitoring data collected by the fourteen major WRRF facilities upstream of the water quality model domain (Figure 3) were downloaded via the OEPA permit website and span 2012-2015. The upstream-downstream data will be used to inform the watershed model calibration.

- USEPA also maintains NPDES data for permitted facilities in their Permit Compliance System (PCS) and Integrated Compliance Information System (ICIS) database[3]. Monthly in-stream water quality data from January 1998 through January 2011 were downloaded for the partner WRRFs, major upstream WRRFs and the major industrial dischargers. The monitoring period and monitored parameters varied by facility. These data will be used to conduct multi-year hydrologic and water quality calibrations and corroborations with the watershed model.ORSANCO Routine Monitoring: ORSANCO has been conducting routine nutrient sampling in the Ohio River and its major tributaries every other month since 2001. They survey one station in the GMR, just below the confluence of the Whitewater River (Figure 3). Solids, organic carbon and physical parameters are also measured in each sample. Data from 2005 to the present were downloaded from ORSANCO's website[4].

- OEPA Water Quality Study Data: OEPA has conducted intensive water quality sampling to support detailed assessments of waterbody health in the GMR watershed over the last approximate 15 years (Figure 4). These studies and associated monitoring data have been documented in several OEPA publications[5]. The water quality data included grab

[2] OEPA permit website: http://www.epa.ohio.gov/dsw/permits/npdes_info.aspx

[3] USEPA PCS-ICIS website: https://www.epa.gov/enviro/pcs-icis-customized-search

[4] ORSANCO's bi-monthly monitoring data website: http://www.orsanco.org/ammonia-15

[5] OEPA Biological/Water Quality Studies in the Great Miami River watershed include:

sampling and continuous monitoring. Grab samples were analyzed for a wide range of parameters, including phosphorus and nitrogen nutrients, and sestonic algae. Data sondes measuring dissolved oxygen, temperature, pH and conductivity were typically deployed for a two-three day period to provide continuous (15-minute) monitoring data at a subset of sampling locations. Sediment sampling, biological community and habitat assessments were also conducted and are discussed separately in this memorandum. Data were provided to LimnoTech in spreadsheet form by OEPA staff. It was not always possible to match the location identifiers on the sonde files to the grab sampling locations so the sonde data within the water quality model domain that could be readily identified were reviewed and added to the project database (48 locations). All of the grab sampling data for the relevant parameters were also reviewed and added to the project database.

- USGS-OH Water Quality Sampling: The USGS Ohio Water Science Center has conducted occasional water quality sampling at a several gage locations in the Great Miami River waterways, including phosphorus and nitrogen nutrients, solids, organic carbon and physical parameters (Figure 4). Data spanning 1998-2013 were downloaded from the Water Quality Portal[6], a data clearinghouse jointly managed by the National Water Quality Monitoring Council, USGS and USEPA.

- Greater Cincinnati Water Works Source Water Monitoring: The Greater Cincinnati Water Works conducts in-stream water quality at three locations in the LGMR as part of several source water investigations for the Hamilton to New Baltimore Ground Water Consortium (Figure 4). The project reports for 2010, 2011, 2014 and 2015 were downloaded from the MCD website[7]. Parameter results relevant to this project include physical parameters and nitrogen nutrients.

Table 3 presents a summary of all of the available in-stream surface water quality data for each agency, compiled and reviewed in this effort, and organized by the key project parameters. This table provides an indication of the amount of data to inform both the calibration and development of the water quality and watershed models. Table 4 gives a rough indication of the amount of data in Table 3 that could potentially be used to calibrate the water quality model. The data from the fourteen upstream WRRFs will be used to inform the calibration the watershed model. The OEPA and USGS-OH datasets will provide data to potentially inform the watershed and

- Biological and Water Quality Study of the Lower Great Miami River and Select Tributaries (2012), OEPA Technical Report EAS/2012-5-7
- Biological and Water Quality Study of the Stillwater River Basin (2015), OEPA Technical Report EAS/2014-10-08
- Biological and Habitat Assessment Stillwater River – West Milton (2010), OEPA Technical Report DSW/EAS 2010-11-12
- Biological and Habitat Study of the Stillwater River, 2008, 2010, and 2011 (2012), OEPA Technical Report DSW/EAS 20112-2-4
- Biological and Water Quality Study of the Middle Great Miami River and Principal Tributaries (2013), OEPA Technical Report EAS/2012-1-2
- Biological and Water Quality Study of the Upper Great Miami River and Selected Tributaries 2008 (2011), OEPA Technical Report EAS/2011-1-1
- Biological and Water Quality Study of Sevenmile Creek and Select Tributaries, 2002 (2005), OEPA Technical Report EAS/2005-12-8
- Biological and Water Quality Study of Twin Creek and Selected Tributaries, 2005 (2007), OEPA Technical Report EAS/2007-10-03

[6] NWQMC Water Quality Portal website: http://waterqualitydata.us/

[7] MCD report library website: http://www.miamiconservancy.org/resources/index.asp

water quality model calibrations. All of data from the remaining data sources (MCD, WWRF partners, ORSANCO) are potentially of use in calibrating the water quality model.

In-stream Biological Community and Habitat Assessments

The OEPA conducted biological community and habitat assessments in the LGMR in 2010. Other portions of the Great Miami River watershed were assessed in other years. Although the water quality model endpoint is water quality-based (e.g. dissolved oxygen) rather than biological community health, a review of the community and habitat results will provide additional context for relating the water quality model results to aquatic life conditions. Thus, the results associated with the sixty-eight (68) locations within the potential water quality model domain (Figure 4) were reviewed for this data inventory.

In-stream Sediment Quality

In-stream sediment quality provides information to characterize the role of sediment in nutrient fate and transport and eutrophication. In depositional reaches of the river, a portion of the solid-associated nutrients may settle out and have limited effect on algal or dissolved oxygen levels downstream reaches. Phosphorus release from sediments under anoxic conditions is another potential source of phosphorus that can affect algal production and contribute to impairing low levels of dissolved oxygen. Sediment data were obtained from OEPA and the USGS-OH sampling surveys spanning the period 2000-2015 (Figure 5). Parameters include phosphorus and nitrogen nutrients, and organic carbon (Table 5). Since OEPA and USGS-OH assigned benthic algae to a sediment matrix in their databases, that convention was maintained for this project and benthic algae results are included in the tally of sediment results. MCD and Wright State University collaborated on a sediment phosphorus flux study in summer 2015 and the data were provided by MCD in May 2016. Results from this study include phosphorus flux and the standard error associated with the flux result at ten locations (Figure 5). To date, approximately 750 observations have been obtained, reviewed and compiled in the project database.

Point Source Discharge Flow and Quality

Major WRRF and industrial facilities are permitted to discharge nutrients and other constituents to local waterways under the NPDES, which is administered by OEPA. Accounting for these pollutant loads is an important component of the river system mass balance, as these loads may be the predominant source of both flow and nutrients to the local rivers during low flow periods.

The WRRF partners have been conducting water quality sampling of their facility and system discharges as part of their NPDES permit requirements (Figure 6). The facilities provided monthly average flow, phosphorus and nitrate/nitrite results from 2008 to present for their treated effluents. Data for other parameters (other nutrients, physical parameters) that the WRRFs monitor in their effluents were downloaded via the OEPA permit website. Water quality and flow data from other permitted outfalls (e.g. CSO, SSO, bypass locations) were also downloaded via the OEPA permit website. Older monthly flow and water quality data were available and downloaded from the PCS database. These data nominally span January 1998 – January 2011 and were used to fill gaps in the periods covered by the other data sources. The monitoring requirements for these parameters vary by facility.

Similarly, discharge flow and water quality monitoring data from the major industrial facility permittees in the LGMR and major WRRF facilities in the upper GMR and tributaries were

acquired from the OEPA permit website (spanning 2012-2015) and the PCS database (nominally spanning 1998-2010). A tally of the available data for each facility and outfall type are summarized in Table 6 (over 45,000 records) and have been compiled in the project database. Fifteen of the major WRRF facilities and five major industrial dischargers are located within the water quality model domain. Fourteen major WRRF dischargers are located upstream or in tributaries that are within the watershed model domain.

Groundwater Quality

Groundwater is a potential source of pollutants to the LGMR waterways since it is a primary source of base flow in the surface waters. Groundwater quality sampling has been conducted at many locations in the GMR watershed (Figure 7), but each location has a limited number of sampling surveys (Table 7). Data were obtained from several sources and are described briefly below:

- MCD Spring/Fall Surveys: MCD conducted sampling at six groundwater wells in Spring 2015 and Fall 2015. Parameters included phosphorus and nitrogen nutrients, physical parameters, organic carbon and oxygen-demanding constituents. Data were provided by MCD as Excel spreadsheets.
- USGS-OH Groundwater Quality Sampling: The USGS Ohio Water Science Center has conducted water quality sampling at over 100 well locations in the GMR watershed, including phosphorus and nitrogen nutrients, dissolved solids, organic carbon and physical parameters. Although the data span 1996 through 2011, the bulk of the data were collected between 1999 and 2004. The water quality data were downloaded from the Water Quality Portal.
- Ohio Division of Drinking and Ground Water (OHDDGW): The ODDDGW has conducted water quality sampling at approximately 20 well locations in the GMR watershed, including phosphorus and nitrogen nutrients, organic carbon and physical parameters. Data were available from 1996 through 2005 and in 2012. The water quality data were downloaded from the Water Quality Portal.
- Greater Cincinnati Water Works Source Water Monitoring: The Greater Cincinnati Water Works conducts groundwater quality sampling at approximately 20 locations in the LGMR as part of several source water investigations for the Hamilton to New Baltimore Ground Water Consortium. The project reports for 2010, 2011, 2014 and 2015 were downloaded from the MCD website. Parameter results relevant to this project include physical parameters and nitrogen nutrients.

These groundwater quality datasets have been reviewed and compiled in the project database.

Geographic Information Systems (GIS) Data

Spatial data are an important type of data that is used extensively to characterize watershed conditions and to support the development of the water quality model. The geographic datasets compiled to build the model framework include: watershed boundaries, hydrography, digital elevation model (DEM), municipal boundaries, land use/land cover, and soils. Sampling locations and point source outfalls were mapped using latitude/longitude information provided with the data or, if coordinates were not available, using descriptive information of the sampling location.

Bathymetry Data

River bathymetry data are used to construct the physical representation of the river in the model. A lack of bathymetry data increases uncertainty in the model's simulation of transport characteristics (e.g., stream velocity, depth, loss rates via settling). Sources of bathymetry data include transect surveys, often acquired using Acoustic Doppler Current Profiler (ADCPs), and hydraulic models previously developed for flooding analyses. Data that have been obtained to date are shown in Figure 8.

Other Data Types

Additional relevant data and information have been provided by MCD, including information on dams in the LGMR and results from a dye study. Although these data do not lend themselves to inclusion in the project database, they are important data to consider because they provide information related to hydraulic transport that will be important to capture in the water quality model.

- Dam information: The LGMR has multiple dams, with most of them being low head, run of the river variety. MCD has provided information on the locations and use of 14 dams in the LGMR between river mile 92.6 and river mile 14.8, one dam on the Stillwater River and three dams on the Mad River. Physical dimensions (height, length) and hydraulic characteristics (maximum discharge, capacity) were included for the larger dams.
- Dye study: A time-of-travel study in the LGMR between Dayton and Cleves was conducted in 1966 by the USGS and summarized in a report[8] provided to LimnoTech. Although the raw data are not available and the survey is dated (~50 years ago), the study results are expected to provide useful information on longitudinal transport within a portion of the water quality model domain.

Data Quality Review

The data in each water quality dataset were reviewed for potential data quality issues that would affect their use in developing and calibrating the water quality model. Erroneous data were identified based on unreasonable values and unreasonable parameter relationships. Criteria used to identify unreasonable values include:

- Dissolved oxygen values exceeding 30 mg/L or less than 0 mg/L;
- pH values greater than 10 S. U. or less than 4 S.U.;
- Water temperature values greater than 35°C; and
- Negative values for the other parameters.

Criteria for unreasonable parameter relationships include:

- Soluble reactive phosphorus/ortho-phosphate values significantly greater than total phosphorus values;
- Total ammonia greater than total Kjeldahl nitrogen; and

[8] Bauer, D. P. 1966. Time of Travel of Water in the Great Miami River, Dayton to Cleves, Ohio. U.S. Geological Survey Water Resources Division. Prepared in cooperation with the Miami Conservancy District. June 1966. Columbus, OH

- Nitrite greater than nitrate (when measured individually).

Examples of unreasonable values and unreasonable relationships are shown in Figures 9 and 10, respectively. In addition, the continuous monitoring data were inspected for occasional spurious points and periods where the data appears unreliable due to instrument drift or fouling. Data were also flagged for poor quality if the reporting agency indicated that the result should be rejected.

Data that were identified as having unacceptable quality were flagged with an "R" qualifier in the project database. In addition, incomplete data, such as data reported as non-detect without an accompanying detection or reporting limit, were also flagged with an "R" qualifier. These data will not be used to parameterize the model, develop model inputs or for model calibration.

In general, the datasets had relatively few values that were deemed unreliable. Most of the flagged data were associated with field parameters. A tally of the percent of qualified data is presented in Table 8 for all of the data and Table 9 for the portion of the data within the potential model domain. Less than 1% of the acquired data were qualified with an "R" flag. Exceptions were pH (>10%) and chlorophyll *a* (~2%) in the daily MCD dataset, and ~3% in the chlorophyll *a* and blue-green algae observations from the MCD/YSI continuous monitoring dataset (negative values were flagged). Overall, the compiled data are of good quality.

Data Management

The data described in this technical memorandum have been compiled into a project database using MS Access. The project database serves as a central repository for the data and ensures that the data are maintained in a consistent format (e.g. reporting units) across data sources. It also offers efficiency in data handling through the use of relational tables and rigor through the implementation of data integrity rules (Figure 11). The database is also linked to the model and visualization tools to facilitate model-data comparisons and site understanding.

The maps provided in this memorandum provide a foundation for evaluating the spatial extent of available data. The temporal extent of the datasets is summarized in Figure 12, which shows the amount of data available each year over the last 20 years for the key parameters (dissolved oxygen, chlorophyll *a*, phosphorus nutrients) at the locations within the model domain. The totals shown represent the unqualified data only.

Data Gap Analysis

The data described in this memo been reviewed by the project team to determine whether there are significant data gaps with respect to constructing and calibrating the water quality model and the model/methods used to specify upstream/tributary conditions. The gap analysis considered factors such as:

- Spatial extent of available data;
- Temporal extent of key parameters;
- Quality of available data; and
- Availability of related parameters at a given location.

Overall, the available data are sufficient to develop, calibrate and corroborate the water quality and watershed model. However, three potential data gaps were identified:

1. Bathymetry
2. Light extinction information
3. Process data for calibration

These gaps will not affect the model development or reliability, rather, if addressed, they will reduce uncertainty in the model configuration (bathymetry) and reliance on literature values in the model parameterization (light extinction and process data). Each of these potential gaps are discussed in more detail below.

Bathymetry

As shown in Figure 8, there are several sections within the potential model domain that do not have bathymetry data, including the Great Miami River between Tipp City and Vandalia, and the Stillwater River north of the Englewood. In addition, the HEC models are over 30 years old and the transect data may not reflect contemporary river bathymetry.

Options to address this gap include 1) work with existing data; and, 2) conduct bathymetry surveys to fill gaps and confirm HEC model transects. Because it is not uncommon for river systems to have bathymetry data gaps, LimnoTech has developed analysis methods to estimate the river's physical characteristics using a variety of secondary data sources, including digital elevation model data, flood insurance profiles, historical aerial photography and in-stream hydraulic data. LimnoTech would apply these methods to implement Option 1.

For Option 2, LimnoTech recommends conducting survey transects approximately every half-mile in the reaches without data. This roughly corresponds to the transect distance in the HEC models. In addition, three longitudinal surveys would help fill in gaps in bathymetry between the transects. In the area covered solely by the HEC models, LimnoTech recommends surveying 3-4 transects that correspond to transect locations in the HEC models so that the channel characteristics can be compared. If the transects are significantly different, then additional surveys would be needed for the rest of the HEC-modeled areas of the river. It is expected that the level of effort for Option 2 would require an adjustment to the model development schedule so that the new bathymetry data could be incorporated into the model.

After confirming that there have been no major dam removals since the 1970s and no major floods that have reshaped the channel, LimnoTech recommends working with existing data (Option 1). This will avoid affecting the project schedule for model development and preserve project resources for the model development and calibration.

Light Extinction Information

Light extinction inputs affect the rate of sestonic and benthic algal growth and can be characterized with collection of chlorophyll *a*, total suspended solids (TSS), total organic carbon (TOC), turbidity, and Secchi depth or photosynthetically active radiation (PAR) under various environmental conditions. Understanding the variability in light extinction will result in a better, more site-specific description of its impact on algal growth.

Options to address this gap include: 1) work with existing data; 2) conduct additional sampling. Option 1 would result in specification of literature values in the model that would be adjusted to a final set of inputs during the model calibration process. This approach is likely to be fairly well constrained by the amount of data available to calibrate the water quality model.

For Option 2, if it is possible to collect additional data in the future, LimnoTech recommends conducting water quality sampling for chlorophyll *a*, TSS, TOC, turbidity and PAR during three distinct environmental conditions:

1. High flow with muddy conditions
2. Low flow without algae present
3. Low flow with algae present

It is recommended that two surveys be conducted for each of the environmental conditions and sampling be conducted at four or five in-stream locations. Ideally, these surveys could be piggy-backed onto planned sampling programs. However, the sampling would need to be conducted by the end of June, with laboratory results provided by mid-July for the water quality model development schedule to stay on track. In all likelihood, the third condition (low flow with algae present) would not occur until later in the summer, which would likely delay the project schedule for completing the water quality model calibration.

After determining that Option 2 could not be readily added to an existing or planned monitoring program, the project schedule implications and the robustness of available data for model calibration, LimnoTech recommends proceeding with working with existing data (Option 1).

Process Data

Uncertainty in several processes simulated in the model occurs when they are parameterized using literature values and refined through model calibration rather than informed by site specific data. For this project, organic content of water are not well characterized in the data compiled to date for the project.

Options to address this gap include: 1) work with existing data; 2) conduct additional sampling. As with light extinction, Option 1 would result in specification of literature values in the model that would be adjusted to a final set of inputs during the model calibration process. This approach is likely to be fairly well constrained by the amount of data available to calibrate the water quality model.

After determining that there were no convenient monitoring programs that could accommodate additional sampling, LimnoTech recommends proceeding with working with existing data (Option 1).

Table 2. Summary of Hydrology and Hydraulic Data.

USGS Gage ID	Gage Description	Daily Flow (cfs)			Field Measurements		
		Start Year	End Year	# of Records	Start Year	End Year	# of Records
03260706	Bokengehalas Creek at De Graff OH	2002	2016	4928	2002	2015	86
03261500	Great Miami River at Sidney OH	1998	2016	6662	2000	2015	104
03262500	Great Miami River at Piqua OH	2012	2016	1305	2012	2015	21
03262700	Great Miami River at Troy OH	1998	2016	6662	2000	2015	100
03263000	Great Miami River at Taylorsville OH	1998	2016	6662	2000	2015	100
03270500	Great Miami River at Dayton OH	1998	2016	6662	2000	2015	123
03271207	Great Miami River at Sellars Rd at West Carrollton, OH	No data			2012	2013	9
03271500	Great Miami River at Miamisburg OH	Discontinued in 1995			2005	2015	4
03271601	Great Miami River below Miamisburg OH	1998	2016	6661	2000	2015	103
03271620	Great Miami River at Franklin, OH	2012	2016	1336	2012	2015	23
03272100	Great Miami River at Middletown OH	1998	2016	6662	2000	2015	106
03274000	Great Miami River at Hamilton OH	1998	2016	6662	2000	2015	103
03264000	Greenville Creek near Bradford OH	1998	2016	6662	2000	2015	104
03271300	Holes Creek near Kettering OH	2002	2016	4928	2000	2015	106
03261950	Loramie Creek near Newport OH	1998	2016	6662	2000	2015	104
03262000	Loramie Creek at Lockington OH	1998	2016	6662	2000	2015	99
03267000	Mad River near Urbana OH	1998	2016	6662	2002	2015	82
03267900	Mad River at St Paris Pike at Eagle City OH	1998	2016	6389	2000	2015	112
03269500	Mad River near Springfield OH	1998	2016	6662	2000	2015	99
03270000	Mad River near Dayton OH	1998	2001	1171	2000	2015	93
03265000	Stillwater River at Pleasant Hill OH	1998	2016	6662	2000	2015	108
03266000	Stillwater River at Englewood OH	1998	2015	6510	2000	2015	98
03272000	Twin Creek near Germantown OH	1998	2016	6662	2000	2015	105
03271000	Wolf Creek at Dayton OH	2002	2016	4928	2002	2015	85
03272700	Sevenmile Creek at Camden OH	1998	2016	6662	2000	2015	95

Table 3. Summary of Surface Water Quality Data by Agency.

Data Source	Sample Matrix	Dissolved Oxygen	Chlorophyll a[a]	Blue-Green Algae	Total Phosphorus	Orthophosphorus
Miami Conservancy District	Surface Water	2005-2015 (8,935)	2010-2015 (4,104)	No data	2002-2015 (9,178)	2002-2015 (9,193)
Heidelberg University	Surface Water	No data	No data	No data	1996-2015 (8,681)	1996-2015 (8,625)
MCD/YSI Continuous Monitoring	Surface Water	2010-2015 (94,321)	2011-2015 (92,615)	2012-2015 (70,569)	No data	No data
Ohio Environmental Protection Agency	Surface Water	2005-2013 (5,814)	2008-2015 (296)	No data	1999-2015 (5,389)	2009-2015 (1,369)
Troy WWTP	Surface water	No data	No data	No data	2002-2016 (383)	No data
Tri-Cities WW Authority	Surface water	2012-2015 (78)	No data	No data	2003-2016 (220)	No data
Dayton WWTP	Surface water	2012-2015 (78)	No data	No data	2003-2016 (445)	No data
Montgomery County/Western Regional WWTP	Surface water	2012-2015 (78)	No data	No data	1998-2016 (543)	No data
West Carrollton WWTP	Surface water	2012-2015 (78)	No data	No data	2000-2016 (403)	No data
Maimisburg WWTP	Surface water	2012-2015 (78)	No data	No data	1998-2015 (466)	No data
Springboro WWTP	Surface water	2012-2015 (78)	No data	No data	2003-2016 (206)	No data
Franklin WWTP	Surface water	2012-2015 (78)	No data	No data	1998-2009 (252)	No data
Middletown WWTP	Surface water	2012-2015 (78)	No data	No data	1998-2009 (282)	No data
Lesourdesville WWTP	Surface water	2012-2015 (78)	No data	No data	1998-2016 (550)	No data
Hamilton WWTP	Surface water	2012-2015 (78)	No data	No data	2003-2016 (329)	No data
Fairfield WWTP	Surface water	2012-2015 (78)	No data	No data	2003-2016 (427)	No data
Union WWTP	Surface water	2012-2015 (78)	No data	No data	2008-2016 (272)	No data
Englewood WWTP	Surface water	2012-2015 (78)	No data	No data	2012-2016 (176)	No data
Taylor Creek WWTP	Surface water	2012-2015 (78)	No data	No data	1999-2015 (229)	No data
Ohio River Valley Water Sanitation Commission	Surface water	No data	No data	No data	2005-2015 (63)	No data
AK Steel	Surface water	No data	No data	No data	No data	No data
Fernald	Surface water	2012-2015 (26)	No data	No data	No data	No data
Wausau Paper	Surface water	2012-2015 (39)	No data	No data	No data	No data
USGS Ohio Water Science Center	Surface water	1998-2013 (216)	2004-2013 (7)	No data	1998-2013 (215)	1998-2013 (221)
Greater Cincinnati Water Works	Surface water	2010-2015 (27)	No data	No data	No data	No data
Bellefontaine WWTP	Surface Water	Not compiled	No data	No data	2002-2016 (183)	No data

Data Source	Sample Matrix	Dissolved Oxygen	Chlorophyll a[a]	Blue-Green Algae	Total Phosphorus	Orthophosphorus
Brookville WWTP	Surface Water	Not compiled	No data	No data	2008-2016 (178)	No data
Eaton WWTP	Surface Water	Not compiled	No data	No data	2015-2016 (10)	No data
Fairborn WWTP	Surface Water	Not compiled	No data	No data	2013-2016 (26)	No data
Greenville WWTP	Surface water	Not compiled	No data	No data	2003-2016 (139)	No data
Indian Lake WWTP	Surface water	Not compiled	No data	No data	2001-2016 (213)	No data
Minster WWTP	Surface water	Not compiled	No data	No data	2013-2016 (78)	No data
Oxford WWTP	Surface water	Not compiled	No data	No data	2004-2016 (112)	No data
Piqua WWTP	Surface water	Not compiled	No data	No data	2002-2016 (271)	No data
Sidney WWTP	Surface water	Not compiled	No data	No data	2002-2016 (265)	No data
Southwest Regional WWTP	Surface water	Not compiled	No data	No data	2006-2016 (172)	No data
Springfield WWTP	Surface water	Not compiled	No data	No data	2001-2016 (443)	No data
Urbana WWTP	Surface water	Not compiled	No data	No data	2013-2016 (78)	No data
West Milton WWTP	Surface water	Not compiled	No data	No data	No data	No data

[a]: Count includes samples corrected for pheophytin

Data Source	Sample Matrix	Nitrate+Nitrite[a]	Ammonia	Total Kjeldahl Nitrogen	Total Sus. Solids[b]	Total Organic Carbon[c]
Miami Conservancy District	Surface Water	2002-2015 (9,315)	2002-2015 (9,010)	2002-2015 (9,320)	2002-2015 (9,164)	No data
Heidelberg University	Surface Water	1996-2015 (8,680)	No data	1996-2015 (8,638)	1996-2015 (8,660)	No data
MCD/YSI Continuous Monitoring	Surface Water	No data	No data	No data	No data	No data
Ohio Environmental Protection Agency	Surface Water	1999-2015 (5,388)	1999-2015 (5,405)	1999-2015 (5,389)	1999-2015 (5,225)	2005-2015 (338)
Troy WWTP	Surface water	2002-2015 (283)	1998-2015 (313)	No data	No data	No data
Tri-Cities WW Authority	Surface water	No data	1999-2015 (387)	2003-2015 (157)	No data	No data
Dayton WWTP	Surface water	2003-2016 (326)	1998-2015 (449)	No data	2015 (4)	No data
Montgomery County/Western Regional WWTP	Surface water	2003-2015 (434)	1998-2015 (443)	2009-2015 (94)	No data	No data
West Carrollton WWTP	Surface water	2003-2015 (330)	1998-2015 (228)	No data	No data	No data
Maimisburg WWTP	Surface water	2003-2015 (239)	1998-2015 (445)	No data	No data	No data
Springboro WWTP	Surface water	2013-2015 (44)	1999-2015 (210)	No data	No data	No data
Franklin WWTP	Surface water	2003-2009 (142)	1998-2015 (200)	No data	No data	No data
Middletown WWTP	Surface water	2003-2009 (171)	1998-2015 (298)	No data	No data	No data
Lesourdesville WWTP	Surface water	2003-2015 (434)	1998-2015 (404)	No data	No data	No data
Hamilton WWTP	Surface water	2003-2015 (326)	1998-2015 (346)	No data	No data	No data
Fairfield WWTP	Surface water	2003-2015 (434)	1998-2015 (259)	No data	No data	No data
Union WWTP	Surface water	2012-2015 (156)	1998-2015 (440)	No data	No data	No data
Englewood WWTP	Surface water	2012-2016 (176)	1998-2016 (473)	No data	No data	No data
Taylor Creek WWTP	Surface water	2003-2015 (327)	2008-2015 (157)	No data	No data	No data
Ohio River Valley Water Sanitation Commission	Surface water	2005-2015 (63)	2005-2015 (63)	2005-2015 (63)	2005-2015 (63)	2005-2015 (63)
AK Steel	Surface water	No data	No data	No data	2012-2015 (62)	No data
Fernald	Surface water	No data	No data	No data	No data	No data
Wausau Paper	Surface water	No data	No data	No data	2012-2015 (64)	No data
USGS Ohio Water Science Center	Surface water	1998-2013 (225)	1998-2013 (225)	1998-2003 (185)	1998-2013 (198)	1998-2004 (126)
Greater Cincinnati Water Works	Surface water	2010-2015 (27)	2010-2015 (27)	No data	No data	No data
Bellefontaine WWTP	Surface Water	2003-2016 (130)	2003-2016 (205)	2002-2006 (34)	No data	No data

Data Source	Sample Matrix	Nitrate+Nitrite[a]	Ammonia	Total Kjeldahl Nitrogen	Total Sus. Solids[b]	Total Organic Carbon[c]
Brookville WWTP	Surface Water	2003-2016 (176)	1998-2016 (269)	No data	No data	No data
Eaton WWTP	Surface Water	2015-2016 (10)	1998-2016 (305)	2015-2016 (10)	No data	No data
Fairborn WWTP	Surface Water	2013-2016 (26)	1998-2016 (160)	No data	No data	No data
Greenville WWTP	Surface water	2003-2016 (193)	1998-2016 (254)	2003-2016 (85)	No data	No data
Indian Lake WWTP	Surface water	2001-2016 (190)	1998-2016 (159)	No data	No data	No data
Minster WWTP	Surface water	2013-2016 (78)	1998-2016 (350)	2013-2016 (78)	No data	No data
Oxford WWTP	Surface water	2004-2016 (165)	1998-2016 (353)	No data	No data	No data
Piqua WWTP	Surface water	2002-2016 (269)	1998-2016 (337)	No data	No data	No data
Sidney WWTP	Surface water	2002-2016 (274)	1998-2016 (345)	No data	No data	No data
Southwest Regional WWTP	Surface water	2006-2016 (188)	1998-2016 (374)	No data	No data	No data
Springfield WWTP	Surface water	2001-2016 (456)	1998-2016 (458)	No data	No data	No data
Urbana WWTP	Surface water	2013-2016 (78)	1998-2016 (326)	No data	No data	No data
West Milton WWTP	Surface water	No data	2003-2016 (241)	No data	No data	No data

[a]: Count includes samples where only nitrate was measured

[b]: Count includes samples where suspended sediment concentration was measured

[c]: Count includes samples where particulate organic carbon was measured

Data Source	Sample Matrix	Temperature	CBOD-5 Day	CBOD-20 Day	Frac. of Diss. Org. Matter	pH
Miami Conservancy District	Surface Water	2005-2015 (8,893)	No data	No data	No data	2005-2015 (7,934)
Heidelberg University	Surface Water	No data	No data	No data	No data	No data
MCD/YSI Continuous Monitoring	Surface Water	2009-2015 (115,531)	No data	No data	2012-2015 (72,120)	2010-2015 (97,243)
Ohio Environmental Protection Agency	Surface Water	2005-2015 (9,104)	2000-2013 (135)	2000-2015 (1,288)	No data	1999-2015 (9,794)
Troy WWTP	Surface water	No data	No data	No data	No data	No data
Tri-Cities WW Authority	Surface water	2012-2015 (156)	No data	No data	No data	2012-2015 (156)
Dayton WWTP	Surface water	2012-2015 (156)	2015 (4)	No data	No data	2012-2015 (156)
Montgomery County/Western Regional WWTP	Surface water	2012-2015 (156)	No data	No data	No data	2012-2015 (156)
West Carrollton WWTP	Surface water	2012-2015 (156)	No data	No data	No data	2012-2015 (156)
Maimisburg WWTP	Surface water	2012-2015 (156)	No data	No data	No data	2012-2015 (156)
Springboro WWTP	Surface water	2012-2015 (156)	No data	No data	No data	2012-2015 (156)
Franklin WWTP	Surface water	2012-2015 (156)	No data	No data	No data	2012-2015 (156)
Middletown WWTP	Surface water	2012-2015 (156)	No data	No data	No data	2012-2015 (156)
Lesourdesville WWTP	Surface water	2012-2015 (156)	No data	No data	No data	2012-2015 (156)
Hamilton WWTP	Surface water	2012-2015 (156)	No data	No data	No data	2012-2015 (156)
Fairfield WWTP	Surface water	2012-2015 (156)	No data	No data	No data	2012-2015 (156)
Union WWTP	Surface water	2012-2015 (156)	No data	No data	No data	2012-2015 (156)
Englewood WWTP	Surface water	2012-2015 (156)	No data	No data	No data	2012-2015 (156)
Taylor Creek WWTP	Surface water	2012-2015 (156)	No data	No data	No data	2012-2015 (156)
Ohio River Valley Water Sanitation Commission	Surface water	2015 (1)	No data	No data	No data	2015 (1)
AK Steel	Surface water	No data	No data	No data	No data	2012-2015 (78)
Fernald	Surface water	2012-2015 (52)	No data	No data	No data	2012-2015 (52)
Wausau Paper	Surface water	2012-2015 (78)	2012-2015 (44)	No data	No data	No data
USGS Ohio Water Science Center	Surface water	1998-2013 (234)	No data	No data	No data	1998-2013 (239)
Greater Cincinnati Water Works	Surface water	2010-2015 (27)	No data	No data	No data	2010-2015 (27)
Bellefontaine WWTP	Surface Water	2013-2016 (78)	No data	No data	No data	No data

Data Source	Sample Matrix	Temperature	CBOD-5 Day	CBOD-20 Day	Frac. of Diss. Org. Matter	pH
Brookville WWTP	Surface Water	2013-2016 (64)	No data	No data	No data	No data
Eaton WWTP	Surface Water	2015-2016 (10)	No data	No data	No data	No data
Fairborn WWTP	Surface Water	2013-2016 (78)	No data	No data	No data	No data
Greenville WWTP	Surface water	2013-2016 (66)	No data	No data	No data	No data
Indian Lake WWTP	Surface water	2013-2016 (76)	No data	No data	No data	No data
Minster WWTP	Surface water	2013-2016 (78)	No data	No data	No data	No data
Oxford WWTP	Surface water	2013-2016 (62)	No data	No data	No data	No data
Piqua WWTP	Surface water	2013-2016 (78)	No data	No data	No data	No data
Sidney WWTP	Surface water	2013-2016 (78)	No data	No data	No data	No data
Southwest Regional WWTP	Surface water	2013-2016 (78)	No data	No data	No data	No data
Springfield WWTP	Surface water	2013-2016 (117)	No data	No data	No data	No data
Urbana WWTP	Surface water	2013-2016 (78)	2013-2016 (39)	No data	No data	No data
West Milton WWTP	Surface water	2013-2016 (78)	No data	No data	No data	No data

Table 4. Percent of Surface Water Quality Data within Water Quality Model Domain.

Data Source	Sample Matrix	Dissolved Oxygen	Chlorophyll a[a]	Blue-Green Algae	Total Phosphorus	Orthophosphorus
Miami Conservancy District	Surface Water	100%	100%	No data	100%	100%
Heidelberg University	Surface Water	No data	No data	No data	100%	100%
MCD/YSI Continuous Monitoring	Surface Water	100%	100%	100%	No data	No data
Ohio Environmental Protection Agency	Surface Water	84%	35%	No data	18%	45%
Troy WWTP	Surface water	No data	No data	No data	100%	No data
Tri-Cities WW Authority	Surface water	100%	No data	No data	100%	No data
Dayton WWTP	Surface water	100%	No data	No data	100%	No data
Montgomery County/Western Regional WWTP	Surface water	100%	No data	No data	100%	No data
West Carrollton WWTP	Surface water	100%	No data	No data	100%	No data
Maimisburg WWTP	Surface water	100%	No data	No data	100%	No data
Springboro WWTP	Surface water	100%	No data	No data	100%	No data
Franklin WWTP	Surface water	100%	No data	No data	No data	No data
Middletown WWTP	Surface water	100%	No data	No data	100%	No data
Lesourdesville WWTP	Surface water	100%	No data	No data	100%	No data
Hamilton WWTP	Surface water	100%	No data	No data	100%	No data
Fairfield WWTP	Surface water	100%	No data	No data	100%	No data
Union WWTP	Surface water	100%	No data	No data	100%	No data
Union WWTP	Surface water	100%	No data	No data	100%	No data
Taylor Creek WWTP	Surface water	100%	No data	No data	100%	No data
Ohio River Valley Water Sanitation Commission	Surface water	No data	No data	No data	100%	No data
AK Steel	Surface water	No data	No data	No data	No data	No data
Fernald	Surface water	100%	No data	No data	No data	No data
Wausau Paper	Surface water	100%	No data	No data	No data	No data
USGS Ohio Water Science Center	Surface water	20%	0%	No data	22%	22%
Greater Cincinnati Water Works	Surface water	100%	No data	No data	No data	No data

Note: The following major WRRF facilities are located upstream of the water quality model domain (0% of data within model domain):
Bellefontaine; Brookville; Eaton; Fairborn; Greenville; Indian Lake; Minster; Oxford; Piqua; Sidney; Southwest Regional; Springfield; Urbana; West Milton.

Data Source	Sample Matrix	Nitrate+Nitrite[a]	Ammonia	Total Kjeldahl Nitrogen	Total Sus. Solids[b]	Total Organic Carbon[c]
Miami Conservancy District	Surface Water	100%	100%	100%	100%	No data
Heidelberg University	Surface Water	100%	No data	100%	100%	No data
MCD/YSI Continuous Monitoring	Surface Water	No data	No data	No data	No data	No data
Ohio Environmental Protection Agency	Surface Water	18%	19%	18%	19%	67%
Troy WWTP	Surface water	100%	100%	No data	No data	No data
Tri-Cities WW Authority	Surface water	No data	100%	100%	No data	No data
Dayton WWTP	Surface water	100%	100%	No data	100%	No data
Montgomery County/Western Regional WWTP	Surface water	100%	100%	100%	No data	No data
West Carrollton WWTP	Surface water	100%	100%	No data	No data	No data
Maimisburg WWTP	Surface water	100%	100%	No data	No data	No data
Springboro WWTP	Surface water	100%	100%	No data	No data	No data
Franklin WWTP	Surface water	No data	100%	No data	No data	No data
Middletown WWTP	Surface water	100%	100%	No data	No data	No data
Lesourdesville WWTP	Surface water	100%	100%	No data	No data	No data
Hamilton WWTP	Surface water	100%	100%	No data	No data	No data
Fairfield WWTP	Surface water	100%	100%	No data	No data	No data
Union WWTP	Surface water	100%	100%	No data	No data	No data
Union WWTP	Surface water	100%	100%	No data	No data	No data
Taylor Creek WWTP	Surface water	100%	100%	No data	No data	No data
Ohio River Valley Water Sanitation Commission	Surface water	100%	100%	100%	100%	100%
AK Steel	Surface water	No data	No data	No data	100%	No data
Fernald	Surface water	No data	No data	No data	No data	No data
Wausau Paper	Surface water	No data	No data	No data	100%	No data
USGS Ohio Water Science Center	Surface water	23%	23%	26%	23%	27%
Greater Cincinnati Water Works	Surface water	100%	100%	No data	No data	No data

Note: The following major WRRF facilities are located upstream of the water quality model domain (0% of data within model domain):
Bellefontaine; Brookville; Eaton; Fairborn; Greenville; Indian Lake; Minster; Oxford; Piqua; Sidney; Southwest Regional; Springfield; Urbana; West Milton.

Data Source	Sample Matrix	Temperature	CBOD-5 Day	CBOD-20 Day	Frac. of Diss. Org. Matter	pH
Miami Conservancy District	Surface Water	100%	No data	No data	No data	100%
Heidelberg University	Surface Water	No data	No data	No data	No data	No data
MCD/YSI Continuous Monitoring	Surface Water	100%	No data	No data	100%	100%
Ohio Environmental Protection Agency	Surface Water	62%	10%	33%	No data	57%
Troy WWTP	Surface water	No data	No data	No data	No data	No data
Tri-Cities WW Authority	Surface water	100%	No data	No data	No data	100%
Dayton WWTP	Surface water	100%	100%	No data	No data	100%
Montgomery County/Western Regional WWTP	Surface water	100%	No data	No data	No data	100%
West Carrollton WWTP	Surface water	100%	No data	No data	No data	100%
Maimisburg WWTP	Surface water	100%	No data	No data	No data	100%
Springboro WWTP	Surface water	100%	No data	No data	No data	100%
Franklin WWTP	Surface water	100%	No data	No data	No data	100%
Middletown WWTP	Surface water	100%	No data	No data	No data	100%
Lesourdesville WWTP	Surface water	100%	No data	No data	No data	100%
Hamilton WWTP	Surface water	100%	No data	No data	No data	100%
Fairfield WWTP	Surface water	100%	No data	No data	No data	100%
Union WWTP	Surface water	100%	No data	No data	No data	100%
Union WWTP	Surface water	100%	No data	No data	No data	100%
Taylor Creek WWTP	Surface water	100%	No data	No data	No data	100%
Ohio River Valley Water Sanitation Commission	Surface water	100%	No data	No data	No data	100%
AK Steel	Surface water	No data	No data	No data	No data	100%
Fernald	Surface water	100%	No data	No data	No data	100%
Wausau Paper	Surface water	100%	100%	No data	No data	No data
USGS Ohio Water Science Center	Surface water	20%	No data	No data	No data	22%
Greater Cincinnati Water Works	Surface water	100%	No data	No data	No data	100%

Note: The following major WRRF facilities are located upstream of the water quality model domain (0% of data within model domain):
Bellefontaine; Brookville; Eaton; Fairborn; Greenville; Indian Lake; Minster; Oxford; Piqua; Sidney; Southwest Regional; Springfield; Urbana; West Milton.

Table 5. Summary of Surface Sediment Quality Data by Agency.

Data Source	Sample Matrix	Chlorophyll a[a]	Total Phosphorus[b]	Phosphorus Flux[d]	Ammonia	Total Organic Carbon[c]
Ohio Environmental Protection Agency	Sediment	2008-2013 (97)	2005-2013 (166)	No data	2005-2013 (166)	2005-2013 (166)
USGS Ohio Water Science Center	Sediment	No data	1998-2013 (10)	No data	No data	1998-2001 (18)
MCD/Wright State University	Sediment	No data	No data	2015 (134)	No data	No data

[a]: Count includes samples corrected for pheophytin

[b]: Count includes samples where phosphorus was measured in mg/kg and %

[c]: Count includes samples where organic carbon <2 mm was measured and organic carbon <62.5u was measured

[d]: Count includes phosphorus flux measurements and the associated standard error in $mg/m^2/day$

Table 6. Summary of Major Point Source Discharge Quality Data.

Data Source	Sample Matrix	Facility Flow	Dissolved Oxygen	Chlorophyll a & Blue-Green Algae	Total Phosphorus	Orthophosphorus
AK Steel	Industrial effluent	2012-2015 (450)	No data	No data	No data	No data
Fernald	Industrial effluent	2012-2015 (114)	2012-2015 (39)	No data	2012-2015 (4)	No data
Hamilton MPP	Industrial effluent	2012-2015 (132)	No data	No data	No data	No data
MillerCoors	Industrial effluent	2012-2015 (78)	2012-2015 (39)	No data	2012-2015 (78)	No data
Wausau Paper	Industrial effluent	2012-2015 (168)	2012-2015 (39)	No data	2015 (16)	No data
Hamilton MPP	Industrial intake	2013-2014 (94)	No data	No data	No data	No data
Maimisburg WWTP	WWTP CSO/SSO/Bypass	2013 (2)	No data	No data	No data	No data
Middletown WWTP	WWTP CSO/SSO/Bypass	2012-2015 (305)	No data	No data	No data	No data
Hamilton WWTP	WWTP CSO/SSO/Bypass	2013-2015 (96)	No data	No data	No data	No data
Troy WWTP	WWTP effluent	1999-2016 (3,154)	No data	No data	2002-2016 (594)	No data
Tri-Cities WW Authority	WWTP effluent	1999-2016 (269)	2012-2015 (39)	No data	2003-2016 (222)	2015 (6)
Dayton WWTP	WWTP effluent	1999-2016 (265)	2012-2015 (39)	No data	1998-2016 (268)	No data
Montgomery County/Western Regional WWTP	WWTP effluent	1999-2016 (258)	2012-2015 (39)	No data	1998-2016 (263)	No data
West Carrollton WWTP	WWTP effluent	1999-2016 (213)	2012-2015 (39)	No data	2000-2016 (212)	No data
Maimisburg WWTP	WWTP effluent	1999-2015 (274)	2012-2015 (39)	No data	1998-2015 (282)	No data
Springboro WWTP	WWTP effluent	1999-2016 (239)	2012-2015 (39)	No data	2002-2016 (224)	No data
Franklin WWTP	WWTP effluent	1999-2015 (540)	2012-2015 (39)	No data	1998-2015 (466)	No data
Middletown WWTP	WWTP effluent	1999-2015 (260)	2012-2015 (39)	No data	1998-2015 (269)	No data
Lesourdesville WWTP	WWTP effluent	1999-2016 (272)	2012-2015 (39)	No data	1998-2016 (280)	No data
Hamilton WWTP	WWTP effluent	1999-2016 (261)	2012-2015 (39)	No data	1999-2016 (284)	No data
Fairfield WWTP	WWTP effluent	1999-2016 (264)	2012-2015 (39)	No data	1998-2016 (274)	No data
Union WWTP	WWTP effluent	1999-2016 (276)	2012-2015 (39)	No data	2007-2016 (182)	No data
Englewood WWTP	WWTP effluent	1999-2016 (217)	2012-2015 (39)	No data	2002-2016 (189)	No data
Taylor Creek WWTP	WWTP effluent	1999-2016 (204)	2012-2015 (95)	No data	1999-2015 (205)	No data
Bellefontaine WWTP	WWTP effluent	1999-2016 (169)	Not compiled	No data	2002-2016 (144)	No data
Brookville WWTP	WWTP effluent	1999-2016 (172)	Not compiled	No data	2003-2016 (124)	No data

Data Source	Sample Matrix	Facility Flow	Dissolved Oxygen	Chlorophyll a & Blue-Green Algae	Total Phosphorus	Orthophosphorus
Eaton WWTP	WWTP effluent	1999-2016 (138)	Not compiled	No data	1999-2016 (141)	2015-2016 (5)
Fairborn WWTP	WWTP effluent	1999-2016 (176)	Not compiled	No data	2006-2016 (97)	No data
Greenville WWTP	WWTP effluent	1999-2016 (171)	Not compiled	No data	2003-2016 (135)	No data
Indian Lake WWTP	WWTP effluent	1999-2016 (172)	Not compiled	No data	2001-2016 (145)	No data
Minster WWTP	WWTP effluent	1999-2016 (165)	Not compiled	No data	No data	No data
Oxford WWTP	WWTP effluent	1999-2016 (168)	Not compiled	No data	2000-2016 (160)	No data
Piqua WWTP	WWTP effluent	1999-2016 (163)	Not compiled	No data	1998-2016 (182)	No data
Sidney WWTP	WWTP effluent	1999-2016 (167)	Not compiled	No data	1998-2016 (178)	No data
Southwest Regional WWTP	WWTP effluent	1999-2016 (170)	Not compiled	No data	2006-2016 (92)	2016 (2)
Springfield WWTP	WWTP effluent	1999-2016 (173)	Not compiled	No data	2001-2016 (151)	No data
Urbana WWTP	WWTP effluent	1999-2016 (174)	Not compiled	No data	1998-2016 (185)	2015-2016 (4)
West Milton WWTP	WWTP effluent	1999-2016 (160)	Not compiled	No data	2006-2016 (96)	No data

Data Source	Sample Matrix	Nitrate+Nitrite[a]	Ammonia	Total Kjeldahl Nitrogen	Total Sus. Solids[b]	Total Organic Carbon[c]
AK Steel	Industrial effluent	No data	2012-2015 (218)	No data	2012-2015 (298)	No data
Fernald	Industrial effluent	2012-2015 (76)	No data	No data	2012-2015 (86)	No data
Hamilton MPP	Industrial effluent	No data	No data	No data	2012-2015 (50)	No data
MillerCoors	Industrial effluent	2012-2015 (76)	2012-2015 (37)	2012-2015 (68)	2012-2015 (78)	No data
Wausau Paper	Industrial effluent	No data	2012-2015 (28)	No data	2012-2015 (78)	No data
Hamilton MPP	Industrial intake	No data	No data	No data	No data	No data
Maimisburg WWTP	WWTP CSO/SSO/Bypass	No data	No data	No data	2013 (2)	No data
Middletown WWTP	WWTP CSO/SSO/Bypass	No data	No data	No data	2012-2015 (308)	No data
Hamilton WWTP	WWTP CSO/SSO/Bypass	No data	2013-2015 (18)	No data	2013-2015 (18)	No data
Troy WWTP	WWTP effluent	1998-2016 (242)	1998-2015 (184)	2002-2011 (106)	No data	No data
Tri-Cities WW Authority	WWTP effluent	1998-2016 (227)	1998-2015 (214)	2003-2015 (165)	2012-2015 (78)	No data
Dayton WWTP	WWTP effluent	1998-2016 (221)	1998-2015 (225)	2003-2015 (166)	2012-2015 (78)	No data
Montgomery County/Western Regional WWTP	WWTP effluent	1998-2016 (270)	1998-2015 (217)	2003-2015 (164)	2012-2015 (78)	No data
West Carrollton WWTP	WWTP effluent	1998-2016 (225)	1998-2015 (221)	1998-2015 (177)	2012-2015 (78)	No data
Maimisburg WWTP	WWTP effluent	1998-2015 (225)	1998-2015 (225)	2003-2015 (106)	2012-2015 (78)	No data
Springboro WWTP	WWTP effluent	1998-2016 (131)	1998-2015 (186)	2013-2015 (22)	2012-2015 (78)	No data
Franklin WWTP	WWTP effluent	1998-2015 (284)	1998-2015 (205)	2003-2009 (68)	2012-2015 (78)	No data
Middletown WWTP	WWTP effluent	1998-2015 (271)	1998-2015 (219)	2003-2015 (106)	2012-2015 (78)	No data
Lesourdesville WWTP	WWTP effluent	1998-2016 (284)	1998-2015 (223)	2003-2015 (165)	2012-2015 (78)	No data
Hamilton WWTP	WWTP effluent	1998-2016 (221)	1998-2015 (239)	2003-2015 (152)	2012-2015 (78)	No data
Fairfield WWTP	WWTP effluent	1998-2016 (397)	1998-2015 (219)	1998-2015 (172)	2012-2015 (78)	No data
Union WWTP	WWTP effluent	1998-2016 (346)	1998-2015 (227)	1998-2015 (225)	2012-2015 (78)	No data
Englewood WWTP	WWTP effluent	1998-2016 (229)	1998-2016 (227)	2002-2016 (186)	2012-2015 (78)	No data
Taylor Creek WWTP	WWTP effluent	1998-2015 (212)	1998-2015 (201)	2004-2015 (151)	2012-2015 (106)	No data
Bellefontaine WWTP	WWTP effluent	1998-2016 (179)	1999-2016 (113)	2002-2016 (75)	2013-2016 (39)	No data
Brookville WWTP	WWTP effluent	1998-2016 (157)	1998-2016 (190)	2013-2016 (32)	2013-2016 (39)	No data
Eaton WWTP	WWTP effluent	1998-2016 (150)	1998-2016 (184)	1999-2016 (41)	2013-2016 (39)	No data

Fairborn WWTP	WWTP effluent	1998-2016 (186)	1998-2016 (184)	2006-2016 (32)	2013-2016 (39)	No data
Greenville WWTP	WWTP effluent	1998-2016 (182)	1998-2016 (158)	2003-2016 (52)	2013-2016 (39)	No data
Indian Lake WWTP	WWTP effluent	1998-2016 (178)	1998-2016 (171)	2002-2016 (91)	2013-2016 (38)	No data
Minster WWTP	WWTP effluent	1998-2011 (136)	1998-2011 (136)	1998-2000 (20)	No data	No data
Oxford WWTP	WWTP effluent	2000-2016 (160)	1998-2016 (189)	2004-2016 (102)	2013-2016 (39)	No data
Piqua WWTP	WWTP effluent	1998-2016 (181)	1998-2016 (177)	2002-2016 (133)	2013-2016 (39)	No data
Sidney WWTP	WWTP effluent	1998-2016 (178)	1998-2016 (178)	2002-2016 (139)	2013-2016 (39)	No data
Southwest Regional WWTP	WWTP effluent	1998-2016 (182)	1998-2016 (181)	2013-2016 (13)	2013-2016 (39)	No data
Springfield WWTP	WWTP effluent	1998-2016 (185)	1998-2016 (172)	2001-2016 (150)	2013-2016 (39)	No data
Urbana WWTP	WWTP effluent	1998-2016 (185)	1998-2016 (184)	2013-2016 (39)	2013-2016 (39)	No data
West Milton WWTP	WWTP effluent	1998-2016 (168)	1998-2016 (137)	No data	2013-2016 (39)	No data

Data Source	Sample Matrix	Temperature	CBOD-5 Day	CBOD-20 Day	Frac. of Diss. Org. Matter	pH
AK Steel	Industrial effluent	No data	No data	No data	No data	2012-2015 (450)
Fernald	Industrial effluent	2012-2015 (78)	2012-2015 (8)	No data	No data	2012-2015 (14)
Hamilton MPP	Industrial effluent	2012-2015 (97)	No data	No data	No data	2012-2015 (80)
MillerCoors	Industrial effluent	2012-2015 (78)	No data	No data	No data	2012-2015 (78)
Wausau Paper	Industrial effluent	2012-2015 (78)	2012-2015 (78)	No data	No data	2012-2015 (56)
Hamilton MPP	Industrial intake	2013-2014 (94)	No data	No data	No data	No data
Maimisburg WWTP	WWTP CSO/SSO/Bypass	No data	2013 (2)	No data	No data	No data
Middletown WWTP	WWTP CSO/SSO/Bypass	No data	2012-2015 (308)	No data	No data	No data
Hamilton WWTP	WWTP CSO/SSO/Bypass	No data	2013-2015 (18)	No data	No data	No data
Troy WWTP	WWTP effluent	No data	No data	No data	No data	No data
Tri-Cities WW Authority	WWTP effluent	2012-2015 (78)	2012-2015 (78)	No data	No data	No data
Dayton WWTP	WWTP effluent	2012-2015 (78)	2012-2015 (78)	No data	No data	No data
Montgomery County/Western Regional WWTP	WWTP effluent	2012-2015 (78)	2012-2015 (78)	No data	No data	No data
West Carrollton WWTP	WWTP effluent	2012-2015 (78)	2012-2015 (78)	No data	No data	No data
Maimisburg WWTP	WWTP effluent	2012-2015 (78)	2012-2015 (78)	No data	No data	No data
Springboro WWTP	WWTP effluent	2012-2015 (78)	2012-2015 (78)	No data	No data	No data
Franklin WWTP	WWTP effluent	2012-2015 (78)	2012-2015 (78)	No data	No data	No data
Middletown WWTP	WWTP effluent	2012-2015 (78)	2012-2015 (78)	No data	No data	No data
Lesourdesville WWTP	WWTP effluent	2012-2015 (78)	2012-2015 (78)	No data	No data	No data
Hamilton WWTP	WWTP effluent	2012-2015 (78)	2012-2015 (78)	No data	No data	No data
Fairfield WWTP	WWTP effluent	2012-2015 (78)	2012-2015 (78)	No data	No data	No data
Union WWTP	WWTP effluent	2012-2015 (78)	2012-2015 (78)	No data	No data	No data
Englewood WWTP	WWTP effluent	2012-2015 (78)	2012-2015 (78)	No data	No data	No data
Taylor Creek WWTP	WWTP effluent	2012-2015 (162)	2012-2015 (78)	No data	No data	2012-2015 (67)
Bellefontaine WWTP	WWTP effluent	2013-2016 (39)	2013-2016 (39)	No data	No data	No data
Brookville WWTP	WWTP effluent	2013-2016 (32)	2013-2016 (39)	No data	No data	No data
Eaton WWTP	WWTP effluent	2015-2016 (5)	2013-2016 (39)	No data	No data	No data

Fairborn WWTP	WWTP effluent	2013-2016 (39)	2013-2016 (39)	No data	No data	No data
Greenville WWTP	WWTP effluent	2013-2016 (33)	2013-2016 (39)	No data	No data	No data
Indian Lake WWTP	WWTP effluent	2013-2016 (38)	2013-2016 (38)	No data	No data	No data
Minster WWTP	WWTP effluent	2013-2016 (39)	No data	No data	No data	No data
Oxford WWTP	WWTP effluent	2013-2016 (31)	2013-2016 (39)	No data	No data	No data
Piqua WWTP	WWTP effluent	2013-2016 (39)	2013-2016 (39)	No data	No data	No data
Sidney WWTP	WWTP effluent	2013-2016 (39)	2013-2016 (39)	No data	No data	No data
Southwest Regional WWTP	WWTP effluent	2013-2016 (39)	2013-2016 (39)	No data	No data	No data
Springfield WWTP	WWTP effluent	2013-2016 (39)	2013-2016 (39)	No data	No data	No data
Urbana WWTP	WWTP effluent	2013-2016 (39)	2013-2016 (39)	No data	No data	No data
West Milton WWTP	WWTP effluent	2013-2016 (39)	2013-2016 (39)	No data	No data	No data

Table 7. Summary of Groundwater Quality Data by Data Source.

Data Source	Sample Matrix	Dissolved Oxygen	Chlorophyll a	Blue-Green Algae	Total Phosphorus	Orthophosphorus
Miami Conservancy District	Ground water	2015 (16)	No data	No data	2015 (16)	2015 (16)
USGS Ohio Water Science Center	Ground water	1997-2011 (259)	No data	No data	1997-2004 (60)	1996-2011 (334)
Ohio Division of Drinking and Ground Water	Ground water	No data	No data	No data	1999-2012 (177)	No data
Greater Cincinnati Water Works	Ground water	2010-2015 (216)	No data	No data	No data	No data

Data Source	Sample Matrix	Nitrate+Nitrite[a]	Ammonia	Total Kjeldahl Nitrogen	Total Sus. Solids[b]	Dissolved Org. Carbon[c]
Miami Conservancy District	Ground water	No data	2015 (16)	2015 (16)	2015 (16)	2015 (16)
USGS Ohio Water Science Center	Ground water	No data	1996-2011 (390)	1996-2011 (370)	1996-2011 (205)	1996-2011 (334)
Ohio Division of Drinking and Ground Water	Ground water	No data	1996-2012 (177)	1996-2012 (177)	1996-2012 (171)	No data
Greater Cincinnati Water Works	Ground water	No data	2010-2015 (216)	2010-2015 (216)	2010-2015 (216)	No data

Data Source	Sample Matrix	Temperature	CBOD-5 Day	CBOD-20 Day	Frac. of Diss. Org. Matter	pH
Miami Conservancy District	Ground water	2015 (16)	2015 (16)	No data	No data	2015 (16)
USGS Ohio Water Science Center	Ground water	1996-2011 (169)	No data	No data	No data	1996-2011 (205)
Ohio Division of Drinking and Ground Water	Ground water	1996-2012 (175)	No data	No data	No data	1996-2012 (171)
Greater Cincinnati Water Works	Ground water	2010-2015 (216)	No data	No data	No data	2010-2015 (216)

Table 8. Summary of Count of Data Failing Quality Assurance/Quality Control Review.

Parameter	Count	"R" Flagged	% "R" Flagged
Dissolved oxygen	111,189	94	0.1%
Carbonaceous biochemical oxygen demand, 5-day	1,820	108	5.6%
Carbonaceous biochemical oxygen demand, 20-day	1,294	0	0.0%
Total phosphorus[a]	36,144	100	0.3%
Orthophosphorus	19,476	9	<0.1%
Ammonia[b]	28,774	108	0.4%
Total Kjeldahl nitrogen	26,967	1	<0.1%
Nitrate+Nitrite[c]	35,110	5	<0.1%
Chlorophyll a[d]	97,119	78	0.1%
Blue-green algae	70,569	1,711	2.4%
Total organic carbon[e]	716	0	0.0%
Fraction of dissolved organic matter	72,120	160	0.2%
pH	118,492	1,513	1.3%
Temperature	137,895	172	0.1%
Total suspended solids[f]	25,706	314	1.2%

[a]: Total phosphorus count includes 167 sediment samples measured in mg/L and 9 sediment samples measured in percent

[b]: Ammonia count includes 166 samples measured in sediment

[c]: Nitrate and nitrite count includes 9,539 records where only nitrate was measured

[d]: Chlorophyll a count includes 293 samples corrected for pheophytin, and 100 records corrected for pheophytin and measured in sediment

[e]: Total organic carbon count includes 9 samples where organic carbon <2 mm was measured, 9 samples where organic carbon <62.5 u was measured, 126 samples where particulate organic carbon was measured, and 166 samples where total organic carbon was measured in sediment

[f]: Total suspended solids count includes 198 records where suspended sediment concentration was measured

Table 9. Summary of Count of Data within Water Quality Model Domain Failing Quality Assurance/Quality Control Review.

Parameter	Count	"R" Flagged	% "R" Flagged
Dissolved oxygen	110,099	94	0.1%
Carbonaceous biochemical oxygen demand, 5-day	1,626	108	6.2%
Carbonaceous biochemical oxygen demand, 20-day	432	0	0.0%
Total phosphorus[a]	28,534	100	0.4%
Orthophosphorus	18,507	9	<0.1%
Ammonia[b]	18,870	108	0.6%
Total Kjeldahl nitrogen	21,655	1	<0.1%
Nitrate+Nitrite[c]	26,982	5	<0.1%
Chlorophyll a[d]	96,846	78	0.1%
Blue-green algae	70,569	1,711	2.4%
Total organic carbon[e]	369	0	0.0%
Fraction of dissolved organic matter	72,120	160	0.2%
pH	113,998	1,512	1.3%
Temperature	134,140	172	0.1%
Total suspended solids[f]	21,191	138	0.6%

[a]: Total phosphorus count includes 39 sediment samples measured in mg/L and 1 sediment samples measured in percent

[b]: Ammonia count includes 39 samples measured in sediment

[c]: Nitrate and nitrite count includes 9,366 records where only nitrate was measured

[d]: Chlorophyll a count includes 100 samples corrected for pheophytin, and 27 records corrected for pheophytin and measured in sediment

[e]: Total organic carbon count includes 1 sample where organic carbon <2 mm was measured, 1 sample where organic carbon <62.5 u was measured, 34 samples where particulate organic carbon was measured, and 39 samples where total organic carbon was measured in sediment

[f]: Total suspended solids count includes 45 records where suspended sediment concentration was measured

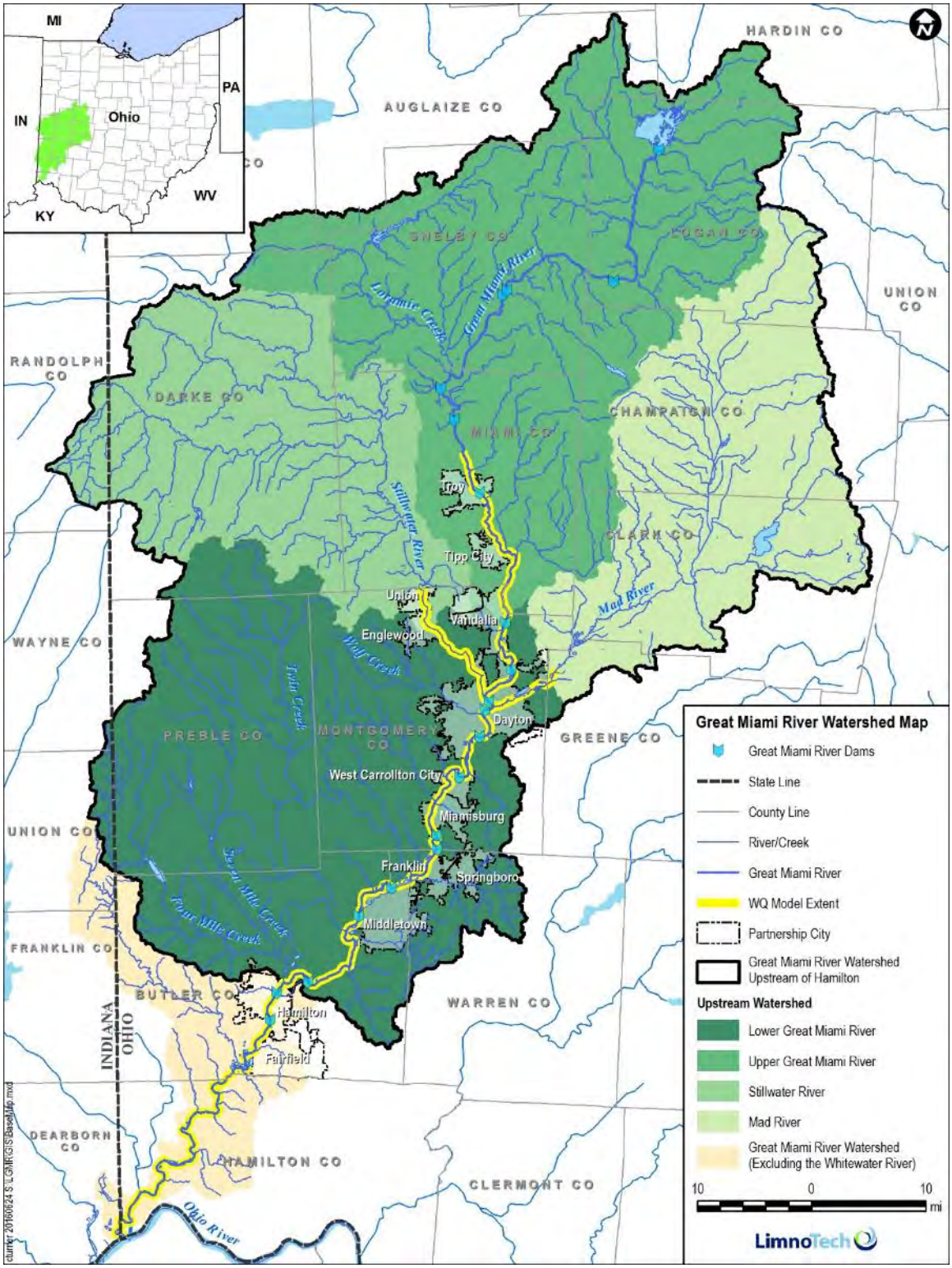

Figure 1. Base Map Features of the Great Miami River Watershed.

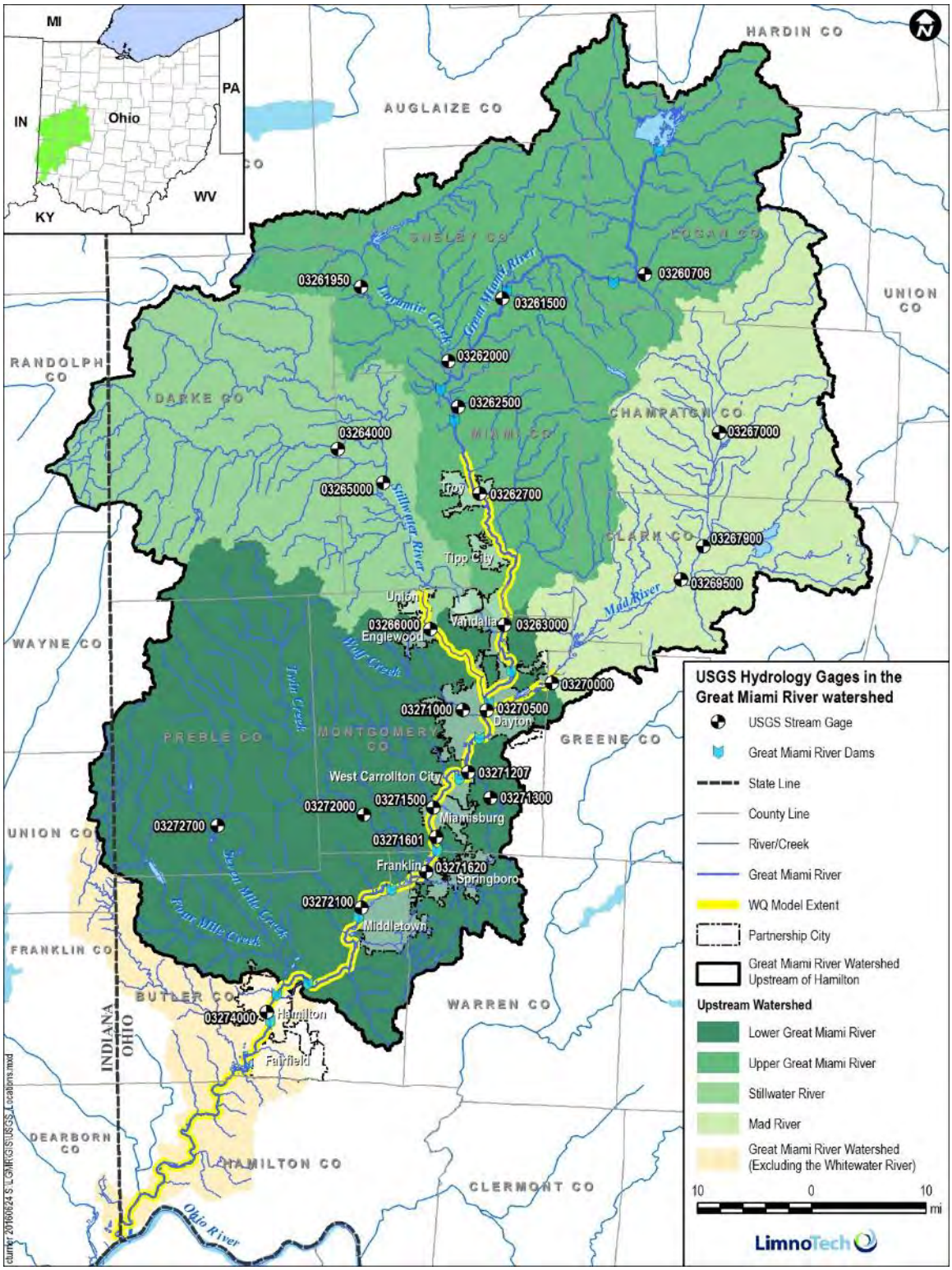

Figure 2. Locations of Hydrologic and Hydraulic Data in the Great Miami River Watershed.

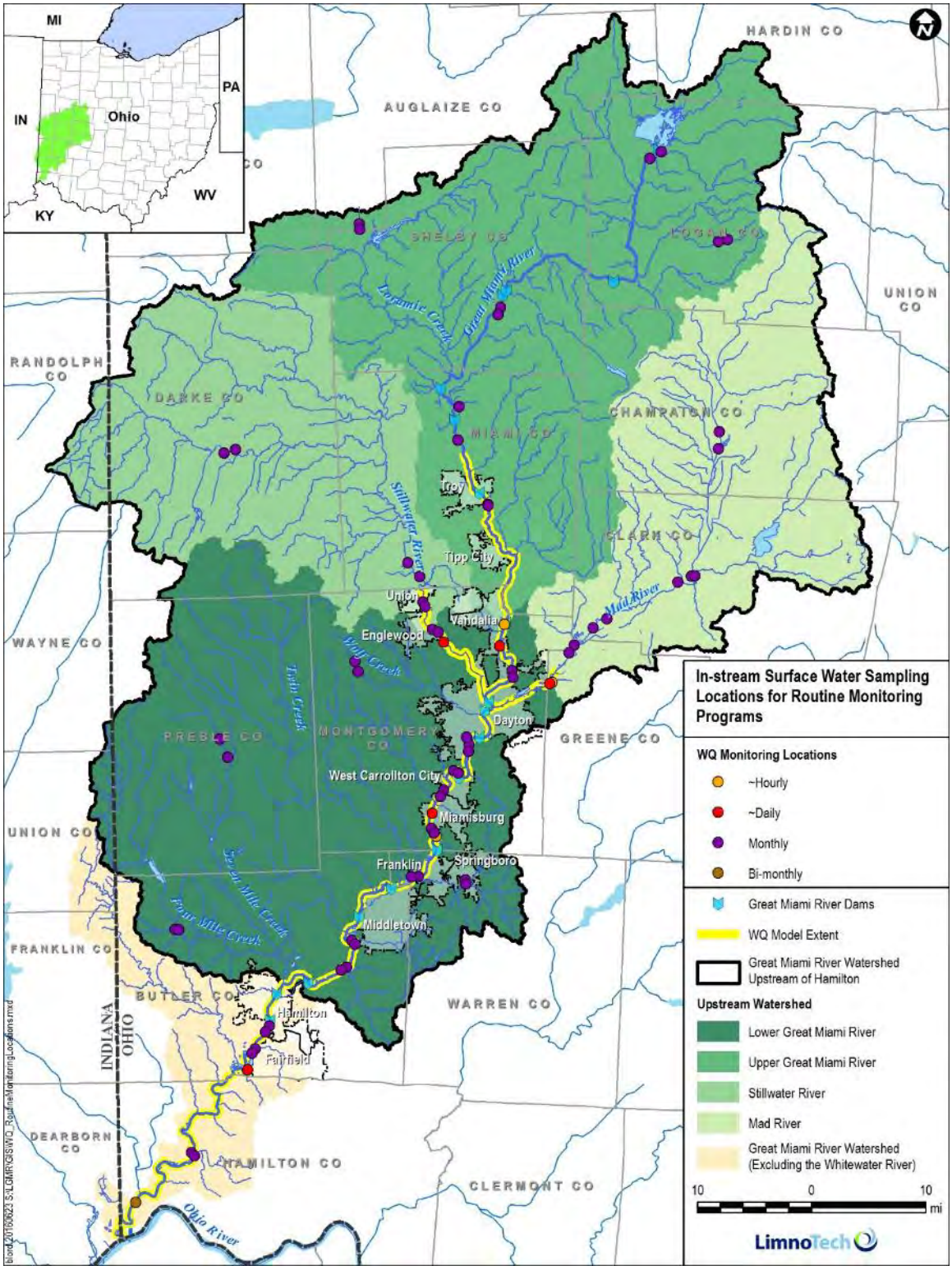

Figure 3. In-Stream Water Quality Sampling Locations of Routine Monitoring Programs in the Great Miami River Watershed.

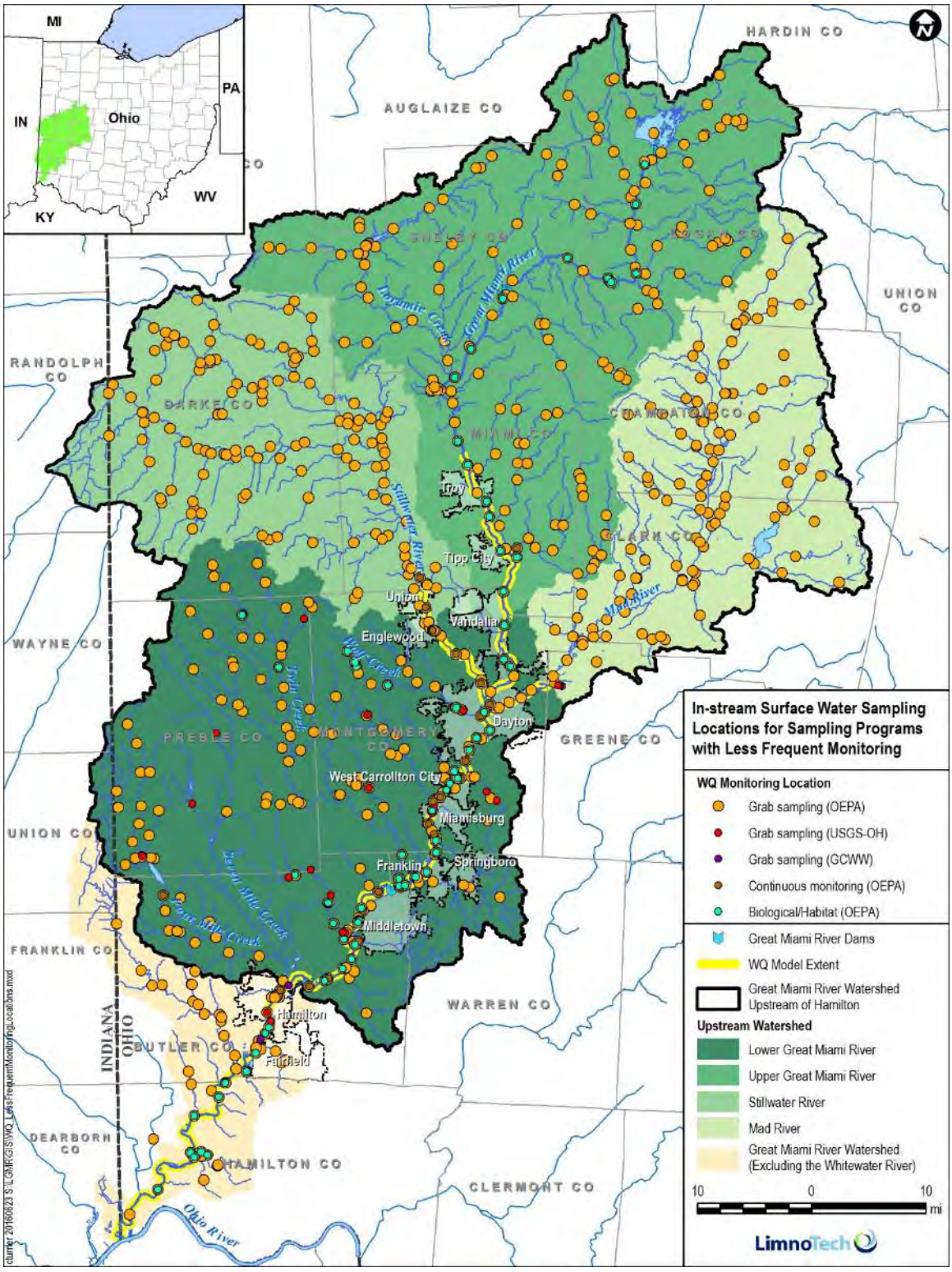

Figure 4. In-stream Surface Water Sampling Locations of Programs Conducting Periodic Monitoring in the Great Miami River Watershed.

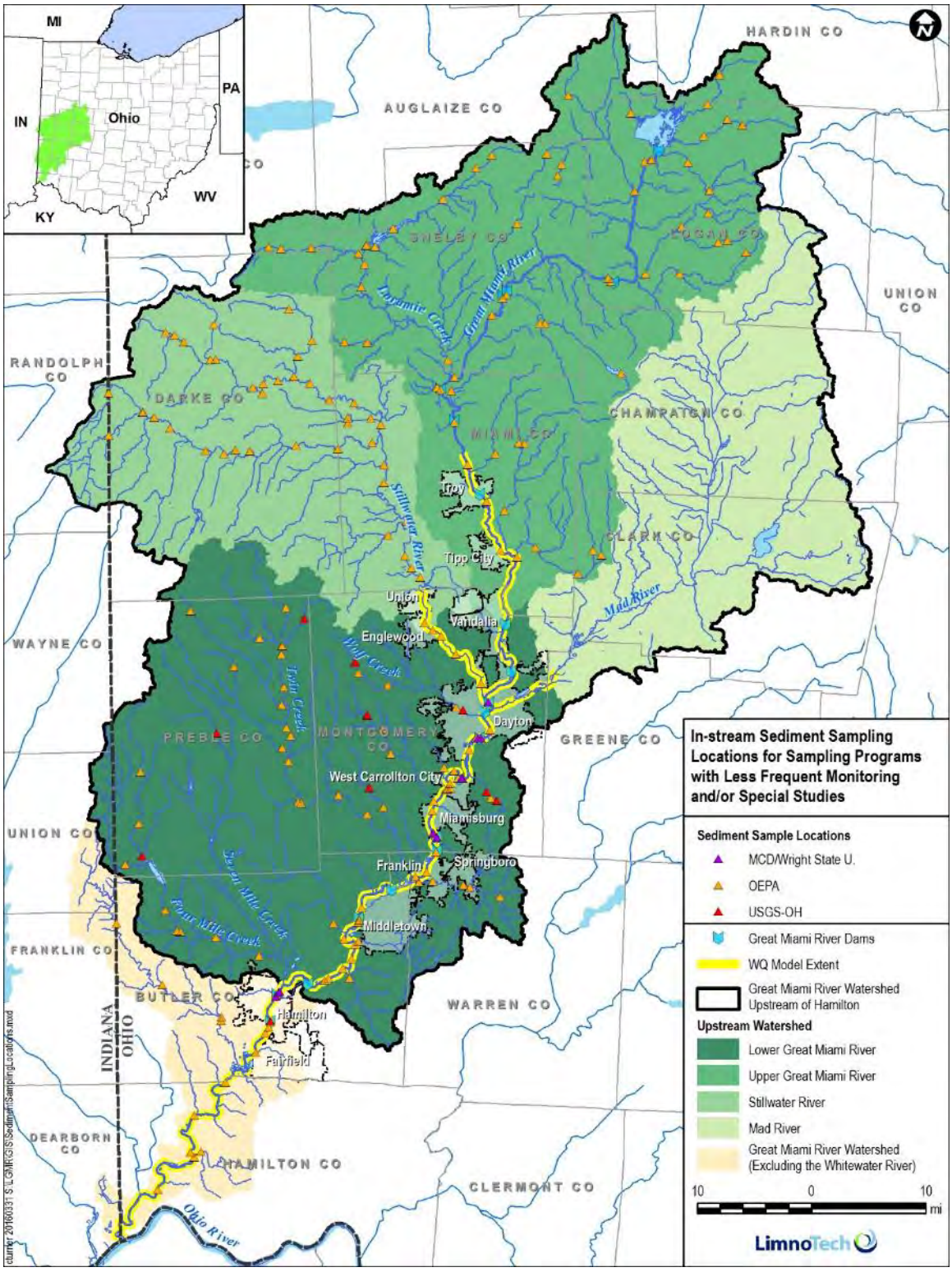

Figure 5. Sediment Sampling Locations in the Great Miami River Watershed.

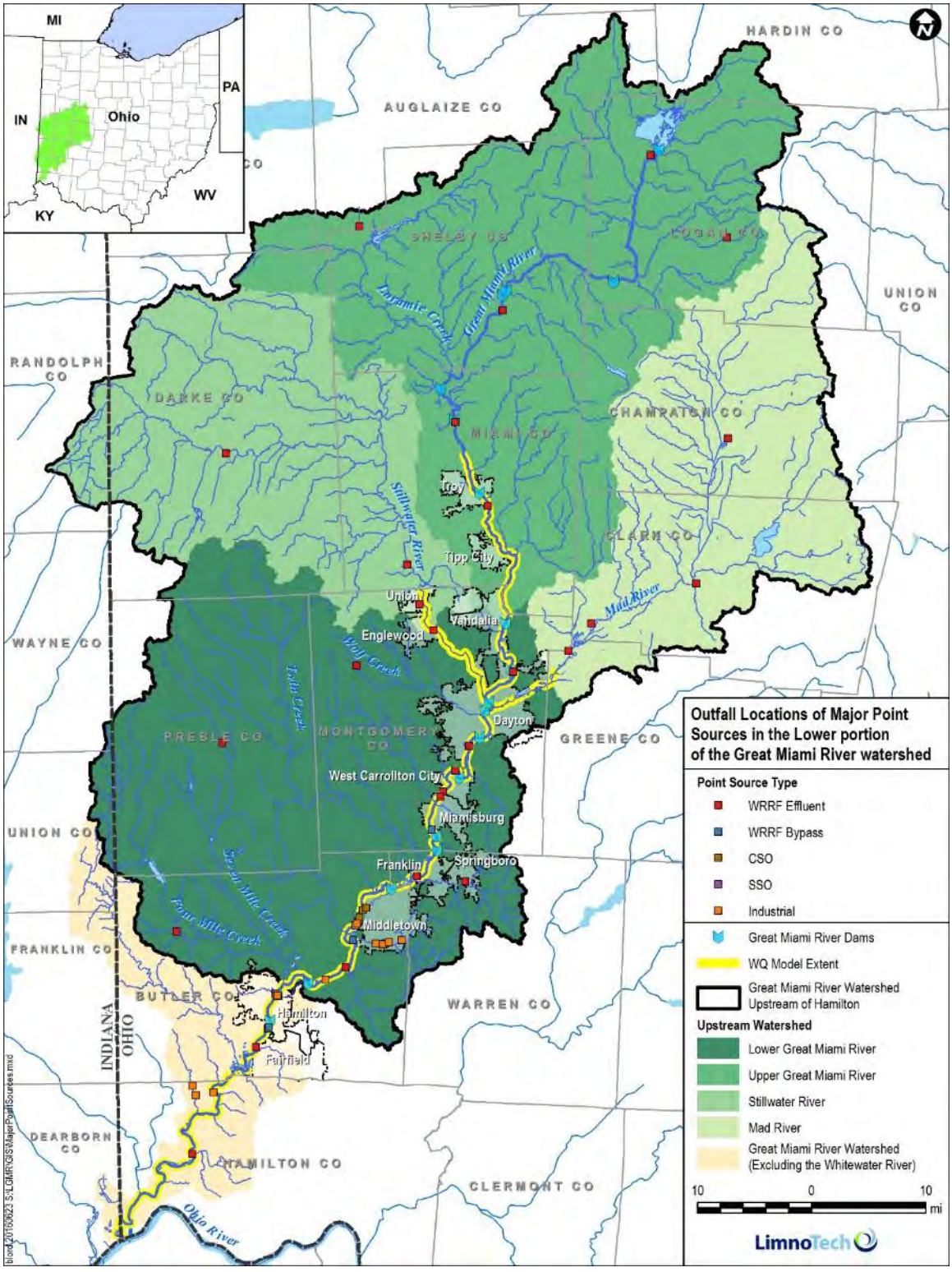

Figure 6. Outfall Locations in the Lower Great Miami River of Major Point Sources.

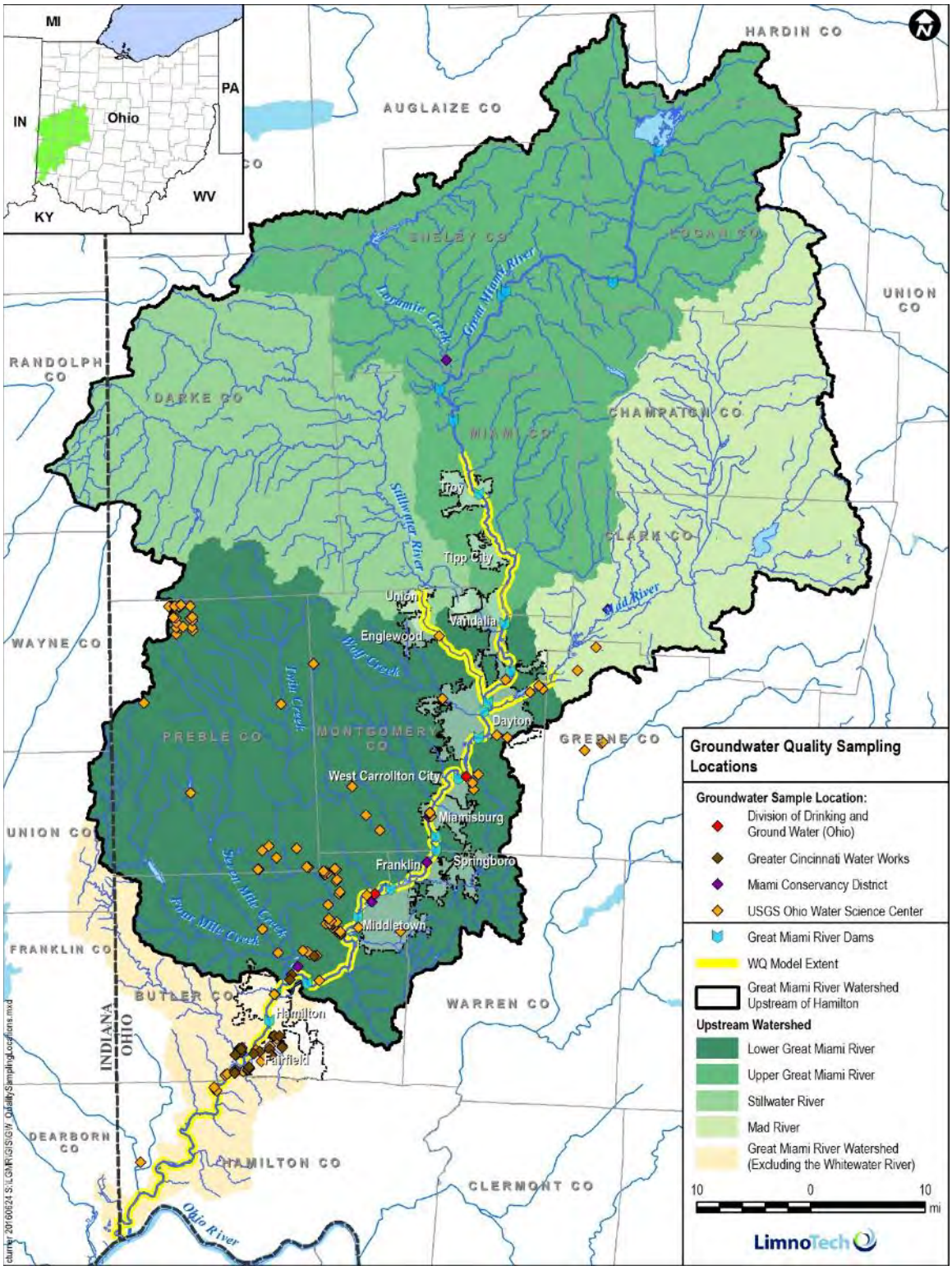

Figure 7. Groundwater Quality Sampling Locations in the Lower Great Miami River Watershed.

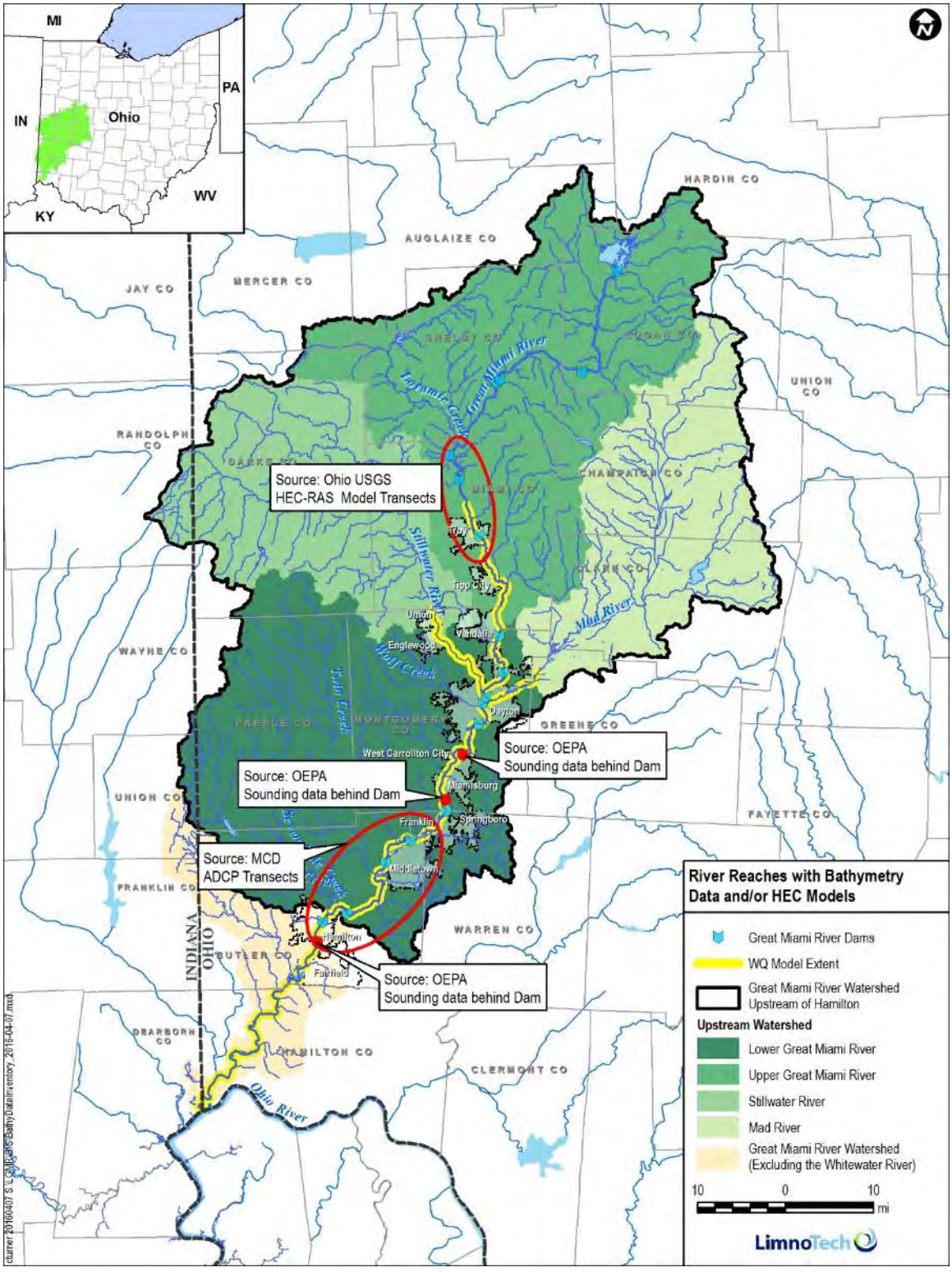

Figure 8. Locations of Bathymetry Data in the Lower Great Miami River Watershed.

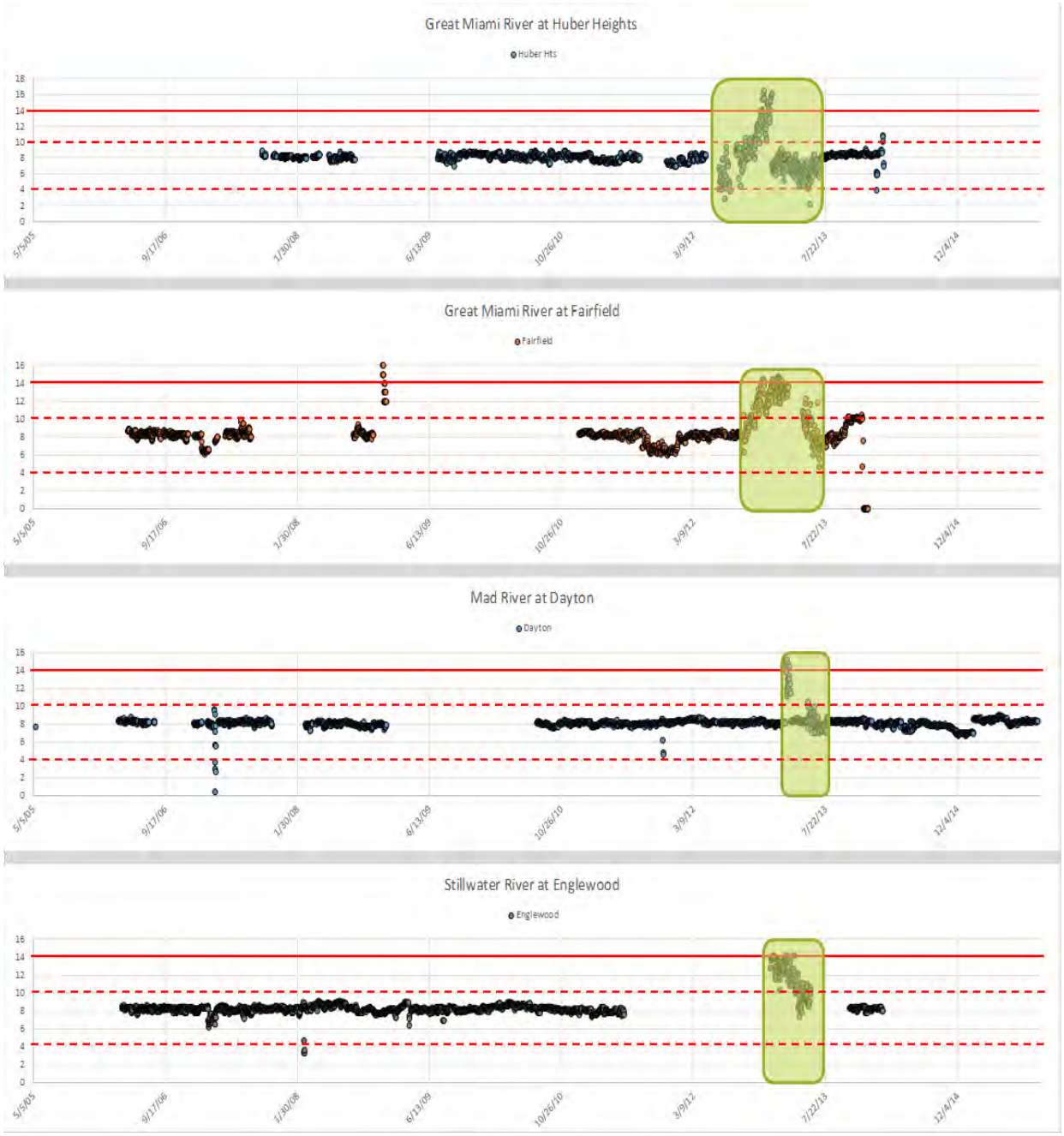

Figure 9. Example of Poor pH Data Quality Resulting from Unreasonable Values.

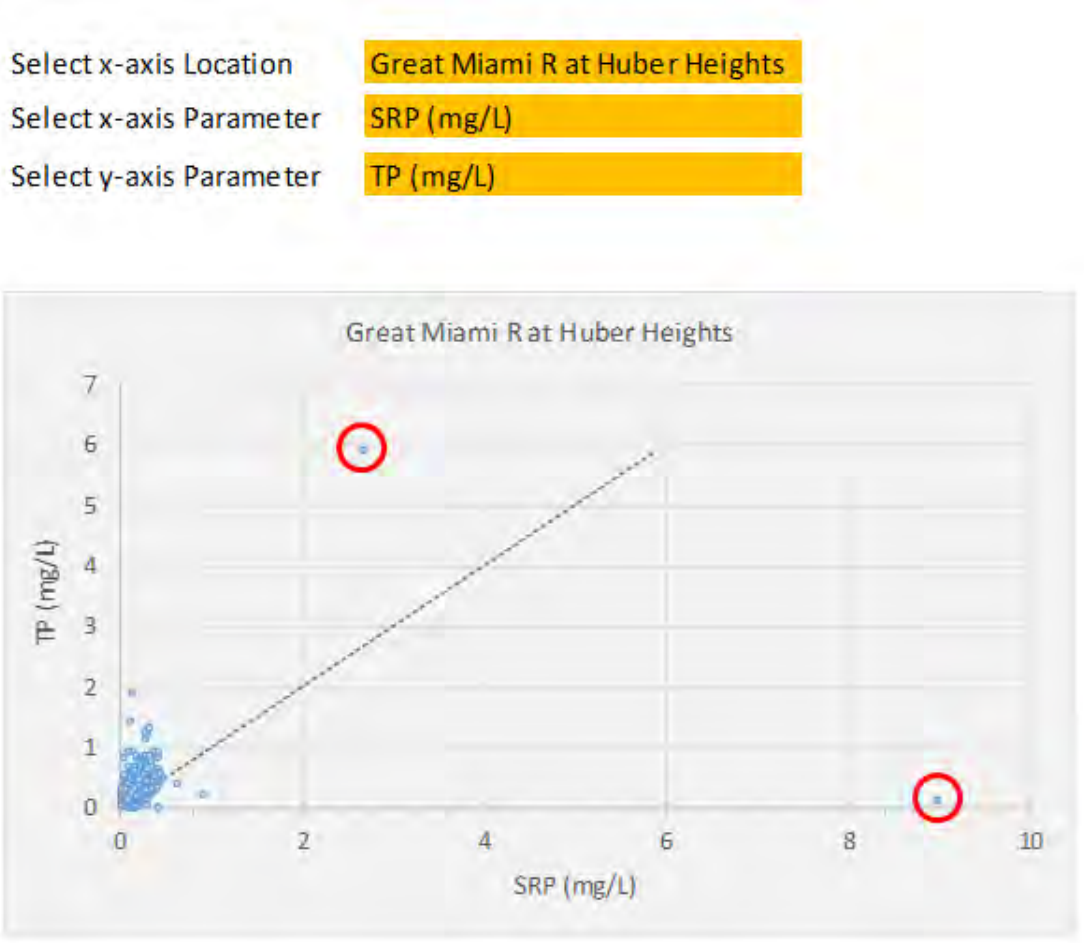

Figure 10. Example of Poor Total Phosphorus and Soluble Reactive Phosphorus Data Quality Resulting from Unreasonable Relationship Results.

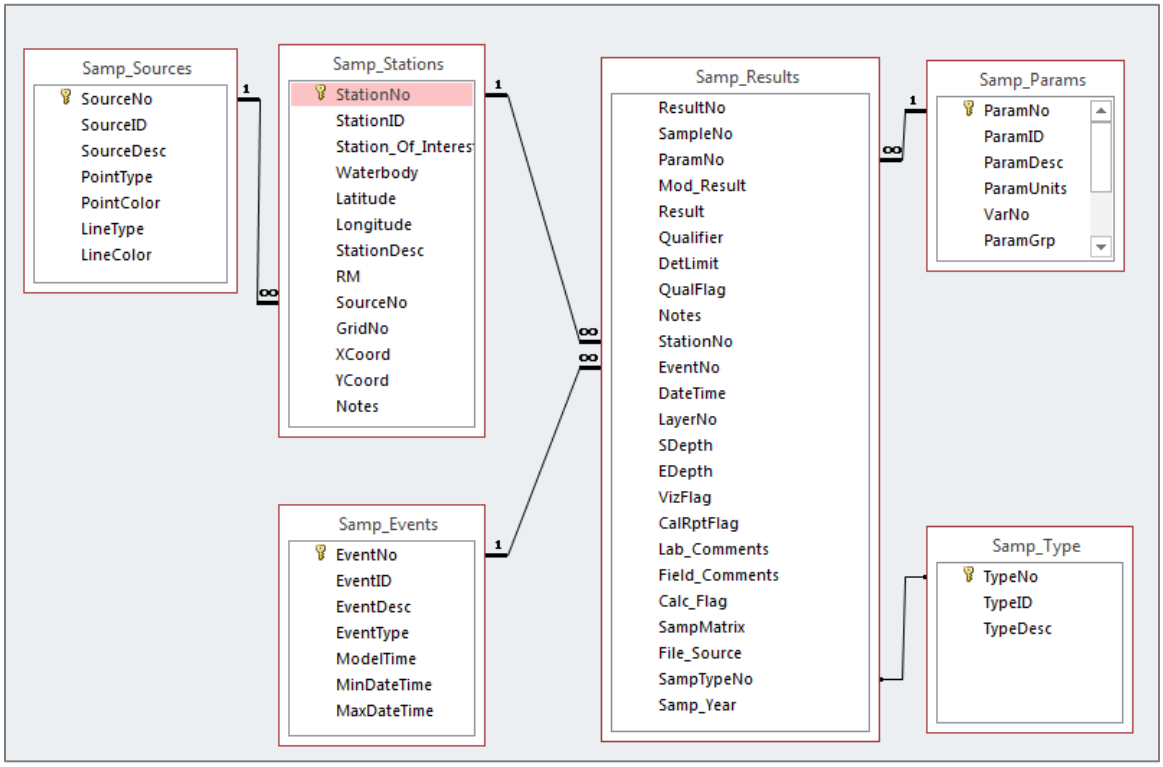

Figure 11. Project Database Structure and Relationships.

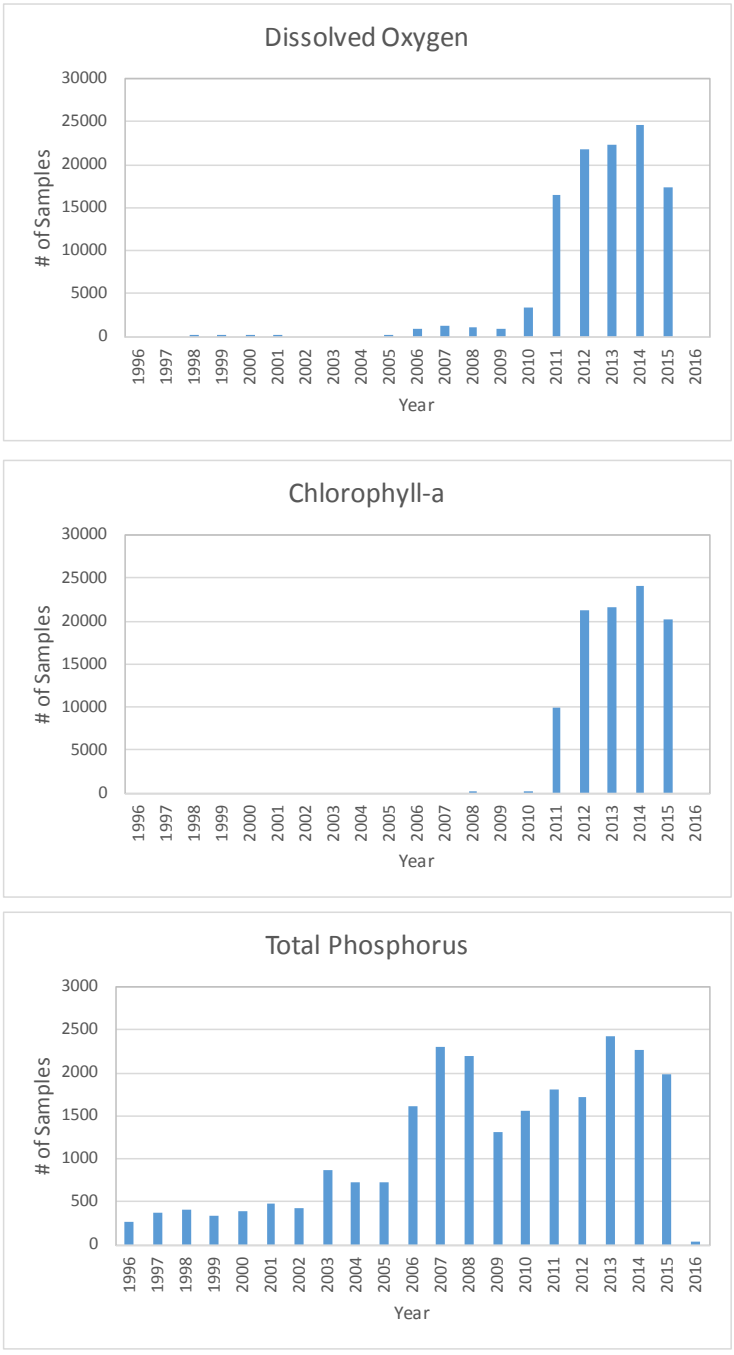

Figure 12. Number of Available Data by Year for Dissolved Oxygen, Chlorophyll a, and Total Phosphorus, 1996-2015.

Appendix B:
Model Selection Memo

Blank

LimnoTech
Water Environment | Scientists Engineers

501 Avis Drive
Ann Arbor, MI 48108
734.332.1200
www.limno.com

Memorandum

From: Dave Dilks, Todd Redder, Carrie Turner, Scott Bell

Date: June 20, 2016

Project: Lower Great Miami River Nutrient Management Project

To: Sarah Hippensteel (MCD)

CC:

SUBJECT: Model Selection for the Lower Great Miami River Water Quality Model

Summary

LimnoTech has been contracted by the Miami Conservancy District (MCD) to select and apply a water quality model to support nutrient management of the Lower Great Miami River (LGMR). This memorandum presents LimnoTech's recommended modeling platform, based on the following considerations:

- *Project understanding* – LimnoTech has acquired a good understanding of the project and the needs of MCD and the Water Resource Recovery Facility (WRRF) partners through numerous discussion with them, as well as a review of background materials.
- *Data review and gap analysis* – As part of this project LimnoTech has conducted a thorough compilation, review and gap analysis of the relevant data available to support development of the LGMR water quality model. This data review and gap analysis is documented in a separate memorandum.
- *Modeling objectives* – LimnoTech previously prepared a draft memorandum (dated 3/18/16) outlining modeling objectives for review, consideration and discussion. This memo was presented and discussed at the March 22 project meeting and subsequently reviewed and commented on by the Ohio EPA. As a result of comments received, the modeling objectives for the LGMR water quality model were refined and are presented in this memorandum.
- *Available modeling platforms* – LimnoTech has knowledge of, and experience with, most of the available water quality modeling platforms used to model nutrients in surface water bodies. In addition, LimnoTech recently led a research project for the Water Environment Research Foundation (WERF) to develop a modeling tool box for assessment of nutrient impacts on water quality, as well as guidance and tools to support selection of appropriate models to address site-specific considerations. Application of the model selection decision tool developed for that project is presented in this memo.
- *Consideration of benthic algae* - Data provided by Ohio EPA and discussions with MCD and project partners indicate that benthic algae may play a significant role in dissolved oxygen conditions at some locations in the river, under certain conditions. Therefore, plant productivity will be simulated by representation of both sestonic and benthic algae.

With these considerations in mind, LimnoTech reviewed a range of potentially applicable hydrodynamic and water quality models and has identified the linked Environmental Fluid Dynamics Code (EFDC) - Advanced Aquatic Ecosystem Model (A2EM) as the model framework most appropriate for the LGMR water quality model. This modeling framework links

hydrodynamic predictions from the EFDC model to the advanced eutrophication model A2EM (Figure 1). EFDC-A2EM is selected over other candidate modeling frameworks due to its flexible and scalable design, computational efficiency and wide application base at similar sites around the United States.

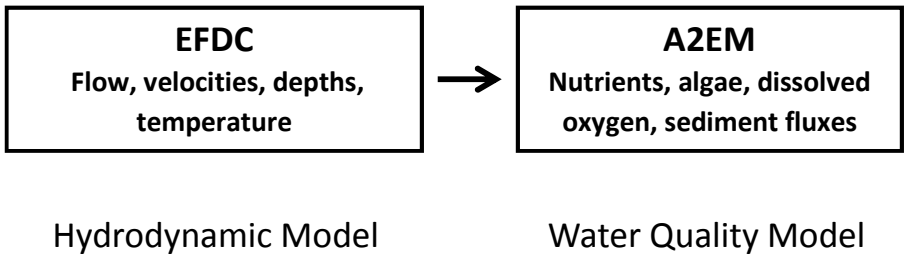

Figure 1. Linked EFDC-A2EM Model Framework

This memorandum describes the model selection process, and provides a description of the capabilities of the linked EFDC-A2EM model framework.

Introduction

A partnership of WRRFs with permitted outfalls to the LGMR, in conjunction with the MCD, have been investigating the causes and impacts of nutrient enrichment of the lower section of the Great Miami River, and are actively monitoring this issue as it relates to the renewal of individual National Pollutant Discharge Elimination System (NPDES) permits for their respective facilities. This project requires development and calibration of a water quality model that can accurately simulate water quality in the LGMR under a range of environmental conditions and can be used to evaluate the effects of nutrient reduction scenarios. Careful selection of the most suitable modeling platform is needed before model development can begin. LimnoTech has considered a number of factors including our understanding of the project, our knowledge of the available data (gained through our review and gap analysis of the available data, documented in a separate memorandum), the project modeling objectives and knowledge of the available modeling platforms. The latter two considerations are discussed in detail in this memorandum. The memorandum is organized into the major sections below, following this introduction:

- LGMR Modeling Objectives;
- Available Modeling Platforms; and
- Selection of Recommended Modeling Platform.

LGMR Modeling Objectives

Explicit delineation of management objectives is an essential first step towards selecting a modeling platform. Based on our current understanding, the overarching management objective can be stated as "the model must be capable of supporting future regulatory decisions regarding management of point and nonpoint nutrient sources to the Lower Great Miami River." Several more explicit modeling objectives were developed by LimnoTech for consideration by the MCD and WRRF partners. These were presented in a draft memorandum dated March 18, 2016. The memorandum was subsequently reviewed by and commented on by Ohio EPA. Further

discussions with MCD and WRRF partners resulted in the modeling objectives described below. The model attributes needed to support the modeling objectives are also discussed below.

Modeling Objectives

The final modeling objectives for this project are described below.

Quantify the benefits to in-stream dissolved oxygen levels and algal production from reduced phosphorus discharges from the WRRF partners

The major WRRFs in the Great Miami River watershed are facing or have recently received permit limits of 1.0 mg/l for total phosphorus. The 1.0 mg/l limit is in keeping with the guidelines described in the Ohio Nutrient Reduction Strategy (Ohio EPA, 2013) for discharges to receiving waters that are currently impaired for nutrients. Furthermore, these limits are referred to as "initial limits" in the Strategy, and lower limits in the future are not precluded. Given the high cost of enhanced phosphorus treatment at WRRFs, a scientifically sound evaluation of the effect of reduced phosphorus loading on the river is required, and this can be best achieved by development and application of an appropriate, calibrated water quality model.

Evaluate the benefits to in-stream dissolved oxygen levels and algal production from controls of different sources of phosphorus

Loading of phosphorus occurs from both point sources (including WRRFs) and non-point sources such as agricultural runoff, although, at present, the relative contribution of phosphorus from various sources is not known. The Ohio Nutrient Reduction Strategy recognizes this and recommends strategies for reducing non-point source phosphorus loads, as well as for controlling point sources. In light of this, the LGMR water quality model should be capable of quantifying and comparing the benefits of various point source and non-point source phosphorus control actions.

Identify and evaluate phosphorus-sensitive areas

It is likely that not all parts of the LGMR are equally affected by phosphorus loading; therefore, it is of interest to identify those reaches for which water quality is most sensitive to phosphorus loading and develop an understanding of the sources that are most closely tied to those reaches. This will allow evaluation of potential phosphorus control actions that will have the greatest benefit across the LGMR system.

Identify critical conditions

As with all rivers, dissolved oxygen concentrations and algal production respond to a range of factors in addition to phosphorus concentrations. The conditions that result in the greatest impacts (e.g., lowest dissolved oxygen, largest diurnal swings, highest algal growth) are referred to as critical conditions. These critical conditions may be described by attributes such as length of day, river flow and temperature, as well as phosphorus loading. Understanding of these critical conditions, including where, when and how often they occur, is important to developing effective water quality improvement strategies.

Estimate downstream distance of impact for WRRFs

This objective is related to the first objective (evaluate the benefits to in-stream dissolved oxygen levels and algal production from reduced phosphorus discharges from the WRRF partners) but more explicitly defines as an objective each WRRF's interest in understanding, to the extent practicable, the downstream extent of impact of their discharge in terms of phosphorus

concentrations, dissolved oxygen, sestonic algae (as represented by chlorophyll *a* in the water column) and benthic algae. Linking this information to phosphorus-sensitive areas may provide additional insight into the appropriate level of phosphorus control for each WRRF. This objective may help utility managers make better-informed decisions regarding investments in control technologies and monitoring activities.

Ensure that the LGMR model is scientifically sound

Because there are multiple parties interested in future phosphorus control strategies for the LGMR, the LGMR water quality model will likely be subject to close scrutiny and will undergo review by parties other than the MCD and WRRF partners. For this reason, it is important that the LGMR water quality model be developed in a scientifically sound manner. This means that the model should be developed using generally accepted methods in current practice, be developed and calibrated using quality site-specific data, be fully and clearly documented, and be internally reviewed before being made public.

Model Attributes to Support Model Objectives

The objectives described above lead to a better understanding of the various model attributes required, which directly informs model selection. The key model attributes informed by the objectives include:

- State variables to be modeled;
- Time scale;
- Spatial scale;
- Accuracy; and
- Processes.

Each of these attributes is described in greater detail below.

State Variables to be Modeled

The ultimate goal of the modeling effort is to develop a predictive relationship between phosphorus loads and support of designated beneficial uses. Ideally, the selected model would be capable of representing all important state variables included in the link between nutrient loading and designated use support, i.e.

- Nitrogen and phosphorus (in their various forms);
- Biochemical oxygen demand;
- Dissolved oxygen;
- Aquatic plants (both abundance and type);
- Water clarity;
- Fish community structure; and
- Benthic macroinvertebrate community.

Two practical matters complicate the selection of state variables. First, the majority of available data on aquatic plants consists of chlorophyll *a* measurements representing sestonic (i.e. suspended in the water column) algae, with relatively limited data available describing attached or rooted aquatic plants. Second, recent nutrient modeling research (DePinto et al., 2013) conducted for the WERF has concluded that the field of water quality modeling has not yet

advanced to the point where the mechanistic relationship between water quality and resulting fish and/or benthic macroinvertebrate community can be accurately modeled.

We propose that the following state variables be simulated in the LGMR water quality model, with reasons (and ramifications) provided subsequently:

- Nitrogen and phosphorus (in their various forms);
- Biochemical oxygen demand (likely derived from organic carbon forms);
- Dissolved oxygen;
- Benthic and sestonic algae (both biomass and type); and
- Total suspended solids/Water clarity (as Secchi depth and/or a light extinction coefficient).

As previously stated, data provided by Ohio EPA and discussions with MCD and project partners indicate that benthic algae may play a significant role in dissolved oxygen conditions at some locations in the river, under certain conditions. Therefore, plant productivity will be simulated by representation of both sestonic and benthic algae.

We propose to consider effects on macroinvertebrates and fish community via empirical relationships between these indicators and state variables in the model representing benthic and sestonic algae and dissolved oxygen. This recommendation is consistent with that of WERF's Modeling Guidance for Developing Site-Specific Nutrient Goals project, which reviewed a compiled Toolbox of models capable of evaluating nutrient impacts and concluded:

> (O)nly a few models in the Toolbox have the capabilities to represent submerged aquatic vegetation (AQUATOX and CE-QUAL-W2), macroinvertebrates (AQUATOX and CE-QUAL-ICM) or fish (AQUATOX). However, even when including AQUATOX, the most complex model in the Toolbox, these higher-order ecological response indicators are represented by only a few individual species or groups. None of the models in the Toolbox represents the full complexities of actual ecosystem structure or function, or its multiple feedback loops. Again, although additional site-specific data would partially address this limitation, there is a lack of scientific understanding of fundamental ecosystem processes. One solution is to use hybrid models to bridge the gap between process-based models and ecological response indicators. Of course, the success of a hybrid approach hinges on having sufficient site-specific data to develop scientifically credible empirical relationships between state variables in process-based models and ecological indicators. Another consideration is that higher-order ecological responses reflect the influence of a myriad of physical, chemical and biological factors, and may not be adequately characterized solely by the dissolved oxygen, chlorophyll, or nutrient concentrations computed by the models in the Toolbox.

Time Scale

Models can be developed with different time scales, ranging from steady-state models capable only of predicting seasonal average concentrations to time-variable models that can predict day-to-day variability. It is understood that:

1) The Request for Proposals explicitly stated that a key requirement of the modeling effort is developing "An understanding of seasonality and critical conditions most important to the nutrient enrichment of the river and applicable water quality standards", and

2) Diurnal variability in dissolved oxygen is known to be an important influence on designated use support.

Based on these factors, we recommend that a time-variable model capable of simulating day-to-day and within-day (i.e., diurnal) variations in water quality over the course of one or more years be developed. This may also have the potential benefit of allowing examination of the long-term response of sediment phosphorus flux to changes in external phosphorus loads. The feasibility of doing this type of long-term analysis will be determined following model calibration.

Spatial Scale

The spatial scale required by a model depends upon the expected variability in water quality as well as the regulatory objectives. Given that discussions with MCD staff indicate that vertical profiles of observed dissolved oxygen above Great Miami River dams show no indication of stratification, we do not see a need to include a vertical dimension in the model during this initial development phase.

In terms of horizontal discretization of the model, the model must be sufficiently segmented to reasonably represent longitudinal variation in water quality. In addition, physical conditions in certain reaches of the river may require varied representation of hydraulics across the river width, which would dictate the use of multiple lateral segments in those areas.

Accuracy

Ideally, model development would include *a priori* specification of the accuracy in model predictions necessary to support management decisions. High-level eutrophication models such as the one planned for the LGMR are not amenable to rigorous uncertainty analyses. This model uncertainty (and the difficulty in quantifying it) will not prevent the model from being used to support management decisions, but it should be factored into decision-making. This will be accomplished as follows:

- Specify quality objectives for model calibration, i.e. how well the model should perform to be considered acceptable. While these objectives will not translate directly into estimates of model uncertainty, meeting the objectives will at least qualitatively constrain model uncertainty.
- Conduct diagnostic/sensitivity analyses with the calibrated model to gain a qualitative understanding of overall uncertainty and an increased understanding of the relative uncertainty in projections between management alternatives.
- Factor the above understanding into the decision-making process, e.g. use the model results to support adaptive management and/or comparisons of relative effectiveness of alternative scenarios.

Processes

The model must be capable of simulating hydrodynamic, nutrient fate and transport (including sediment nutrient flux), and primary production processes necessary to accurately simulate the indicators of interest.

Selection of Recommended Modeling Platform

In 2013, the WERF (with support from U.S. EPA) sponsored a research team to develop a Nutrient Modeling Toolbox of potential models for support in developing and achieving nutrient

goals. The Nutrient Modeling Toolbox contains 30 public domain models capable of quantifying the relationship between nutrient loads and their impacts on water quality or ecological response indicators. A Model Selection Decision Tool (MSDT) was also developed as part of this work to filter and select potential models for their specific site, problem, response indicator(s), and time and spatial scales (DePinto et al., 2013).

Application of the MSDT

The MSDT was applied using the results of the LGMR problem specification as input. The MSDT consists of two windows in which the user enters the appropriate specifications. The first window is shown in Figure 2 and the second (final) window is shown in Figure 3, below.

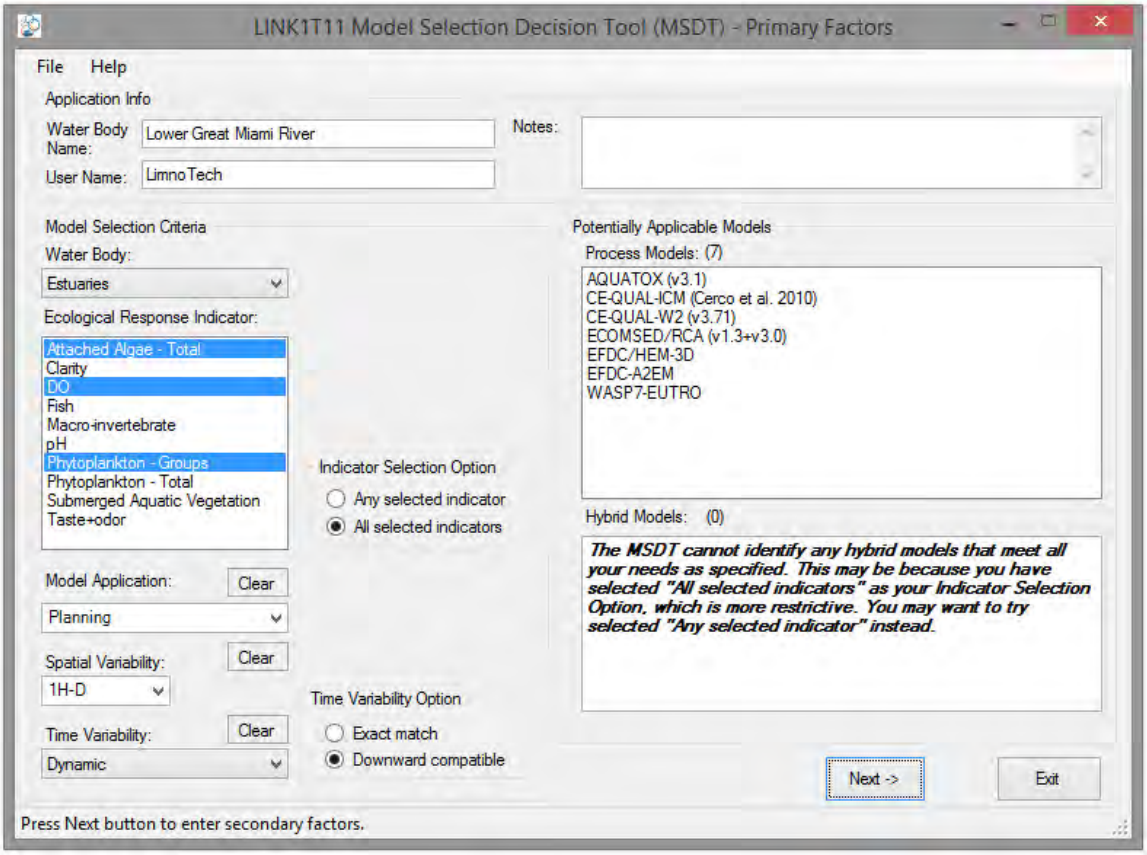

Figure 2. First Model Specification Window of the Model Selection Decision Tool for the Lower Great Miami River.

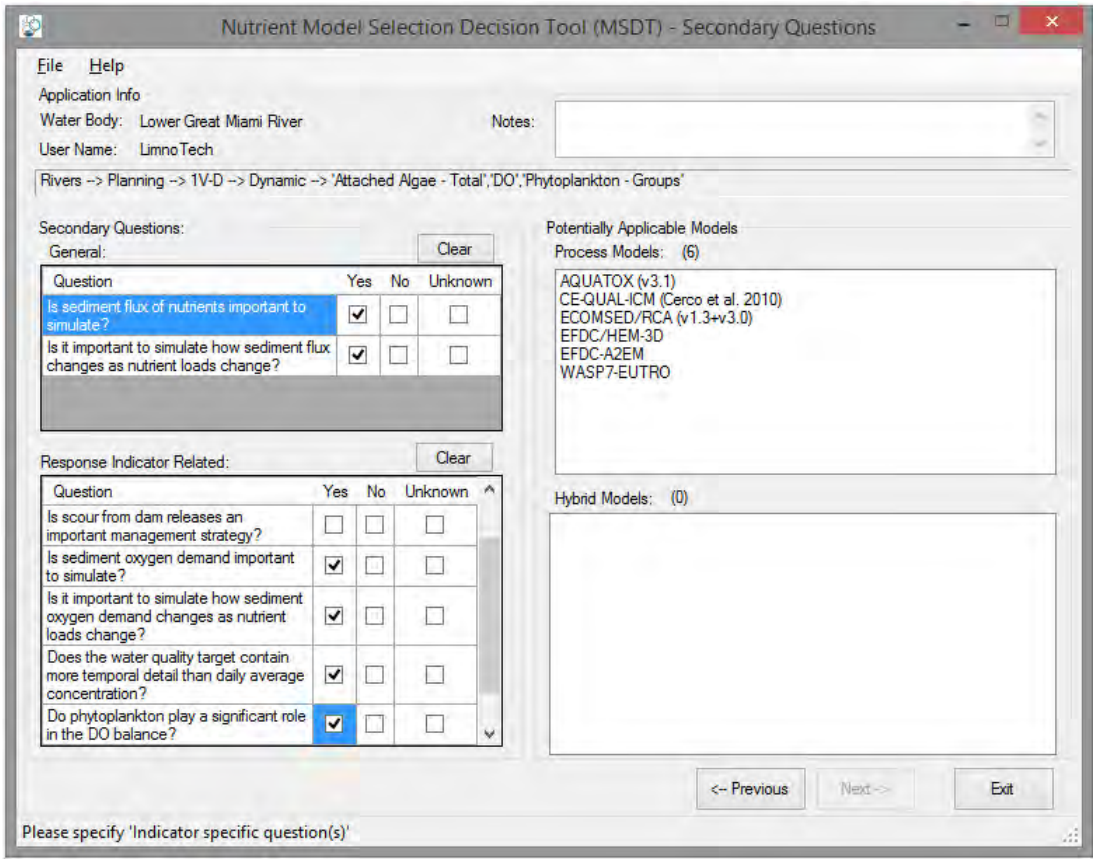

Figure 3. Second Model Specification Window of the Model Selection Decision Tool for the Lower Great Miami River, Showing Final List of Selected Model Platforms.

As shown in Figure 3, the following candidate model frameworks were identified:

- AQUATOX;
- CE-QUAL-ICM;
- ECOMSED/RCA;
- EFDC (either as a standalone model or linked to a separate water quality module);
- EFDC-A2EM; and
- EFDC-WASP7.

An overview of each of the modeling frameworks, including specific pros and cons, is provided below.

AQUATOX

AQUATOX is a freshwater ecosystem simulation model that predicts the fate of various pollutants, such as nutrients and organic chemicals, and their effects on the ecosystem, including fish, invertebrates, and aquatic plants. AQUATOX simulates multiple environmental stressors (including nutrients, organic loadings, sediments, toxic chemicals, and temperature) and their

effects on the algal, macrophyte, invertebrate, and fish communities. AQUATOX does not have the capability of predicting hydrodynamic transport nor has it been commonly applied by being linked to a hydrodynamic model. If the need arises to simulate lateral variability in hydraulics or water quality, AQUATOX would be excluded from selection by the MSDT.
http://water.epa.gov/scitech/datait/models/aquatox/

CE-QUAL-ICM

The CE-QUAL-ICM water quality model was initially developed as one component of a model package employed to study eutrophication processes in Chesapeake Bay. The model computes constituent concentrations resulting from transport and transformations in well-mixed cells that can be arranged in arbitrary one-, two-, or three-dimensional configurations. The model computes and reports concentrations, mass transport, kinetic transformations, and mass balances. While potentially applicable for the LGMR, the CE-QUAL-ICM framework has not been widely applied outside of Chesapeake Bay and is judged less desirable than other models that have had wider application.
http://ches.communitymodeling.org/models/CEQUALICM/index.php

ECOMSED-RCA

The Row-Column AESOP (RCA) model is part of a family of generalized water quality models known as the "Advanced Ecological Systems Modeling Program". RCA, commonly linked to the ECOMSED (Estuarine, Coastal, and Ocean Model) three-dimensional hydrodynamic and sediment transport model, is based on the original WASP water quality model. Kinetic subroutines have been developed that permit RCA to model coliforms, pathogens, BOD/DO, and simple and advanced eutrophication. In addition, the advanced eutrophication kinetics subroutine has been constructed to link to a sediment nutrient flux subroutine which permits the coupling of the water column and sediment bed, so as to account for the deposition of particulate organic matter, its diagenesis in the sediment bed, and the resulting flux of inorganic nutrients and sediment oxygen demand back to the overlying water column. The sediment nutrient flux subroutine also takes into account the effects of bioturbation on dissolved and particulate mixing in the sediment bed. While available in the public domain, the stock version of ECOMSED/RCA has generally only been applied by HDR/Hydroqual, the firm that developed it. In addition, previous attempts to apply ECOMSED in the Upper Mississippi River revealed limitations of the model's use in riverine systems. http://www.hydroqual.com/wr_rca.html

EFDC

The Environmental Fluid Dynamics Code (EFDC Hydro) is a state-of-the-art hydrodynamic model that can be used to simulate aquatic systems in one, two, and three dimensions. It has evolved over the past two decades to become one of the most widely used and technically defensible hydrodynamic models in the world. EFDC uses either stretched (or "sigma") vertical coordinates or a more flexible "generalized vertical coordinate" (GVC) system and Cartesian or curvilinear, orthogonal horizontal coordinates to represent the physical characteristics of a waterbody. It solves the three-dimensional, vertically hydrostatic, free surface, turbulent averaged equations of motion for a variable-density fluid. Dynamically-coupled transport equations for turbulent kinetic energy, turbulent length scale, salinity and temperature are also solved. The EFDC model allows for drying and wetting in shallow areas by a mass conservation scheme. While EFDC also has the capability of simulating water quality parameters, EFDC's primary role has been to provide necessary hydrodynamic inputs to receiving water quality models. Because applications of EFDC's water quality sub-model have been limited, the water quality component

has not been proven to the extent that other water quality frameworks discussed in this memorandum have been. Consequently, there is greater potential for errors or inaccuracies in the EFDC water quality outputs. Another significant disadvantage of applying EFDC to simulate water quality for the LGMR is computational efficiency. While the other modeling frameworks discussed herein represent linked hydrodynamic/water quality models, EFDC computes hydrodynamics and water quality responses simultaneously. As a result, EFDC would require considerably more runtime, as the hydrodynamic simulation would be unnecessarily reproduced with each water quality simulation. This additional runtime would significantly increase the amount of time required to test, calibrate, and apply the water quality model.
http://www.epa.gov/athens/wwqtsc/html/efdc.html

EFDC-A2EM (Advanced Aquatic Ecosystem Model)

EFDC-A2EM (Advanced Aquatic Ecosystem Model) is a publically available, three-dimensional, linked hydrodynamic-advanced eutrophication model developed by LimnoTech based on the original public domain versions of EFDC and RCA. The linked models can simulate suspended solids and nutrient fate and transport, the entire low food web through zooplankton (including up to five phytoplankton and three zooplankton functional groups) and a benthic alga functional group (e.g., Cladophora), two benthic filter feeder species (e.g., to represent *Dreissenid* mussels), a sediment diagenesis sub-model, and dissolved oxygen kinetics. A2EM has been successfully applied at a number of freshwater sites to answer management questions concerning eutrophication and ecosystem function (LimnoTech, 2009; Bierman et al., 2005; DePinto et al., 2009a; DePinto et al., 2009b; Verhamme et al., 2009). In addition, in contrast to the EFDC water quality sub-model, A2EM provides the important capability of externally linking the results of the hydrodynamic model to the water quality sub-model. The external linkage setup provides for optimal efficiency when developing, testing, calibrating, and applying the model framework.

EFDC-WASP7

The Water Quality Analysis Simulation Program (WASP7) is a dynamic compartment-modeling program for aquatic systems, and it includes representation of both the water column and the underlying benthos. WASP, which has been in use for about 30 years in a series of numbered versions, allows the user to investigate 1, 2, and 3 dimensional systems, and a variety of pollutant types. The time varying processes of advection, dispersion, point and diffuse mass loading and boundary exchange are represented in the model. The current version of WASP, WASP7, has a EUTRO module that addresses both conventional pollutants and eutrophication issues in receiving waters and associated bottom sediments. WASP7 also can be linked with the EFDC hydrodynamic model, which provides spatially- and temporally-varying flows, depths, velocities, temperature, and salinity. The EFDC-WASP7 framework provides some of the same advantages that the A2EM framework provides, including an external linkage between the hydrodynamic and water quality models and the use of the preferred “generalized vertical coordinate” system. However, while technically available in the public domain, the model source code for WASP7 has not been publically released. As a result, EFDC-WASP7 provides a rigid modeling framework that cannot be readily modified or optimized to support site-specific applications.
http://www.epa.gov/athens/wwqtsc/html/wasp.html

Model Selection

Each of the models described above is potentially applicable to meet the management objectives for the LGMR. AQUATOX is not recommended because it does not simulate hydrodynamics, and it cannot readily be linked to an external hydrodynamic model. CE-QUAL-ICM is not

recommended because it has not been widely applied outside of Chesapeake Bay and because it is configured to represent some eutrophication variables and processes that are specific to the Chesapeake Bay system. ECOMSED/RCA is not recommended because the EFDC-A2EM alternative includes a hydrodynamic model (EFDC) that is more suitable than ECOMSED for a riverine environment, as well as an enhanced version of the original RCA code. EFDC/WASP7 is not recommended due to the unavailability of model source code, which renders the modeling framework less flexible in regard to addressing site-specific eutrophication and contaminant issues. This leaves EFDC (full version) and EFDC-A2EM as the remaining candidate models. We recognize that the LGMR modeling could be conducted solely using EFDC (i.e. using the water quality component of EFDC in place of A2EM), but we recommend that A2EM be used for this project for three reasons:

1. *Efficiency*: Use of separate models for hydrodynamics and water quality, as we propose, allows these calculations to be "uncoupled" during calibration and scenario runs. In contrast, the water quality module of EFDC requires hydrodynamic calculations (which consume the large majority of processing time) to be repeated each time a new water quality simulation is conducted. With separate hydrodynamic and water quality modules, there is no need to repeat these calculations once the hydrodynamics of the lake are calibrated. A2EM water quality routines can read the hydrodynamics results from a file, allowing much more efficient calculations and faster run times, making it easier to generate additional simulations within project schedule. Furthermore, LimnoTech has developed an extensive set of processing and visualization tools to support the EFDC and A2EM models, which further improves the efficiency of applying the linked EFDC-A2EM modeling framework for the LGMR.
2. *Reliability*: As demonstrated above, LimnoTech has a wealth of experience applying the linked EFDC-A2EM model code, and is fully confident in the accuracy of the water quality model calculations. While EFDC has been used extensively for hydrodynamic and sediment transport modeling, its eutrophication modeling capacity has not been nearly as well-vetted, and undiscovered problems may still exist in the water quality code.
3. *Superior Process Representation* – A2EM includes processes that are likely to be significant in the LGMR, such as benthic algae, which are not included in EFDC or which are represented simplistically.

Model Capabilities

The capabilities of the EFDC-A2EM modeling framework are discussed in greater detail below.

EFDC Background and General Capabilities

The EFDC model is a state-of-the-art finite difference model that can be used to simulate hydrodynamic and sediment transport behavior in one, two, or three dimensions in riverine, lacustrine, and estuarine environments. EFDC was developed at the Virginia Institute of Marine Science in the 1980s and 1990s, and the model is currently maintained under support from the U.S. EPA. Recently, LimnoTech has successfully applied EFDC to a number of sites, including a portion of the lower Great Miami River, the Ohio River (near Cincinnati, Evansville (IN) and Wheeling (WV)), the lower Licking River (Northern Kentucky), Missisquoi Bay (Lake Champlain), Saginaw Bay (Lake Huron), Maumee Bay (Lake Erie), Saginaw River (Michigan), and the Tittabawassee River (Michigan). The EFDC model is both public domain and open source,

meaning that the model can be used free of charge, and the original source code can be modified if necessary to tailor the model to the specific needs of a particular application.

The model input parameters include variable hydrologic inflows and outflows from tributaries, water level boundary conditions, and atmospheric conditions such as air temperature, relative humidity, solar radiation, and wind speed. EFDC represents the model grid using a generalized vertical coordinate (GVC) system, which is capable of accurately describing vertical gradients in systems with rapidly changing bathymetry, if necessary. The model outputs will include the movement of water in the river (i.e., flows and velocities), water level, bottom shear stresses, and water temperature throughout the model domain. Furthermore, the version of EFDC maintained by LimnoTech provides a well-tested, optimized linkage to an enhanced version of the RCA model within the A2EM framework. As a result, EFDC provides a powerful and highly flexible framework for simulating hydrodynamic behavior in the LGMR that can be readily linked to the associated A2EM water quality model.

A2EM Background and General Capabilities

A2EM is the LimnoTech version of the RCA model framework and is capable of simulating water quality dynamics on a fine-scale, three-dimensional computational grid, based on a linkage to an external hydrodynamic model application (in this case, EFDC). More than 30 water quality state variables are available for simulation within the framework, including organic and inorganic nutrients (carbon, nitrogen, phosphorus, and silica), dissolved oxygen, multiple phytoplankton classes (up to five, including cyanobacteria), multiple zooplankton classes (up to three), and the benthic alga Cladophora. In addition, the model is capable of simulating the impact of benthic filter feeders on nutrient cycling and their impact on water clarity and primary productivity in the water column. A2EM also includes a full sediment diagenesis model that simulates the deposition, transformation, burial, and release of carbon, phosphorus, nitrogen, and silica. Similar to EFDC, A2EM is an open source, public domain model that provides a flexible environment for simulating and evaluating system water quality responses.

References

Bierman, V.J., J. Kaur, J.V. DePinto, T.J. Feist, and D.W. Dilks. 2005. “Modeling the Role of Zebra Mussels in the Proliferation of Blue-green Algae in Saginaw Bay, Lake Huron.” J. Great Lakes Res. 31:32-55.

DePinto, J.V., V.J. Bierman Jr., D.W. Dilks, P.E. Moskus, T.A.D. Slawecki, C.F. Bell, W.C. Chapra, K.F. Flynn. 2013. Modeling Guidance for Developing Site-Specific Nutrient Goals. Final Technical Report for Water Environment Research Foundation (WERF).

DePinto, J.V., P.L. Freedman, D.W. Dilks, and W.M. Larson. 2004. Models quantify the Total Maximum Daily Load process. Journal of Environmental Engineering. 130(6):703-713.

DePinto, J.V., H. Holmberg, T. Redder, E. Verhamme, W. Larson, N.J. Senjem, H. Munir. 2009a. Linked hydrodynamic –sediment transport – water quality model for support of the Upper Mississippi River – Lake Pepin TMDL. Proceedings of the WEF Specialty Conference: TMDL 2009. Minneapolis, MN. August 9-12, 2009.

DePinto, J.V., M.T. Auer, T.M. Redder, E. Verhamme. 2009b. “Coupling the Great Lakes Cladophora Model (GLCM) with a whole lake Advanced Eutrophication Model (A2EM-

3D).” Presented at 52nd Annual Conference on Great Lakes Research, University of Toledo, Toledo, OH (May 18- 22, 2009).

LimnoTech. 2009. Upper Mississippi River –Lake Pepin Water Quality Model: Development, Calibration, and Application. Prepared for the Minnesota Pollution Control Agency. July 2009.

Ohio Environmental Protection Agency (Ohio EPA). Ohio Nutrient Reduction Strategy. Ohio EPA Division of Surface Water. June 28, 2013.

Verhamme, E., J.V. DePinto, T.M. Redder, D. Rucinski. 2009. “Development of a linked fine-scale hydrodynamic and ecosystem model for assessing the impact of multiple stressors in Saginaw Bay, Lake Huron. Presented at 52nd Annual Conference on Great Lakes Research, University of Toledo, Toledo, OH (May 18- 22, 2009).

Appendix C:
HSPF Watershed Model Calibration

Introduction

A *Hydrologic Simulation Program - FORTRAN* (HSPF) model was developed by the United States Geological Survey (USGS) in cooperation with the Miami Conservancy District (MCD) for forecasting peak discharge in the Great Miami River Watershed. The Great Miami River Watershed HSPF (GMRWHSPF) model framework consisted of eight individual user control input (UCI) files and was initially calibrated for a four-year period (1999-2002) but was later extended to simulate hydrology for the Jan 1999-Feb 2009 period. LimnoTech acquired the GMRWHSPF modeling files, reviewed the existing setup and hydrology calibration, made several enhancements to the model, updated the hydrology calibration, and calibrated the model for phosphorus and nitrogen species. Model enhancements included merging the eight individual UCI files into one UCI file, extending the simulation period to cover calendar years 1999 through 2015, adding the capability of phosphorus and nitrogen simulation, and adding point source flows and loads.

Model Development

This section provides a brief overview of enhancements made to the GMRWHSPF model. In collaboration with the original model developer, Barry Puskas (MCD, formerly with USGS), LimnoTech obtained and modified the model beginning with the file set listed in Table C-1 below. The files were configured to simulate the 1/1/1999-3/4/2009 period using a one-hour time step. LimnoTech was able to successfully run the eight interconnected models in sequence from upstream to downstream and visualize model output using the files provided in their original form using a newer version of the HSPF executable (WinHSPFLt.exe version 12.3, dated 8/27/2012).

Table C-1. List of the original GMRWHSPF modeling files provided to LimnoTech.

File Name	Description	Date Modified
mcdm1.uci	Upper Great Miami River (above Loramie Creek)	3/2/2009
mcdm2.uci	Loramie Creek	3/2/2009
mcdm3.uci	Upper Great Miami River (below Loramie Creek)	3/2/2009
mcdm4.uci	Stillwater River	3/2/2009
mcdm5.uci	Mad River	3/2/2009
mcdm6.uci	LGMR (above Twin Creek)	3/2/2009
mcdm7.uci	Twin Creek	3/2/2009
mcdm8.uci	LGMR (below Twin Creek)	3/2/2009
MCDHPCPf.wdm	Precipitation time series	4/28/2009
PETairtempf.wdm	Air temperature & Potential Evapotranspiration time series	4/28/2009
RUNOFF_Q.wdm	Flow linkage time series	4/28/2009

Configuration

The following structural changes were made to the GMRWHSPF model as part of this project:

- The eight individual UCI files were merged into a single UCI file;
- The simulation period was extended to cover 1/1/1999-12/31/2015;
- The ability to simulate landside phosphorus (P) and nitrogen (N) was added using the PQUAL (for pervious land areas) and IQUAL (for impervious land areas) modules, which resulted in additional state variables for: 1) three forms of phosphorus (organic P, dissolved inorganic P, and particulate inorganic P), and 2) three forms of nitrogen (organic N, ammonia, and nitrate+nitrite); and
- The ability to simulate riverine transport of phosphorus and nitrogen species was added using the GQUAL module.

No changes were made to the total land area, land use/land cover distribution, subbasin delineations, or reach segmentation.

Meteorological Forcing Functions

Although a total of twenty precipitation time series were provided in the original watershed data management (WDM) file, a quality control review of the time series revealed that some stations had significant gaps or significant deviation in annual rainfall relative to nearby stations. Therefore, the original precipitation time series were not used in the updated model. LimnoTech created a total of four new hourly precipitation time series to be used for the updated model, derived from six unique locations. The updated GMRWHSPF model was split into the four precipitation regions using the precipitation datasets described in Table C-2.

Table C-2. List of precipitation stations used to create new time series for the GMRWHSPF model.

Region	Station Description	Station ID	Data Source	Period of Record
North	Sidney Highway Dept.	OH337698	BASINS	1999-2009
			NCDC	2010-2015
West	Winchester Airport	IN129678	BASINS	1999-2009
	Greenville Water Plant	OH333375	NCDC	2010-2015
Central	Dayton Airport	OH332075	BASINS	1999-2009
			NCDC	2010-2015
South	Fairfield	OH332651	BASINS	1999-2009
	Butler County Airport	725217	NCDC	2010-2015

The original air temperature and potential evapotranspiration (PET) time series from the original WDM file (1999-2008) were merged with new time series for the 2009-2015 period. An hourly air temperature time series from the Dayton Airport station (OH332075) was appended to the existing air temperature time series. It was also used to compute the daily PET time series for 2009-2015 using the Hamon PET method and the same monthly coefficients used by USGS to develop the original PET time series.

Point Sources

Monthly variable municipal and industrial point source flow and load time series were added to the GMRWHSPF model. A total of 60 unique flow time series were developed for the largest point source discharges in the watershed. Relatively small point sources were not included. The criteria for inclusion of

point sources was a facility type description of "0.1 to 0.5 MGD" or larger. Development of the flow time series included a screening process to remove outlier values. Data gaps were filled using monthly median values for each facility. If enough data were available for each facility/water quality constituent combination, monthly load time series were developed for organic N, ammonia, nitrate+nitrite, and/or total P. Like the discharges, reported effluent concentrations were screened for outlier values prior to computation of the load time series and data gaps were filled using monthly median values for each facility. If insufficient effluent concentration data were available to compute a load time series for a given facility/constituent, the following constant concentrations were assumed: total P 3.0 mg-P/l, organic N 1.5 mg-N/l, ammonia 3.0 mg-N/l, and nitrate+nitrite 10.0 mg-N/l/

Atmospheric Deposition

Atmospheric deposition of NH4-N and NO3-N was included in the GMRWHSPF model. Dry deposition data were downloaded from the USEPA Clean Air Status and Trends Network (CASTNET). Data were available at the Oxford, OH (OXF122) station for the 1988-2015 time period. Wet deposition data were downloaded from the National Atmospheric Deposition Program (NADP) National Trends Network (NTN). Data were available at the Oxford, OH (OH09) station for the 1984-2015 time period.

Model Calibration

GMRWHSPF model calibration followed standard protocols for HSPF calibration. The evaluation of model performance was performed using a "weight of evidence" approach, which consisted of using multiple model comparisons, both graphical and statistical.

A split calibration/corroboration approach was used for the hydrology calibration. 2008 through 2015 served as the calibration period, and 2000 through 2007 was used for the corroboration period. Calendar year 1999 was effectively used as a model "spin-up" year. The hydrology calibration protocol followed this order:

- Adjust landside parameters until the correct balance of evaporation and runoff is achieved on an annual/long-term basis;
- Adjust landside parameters to distribute the total streamflow volume appropriately into baseflow and stormflow (surface runoff plus interflow);
- Distribute streamflow seasonally according to patterns in observed data; and
- Consider individual storms and modify the simulated hydrograph shape (e.g., magnitude of peak flows, timing of rising and falling limbs) to match patterns in the observed data by balancing the timing and distribution of stormflow between surface runoff and interflow.

A split calibration/corroboration approach was also used for the nutrient calibration, but the periods did not align with those of the hydrology calibration due to greater nutrient data availability in recent years. The timeframe 2011 through 2015 served as the calibration period, and 2000 through 2010 was used for the corroboration period. The nutrient calibration protocol included:

- Estimate land use specific accumulation rates, removal rates, and subsurface concentrations;
- Adjust landside parameters until nonpoint source loadings from each land use category fell within reasonable limits of reported literature ranges;
- Compare simulated and observed instream concentrations for TP and TN, as well as for individual nutrient species; and

- Compare simulated TP, DPO4, TN, and NO2+NO3 loads against loads estimated from observed streamflow and constituent concentration data at key calibration stations in the LGMR.

Hydrology Calibration Results

The hydrology calibration was constrained using regional estimates of water balance components (e.g. evapotranspiration vs. streamflow), tributary-specific estimates of baseflow from annual MCD water data reports, and USGS streamflow data. GMRWHSPF model-predicted streamflow was compared against USGS measured streamflow at daily, monthly, seasonal, and annual time scales for 21 locations. Eight locations were considered primary calibration locations, one for each of the original eight individual models, and the other 13 locations were considered as secondary calibration locations.

A breakdown of simulated water balance components, tabulated by the eight original HSPF models, is shown in Table C-3. The portion of incoming precipitation lost to evapotranspiration, approximately 25 inches for the entire watershed or 62%, matched reasonably well to targets for the southwest Ohio region. Further, the ability of the model accurately simulate annual streamflow volumes suggests an adequate distribution of precipitation into streamflow and evapotranspiration. Figure C-1 compares simulated and target baseflow as a portion of total streamflow for seven key locations in the Great Miami River watershed. Overall, the model adequately represents the distribution of total streamflow into stormflow and baseflow.

Table C-3. Average annual breakdown of water balance components as simulated by the GMRWHSPF model.

Subwatershed	Evapotranspiration	Streamflow	Surface	Interflow	Baseflow
Great Miami River Headwaters	63%	36%	15%	35%	50%
Loramie Creek	66%	34%	17%	55%	28%
Upper Great Miami River	60%	40%	30%	28%	42%
Stillwater River	62%	37%	20%	40%	40%
Mad River	61%	39%	21%	16%	63%
Lower Great Miami River (above Twin Ck.)	53%	47%	48%	20%	32%
Twin Creek	63%	37%	18%	37%	45%
Lower Great Miami River & Fourmile Creek	57%	43%	32%	28%	40%

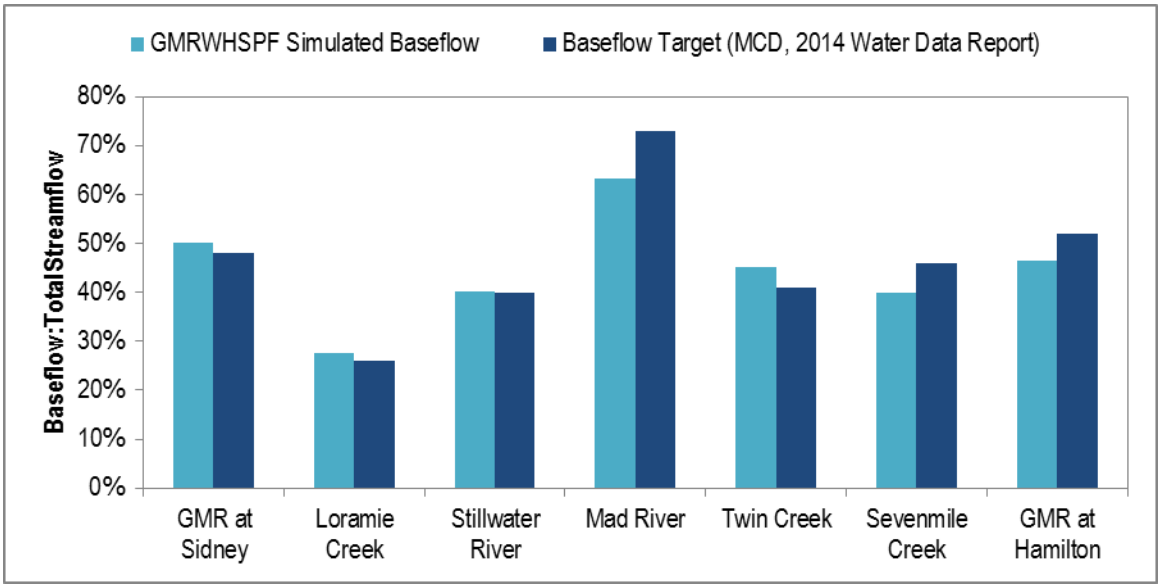

Figure C-1. Annual average baseflow as simulated by the GMRWHSPF model compared against baseflow targets derived from USGS streamflow gages for seven key locations in the watershed.

Summary performance metrics for the hydrology calibration and corroboration periods for the eight primary streamflow stations are shown in Tables C-3 and C-4. The statistics chosen to evaluate model performance were the coefficient of determination (R-Squared), Nash-Sutcliffe efficiency (NSE), percent bias (PBIAS), and mean relative percent difference (RPD). Nearly all statistical measures indicated acceptable model performance, and the large majority indicated that the hydrology calibration could be categorized as "very good" to "excellent."

Table C-4. Summary performance metrics for simulation of streamflow at primary calibration locations for the calibration period (2008-2015).

Scale	Statistic	GMR at Hamilton # 03274000	Twin Ck near Germantown # 03272000	GMR below Miamisburg # 03271601	Mad R near Dayton # 03270000	Stillwater R at Englewood # 03266000	GMR at Taylorsville # 03263000	Loramie Ck at Lockington # 03262000	GMR at Sidney # 03261500
Annual	*Count*	8	8	8	8	8	8	8	8
	R-Squared	0.97	0.93	0.98	0.93	0.93	0.96	0.93	0.97
	Nash-Sutcliffe Efficiency	0.96	0.84	0.97	0.91	0.91	0.96	0.91	0.94
	Relative Percent Difference	1.2%	-12.8%	3.6%	-3.3%	-2.1%	3.0%	-2.6%	7.2%
Seasonal	*Count*	33	33	33	33	31	33	33	33
	R-Squared	0.92	0.87	0.92	0.93	0.83	0.93	0.92	0.92
	Nash-Sutcliffe Efficiency	0.91	0.84	0.92	0.93	0.83	0.93	0.91	0.92
	Relative Percent Difference	5.9%	-5.0%	7.6%	-2.9%	-0.8%	6.8%	7.5%	11.0%
Monthly	*Count*	96	96	96	96	92	96	96	96
	R-Squared	0.89	0.82	0.89	0.87	0.80	0.89	0.83	0.86
	Nash-Sutcliffe Efficiency	0.89	0.81	0.89	0.86	0.79	0.89	0.83	0.86
	P-Bias	-0.94	11.10	-2.82	3.84	1.24	-1.13	4.40	-4.80
	Relative Percent Difference	8.5%	0.5%	10.0%	-1.0%	1.7%	9.2%	15.4%	13.5%
Daily	*Count*	2922	2922	2922	2922	2789	2922	2922	2922
	R-Sq	0.82	0.73	0.80	0.70	0.71	0.78	0.71	0.72
	Nash-Sutcliffe Efficiency	0.82	0.73	0.80	0.70	0.69	0.78	0.71	0.69
	Relative Percent Difference	8.4%	5.5%	9.9%	-1.9%	2.7%	13.1%	35.6%	18.2%

Table C-5. Summary performance metrics for simulation of streamflow at primary calibration locations for the corroboration period (2000-2007).

Scale	Statistic	GMR at Hamilton # 03274000	Twin Ck near Germantown # 03272000	GMR below Miamisburg # 03271601	Mad R near Dayton # 03270000	Stillwater R at Englewood # 03266000	GMR at Taylorsville # 03263000	Loramie Ck at Lockington # 03262000	GMR at Sidney # 03261500
Annual	*Count*	8	8	8	8	8	8	8	8
	R-Squared	0.91	0.52	0.95	0.92	0.88	0.94	0.95	0.95
	Nash-Sutcliffe Efficiency	0.64	0.33	0.92	0.90	0.87	0.93	0.91	0.95
	Relative Percent Difference	10.7%	-8.4%	4.1%	-2.9%	1.7%	3.5%	8.2%	2.1%
Seasonal	*Count*	33	33	33	33	33	33	33	33
	R-Squared	0.92	0.82	0.95	0.91	0.86	0.95	0.96	0.93
	Nash-Sutcliffe Efficiency	0.89	0.78	0.94	0.90	0.86	0.95	0.95	0.92
	Relative Percent Difference	14.6%	1.3%	7.6%	-2.2%	9.0%	5.9%	17.0%	2.9%
Monthly	*Count*	96	96	96	96	96	96	96	96
	R-Squared	0.92	0.83	0.94	0.90	0.86	0.94	0.92	0.90
	Nash-Sutcliffe Efficiency	0.90	0.81	0.94	0.90	0.85	0.94	0.91	0.88
	P-Bias	-10.39	9.13	-2.97	2.94	-0.57	-2.85	-7.14	-1.96
	Relative Percent Difference	15.5%	5.1%	9.1%	-0.7%	10.5%	6.3%	19.2%	2.7%
Daily	*Count*	2922	2922	2922	2922	2922	2922	2922	2922
	R-Sq	0.80	0.70	0.79	0.67	0.72	0.77	0.73	0.69
	Nash-Sutcliffe Efficiency	0.74	0.69	0.78	0.66	0.71	0.75	0.71	0.61
	Relative Percent Difference	13.1%	10.9%	8.1%	-1.5%	6.7%	9.0%	37.3%	10.0%

Nutrient Calibration Results

The nutrient calibration was constrained by land use specific nonpoint source unit area load (UAL) ranges reported in literature, Great Miami River watershed-specific nutrient yield estimates, and measured nutrient concentrations and estimated nutrient loads at the following instream stations: Great Miami River near Huber Heights, the Stillwater River at Englewood, the Mad River near Dayton, and the Great Miami River at Miamisburg.

Summary performance metrics for the nutrient calibration and corroboration periods for the four primary locations are shown in Tables C-5 and C-6. The statistics chosen to evaluate model performance were R-Squared, NSE, PBIAS, and mean RPD. Due to greater uncertainty in daily loads estimated from measured data, statistics were only computed for annual, seasonal, and monthly time scales. Nearly all statistical measures indicated acceptable model performance, and the large majority indicated that the nutrient calibration could be categorized as "good" to "very good."

Table C6 – Summary performance metrics for simulation of nutrient loads at primary calibration locations for the calibration period (2011-2015).

Scale	Statistic	GMR near Huber Heights (2011-2015)				Stillwater River at Englewood (2011-2015)			
		DPO4	TP	NO2+NO3	TN	DPO4	TP	NO2+NO3	TN
Annual	*Count*	5	5	5	5	5	5	5	5
	R-Squared	0.94	0.98	0.94	0.94	0.74	0.84	0.79	0.80
	Nash-Sutcliffe Efficiency	0.56	0.63	0.83	0.83	0.65	0.82	0.40	0.58
	Relative Percent Difference	-23.7%	-19.1%	-1.9%	-14.5%	-11.8%	4.8%	9.2%	-2.4%
Seasonal	*Count*	21	21	21	21	19	19	19	19
	R-Squared	0.88	0.85	0.90	0.91	0.81	0.85	0.83	0.83
	Nash-Sutcliffe Efficiency	0.81	0.77	0.77	0.85	0.77	0.84	0.49	0.65
	Relative Percent Difference	-18.3%	-9.2%	-4.1%	-16.2%	-12.8%	1.7%	-1.6%	-13.4%
Monthly	*Count*	60	60	60	60	56	56	56	56
	R-Squared	0.75	0.76	0.76	0.75	0.69	0.69	0.70	0.70
	Nash-Sutcliffe Efficiency	0.70	0.70	0.60	0.67	0.68	0.59	0.20	0.39
	P-Bias	22.5	23.2	-0.8	11.5	16.5	-0.8	-14.2	-1.9
	Relative Percent Difference	-14.9%	-1.7%	2.8%	-11.5%	-11.5%	-1.1%	1.6%	-12.8%
Scale	**Statistic**	**Mad River near Dayton (2011-2015)**				**GMR at Miamisburg (2011-2015)**			
		DPO4	TP	NO2+NO3	TN	DPO4	TP	NO2+NO3	TN
Annual	*Count*	5	5	5	5	5	5	5	5
	R-Squared	0.92	0.82	0.92	0.90	0.77	0.83	0.62	0.68
	Nash-Sutcliffe Efficiency	0.74	0.26	0.83	0.19	0.22	0.52	0.08	0.59
	Relative Percent Difference	-9.2%	-24.3%	-6.3%	-26.0%	17.6%	-18.1%	12.7%	-3.1%
Seasonal	*Count*	21	21	21	21	19	19	19	19
	R-Squared	0.93	0.82	0.93	0.92	0.75	0.83	0.53	0.62
	Nash-Sutcliffe Efficiency	0.86	0.66	0.85	0.77	0.48	0.72	0.09	0.50
	Relative Percent Difference	-8.0%	-15.8%	-9.2%	-25.4%	15.2%	-10.3%	6.8%	-6.0%
Monthly	*Count*	60	60	60	60	55	55	55	55
	R-Squared	0.73	0.52	0.76	0.73	0.65	0.75	0.63	0.68
	Nash-Sutcliffe Efficiency	0.70	0.45	0.64	0.63	0.26	0.71	0.11	0.53
	P-Bias	10.2	22.9	4.9	22.4	-20.6	17.5	-16.8	0.9
	Relative Percent Difference	-5.5%	-10.3%	-7.6%	-22.4%	16.9%	-1.1%	16.9%	3.4%

Table C7 – Summary performance metrics for simulation of nutrient loads at primary calibration locations for the corroboration period (2000-2010).

Scale	Statistic	GMR near Huber Heights (2007-2010)				Stillwater River at Englewood (2005-2010)			
		DPO4	TP	NO2+NO3	TN	DPO4	TP	NO2+NO3	TN
Annual	*Count*	4	4	4	4	6	6	6	6
	R-Squared	0.94	0.98	1.00	1.00	0.41	0.89	0.34	0.51
	Nash-Sutcliffe Efficiency	0.66	0.70	0.91	0.86	-0.13	0.74	-0.38	0.12
	Relative Percent Difference	-20.3%	-18.2%	0.8%	-16.0%	-33.8%	-12.4%	1.8%	-14.7%
Seasonal	*Count*	17	17	17	17	25	25	25	25
	R-Squared	0.89	0.89	0.89	0.90	0.65	0.65	0.67	0.69
	Nash-Sutcliffe Efficiency	0.78	0.77	0.86	0.88	0.45	0.58	0.64	0.68
	Relative Percent Difference	-2.1%	7.7%	19.9%	3.8%	-8.6%	13.3%	16.7%	1.4%
Monthly	*Count*	48	48	48	48	72	72	72	72
	R-Squared	0.84	0.86	0.84	0.86	0.72	0.70	0.64	0.68
	Nash-Sutcliffe Efficiency	0.77	0.76	0.81	0.85	0.59	0.67	0.53	0.66
	P-Bias	18.7	20.3	-3.9	13.1	31.9	14.0	-4.9	11.4
	Relative Percent Difference	7.6%	17.6%	31.2%	13.5%	-9.4%	9.5%	15.5%	-2.9%
Scale	**Statistic**	**Mad River near Dayton (2006-2010)**				**GMR at Miamisburg (2000-2010)**			
		DPO4	TP	NO2+NO3	TN	DPO4	TP	NO2+NO3	TN
Annual	*Count*	5	5	5	5	11	11	11	11
	R-Squared	0.79	0.91	0.87	0.91	0.90	0.85	0.34	0.50
	Nash-Sutcliffe Efficiency	0.25	0.69	0.76	0.11	0.33	0.60	0.22	0.17
	Relative Percent Difference	-18.8%	-10.4%	-6.0%	-23.6%	17.8%	-12.6%	-1.4%	-13.1%
Seasonal	*Count*	21	21	21	21	45	45	45	45
	R-Squared	0.88	0.79	0.85	0.86	0.78	0.69	0.57	0.64
	Nash-Sutcliffe Efficiency	0.70	0.73	0.75	0.70	0.55	0.61	0.47	0.59
	Relative Percent Difference	-18.3%	-5.8%	-8.3%	-23.4%	18.8%	-2.8%	3.6%	-6.5%
Monthly	*Count*	60	60	60	60	132	132	132	130
	R-Squared	0.81	0.75	0.71	0.74	0.76	0.71	0.53	0.61
	Nash-Sutcliffe Efficiency	0.72	0.71	0.47	0.62	0.59	0.64	0.43	0.57
	P-Bias	18.0	11.7	4.8	20.8	-18.8	13.9	0.8	11.6
	Relative Percent Difference	-18.3%	-3.3%	-8.6%	-22.7%	18.1%	2.6%	10.4%	-1.1%

Discussion and Model Limitations

The GMRWHSPF model was updated, re-calibrated for hydrology, and calibrated for simulation of TP, TN, and select P and N species. Evaluation of the hydrology calibration indicates the model is capable of accurately reproducing daily, monthly, seasonal, and annual flow volumes for major tributaries throughout the watershed and at the watershed outlet, which suggests that GMRWHSPF model streamflow output can be used to estimate LGMR hydrodynamic model flow inputs. Evaluation of the nutrient calibration indicates satisfactory capabilities in predicting monthly, seasonal, and annual loadings from dominant land use types present in the watershed. The GMRWHSPF model nutrient calibration is sufficiently representative of observed data such that nutrient loading output can be used to estimate LGMR water quality model concentration (or load) inputs for tributaries and direct drainage areas.

Although the GMRWHSPF model calibration indicates sufficient quality to provide estimates of boundary inputs for the LGMR hydrodynamic and water quality models, the following limitations exist with the watershed model:

1. The overall temporal and spatial accuracy of the watershed model is limited by the temporal and spatial resolution of its inputs. For example, the model relied on monthly variable inputs for point source discharges and nutrient loads and therefore should not be expected to precisely reproduce daily variable loads, especially during extremely low flow periods when point sources become the major nutrient load contributor. Additionally, four precipitation stations and a single air temperature station were used as meteorological inputs, which, although adequate for the purposes of this model application, represent a relatively coarse spatial resolution.

2. A simplified, generalized quality constituent approach was used to represent landside loading and instream transport of P and N species in HSPF. As such, the watershed model cannot be used to predict several other state variables needed for the LGMR water quality model, including inorganic suspended solids, organic carbon, dissolved oxygen, and sestonic algae biomass.
3. The watershed model does not represent instream (i.e., internal) P and/or N sources such as sediment release of inorganic P/N and bed/bank erosion of sediment-bound P/N.
4. Representation of instream transformation (e.g., P mineralization, nitrification) and loss mechanisms (e.g., settling, denitrification) in the watershed model was accomplished using a generalized first-order decay approach.
5. The GMRWHSPF nutrient calibration focused on key water quality sampling stations with the most robust datasets, namely the Great Miami River at Huber Heights, Stillwater River at Englewood, Mad River at Dayton, and Great Miami River at Miamisburg. The ability of the watershed model to predict absolute P and/or N concentrations at other locations in the watershed (i.e., within other tributaries such as Wolf Creek, Twin Creek and Fourmile Creek) is not as well constrained. The calibration ideally should be further evaluated against observed water quality datasets, and updated if deemed necessary, before being used to predict the impact of management actions at altering instream P and/or N concentrations in smaller tributaries.

Blank

Appendix D:
Supplementary A2EM Development Material

Table D-1. Flow-concentration relationships used to fill in gaps at upstream boundaries when no measured water quality data were available. All concentrations are in mg/l.

Great Miami River at Huber Heights						
Flow Percentile	**TP**	**SRP**	**TKN**	**NO23**	**NH3**	**SS**
0-10 (low)	0.35	0.28	0.88	1.23	0.09	31
10-20	0.29	0.24	1.06	1.22	0.09	30
20-30	0.27	0.22	1.09	2.01	0.08	34
30-40	0.22	0.16	0.99	2.27	0.09	33
40-50	0.20	0.14	0.93	2.56	0.09	34
50-60	0.20	0.14	1.00	2.98	0.11	38
60-70	0.19	0.14	0.96	3.12	0.10	36
70-80	0.20	0.14	1.09	3.71	0.10	41
80-90	0.26	0.16	1.19	3.92	0.11	73
90-100 (high)	0.45	0.20	1.58	4.07	0.12	169
Stillwater River at Englewood						
Flow Percentile	**TP**	**SRP**	**TKN**	**NO23**	**NH3**	**SS**
0-10 (low)	0.15	0.13	0.88	1.08	0.19	31
10-20	0.23	0.13	1.19	1.27	0.12	70
20-30	0.22	0.13	1.11	1.94	0.12	62
30-40	0.18	0.13	1.06	2.51	0.15	46
40-50	0.16	0.11	1.07	3.55	0.12	36
50-60	0.14	0.10	1.06	4.08	0.11	36
60-70	0.15	0.11	1.19	4.55	0.11	36
70-80	0.19	0.14	1.28	4.91	0.15	53
80-90	0.25	0.18	1.54	5.56	0.23	81
90-100 (high)	0.50	0.30	2.13	4.96	0.16	173
Mad River near Dayton						
Flow Percentile	**TP**	**SRP**	**TKN**	**NO23**	**NH3**	**SS**
0-10 (low)	0.23	0.19	0.74	2.53	0.13	37
10-20	0.22	0.15	0.79	2.53	0.14	30
20-30	0.19	0.13	0.71	2.56	0.12	41
30-40	0.18	0.12	0.80	2.65	0.11	43
40-50	0.16	0.11	0.70	2.83	0.09	35
50-60	0.15	0.11	0.77	2.90	0.09	38
60-70	0.16	0.10	0.86	2.90	0.22	41
70-80	0.17	0.10	0.99	2.80	0.11	74
80-90	0.22	0.11	1.23	2.74	0.12	128
90-100 (high)	0.38	0.14	1.64	2.30	0.13	250

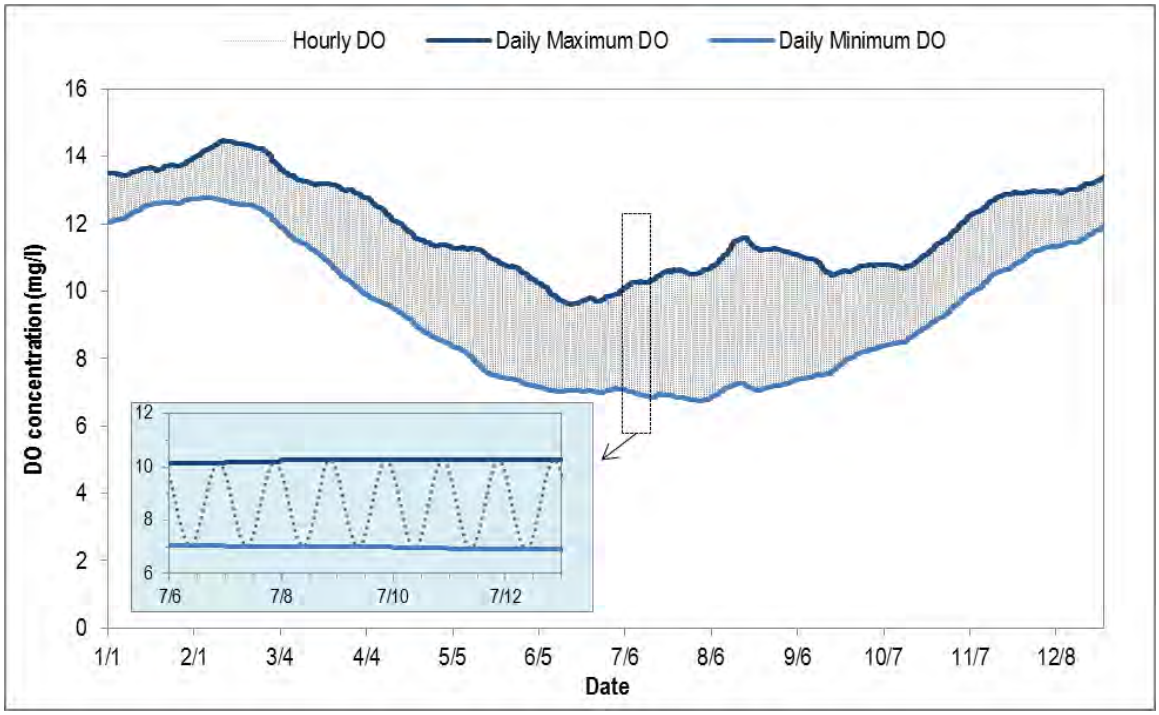

Figure D-1. DO concentration time series used for Stillwater River upstream boundary and all HSPF boundaries.

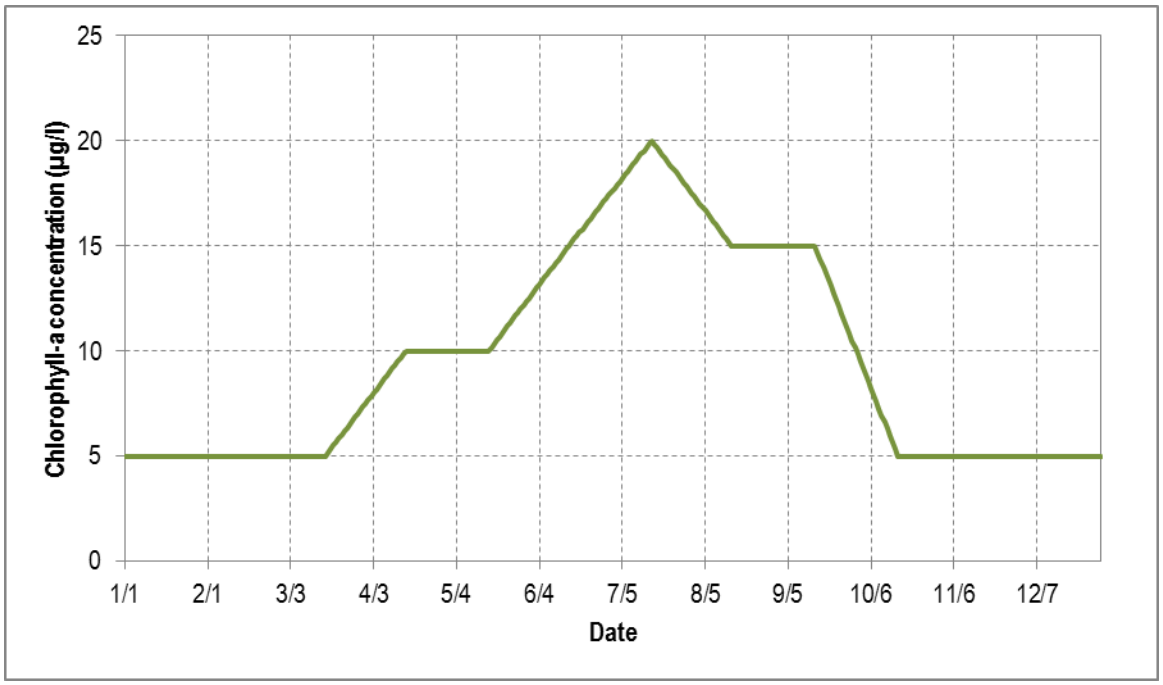

Figure D-2. Chlorophyll *a* concentration time series used for all HSPF boundaries and to fill gaps for Stillwater and Upper Great Miami River boundaries.

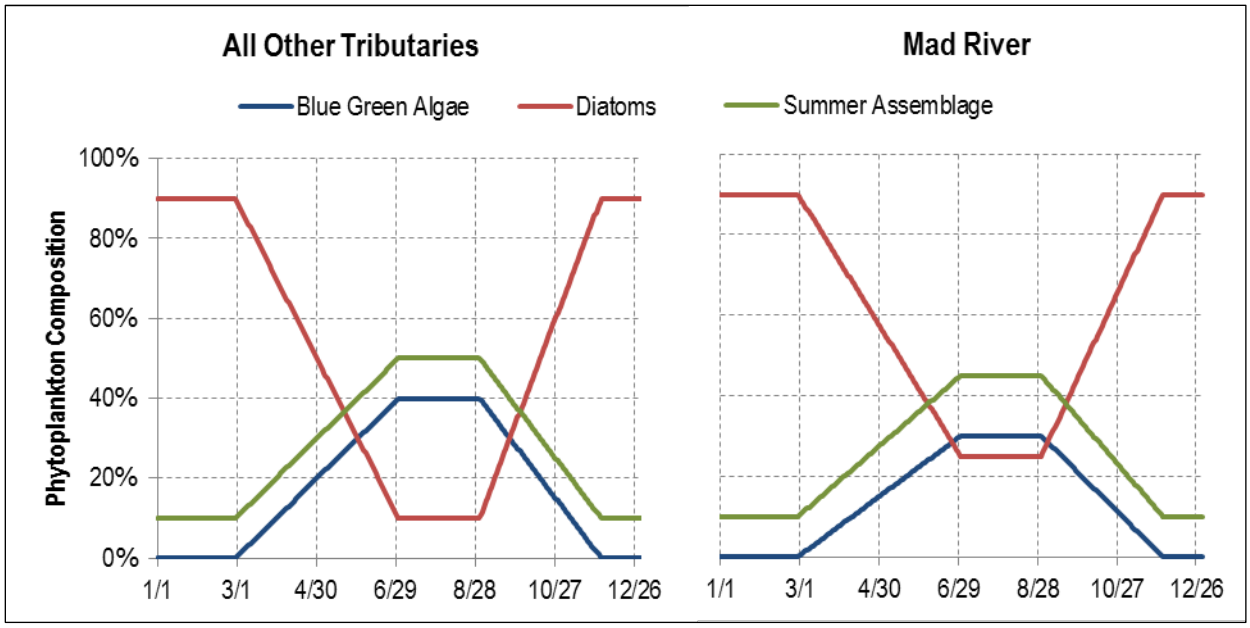

Figure D-3. Phytoplankton community composition assumptions for water quality model tributaries.

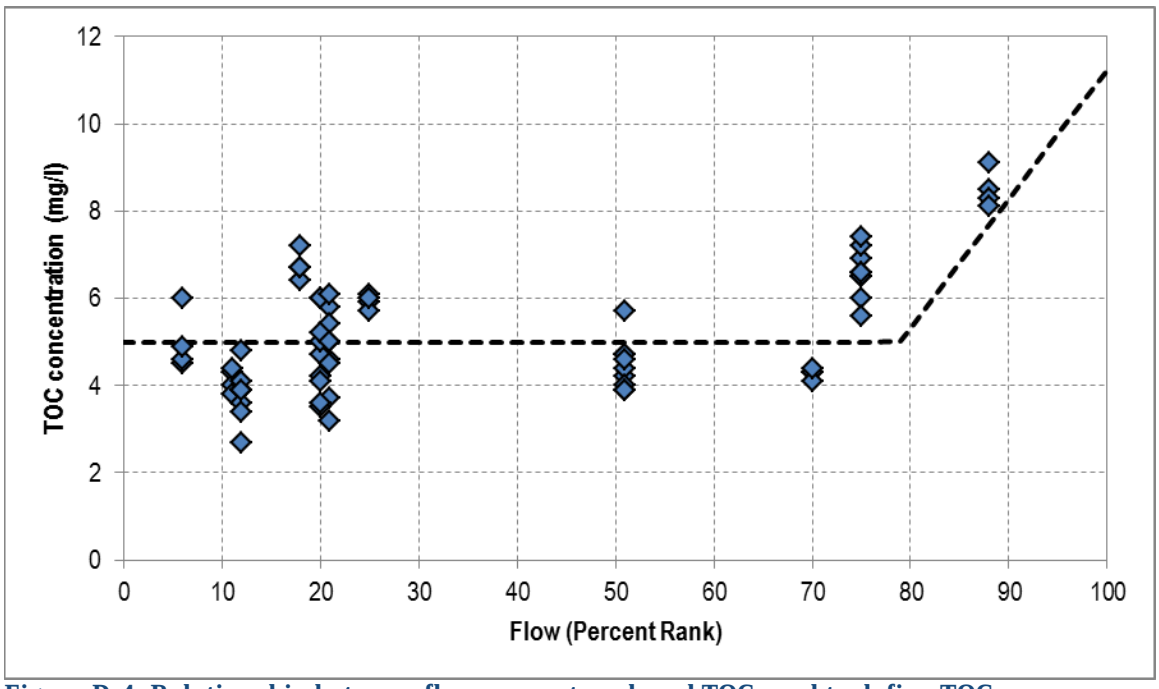

Figure D-4. Relationship between flow percent rank and TOC used to define TOC concentrations for upstream and HSPF boundaries.

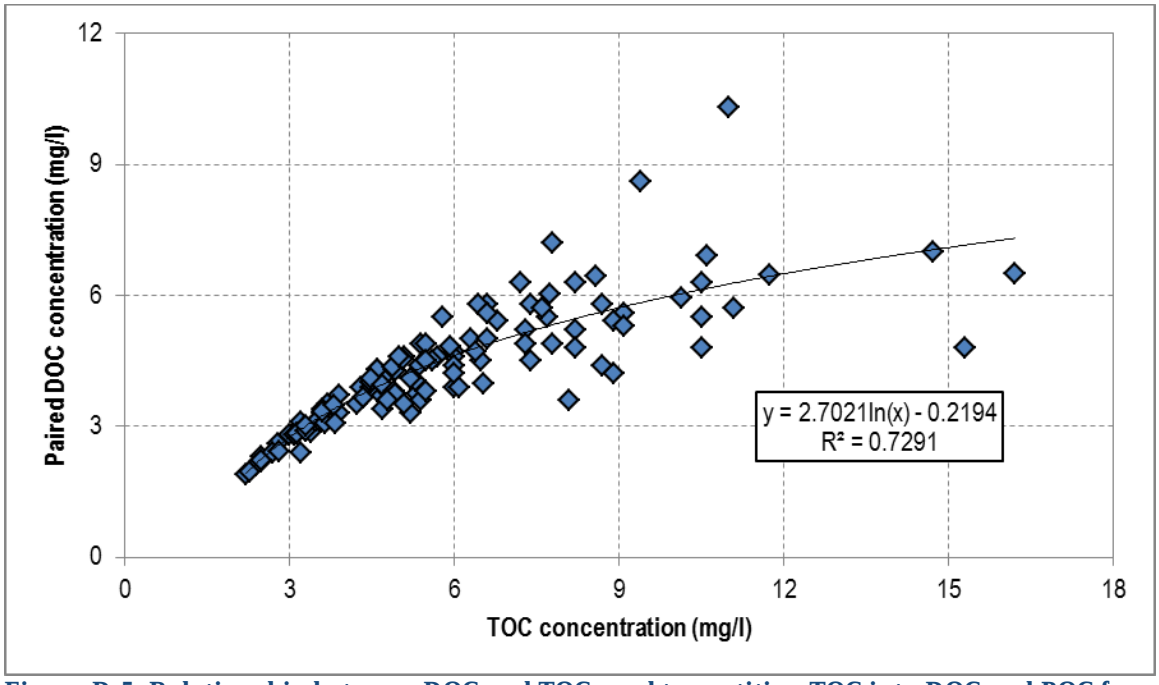

Figure D-5. Relationship between DOC and TOC used to partition TOC into DOC and POC for upstream and HSPF boundaries.

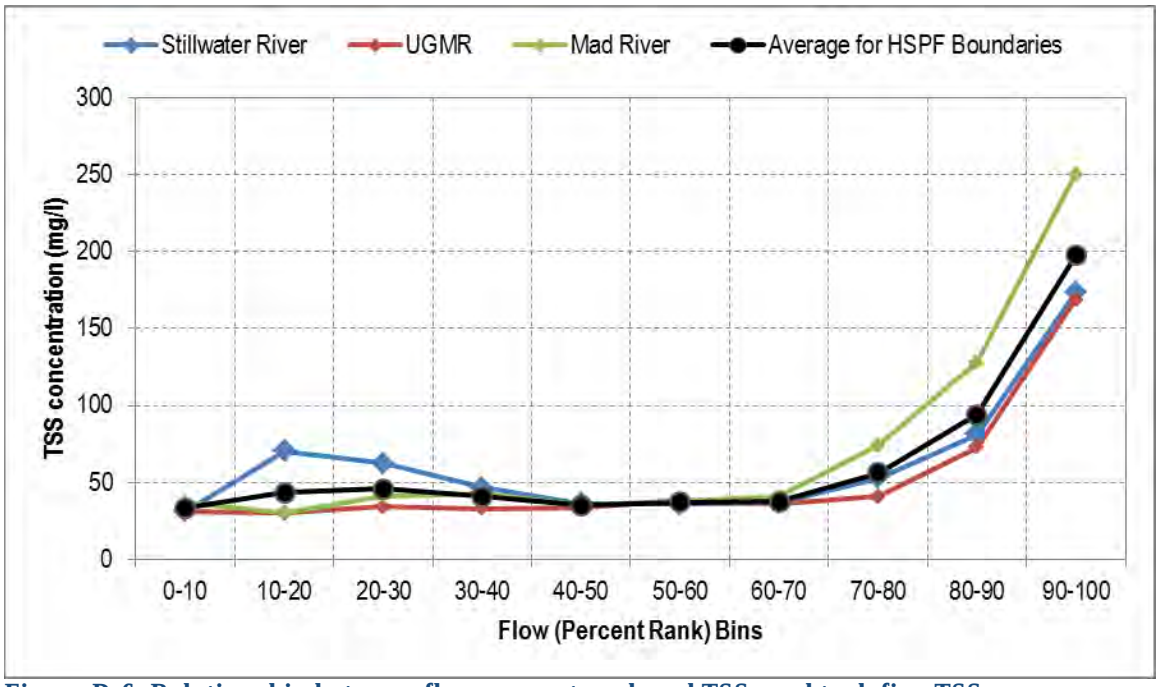

Figure D-6. Relationship between flow percent rank and TSS used to define TSS concentrations for HSPF boundaries.

Blank

Appendix E:
Supplementary A2EM Calibration Material

Table E-1. LGMR water quality model input coefficients.

Constant ID	Constant Description	Value	Units
AGOPT	Algal growth model option (0=standard, 1=Laws-Chalup)	0	
ACTALG	Number of algal groups to simulate (1-5)	5	
KAOPT	Reaeration formulation option	6	
KEOPT	Extinction coefficient option	12	
ZGMOPT	Zooplankton growth/grazing model option	0	
MGMOPT	Mussel bioenergetics model flag	0	
BALGOPT	Benthic algae sub-model flag	2	
KADOPT	Inorganic P adsorption approach	0	
TOPT1	Optimal growth temperature	26.5	deg C
K1BETA1	Temperature correction effect on growth rate below TOPT*	0.01	(deg C)-2
K1BETA2	Temperature correction effect on growth rate above TOPT*	0.005	(deg C)-2
K1C	Saturated phytoplankton growth rate at TOPT*	2.2	/day
K1T	Temperature coefficient for K*C	-0.005	
IS1	Saturating algal light intensity	50	ly/day
KMN1	Half saturation constant for nitrogen	0.01	mg-N/L
KMP1	Half saturation constant for phosphorus	0.005	mg-P/L
KMS1	Half saturation constant for silica	0.002	mg-Si/L
K1RB	Endogenous respiration rate at 30 deg. C	0.2	/day
K1RT	Temperature coefficient for K*RB	1.08	
K1RG	Growth-rate-dependent respiration coefficient	0	
K1GRZC	Death rate due to (zooplankton) grazing	0	/day
K1GRZT	Temperature coefficient for K*GRZC	1.08	
CCHL1	Carbon to chlorophyll ratio	33	mg-C/mg-Chla
CRBP11	Carbon to phosphorus ratio (non-P-limited)	40	mg-C/mg-P
CRBP12	Carbon to phosphorus ratio (P-limited)	90	mg-C/mg-P
CRBP13	Coefficient determining range of P limitation	50	L/mg-P
CRBN11	Carbon to nitrogen ratio (non-N-limited)	5.68	mg-C/mg-N
CRBN12	Carbon to nitrogen ratio (N-limited)	8.5	mg-C/mg-N
CRBN13	Coefficient determining range of N limitation	10	L/mg-N
CRBS11	Carbon to silica ratio (non-S-limited)	8	mg-C/mg-S
CRBS12	Carbon to silica ratio (S-limited)	20	mg-C/mg-S
CRBS13	Coefficient determining range of S limitation	20	L/mg-S

Constant ID	Constant Description	Value	Units
XKC1	Chlorophyll self-shading extinction coefficient	0.017	m2/mg-Chla
VSBAS1	Base algal settling rate	-2	m/day
VSNTR1	Nutrient stressed algal settling rate	0	m/day
TOPT2	Optimal growth temperature	12	deg C
K2BETA1	Temperature correction effect on growth rate below TOPT*	0.003	(deg C)-2
K2BETA2	Temperature correction effect on growth rate above TOPT*	0.006	(deg C)-2
K2C	Saturated phytoplankton growth rate at TOPT*	2.6	/day
K2T	Temperature coefficient for K*C	-0.005	
IS2	Saturating algal light intensity	50	ly/day
KMN2	Half saturation constant for nitrogen	0.02	mg-N/L
KMP2	Half saturation constant for phosphorus	0.005	mg-P/L
KMS2	Half saturation constant for silica	0.02	mg-Si/L
K2RB	Endogenous respiration rate at 30 deg. C	0.14	/day
K2RT	Temperature coefficient for K*RB	1.04	
K2RG	Growth-rate-dependent respiration coefficient	0	
K2GRZC	Death rate due to (zooplankton) grazing	0.03	/day
K2GRZT	Temperature coefficient for K*GRZC	1.08	
CCHL2	Carbon to chlorophyll ratio	50	mg-C/mg-Chla
CRBP21	Carbon to phosphorus ratio (non-P-limited)	40	mg-C/mg-P
CRBP22	Carbon to phosphorus ratio (P-limited)	90	mg-C/mg-P
CRBP23	Coefficient determining range of P limitation	200	L/mg-P
CRBN21	Carbon to nitrogen ratio (non-N-limited)	5.68	mg-C/mg-N
CRBN22	Carbon to nitrogen ratio (N-limited)	8.5	mg-C/mg-N
CRBN23	Coefficient determining range of N limitation	10	L/mg-N
CRBS21	Carbon to silica ratio (non-S-limited)	3	mg-C/mg-S
CRBS22	Carbon to silica ratio (S-limited)	10	mg-C/mg-S
CRBS23	Coefficient determining range of S limitation	20	L/mg-S
XKC2	Chlorophyll self-shading extinction coefficient	0.017	m2/mg-Chla
VSBAS2	Base algal settling rate	0.3	m/day
VSNTR2	Nutrient stressed algal settling rate	0	m/day
TOPT3	Optimal growth temperature	22	deg C
K3BETA1	Temperature correction effect on growth rate below TOPT*	0.007	(deg C)-2
K3BETA2	Temperature correction effect on growth rate above TOPT*	0.005	(deg C)-2

Constant ID	Constant Description	Value	Units
K3C	Saturated phytoplankton growth rate at TOPT*	2.4	/day
K3T	Temperature coefficient for K*C	0	
IS3	Saturating algal light intensity	50	ly/day
KMN3	Half saturation constant for nitrogen	0.02	mg-N/L
KMP3	Half saturation constant for phosphorus	0.005	mg-P/L
KMS3	Half saturation constant for silica	0.02	mg-Si/L
K3RB	Endogenous respiration rate at 30 deg. C	0.14	/day
K3RT	Temperature coefficient for K*RB	1.04	
K3RG	Growth-rate-dependent respiration coefficient	0	
K3GRZC	Death rate due to (zooplankton) grazing	0.02	/day
K3GRZT	Temperature coefficient for K*GRZC	1.08	
CCHL3	Carbon to chlorophyll ratio	33	mg-C/mg-Chla
CRBP31	Carbon to phosphorus ratio (non-P-limited)	40	mg-C/mg-P
CRBP32	Carbon to phosphorus ratio (P-limited)	90	mg-C/mg-P
CRBP33	Coefficient determining range of P limitation	50	L/mg-P
CRBN31	Carbon to nitrogen ratio (non-N-limited)	5.68	mg-C/mg-N
CRBN32	Carbon to nitrogen ratio (N-limited)	8.5	mg-C/mg-N
CRBN33	Coefficient determining range of N limitation	10	L/mg-N
CRBS31	Carbon to silica ratio (non-S-limited)	8	mg-C/mg-S
CRBS32	Carbon to silica ratio (S-limited)	20	mg-C/mg-S
CRBS33	Coefficient determining range of S limitation	20	L/mg-S
XKC3	Chlorophyll self-shading extinction coefficient	0.017	m2/mg-Chla
VSBAS3	Base algal settling rate	0.1	m/day
VSNTR3	Nutrient stressed algal settling rate	0	m/day
KMPHYT	Half-saturation constant for phytoplankton	0.05	mg-C/L
FRPOP	Refractory particulate organic phosphorus	0.1	
FLPOP	Labile particulate organic phosphorus	0.25	
FRDOP	Refractory dissolved organic phosphorus	0.1	
FLDOP	Labile dissolved organic phosphorus	0.1	
FPO4	Dissolved inorganic phosphorus	0.45	
FRPON	Refractory particulate organic nitrogen	0.1	
FLPON	Labile particulate organic nitrogen	0.3	
FRDON	Refractory dissolved organic nitrogen	0.125	

Constant ID	Constant Description	Value	Units
FLDON	Labile dissolved organic nitrogen	0.125	
FNH4	Ammonia	0.35	
FRPOC	Refractory particulate organic carbon	0.1	
FLPOC	Labile particulate organic carbon	0.35	
FRDOC	Refractory dissolved organic carbon	0.1	
FLDOC	Labile dissolved organic carbon	0.45	
K57C	Hydrolysis rate of RPOP to RDOP	0.01	/day
K57T	Temperature correction coefficient	1.08	
K68C	Hydrolysis rate of LPOP to LDOP	0.25	/day
K68T	Temperature correction coefficient	1.08	
K79C	Mineralization rate of RDOP to PO4	0.05	/day
K79T	Temperature correction coefficient	1.08	
K89C	Mineralization rate of LDOP to PO4	0.1	/day
K89T	Temperature correction coefficient	1.08	
K1012C	Hydrolysis rate of RPON to RDON	0.05	/day
K1012T	Temperature correction coefficient	1.08	
K1113C	Hydrolysis rate of LPON to LDON	0.12	/day
K1113T	Temperature correction coefficient	1.08	
K1214C	Mineralization rate of RDON to NH4	0.05	/day
K1214T	Temperature correction coefficient	1.08	
K1314C	Mineralization rate of LDON to NH4	0.1	/day
K1314T	Temperature correction coefficient	1.08	
K1415C	Nitrification rate at 20 deg. C	0.3	/day
K1415T	Temperature correction coefficient	1.08	
KNIT	Half-saturation constant for nitrogen oxygen limitation	1	mg-O2/L
K150C	Denitrification rate at 20 deg. C	0.05	/day
K150T	Temperature correction coefficient	1.045	
KNO3	Michaelis constant for denitrification oxygen limitation	0.1	mg-O2/L
K1617C	Mineralization rate of biogenic Si to available dissolved Si	0.1	/day
K1617T	Temperature correction coefficient	1.08	
K1820C	Hydrolysis rate of RPOC to RDOC	0.01	/day
K1820T	Temperature correction coefficient	1.08	
K1921C	Hydrolysis rate of LPOC to LDOC	0.1	/day

Constant ID	Constant Description	Value	Units
K1921T	Temperature correction coefficient	1.08	
K200C	Oxidation rate of RDOC	0.01	/day
K200T	Temperature correction coefficient	1.08	
K210C	Oxidation rate of LDOC	0.1	/day
K210T	Temperature correction coefficient	1.08	
KMLDOC	Michaelis constant for LDOC	0.1	mg-C/L
KDOC	Half-saturation for organic carbon	0.2	mg-O2/L
K220C	Algal exudate DOC oxidation rate	0.1	/day
K220T	Temperature correction coefficient	1.08	
FLOCEX	Fraction of primary productivity going to labile OC via exudation	0.1	
K2324C	Hydrolysis rate of REPOC to REDOC	0.3	/day
K2324T	Temperature correction coefficient	1.08	
K240C	Reactive DOC oxidation rate	0.3	/day
K240T	Temperature correction coefficient	1.08	
CTOPCSO	Carbon to phosphorus ratio of CSO solids	0	mg-C/mg-P
CTONCSO	Carbon to nitrogen ratio of CSO solids	0	mg-C/mg-N
K250C	Oxidation rate for aqueous SOD	0.4	/day
K250C	Temperature correction coefficient	1.08	
KO2EQ	Half-saturation constant for dissolved oxygen	0.2	mg-O2/L
KLMIN	Minimum reareation coefficient	1	m/day
DIFUS	Diffusivity of oxygen across air-water interface	0.0001806	m2/day
KAT	Temperature correction coefficient for atmospheric reaeration	1.024	
VSBAST	Temperature correction coefficient for algal settling (all classes)	1.039	
VSPOM	Particulate organic matter settling rate	0.4	m/day
VSPMT	Temperature correction for settling rate	1	
VSSEDT	Temperature correction for deposition to sediment	1	
BVCSO	Power coefficient for CSO solid settling rate (>=1)	1	
CRCSO		1	mg-C/L
VMINCSO		0	m/day
VMAXCSO		0	m/day
KADPO4	Partitioning coefficient scale factor for sorbed phosphorus	1	L/mg-ss
KADSI	Partition coefficient for sorbed silica	0	L/mg-ss
VSPIM	Settling rate for phosphorus/silica sorbed to suspended solids	0	m/day

Constant ID	Constant Description	Value	Units
KECONST	Base (Chla-corrected) extinction coefficient (KEOPT=0,2)	0	/m
KADPO41	Partition coefficient for phosphorus sorption to fine suspended solids	0.0015	L/mg-ss
KADPO42	Partition coefficient for phosphorus sorption to coarse suspended solids	0	L/mg-ss
TAUCR	Critical shear stress for probability of deposition (based on Krohn)	1	dynes/cm2
WSS1	Water column settling rate for SS1	0.5	m/day
WSS2	Water column settling rate for SS2	5	m/day
VSF1	Global scale factor for SS1 settling rate	1	
VSF2	Global scale factor for SS2 settling rate	1	
RSFPO4	resuspension scale factor for PO4 (TIP)	0.2	
RSFORG	resuspension scale factor for all organic species (LPOC, RPOC, LPON, RPON, LPOP, RPOP)	0.4	
KLPIP	Desportion rate (LPIP --> DIP)	0.1	/day
RFLPIP	Fraction of resuspended PIP assigned to LPIP	0.3	
K3809C	Hydrolysis rate of IPOP to RDOP	0.00001	/day
K3809T	Temperature correction for IPOP hydrolysis	1	
K3914C	Hydrolysis rate of IPON to RDON	0.00001	/day
K3914T	Temperature correction for IPON hydrolysis	1	
K4022C	Hydrolysis rate of IPOC to RDOC	0.00001	/day
K4022T	Temperature correction for IPOC hydrolysis	1	
NBASZ	# of benthic algae subzones	8	
BA_RptFlg	Benthic algae reporting flag (0=mg-Chla/m2; 1=???; 2)	0	
CNRBBA	Constant C:N ratio for benthic algae	6	mgC/mgN
CDWRBA	Constant C:DW ratio for benthic algae	0.4	mgC/mg-DW
CCHLBA	Constant C:Chla ratio for benthic algae	40	mgC/mg-Chla
Qinit_P	Initial intercellular P:C ratio	0.0075	mgP/mgC
Qmin_P	Minimum intercellular P:C ratio	0.0075	mgP/mgC
KMPBA	External phosphorus half-saturation constant	0.125	mgP/L
KQPBA	Internal (intercellular) phosphorus half-saturation constant	0.00325	mgP/mgC
RhoPMax	Maximum phosphorus uptake rate	0.125	(mgP/mgC)/day
Qinit_N	Initial intercellular N:C ratio	0.054	mgN/mgC
Qmin_N	Minimum intercellular N:C ratio	0.018	mgN/mgC
KMNBA	External nitrogen half-saturation constant	0.25	mgN/L
KQNBA	Internal (intercellular) nitrogen half-saturation constant	0.08	mgN/mgC
RhoNMax	Maximum nitrogen uptake rate	0.9	(mgN/mgC)/day

Constant ID	Constant Description	Value	Units
Theta_GRBA	Temperature correction for benthic algae growth rate	1.07	
RMAXBA	Maximum respiration rate for benthic algae	0.4	/day
Theta_RSBA	Temperature correction for benthic algae respiration rate	1.07	
EXCBA	Benthic algae excretion rate	0.2	/day
Theta_EXCBA	Temperature correction for benthic algae excretion rate	1.07	
DTHBA	Benthic algae death rate (via grazing and other mortality)	0.2	/day
Theta_DTHBA	Temperature correction for benthic algae death rate	1.07	
KMLBA	Light half-saturation constant	50	langleys/day
KSOBA	Oxygen inhibition parameter for benthic algae respiration rate	0.6	L/mg-O2
KHNXB	Preference coefficient for NH4 by benthic algae	0.025	mgN/L
SLMAX	Maximum sloughing rate coefficient or base rate of death	0.19	/day
SLALPHA	Empirical coefficient relating sloughing loss rate to depth	0.11	
SLTMIN	Temperature at which sloughing is initiated	12	deg. C
SLTOPT	Temperature at of above which the maximum sloughing rate occurs	17	deg. C
VSBA	Settling rate for benthic algae	0	m/day
PDEPBA	Probability of deposition	1	
K34C	Degradation rate of detrital benthic algae biomass	0.05	/day
K34T	Temp. correction for detrital benthic algae degradation rate	1.08	

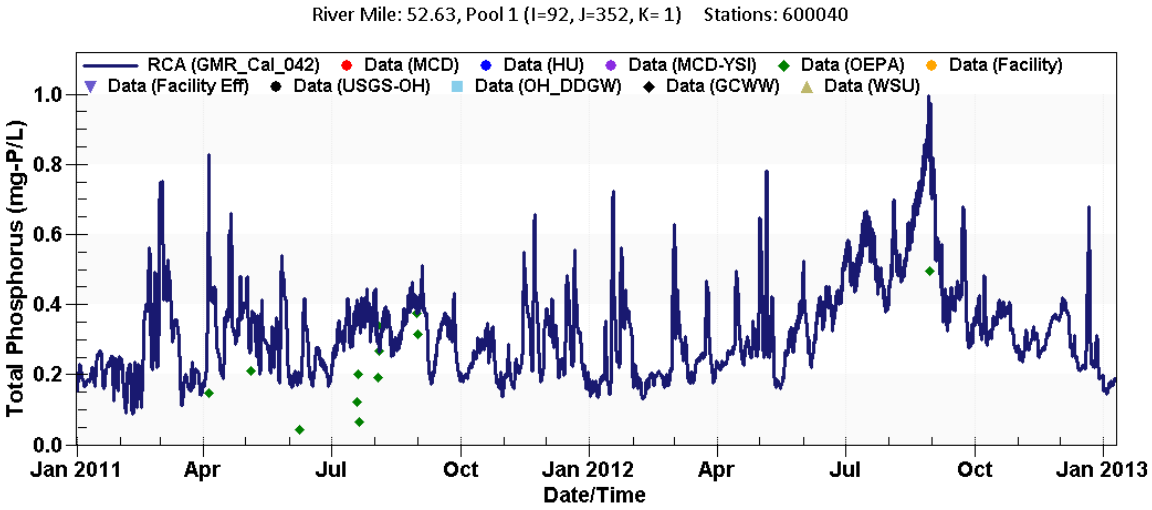

Figure E-1. Time series comparison of simulated and observed TP concentrations for the Great Miami River at Middletown, 2011-2012.

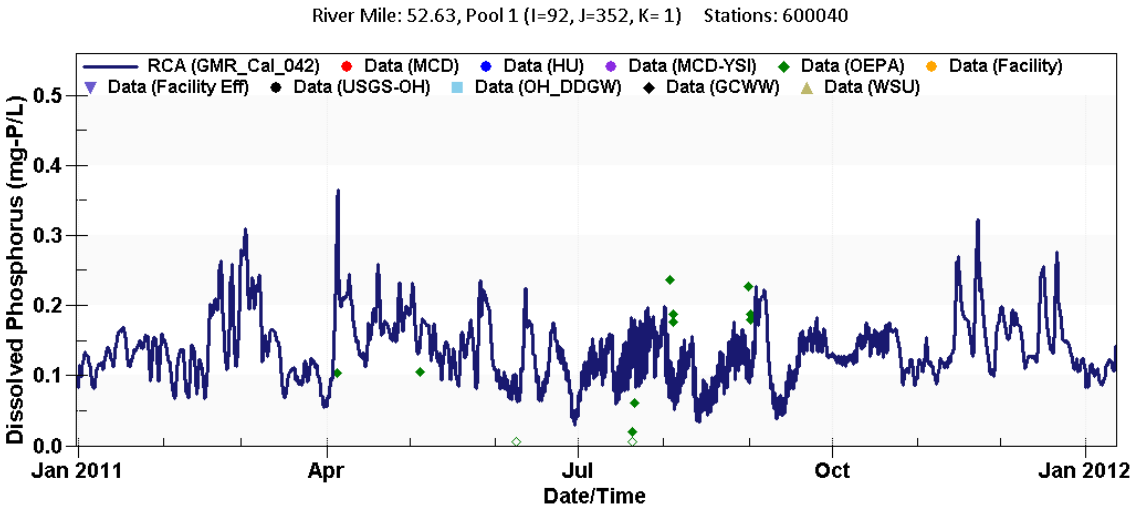

Figure E-2. Time series comparison of simulated and observed DPO4 concentrations for the Great Miami River at Middletown, 2011.

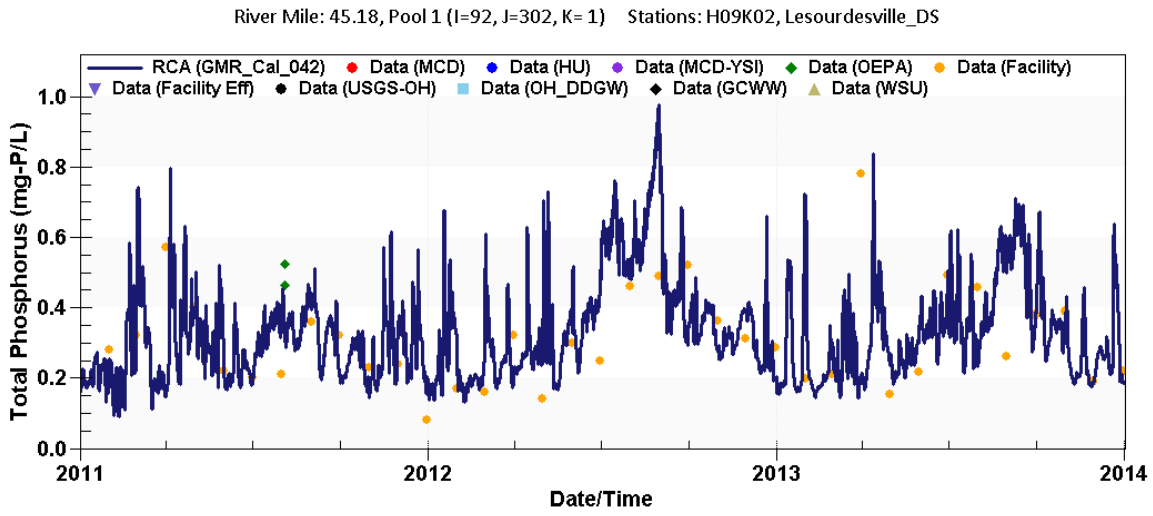

Figure E-3. Time series comparison of simulated and observed TP concentrations for the Great Miami River downstream of the LeSourdsville WRF, 2011-2013.

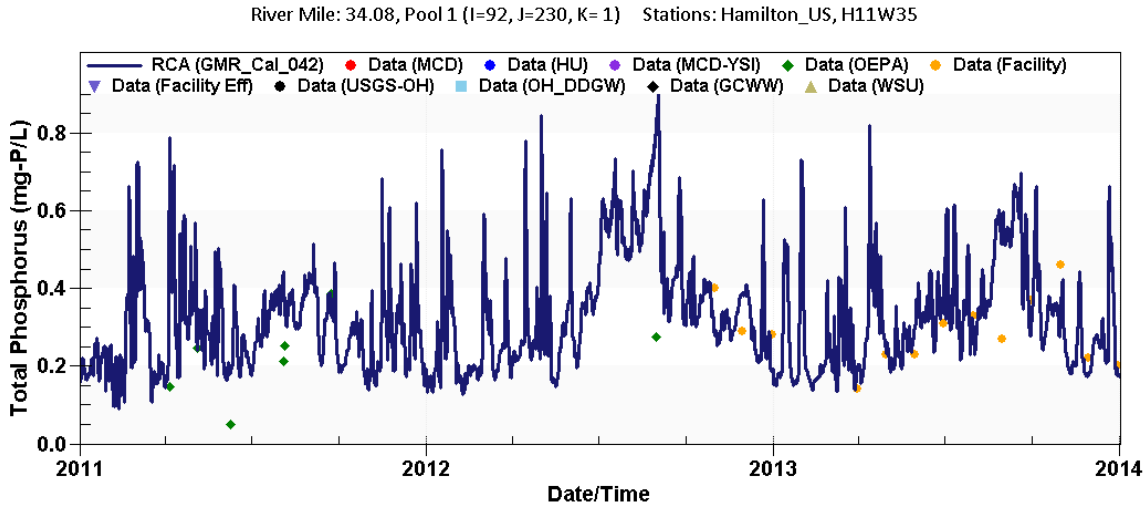

Figure E-4. Time series comparison of simulated and observed TP concentrations for the Great Miami River upstream of the Hamilton WWTP, 2011-2012.

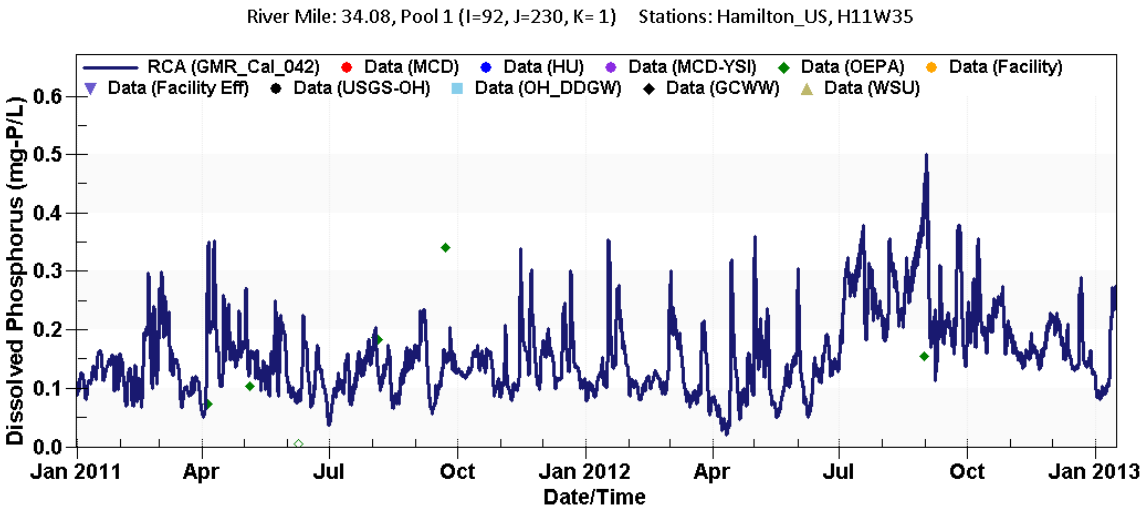

Figure E-5. Time series comparison of simulated and observed DPO4 concentrations for the Great Miami River upstream of the Hamilton WWTP, 2011-2012.

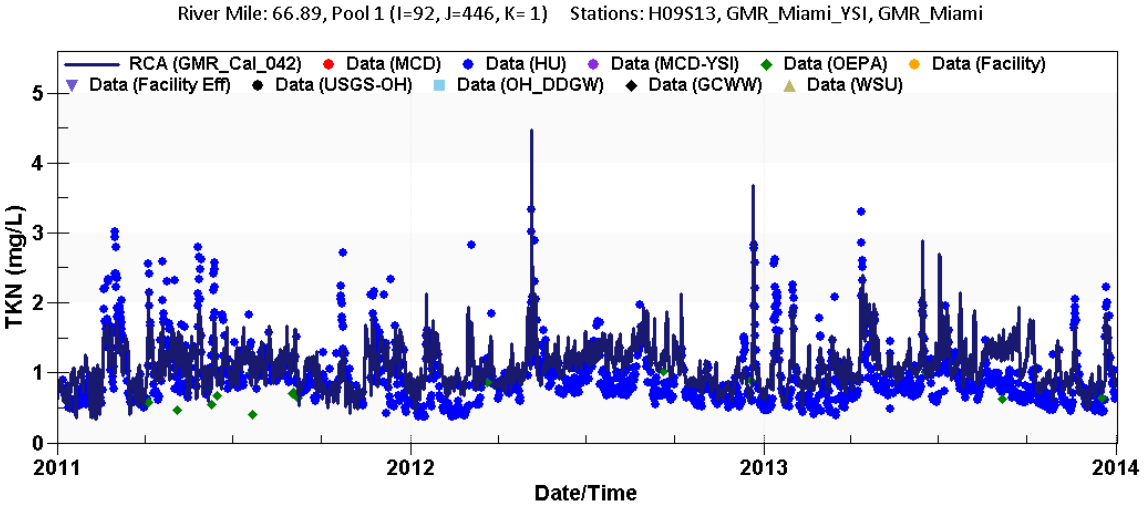

Figure E-6. Time series comparison of simulated and observed TKN concentrations for the Great Miami River at Miamisburg, 2011-2013.

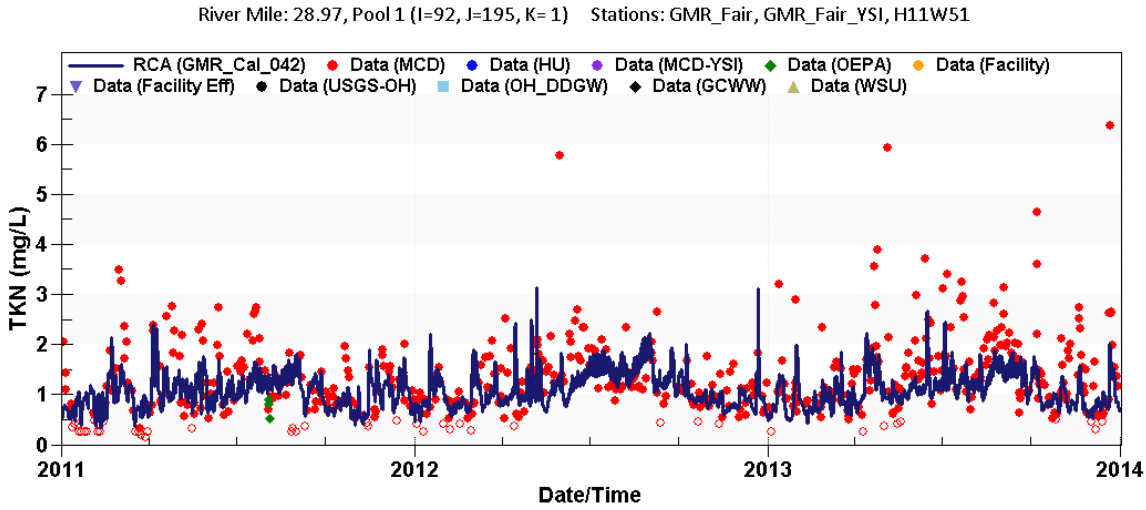

Figure E-7. Time series comparison of simulated and observed TKN concentrations for the Great Miami River at Fairfield, 2011-2013.

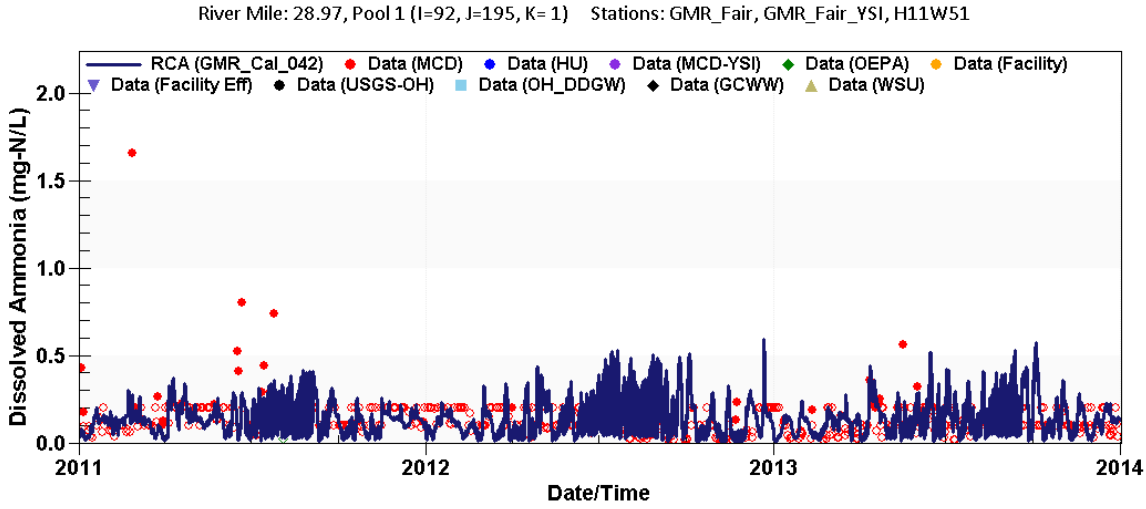

Figure E-8. Time series comparison of simulated and observed NH3 concentrations for the Great Miami River at Fairfield, 2011-2013.

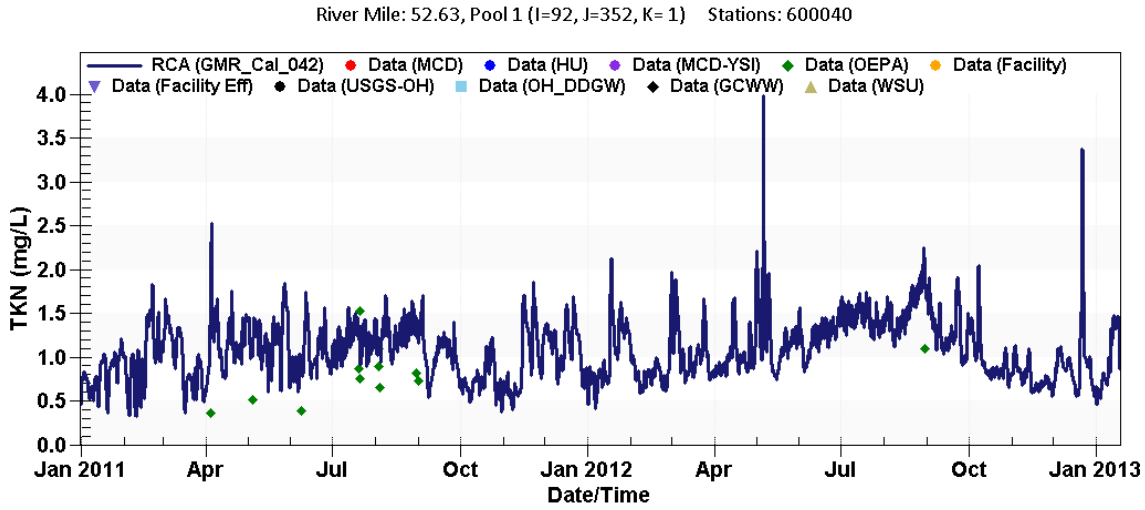

Figure E-9. Time series comparison of simulated and observed TKN concentrations for the Great Miami River at Middletown, 2011-2012.

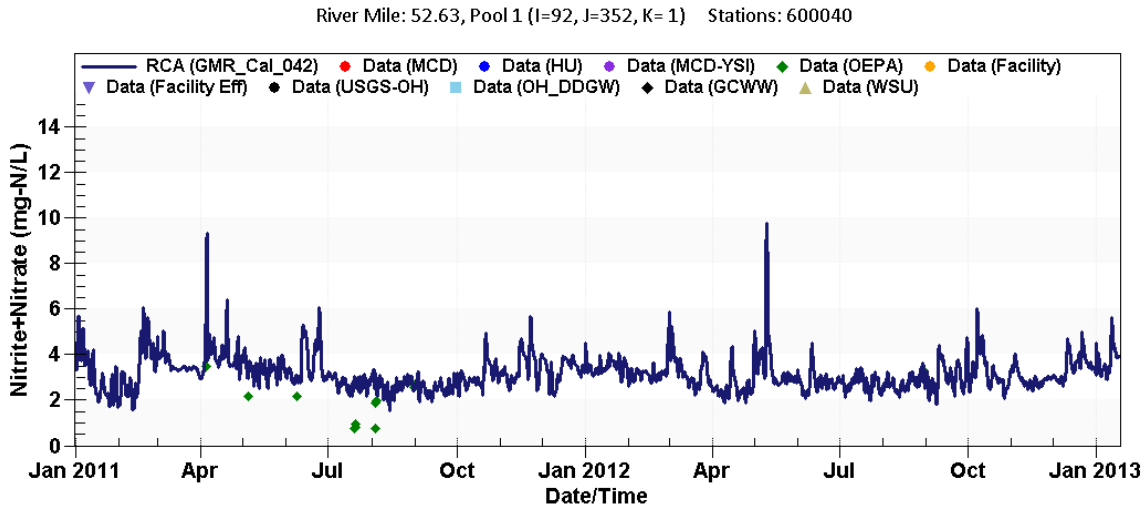

Figure E-10. Time series comparison of simulated and observed NO2+NO3 concentrations for the Great Miami River at Middletown, 2011-2012.

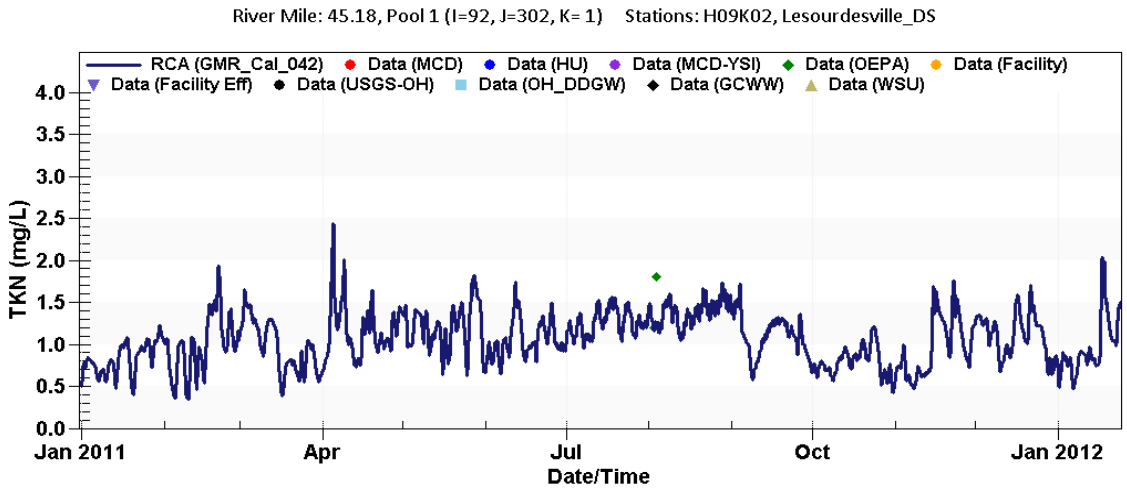

Figure E-11. Time series comparison of simulated and observed NO2+NO3 concentrations for the Great Miami River downstream of the LeSourdsville WRF, 2011.

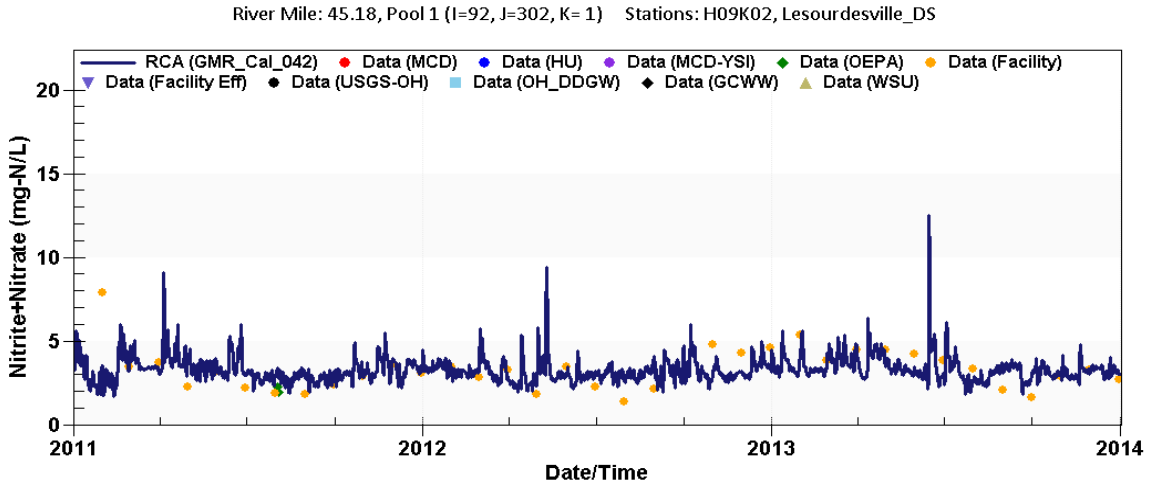

Figure E-12. Time series comparison of simulated and observed NO2+NO3 concentrations for the Great Miami River downstream of the LeSourdsville WRF, 2011-2013.

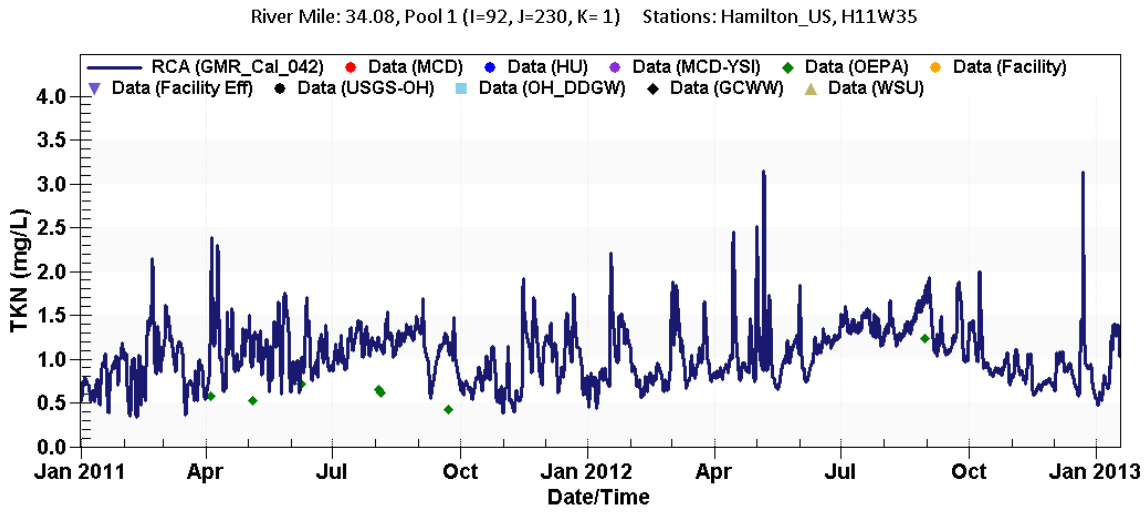

Figure E-13. Time series comparison of simulated and observed TKN concentrations for the Great Miami River upstream of the Hamilton WWTP, 2011-2012.

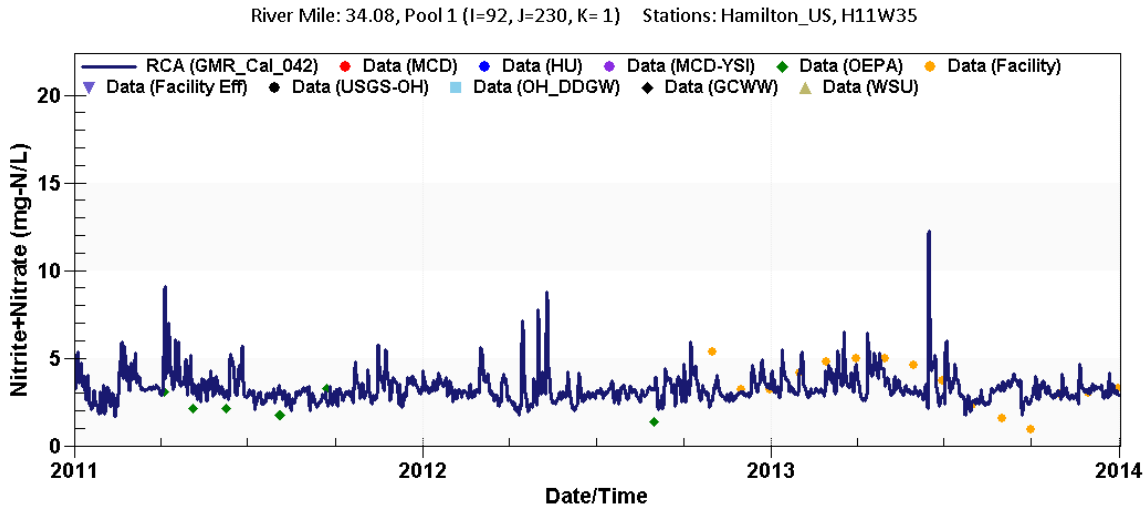

Figure E-14. Time series comparison of simulated and observed NO2+NO3 concentrations for the Great Miami River upstream of the Hamilton WWTP, 2011-2013.

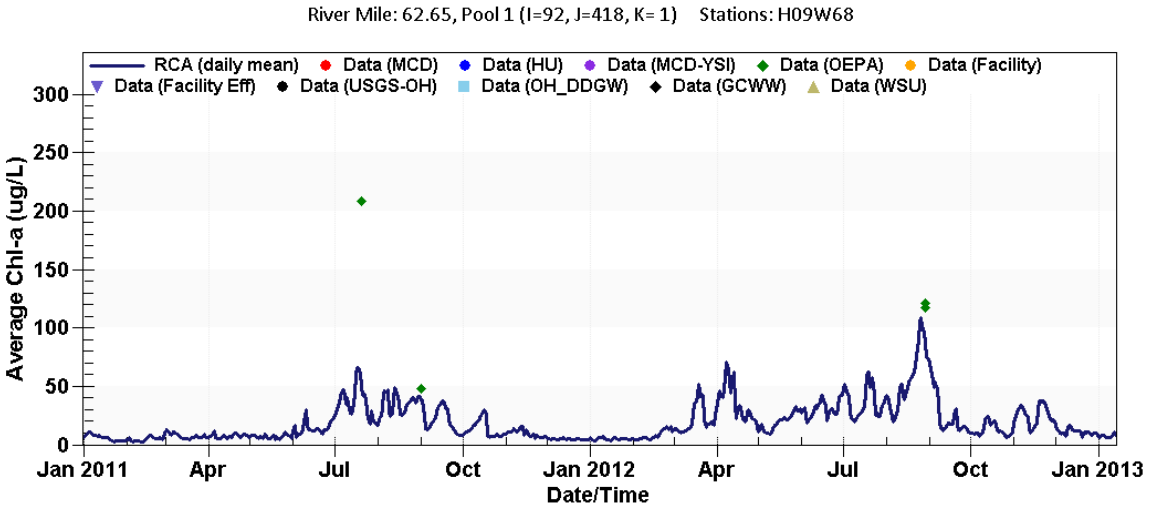

Figure E-15. Time series comparison of simulated and observed chlorophyll *a* concentrations for the Great Miami River N. of Franklin at Chautauqua Dam, 2011-2012.

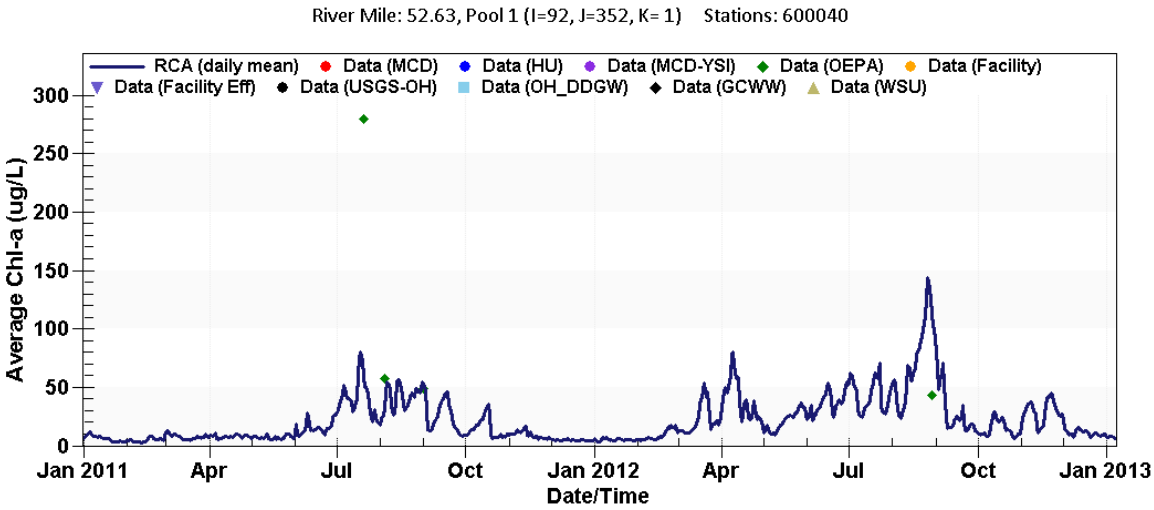

Figure E-16. Time series comparison of simulated and observed chlorophyll *a* concentrations for the Great Miami River at Middletown, 2011-2012.

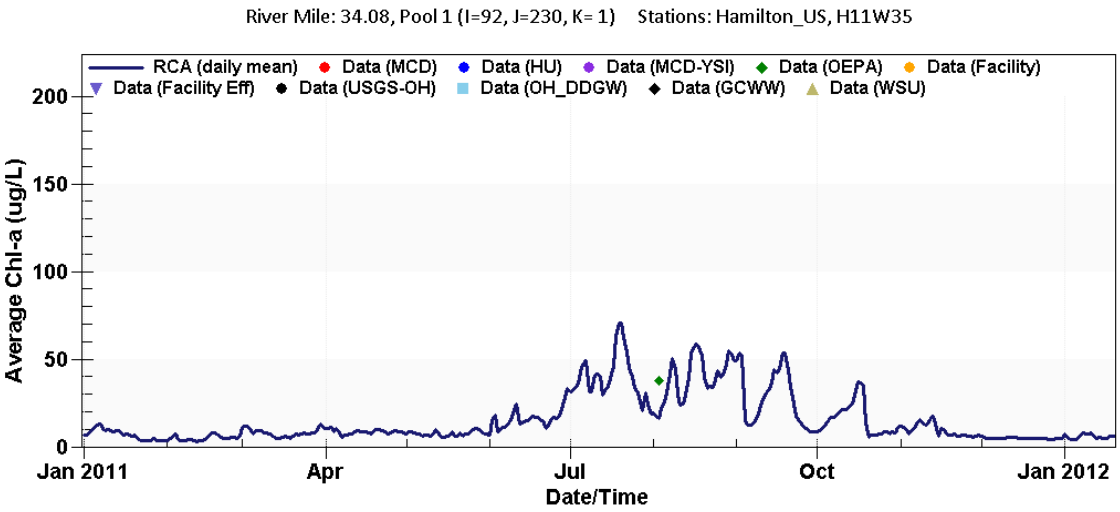

Figure E-17. Time series comparison of simulated and observed chlorophyll *a* concentrations for the Great Miami River upstream of the Hamilton WWTP, 2011.

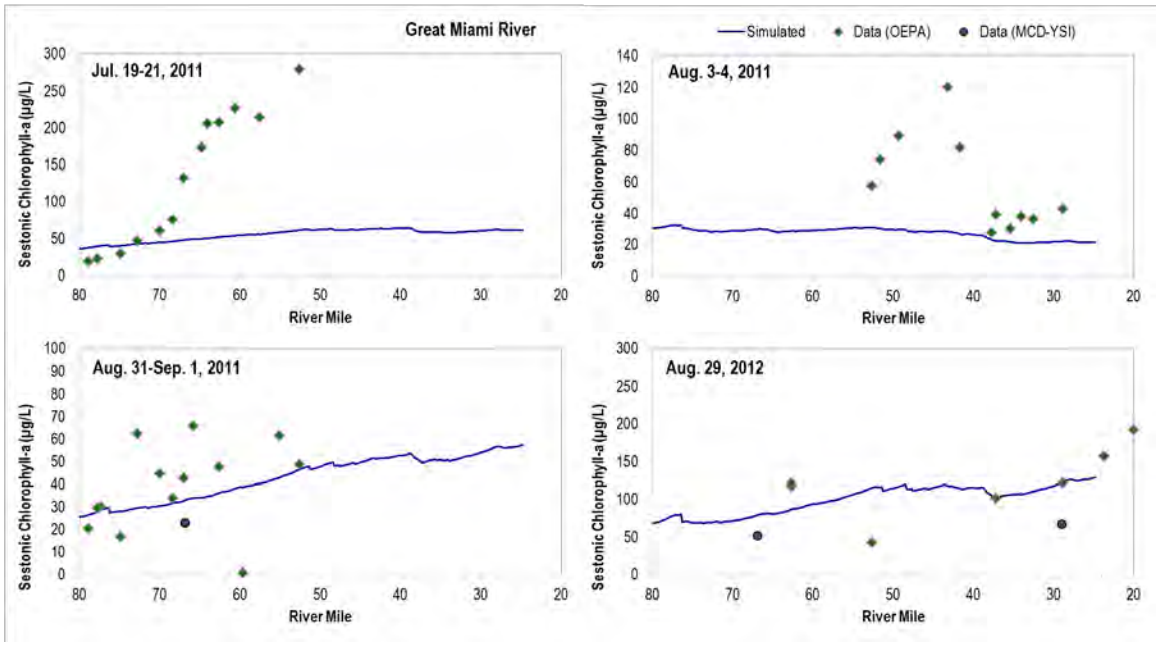

Figure E-18. Longitudinal profile plot of simulated and observed chlorophyll a concentrations for the Great Miami River for four OEPA sampling events. Simulated results represent a 7-day average around the sampling event date (i.e., 3 days before and 3 days after).

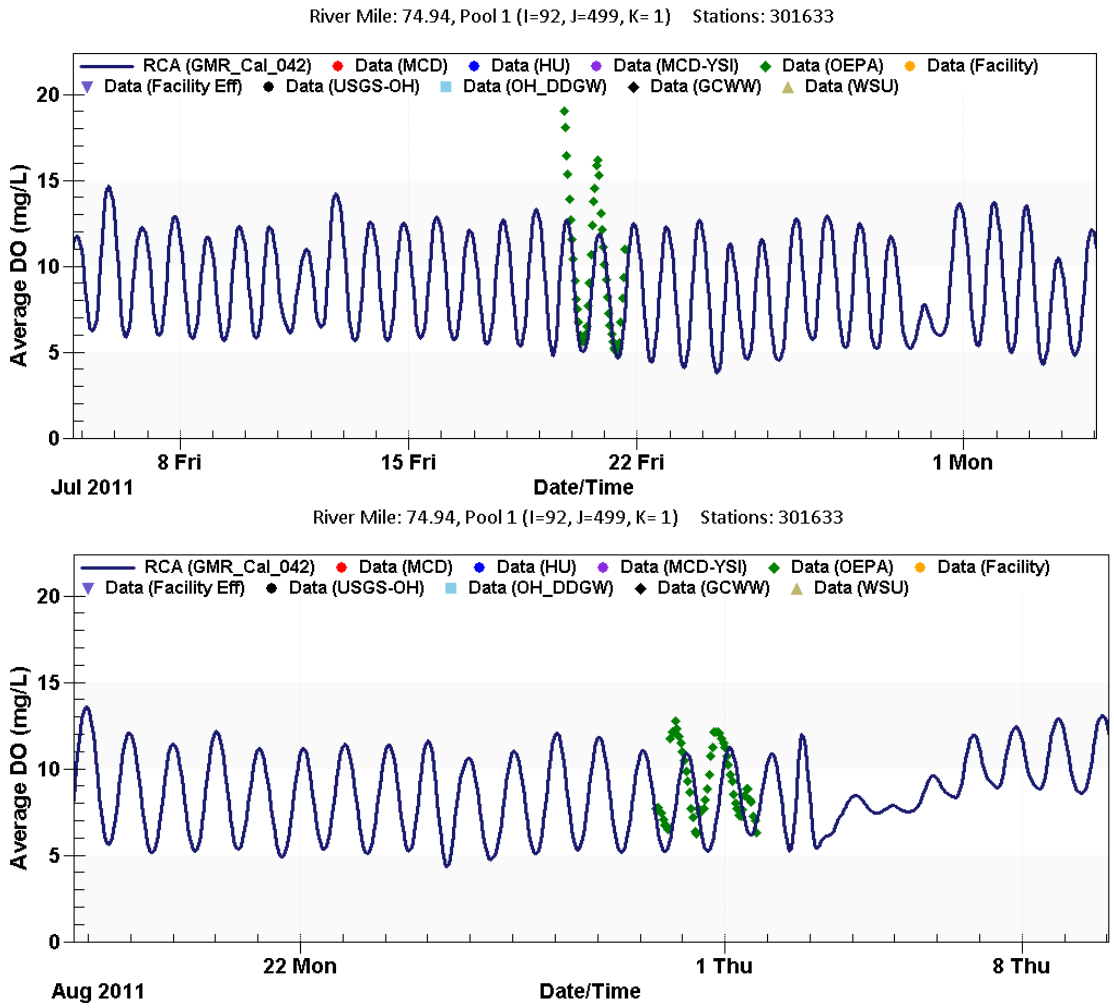

Figure E-19. Hourly time series comparison of simulated and observed DO concentrations for the Great Miami River at Moraine during two OEPA sampling events in 2011.

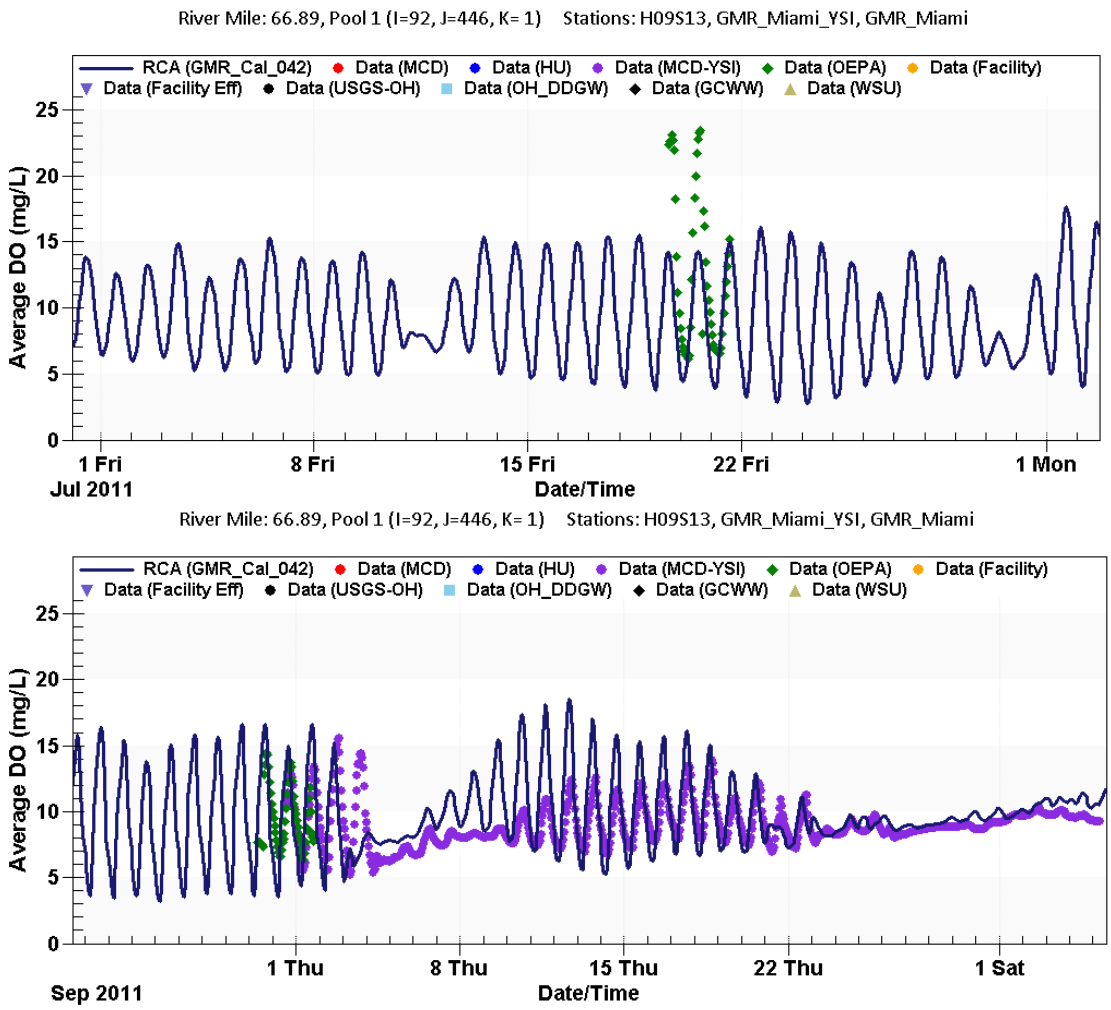

Figure E-20. Hourly time series comparison of simulated and observed DO concentrations for the Great Miami River at Miamisburg during two OEPA sampling events in 2011.

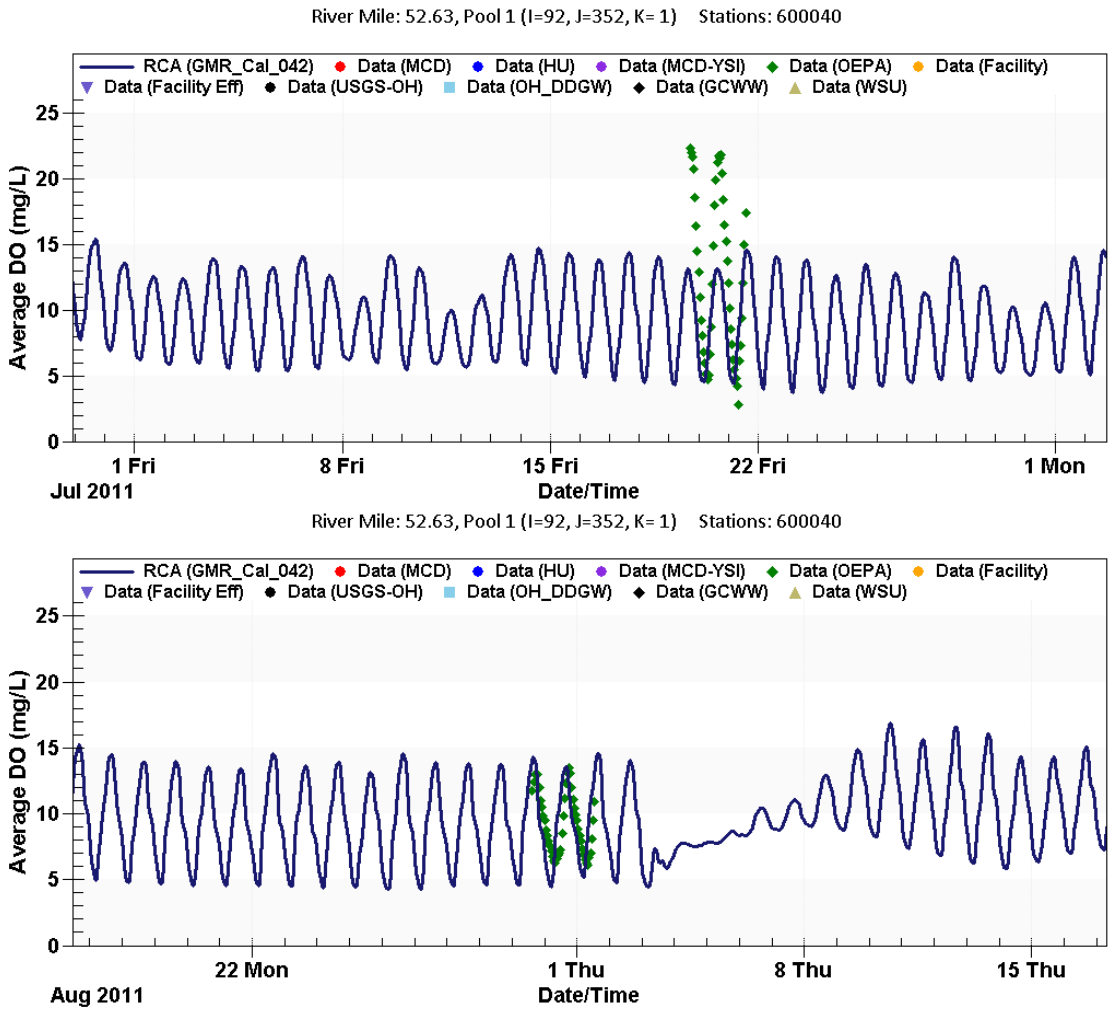

Figure E-21. Hourly time series comparison of simulated and observed DO concentrations for the Great Miami River at Middletown during two OEPA sampling events in 2011.

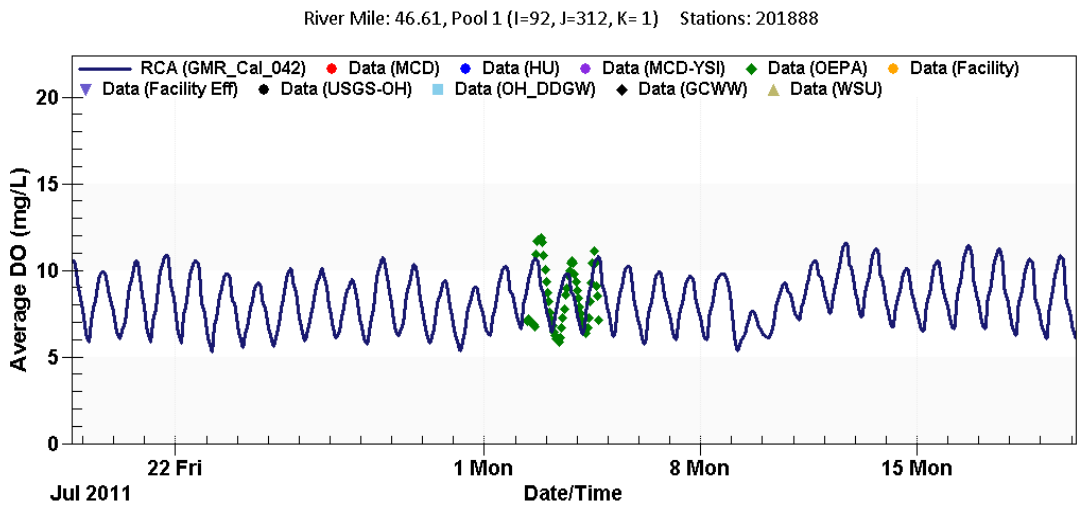

Figure E-22. Hourly time series comparison of simulated and observed DO concentrations for the Great Miami River upstream of the LeSourdsville WRF during an OEPA sampling event in 2011.

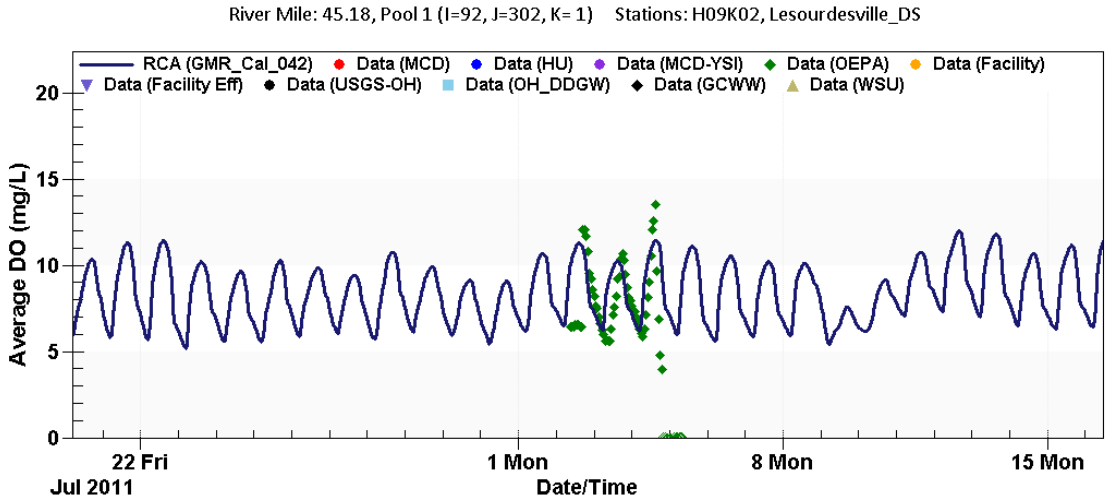

Figure E-23. Hourly time series comparison of simulated and observed DO concentrations for the Great Miami River downstream of the LeSourdsville WRF during an OEPA sampling event in 2011.

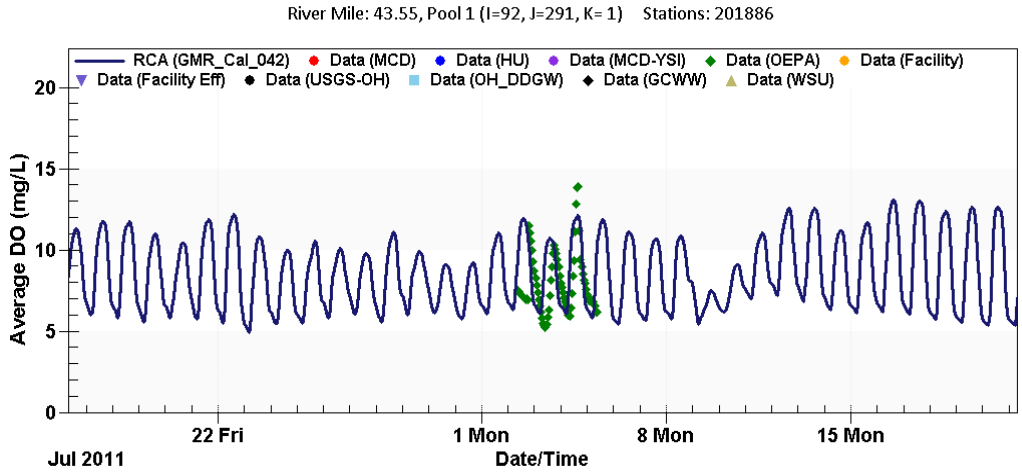

Figure E-24. Hourly time series comparison of simulated and observed DO concentrations for the Great Miami River upstream of Liberty-Fairfield Road during an OEPA sampling event in 2011.

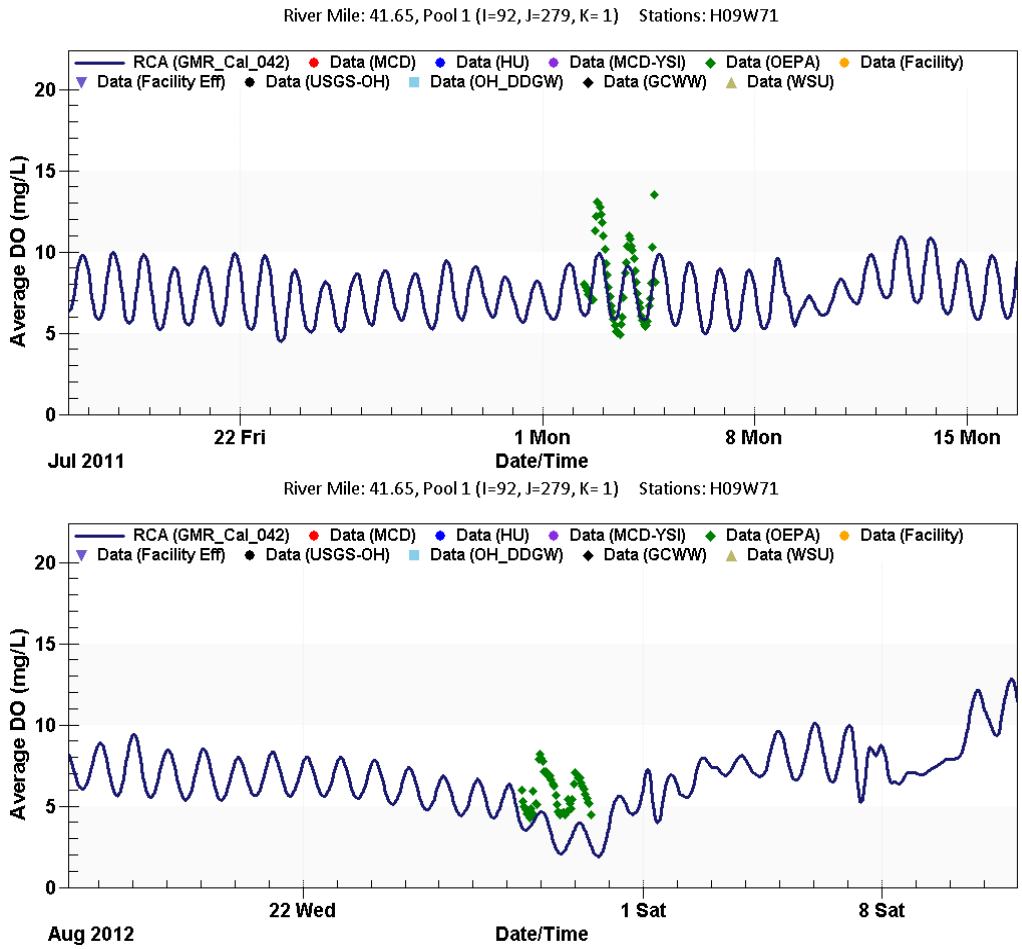

Figure E-25. Hourly time series comparison of simulated and observed DO concentrations for the Great Miami River upstream of the Hamilton Hydraulic Canal during OEPA sampling events in 2011 and 2012.

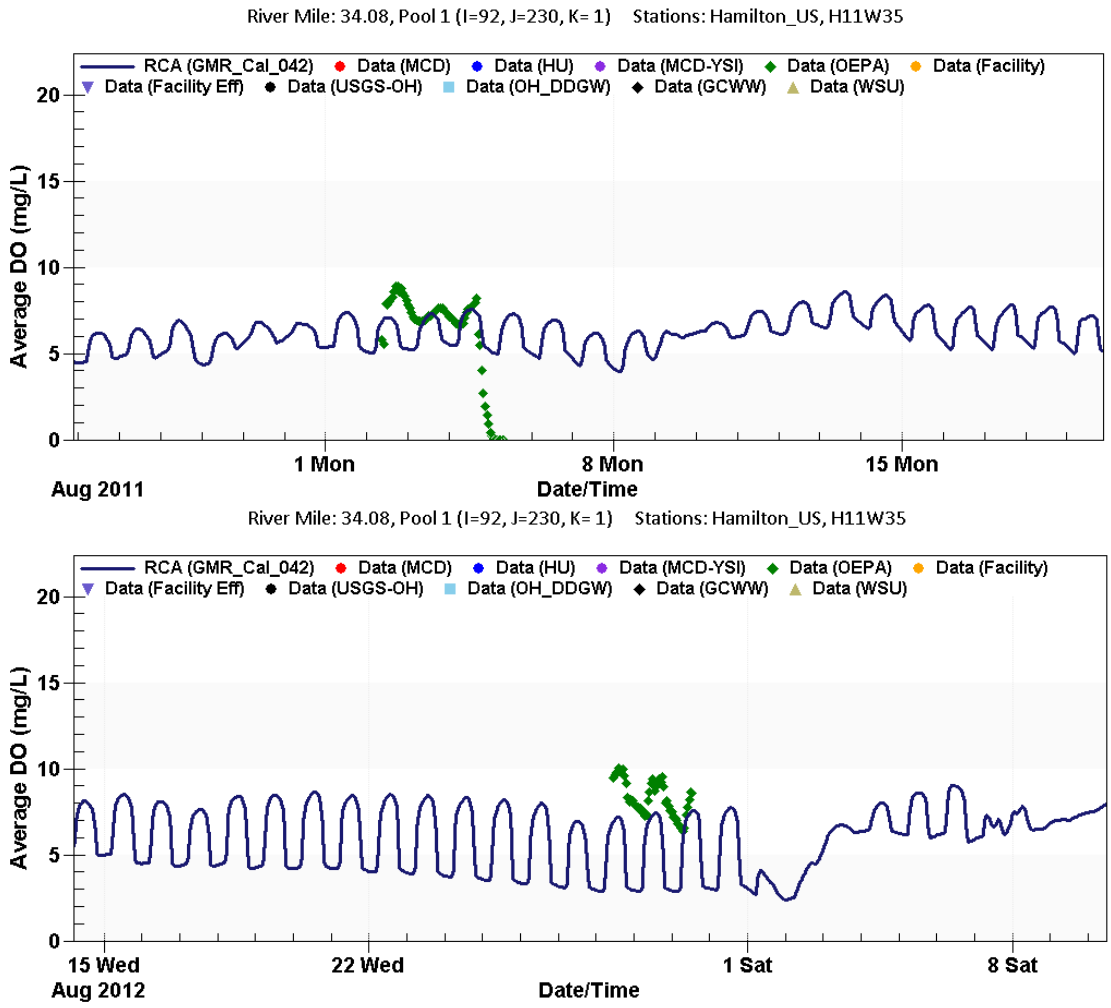

Figure E-26. Hourly time series comparison of simulated and observed DO concentrations for the Great Miami River upstream of the Hamilton WWTP during OEPA sampling events in 2011 and 2012.

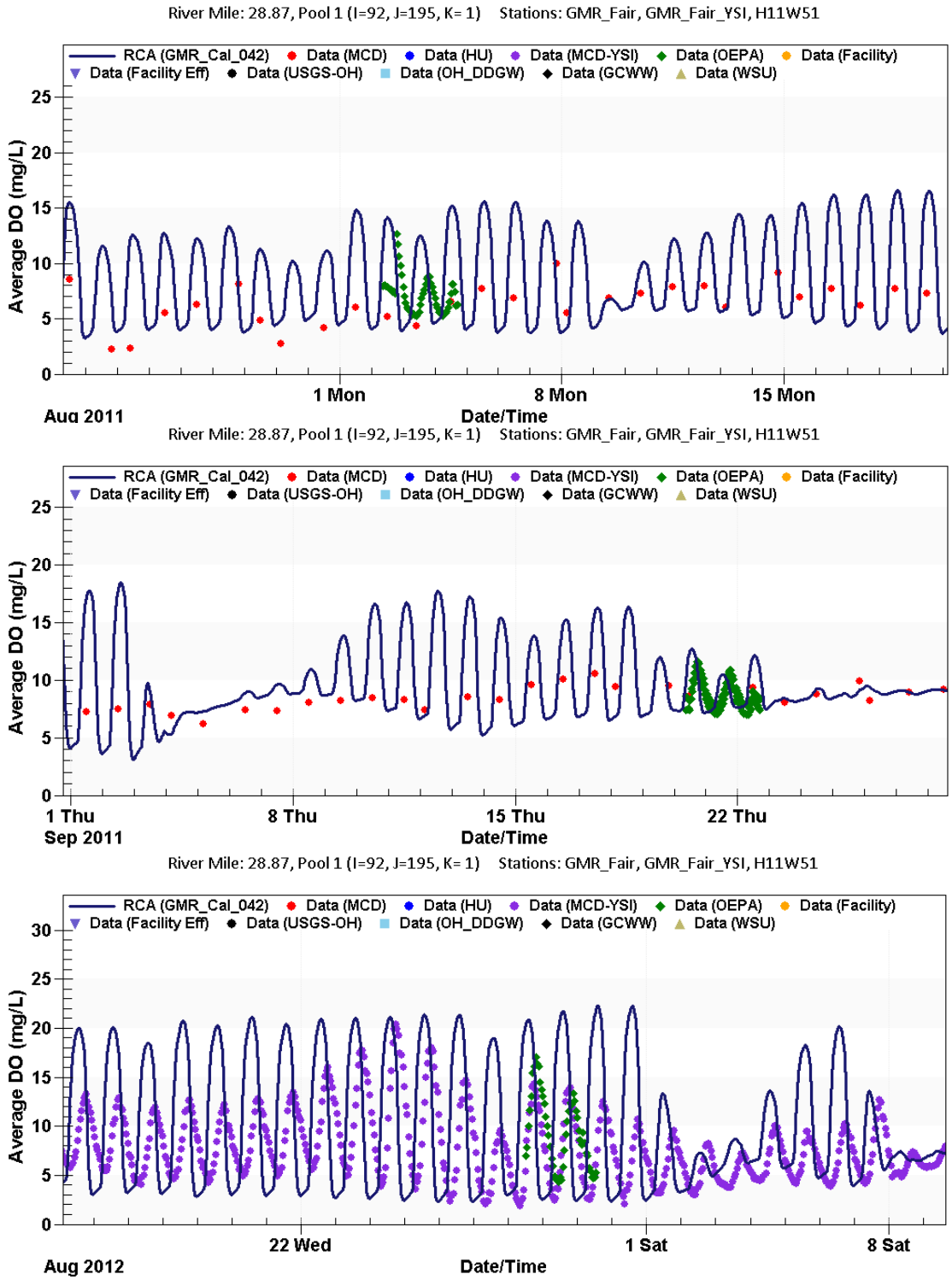

Figure E-27. Hourly time series comparison of simulated and observed DO concentrations for the Great Miami River at Fairfield during OEPA sampling events in 2011 and 2012.

Appendix F:
September 2016 Supplemental Field Investigation

LimnoTech mobilized a field crew on September 16, 2016, to investigate lateral variability of dissolved oxygen (DO) in the lower Great Miami River (LGMR). Although this work was not part of the scope of this project, previous visual observations of the lateral variability of bathymetry and algal growth, along with questions raised while calibrating the LGMR water quality model to DO data collected by deployed sondes, indicated the need for such an investigation. Because the activity was not part of the original project, the scope was limited to one day and a single location on the river.

The Miamisburg data station (Figure F-1) was chosen for this investigation because it is one of two primary stations used for calibration of the LGMR water quality model. Two transects were investigated at this location as shown in Figure F-2. The investigation is summarized below. Each transect was characterized twice on September 16: once in in late morning and once in the late afternoon. The earlier characterization occurred between 11:15 AM and 1:45 PM. The later characterization was performed between 4:05 PM and 5:50 PM. Characterization consisted of a two-person crew traversing the transect in a jon boat; to minimize ambient disturbance, the boat was rowed, as opposed to using a motor.

Each transect characterization consisted of two passes. On the first pass, the crew stopped at intervals across the river and took manual soundings with a weighted tape to get a sense of the bathymetric variability. At each stop, the crew also used a YSI 6920 water quality sonde to measure water temperature, pH, specific conductivity, turbidity and DO. These measurements were manually recorded in the field notes. On the second pass, the boat towed a SonTek Riversurveyor M9 Hydroboard Acoustic Doppler Profiler (ADP) to measure bathymetry and current velocity (see Figure F-3).

The DO data collected during this investigation demonstrate that significant variability in DO can occur across the river channel, even when measurements are made over very short periods of time. Figure F-4 shows these results graphically. Each transect is shown in profile so bathymetry can be viewed. Ambient velocity recorded by the ADP is represented qualitatively using color, from violet (slower) to red (faster). DO results shown in green are from late morning/midday, and DO results shown in blue are from late afternoon.

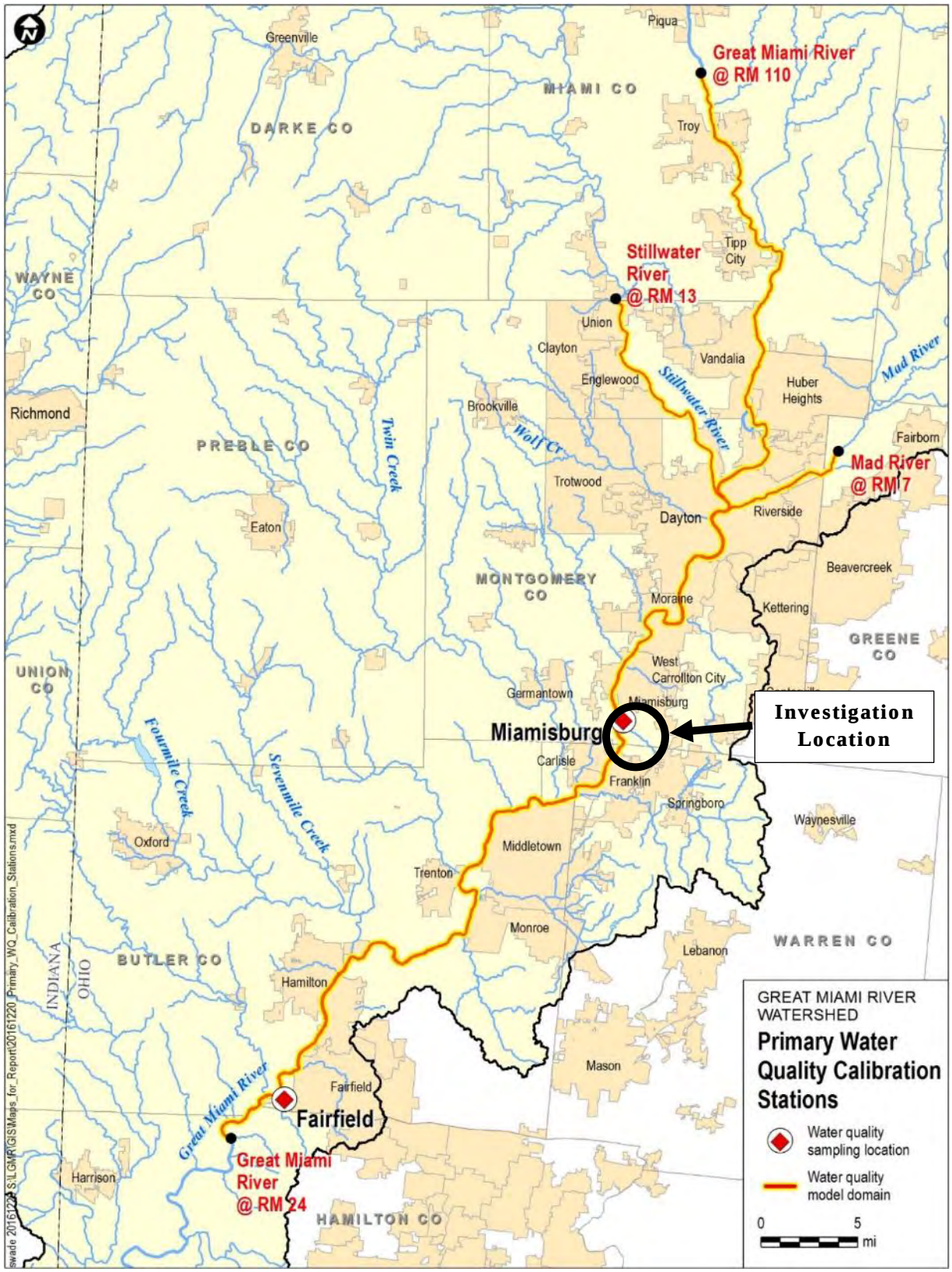

Figure F-1. Location of September 16, 2016, Field Investigation.

Figure F-2. Transects Investigated at Miamisburg on September 16, 2016.

Figure F-3. SonTek Riversurveyor M9 Hydroboard Acoustic Doppler Profiler in use on the Lower Great Miami River.

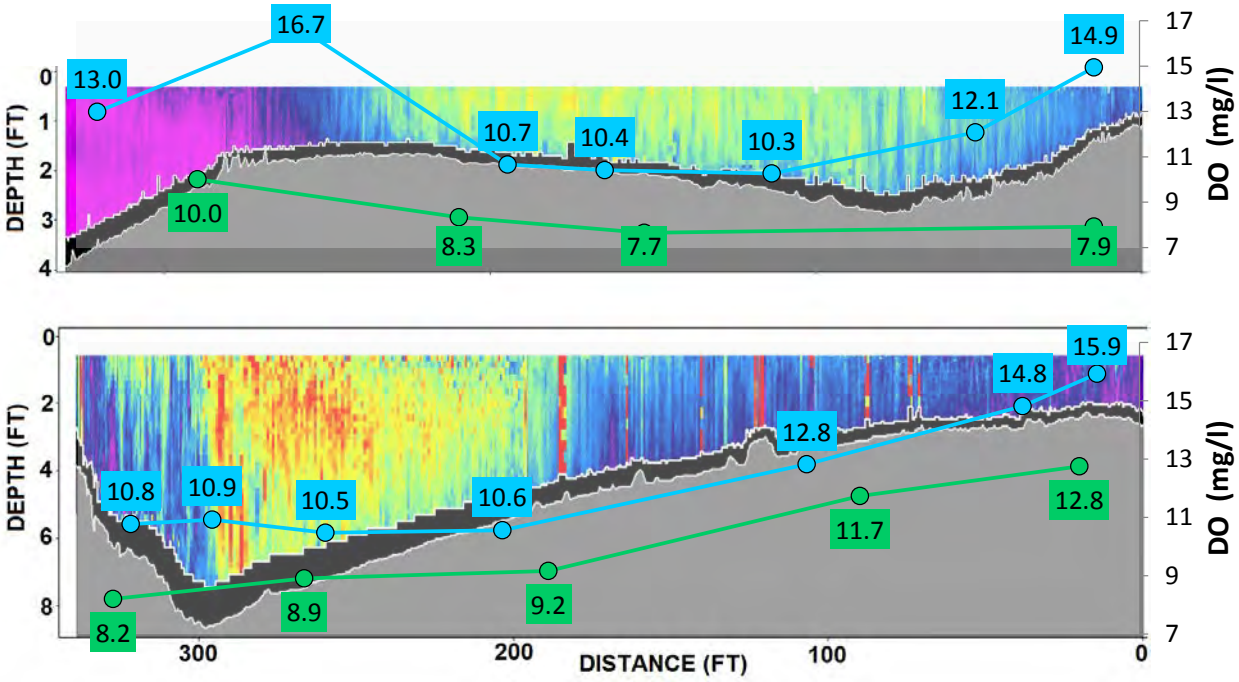

Figure F-4. Transect profiles collected on September 16, 2016, showing bathymetry, ambient velocity (qualitatively using color) and DO measurements. Green DO measurements are late morning/midday and blue DO measurements are from late afternoon.

Appendix G:
Daily Scenario Results

As a supplement to the plots presented in Section 5.6, which show monthly average results for key water quality parameters, the following plots show daily average results at Fairfield comparing the seven scenarios, for six key water quality parameters.

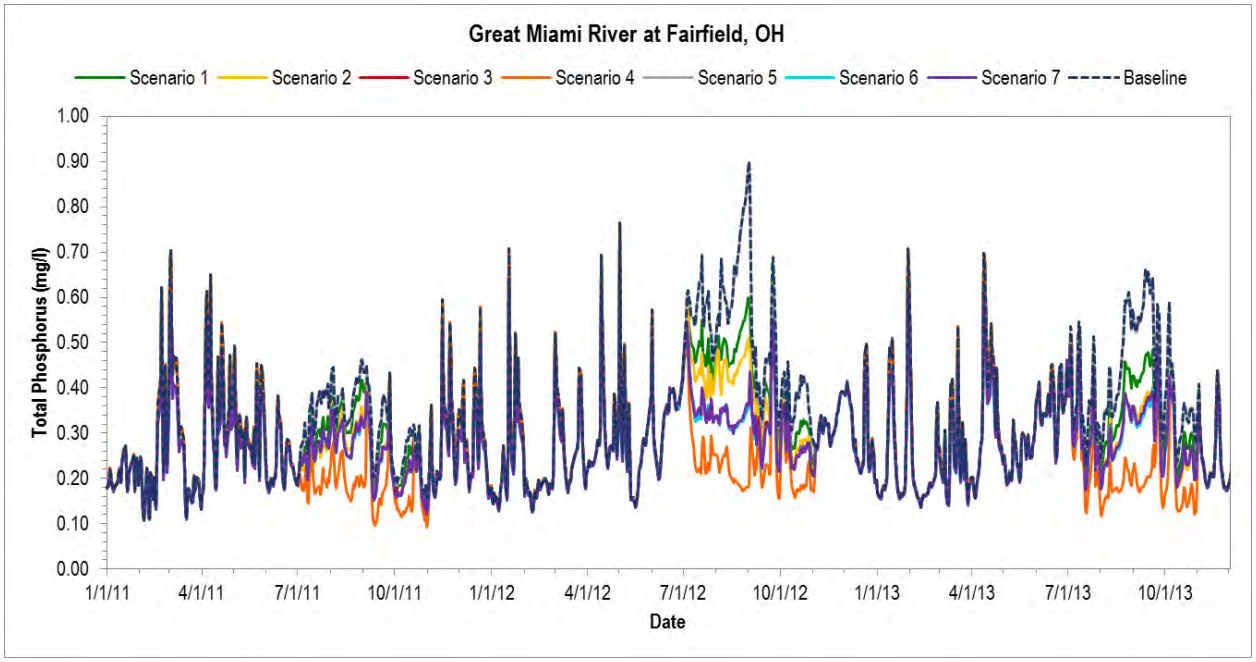

Figure G-1. Daily average TP time series comparison of the baseline conditions scenario and seven management scenarios for the Great Miami River at Fairfield, 2011-2013

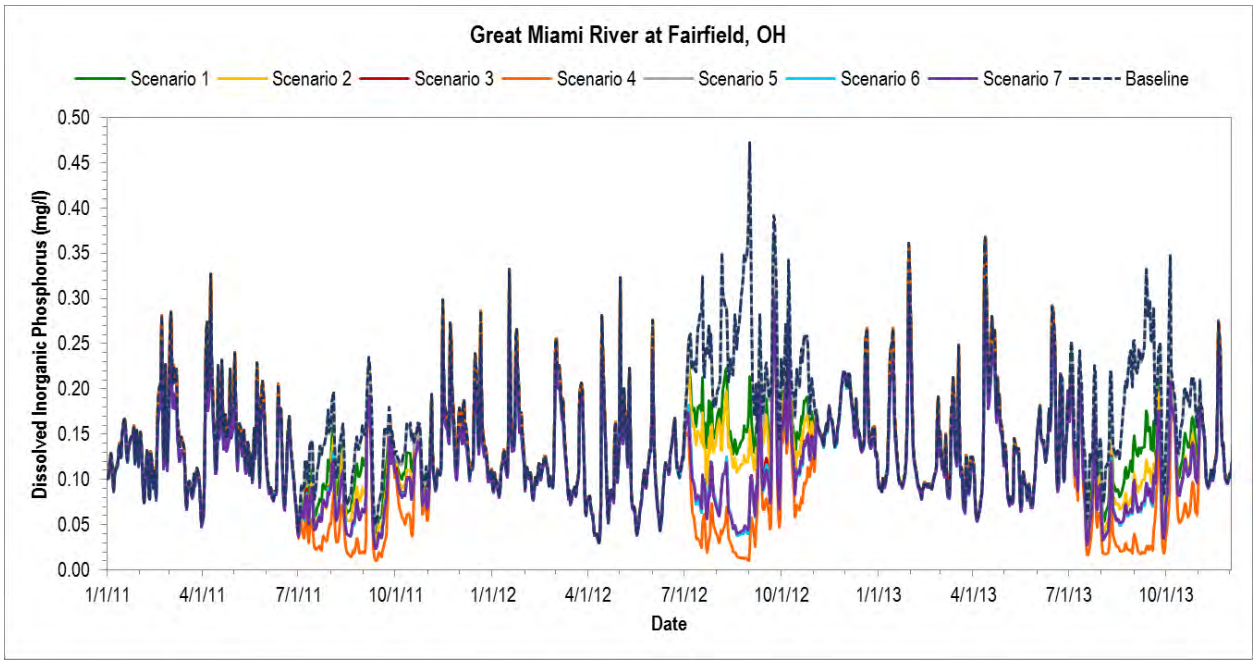

Figure G-2. Daily average DPO4 time series comparison of the baseline conditions scenario and seven management scenarios for the Great Miami River at Fairfield, 2011-2013

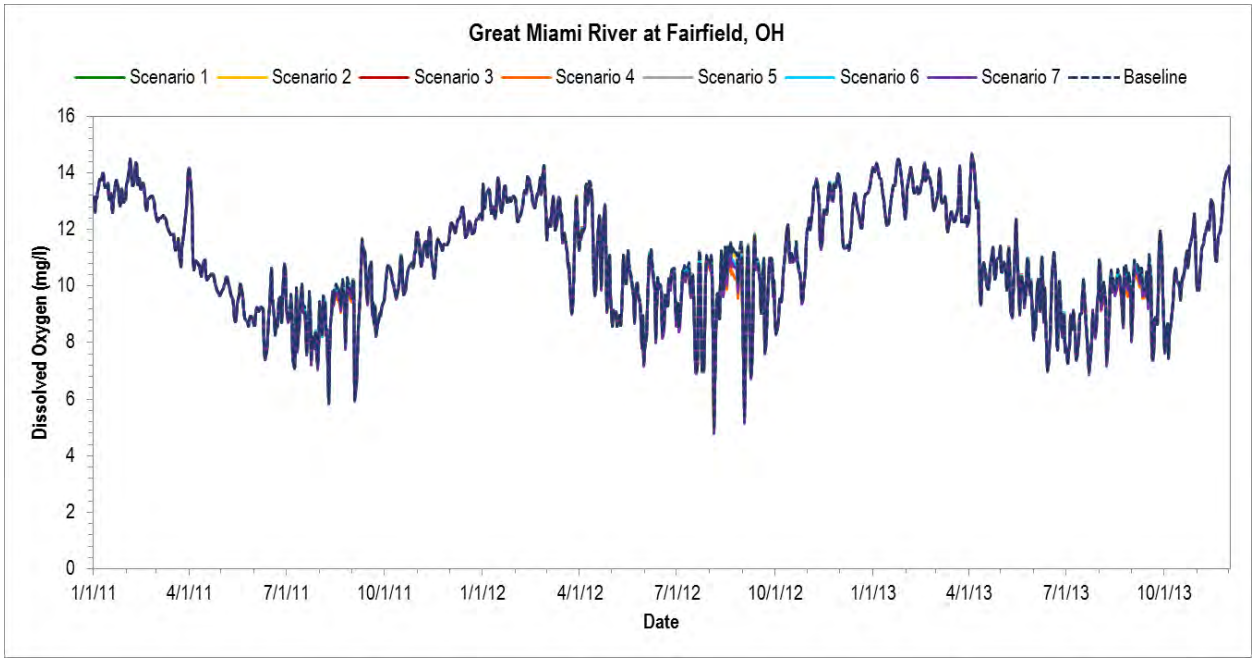

Figure G-3. Daily average DO time series comparison of the baseline conditions scenario and seven management scenarios for the Great Miami River at Fairfield, 2011-2013

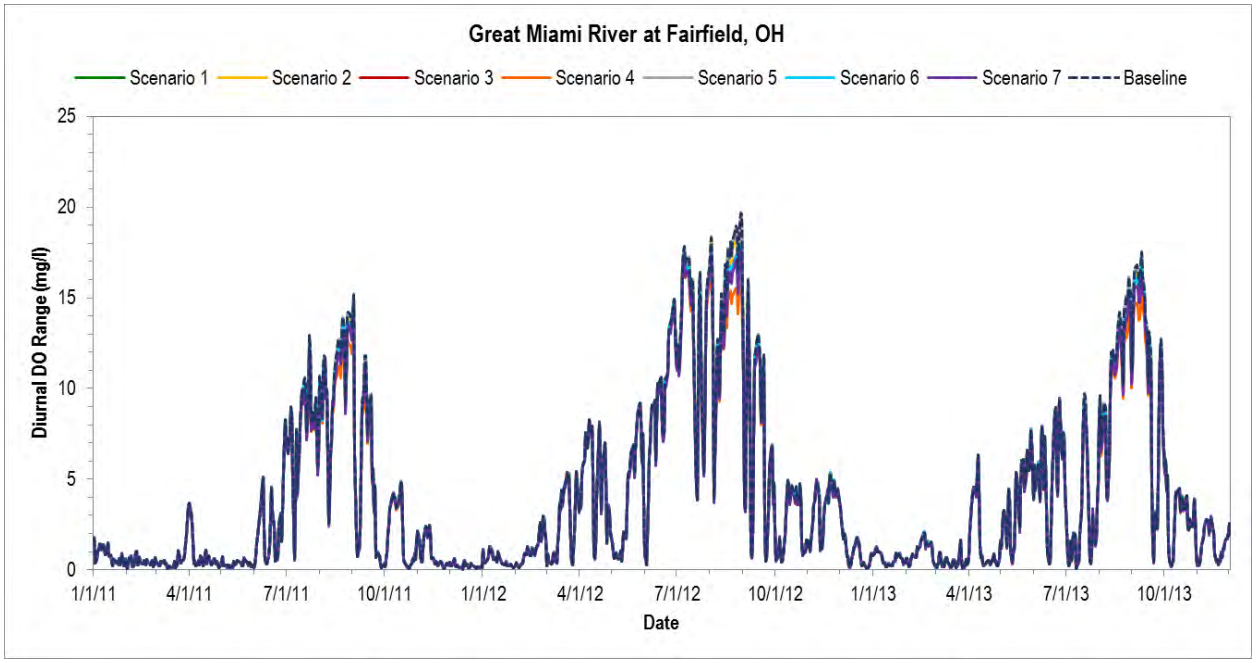

Figure G-4. Daily average diurnal DO range time series comparison of the baseline conditions scenario and seven management scenarios for the Great Miami River at Fairfield, 2011-2013

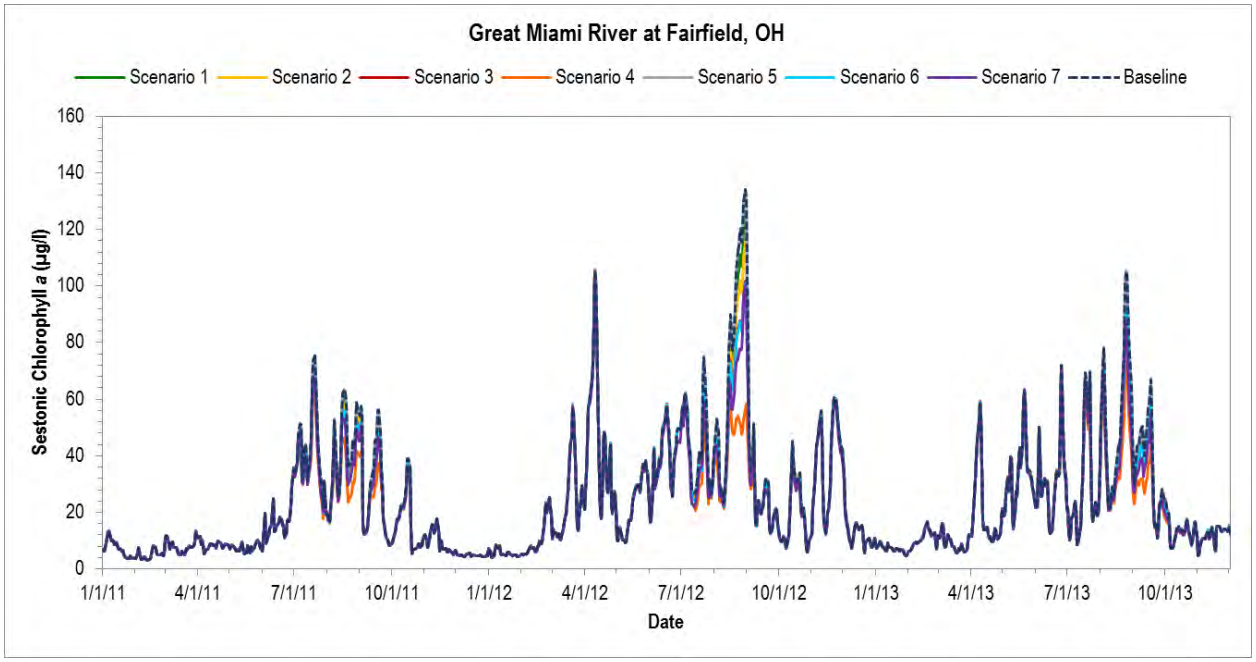

Figure G-5. Daily average sestonic algae chlorophyll *a* time series comparison of the baseline conditions scenario and seven management scenarios for the Great Miami River at Fairfield, 2011-2013

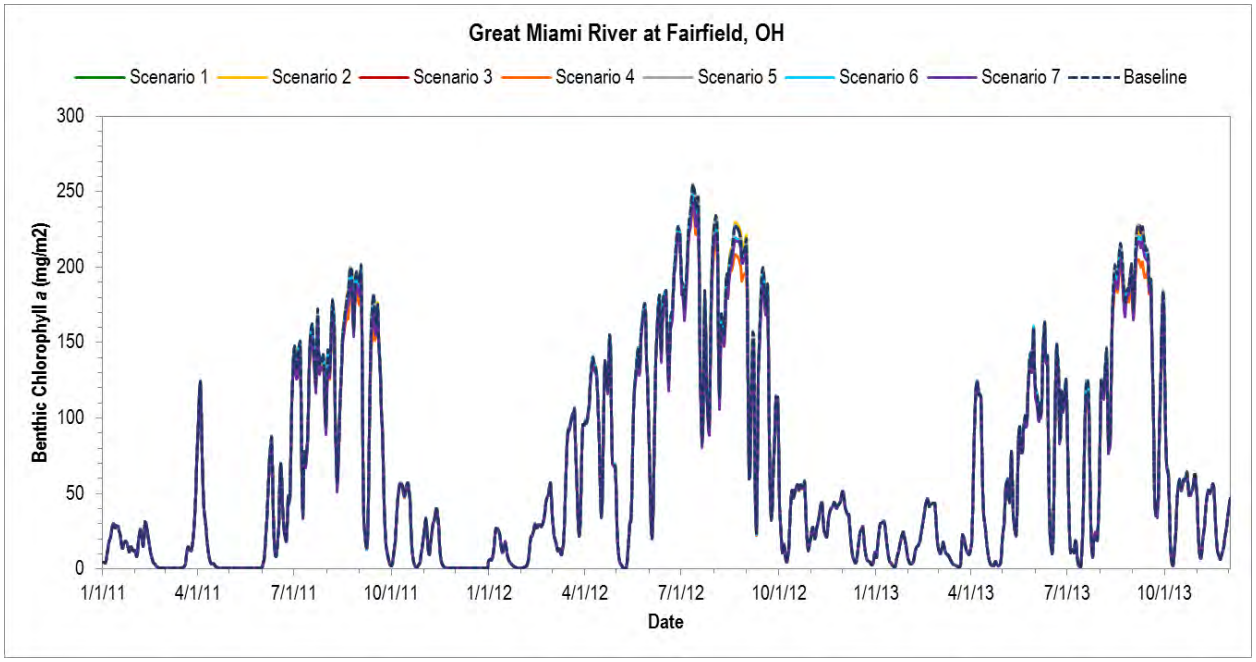

Figure G-6. Daily average benthic algae chlorophyll *a* time series comparison of the baseline conditions scenario and seven management scenarios for the Great Miami River at Fairfield, 2011-2013

Appendix H:
Biosketches of Project Experts

Blank

David W. Dilks, Ph.D.

Dr. Dilks is responsible for the assessment of water quality issues, primarily through the development and/or application of mathematical models. A Vice President at LimnoTech, Dr. Dilks has directed modeling studies on more than 250 water bodies and watersheds nationwide. This work has included watershed simulation models, hydrodynamic models, and water quality models for temperature, conventional pollutants and toxic pollutants. He has also directed the development or review of more than 200 Total Maximum Daily Load (TMDL) determinations.

Dr. Dilks has directed and lectured at water quality and mixing zone modeling training workshops for more than 1,000 State and EPA staff. He has co-authored three national technical guidance manuals on water quality modeling and assessment. Dr. Dilks served as a member of EPA's SWAT team, a group of experts providing nationwide support in the development of watershed-based Total Maximum Daily Loads (TMDLs). He also served as co-Principal Investigator for two Water Environment Research Foundation (WERF) research projects evaluating and designing improvements to the TMDL development process.

With respect to professional activities, Dr. Dilks has served as a technical reviewer for EPA guidance documents, professional journals, and research proposals. He has also served as an Adjunct Professor at the University of Michigan College of Engineering and School of Public Health, where he has taught graduate-level water quality modeling courses. Dr. Dilks has authored more than 40 scientific papers and given approximately 100 presentations at national scientific conferences, including more than two dozen invited presentations. He has also provided expert testimony in several cases related to water quality assessment. Dr. Dilks earned his bachelor's degree (Aquatic Biology/Biostatistics), master's degree (Public Health, Water Quality) and doctorate (Environmental Health Sciences) from the University of Michigan.

Steven Chapra, Ph.D.

Steve Chapra presently holds the Louis Berger Chair for Computing and Engineering in the Civil and Environmental Engineering Department at Tufts University. Professor Chapra is a Fellow of the American Society of Civil Engineers (ASCE). In 2013, he was chosen as one of the 5 inaugural Fellows of the Association of Environmental Engineering & Science Professors (AEESP). He has published over 150 papers, reports and software packages, and has authored seven textbooks including Numerical Methods for Engineers, which has been adopted at over 150 universities throughout the world. He has also authored the book Surface Water-Quality Modeling, the standard text in that area.

Before joining the faculty at Tufts, Dr. Chapra worked for EPA, NOAA, Texas A&M University and the University of Colorado. He has also served as the Associate Director of the Center for Advanced Decision Support in Water and Environmental Systems (CADSWES), and has been a visiting professor or scientist at 9 institutions Duke University, the University of Michigan, Imperial College London, and the University of Washington.

His general research interests focus on surface water-quality modeling and advanced computer applications in environmental engineering. His research has been used in a number of decision-making contexts including the 1978 Great Lakes Water Quality Agreement. He is the recipient of 4 international best paper awards including the 1993 Rudolph Hering Medal, the 2009 Chandler-Misener Award and the 2015 Wesley W. Horner Award. He has developed several environmentally-oriented software packages, including QUAL2K and LAKE2K, which are widely used for water-quality modeling in rivers and lakes.

Aside from his activities in environmental engineering, he has written several texts on computing and engineering for which he was awarded the 1987 Meriam-Wiley Distinguished Author Award by the American Society for Engineering Education. He has also taught over 75 workshops on water-quality modeling in North and South America, Europe, Asia, Africa, and Oceania.

He has been recognized as the outstanding teacher at Texas A&M University (1986 Tenneco Award), the University of Colorado (1992 Hutchinson Award), and Tufts University (2011 Professor of the Year Award). He is also the first recipient of the AEESP Wiley Award for Outstanding Contributions to Environmental Engineering and Science Education (2000). Dr. Chapra earned his bachelor's degree (Civil Engineering) and master's degree (Environmental Engineering) from Manhattan College and his doctorate (Water Resources and Environmental Engineering) from the University of Michigan.

Joseph V. DePinto, Ph.D.

Dr. DePinto is a Senior Scientist at Limno-Tech. He has 41 years' experience (27 of which have been spent in academia as a Professor of Environmental Engineering) conducting aquatic system research, education and management programs, with an emphasis on activities in the Great Lakes region. After earning his Doctorate, Dr. DePinto spent 17 years on the faculty at Clarkson University before joining the faculty at the University at Buffalo in January 1991 as a Full Professor in the Department of Civil, Structural and Environmental Engineering, and Director of the University-wide Great Lakes Program. While in academia, Dr. DePinto has received over $4 million in grants and contracts. Through his research on such topics as nutrient cycling-eutrophication, toxic chemical exposure and bioaccumulation, contaminated sediment assessment and remediation, aquatic ecosystem structure and functioning, and watershed, river, and lake modeling, Dr. DePinto has become internationally recognized as a leader in the development and application of surface water models to address water quality and ecosystem issues.

Recent projects for which Dr. DePinto has either been the Principal Investigator, co-PI, Lead Scientist, or Project Manager include: assessment of nutrient/ eutrophication dynamics in western Lake Erie; Saginaw Bay optimization decision tool: linking management actions to multiple ecological benefits via integrated modeling; restoring the health of the Green Bay ecosystem under a changing climate: modeling land use, management, and future outcomes; recommendation for an approach to determine phosphorus objectives and target loads for Lake Erie; development of a Nutrient Modeling Toolbox and modeling guidance for using load-response models to set site-specific nutrient goals for surface water ecosystems (Lead Scientist); development of a long-term phosphorus mass balance model for Missisquoi Bay, Lake Champlain (PM); extreme events impacts on water quality in the Great Lakes: Prediction and management of

nutrient loading in a changing climate (co-PI); development and application of AnnAGNPS to assess sediment and nutrient export from the Blanchard River watershed in north-western Ohio; development of a revised phosphorus dynamics sub-model for the Chesapeake Bay water quality model; Dr. DePinto has also conducted nutrient-eutrophication assessment studies in a number of lakes ranging in size from small lakes to the Great Lakes. Dr. DePinto's recent development of aquatic ecosystem models for Saginaw Bay, the lower Maumee River and western basin of Lake Erie, and Lake Ontario have greatly expanded our awareness of the impacts of multiple stressors acting in concert on the structure and function of aquatic ecosystems.

Dr. DePinto's studies have led to over 100 publications and the direction of more than 50 Master's theses and 12 Ph.D. dissertations. He has also worked on a great many councils, task forces, and advisory groups on water quality management nationally (e.g., EPA SAB review panels) and in the Great Lakes (e.g., IJC Council of Great Lakes Research Managers). Dr. DePinto earned his bachelor's degree in physics from Miami University of Ohio, as well as two master's degrees (Physics and Environmental Engineering) and his doctorate (Environmental Engineering) from the University of Notre Dame.